



THE UNIVERSITY *of* EDINBURGH

Title	Identification and characterisation of a novel p21 feedback loop in the regulation of p53
Author	Pang, Lisa Y.
Qualification	PhD
Year	2008

Thesis scanned from best copy available: may contain faint or blurred text, and/or cropped or missing pages.

Digitisation notes:

- Pages 46,79,113,181,212,228,252 & 258 are missing from original pagination

IDENTIFICATION AND CHARACTERISATION OF A NOVEL p21

FEEDBACK LOOP IN THE REGULATION OF p53

Lisa Y. Pang B.Sc. (Hons)

Thesis submitted to The University of Edinburgh for the degree of

Doctor of Philosophy

December 2007



“Mischief Managed”

Harry Potter and the Prisoner of Azkaban

J.K. Rowling

TABLE OF CONTENTS

Figures and Tables	x
Acknowledgements	xiii
Declaration	xiv
Abbreviations	xv
Abstract	xx
CHAPTER 1 - INTRODUCTION	1-45
CHAPTER 2 - MATERIALS AND METHODS.....	46-78
CHAPTER 3 - RESULTS	79-112
CHAPTER 4 - RESULTS	113-180
CHAPTER 5 - RESULTS	181-211
CHAPTER 6 - CONCLUSIONS AND FUTURE PERSPECTIVES	212-227
APPENDIX A - SUPPLEMENTARY DATA	228-251
APPENDIX B - BUFFERS AND SOLUTIONS	252-257
REFERENCES.....	258-303

CHAPTER 1 INTRODUCTION

1.1 Cancer.....	1
1.2 The p53 Tumour Suppressor	2
1.2.1 Discovery and classification of p53	2
1.2.2 Structure of p53	4
1.2.2.1 The N-terminal region	5
1.2.2.2 The central region	6
1.2.2.3 The C-terminal region.....	7
1.2.3 Functions of p53	9
1.2.3.1 Cell-cycle arrest	10
1.2.3.2 Apoptosis	11
1.2.3.3 DNA repair	13
1.2.3.4 Senescence	16

1.2.3.5 Metabolism	16
1.2.3.6 Development.....	17
1.2.4 Regulation of p53 transcriptional activity	18
1.2.4.1 Co-regulators of p53-dependent gene expression.....	19
1.2.4.2 Protein stability.....	21
1.2.4.3 Post-translational modifications	24
1.2.4.3.1 Phosphorylation.....	24
1.2.4.3.2 Lysine modification.....	25
1.2.4.3.3 Current controversy.....	27
1.2.4.4 Subcellular localisation.....	29
1.2.5 Autoregulatory feedback loops.....	30
1.3 The p21 Cyclin Dependent Kinase Inhibitor.....	33
1.3.1 Discovery and characterisation of p21	33
1.3.2 Structure of p21	34
1.3.3 Functions of p21	35
1.3.4 Regulation pf p21	37
1.3.5 p21 feedback loops.....	38
1.4 Objectives.....	41

CHAPTER 2

MATERIALS AND METHODS

2.1 General Reagents.....	47
2.2 Equipment	47
2.3 Antibodies	48
2.3.1 Primary antibodies.....	48
2.3.2 Secondary antibodies.....	48
2.4 Plasmids	48
2.5 Sterilisation.....	50
2.6 Molecular Biology Methods.....	50
2.6.1 Bacterial growth media.....	50
2.6.2 Storage of bacterial stocks.....	51
2.6.3 Preparation of competent cells	51

2.6.4 Transformation of <i>E.coli</i> competent cells with plasmid DNA	52
2.6.5 Amplification of plasmid DNA	52
2.6.6 Purification of plasmid DNA.....	52
2.6.7 Quantification of DNA concentration	53
2.6.8 Agarose gel electrophoresis.....	53
2.7 Cell Culture	54
2.7.1 Human cell lines.....	54
2.7.1.1 Cell maintenance	54
2.7.1.1.1 Subculturing.....	54
2.7.1.1.2 Cell storage and recovery.....	55
2.7.2 Harvesting adherent cells	56
2.7.3 Mouse cells.....	56
2.7.3.1 Extraction of B-cells from mouse spleens	56
2.7.3.2 Harvesting suspension cells.....	57
2.8 Manipulation of Mammalian Cells.....	58
2.8.1 Transient transfection	58
2.8.2 Stable transfection	59
2.8.3 RNA interference mediated gene knockdown.....	59
2.8.4 Gene reporter assays.....	60
2.8.4.1 Cell transfection and lysis.....	60
2.8.4.2 Luciferase assay	60
2.8.4.3 β -Galactosidase assay	60
2.8.5 Genotoxic or drug treatment of mammalian cells	61
2.8.5.1 IR treatment	61
2.8.5.2 Treatment with inhibitors.....	62
2.8.5.3 Cyclohexamide treatment	62
2.8.5.4 Poly(I).poly(C) treatment.....	63
2.9 Recovery and Detection of Protein	63
2.9.1 Urea lysis.....	63
2.9.2 Protein precipitation	63
2.9.3 Bradford assay	64
2.9.4 SDS polyacrylamide gel electrophoresis.....	64
2.9.5 Immunoblotting.....	65
2.9.6 Coomassie staining.....	66

2.10 Subcellular Localisation	66
2.10.1 Adherent cells.....	67
2.10.2 Suspension cells	68
2.11 Cell Fractionation and Nuclease Digestion	69
2.12 Proteasome Activity Assay	70
2.13 ATM Kinase Assay	71
2.13.1 Nuclear extraction	71
2.13.2 Immunoprecipitation of ATM	71
2.13.3 Immunochemical detection of kinase activity	72
2.13.4 Radioactive detection of kinase activity	73
2.14 Co-immunoprecipitation Assay.....	73
2.15 Antibody Capture ELISA.....	74
2.16 DNA Microarray	75
2.16.1 Total RNA isolation	76
2.16.2 cRNA target labelling.....	76
2.16.3 Array hybridisation and detection	77
2.16.4 Image and data analysis.....	78

CHAPTER 3

REGULATION OF p53 PROTEIN LEVELS AND TRANSCRIPTIONAL ACTIVITY IS p21-DEPENDENT

3.1 Introduction	80
3.2 Results	82
3.2.1 Basal p53 levels, half-life and transcriptional activity are affected by loss of p21	82
3.2.2 p53 stress responses are not induced in p21 ^{-/-} cells.....	85
3.2.3 p21 regulates basal p53 levels and activity	88
3.2.4 Reintroduction of p21 into p21 ^{-/-} cells rescues the p53 stress response.....	89
3.2.5 The C-terminus of p21 is not required for p53 reactivation	92
3.3 Discussion	93

CHAPTER 4

LOSS OF p21 CAUSES ABERRANT LOCALISATION OF p53 AND REPRESSES EXPRESSION OF p53 TARGET GENES IN THREE MODEL SYSTEMS

4.1 Introduction	114
4.2 Results	118
4.2.1 Loss of p21 influences the cellular localisation of endogenous p53	118
4.2.2 Reintroduction of p21 restores p53 nuclear localisation	121
4.2.3 Aberrant localisation of p53 is not associated with unfolding	122
4.2.4 p53 localisation is independent of DNA damage	125
4.2.5 Microarray analysis of the HCT116 isogenic cell panel	125
4.2.6 The p21-null phenotype characterised in a cancer cell model applies to normal human cells.....	131
4.2.7 Microarray analysis of normal human fibroblast cells shows that loss of p21 suppresses p53-dependent gene expression	132
4.2.8 p21-dependent regulation of p53 subcellular localisation is evolutionarily conserved	136
4.2.9 The mouse model illustrates that p53 activity is <i>p21</i> gene dose dependent.....	137
4.3 Discussion	140
4.3.1 p21-dependent regulation of p53 subcellular localisation	140
4.3.2 Loss of p21 causes a global decrease in p53-dependent gene expression	144
4.3.3 p21 and apoptosis	147

CHAPTER 5

A GENETIC INTERACTION BETWEEN ATM AND p21 MAINTAINS p53 NUCLEAR LOCALISATION

5.1 Introduction	182
5.2 Results	186
5.2.1 Elevated phosphorylation of p53 at serine-15 are ablated by specific inhibition of ATM.....	186

5.2.2 <i>In vitro</i> ATM kinase activity is unaffected by loss p21.....	189
5.2.3 Specific inhibition of ATM disrupts cellular localisation of endogenous p53	191
5.2.4 Lack of evidence that ATM and p21 physically interact.....	193
5.2.5 ATM inhibition of normal human cells mimics loss of p21 by causing p53 mislocalisation.....	194
5.2.6 p53 subcellular localisation is MDM2-independent.....	196
5.3 Discussion	197
5.3.1 Evidence of a genetic interaction between ATM and p21.....	197
5.3.2 Induced ATM kinase activity is associated with loss of p21.....	200
5.3.3 ATM/p21 regulation of p53 localisation is independent of MDM2.....	202

CHAPTER 6

CONCLUSIONS AND FUTURE PERSPECTIVES

6.1 Regulation of p53 transcriptional activity by p21	213
6.1.1 Mechanism of p21-dependent regulation of p53 localisation	213
6.1.2 p53-dependent gene expression is associated with p21 gene dose	215
6.2 Further characterisation of the ATM-p21 interaction	217
6.3 Investigation of p21-dependent regulation of p53 within the cell cycle	219
6.4 Potential therapeutics	221
6.4.1 Specific inhibition of ATM	221
6.4.2 Specific p21 peptides for reactivation of p53	222
6.5 Conclusion.....	224

APPENDIX A

IDENTIFICATION OF NOVEL SMALL MOLECULE COMPOUND INHIBITORS OF hSMG-1

A.1 Introduction	229
A.1.1 Biochemistry of the PIKK family.....	230
A.1.2 Suppressor of morphogenesis in genitalia-1 (hSMG-1)	231

A.1.3 The role of hSMG-1 in nonsense mediated mRNA decay	232
A.1.4 The role of hSMG-1 in the stress response.....	233
A.2 Materials and Methods	235
A.2.1 Screening for small molecule compound inhibitors of hSMG-1	235
A.2.1.1 General equipment and reagents	235
A.2.1.2 Immunoprecipitation of hSMG-1	236
A.2.1.3 hSMG-1 <i>in vitro</i> kinase assay	236
A.3 Results	238
A.3.1 Screening small molecule compound libraries.....	238
A.3.2 IC ₅₀ determination	239
A.4 Discussion	240
 APPENDIX B - Buffers and solutions.....	 253
 REFERENCES.....	 259

FIGURES AND TABLES

Figure 1.1 Functional domains of the human p53 tumour suppressor protein	42
Figure 1.2 The p53 response	43
Figure 1.3 Autoregulatory feedback loops modulate p53 activity	44
Figure 1.4 Human p21 protein and its direct protein-protein interactions	45
Table 2.1 Details of primary antibodies	49
Table 2.2 Human cell lines and culture conditions	54
Table 2.3 Details of inhibitors of cellular targets	62
Figure 3.1 p53 protein levels and half-life are aberrant in the absence of p21	99
Figure 3.2 High basal level of p53 in the HCT116 p21 ^{-/-} cells is due to increased stabilisation	100
Figure 3.3 p53 transcriptional activity is uncoupled from p53 protein stabilisation in p21 ^{-/-} cells	101
Figure 3.4 The p53 viral response is suppressed in p21 ^{-/-} cells	102
Figure 3.5 The p53 DNA damage response is suppressed in p21 ^{-/-} cells	104
Figure 3.6 Basal p53 protein levels are p21-dependent	106
Figure 3.7 Transient transfection of p21 can partially recover p53 activity yet no effect on protein levels	107
Figure 3.8 Stable reintroduction of p21 into HCT116 p21 ^{-/-} cells restores basal levels of p53 and phosphorylation of p53 at serine-15	108
Figure 3.9 Stable reintroduction of p21 into p21 ^{-/-} cells restores the p53 viral response	109
Figure 3.10 Stable reintroduction of p21 into HCT116 p21 ^{-/-} cells restores the p53 DNA damage response	110
Figure 3.11 The C-terminus of p21 is not required for recovery of p53 activity	111
Figure 3.12 A model of p53 regulation by autoregulatory feedback loops	112
Figure 4.1 Loss of p21 is associated with mislocalisation of p53	152
Figure 4.2 p53 nuclear localisation is p21-dependent	153

Figure 4.3 Mislocalised p53 is not unfolded in the absence of p21	154
Figure 4.4 p53 localisation in not DNA damage-dependent	156
Figure 4.5 Analysis of gene expression alterations in the absence of p21	157
Figure 4.6 Graphical representation of microarray results of selected genes indicates aberrant basal and IR-induced gene expression in the absence of p21	158
Figure 4.7 Gene expression profiles show an overall decrease in p53 target gene expression in the absence of p21	160
Table 4.1 Genes expressed in HCT116 isogenic cell panel in response to IR	161
Table 4.2 Ratio of gene expression between HCT116 isogenic cells in response to IR.....	162
Figure 4.8 In normal human fibroblast cells basal levels of BAX protein are reduced by p21 siRNA mediated gene knockdown	163
Figure 4.9 p53 subcellular localisation is p21-dependent in NHF cells.....	164
Figure 4.10 Reduction of p21 protein levels in NHF cells causes defects in basal and IR induced p53-dependent gene expression	165
Figure 4.11 Microarray analysis of individual genes indicates aberrant basal and IR-induced gene expression in the absence of p21 in NHF cells	166
Figure 4.12 Graphical representation of NHF microarray results shows a general reduction of gene expression in the absence of p21 and partial recovery in response to IR.....	168
Figure 4.13 NHF gene expression profiles show an overall decrease in basal and IR-induced p53 target gene expression in the absence of p21	170
Table 4.3 Genes expressed in NHF cells in response to p21 siRNA and IR.....	171
Table 4.4 Ratio of gene expression between NHF cells treated with either control or p21 siRNA and with or without IR	172
Figure 4.14 B-cells extracted from p21 ^{-/-} mice contain mislocalised p53 compared to WT counterparts.....	173
Figure 4.15 Microarray analysis of B-cells extracted from WT, p21 ^{+/-} , and p21 ^{-/-} mice show that p53-dependent gene expression is affected by p21 gene dosage.....	174
Figure 4.16 Graphical representation of microarray results of selected genes indicates p21 gene dosage effects.....	175
Figure 4.17 p53-dependent gene expression is affected by p21 gene dosage	177
Figure 4.18 Gene expression profiles of B-cells extracted from WT, p21 ^{+/-} , and	

p21 ^{-/-} mice show an overall decrease in basal p53 target gene expression in the absence of p21	178
Table 4.5 Genes expressed in B-cells extracted from transgenic mice either wild-type, heterozygous, or nullizygous for the <i>p21</i> gene	179
Table 4.6 Ratio of gene expression in B-cells extracted from transgenic mice either wild-type, , heterozygous, or nullizygous for the <i>p21</i> gene	180
Figure 5.1 Chemical structures of ATM inhibitors	204
Figure 5.2 Small molecule inhibitors of ATM leads to dose dependent decrease in ATM substrate phosphorylation	205
Figure 5.3 Specific inhibition of ATM decreases the elevated p53 serine-15 and CHK2 threonine-68 phosphorylation that are induced by loss of p21	206
Figure 5.4 ATM kinase activity is not affected by loss of p21 by <i>in vitro</i> kinase assays.....	207
Figure 5.5 Specific ATM inhibition mimics the p21 ^{-/-} phenotype	208
Figure 5.6 Endogenous ATM and p21 do not co-immunoprecipitate.....	209
Figure 5.7 p53 nuclear localisation is ATM-dependent in NHF cells.....	210
Figure 5.8 MDM2 is not required for p21-dependent localisation of p53	211
Figure 6.1 A model of the regulation of p53 subcellular localisation	225
Figure 6.2 A model of ATM-dependent regulation of p21 expression and activation of p53.....	226
Figure 6.3 A model of a novel p21 feedback loop in the regulation of p53	227
Figure A.1 Schematic representation of the human PIKK proteins	244
Figure A.2 A model of nonsense mediated mRNA decay pathway	245
Table A.1 Hits identified in the secondary screen.....	246
Figure A.3 Plate layout for IC ₅₀ determination	246
Table A.2 Compounds identified in the secondary screen and their IC ₅₀ values	247
Figure A.4 Inhibitors of hSMG-1	248
Table A.3 Comparison of IC ₅₀ values	249
Figure A.5 Chemical structure of KU-0055958.....	251

ACKNOWLEDGEMENTS

I would first and foremost like to thank my supervisor, Ted Hupp for being a brilliant boss, for his patience, enthusiasm, endless ideas and limitless scientific knowledge, for introducing me to the world of Olaf Stapledon, and for sharing a mutual appreciation for all things Neil Gaimen. I am also grateful to Graeme Smith for all his advice and for giving me the opportunity to do a stint at KuDOS Pharmaceuticals. Thanks to Kate and Ali who looked after me at KuDOS. And I thank the BBSRC and KuDOS for funding me.

I'd like to thank everyone in the lab, past and present, for making my PhD experience a very happy one. Thanks to Ashley, Andrea, Angela, Angeli, Bart, Ben, Bodil, Craig, David, Emma, Euan, Erin, Hannah, Havi, Iro, Jen, Jenny, Kathryn, Lindsey, Liz, Lenny, Lee, Magda, Maura, Mirijam, Natalie, Nicky, Sarah, Suzy, Vikram, Yew-Kwang and Yao. Thanks to Ashley for all her help and advice. Thanks to Jennifer Chrystal for sharing a bench with me, for being my conference buddy, and for going through this together. Thanks to Sarah for lots advice, understanding and always sharing dessert. Thanks to Jenny for teaching me the intricacies of the Doric language, for numerous trips to the gym and/or pub, and for answering all my random science questions. Thank you to Jenny and Sarah for proof reading my thesis.

Many thanks to all my friends and family, all have been fab and are simply irreplaceable. Special thanks to my Mum, Dad, Louise and Floyd, for their unlimited love, encouragement, and patience, and for always believing in me. Finally, thank you to Matthew, for being my best friend and support throughout.

DECLARATION

I declare that I am the author of this thesis and it is entirely the result of my own work except where acknowledged in the text. The work presented has not been submitted or accepted to any other board for any other qualification or degree. All sources of information have been acknowledged by means of a reference.

Lisa Pang

December 2007

ABBREVIATIONS

+/+	Wild Type
+/-	Heterozygous mutant
-/-	Homozygous mutant
aa	Amino acid
Ab	Antibody
A-T	Ataxia-telangiectasia
AMC	7-amino-4-methylcoumarin
APC/C	Anaphase-promoting complex/cyclosome
ATM	Ataxia-telangiectasia Mutated
ATP	Adenosine triphosphate
ATR	ATM and Rad-3 related
β GP	Beta Glycerol Phosphate
BAX	Bcl-2 associated protein X
Bcl-2	B-cell lymphoma-2
BSA	Bovine serum albumin
C-terminus	Carboxy terminus of protein
CBP	CREB binding protein
CDK	Cyclin dependent kinase
CHK1	Checkpoint kinase 1
CHK2	Checkpoint kinase 2
CIP1	CDK interacting protein 1

Cont	Control
CPM	Counts per minute
DBD	DNA binding domain
DMEM	Dulbecco's modified eagle's medium
DMSO	Dimethyl Sulfoxide
DNA	Deoxyribonucleic acid
DNA-PK	DNA-dependent protein kinase
DSB	Double strand break
dsRNA	Double stranded RNA
DTT	Dithiolthretiol
<i>E. Coli</i>	Escherichia Coli
ECL	Enhanced chemiluminescence
EDTA	Ethylene diamine tetra-acetic acid
EJC	Exon junction complex
ELISA	Enzyme linked immunosorbent assay
FBS	Foetal bovine serum
G1	Gap phase 1
G2	Gap phase 2
GADD	Growth arrest and DNA damage gene
GST	Glutathione S-transferase
Gy	Gray
H	Histone
HAT	Histone acetyltransferase

HDAC	Histone deacetylase
HEPES	N-(2-Hydroxyethyl)piperazine-N'-(2-ethanesulfonic acid)
HR	Homologous recombination
HRP	Horse radish peroxidase
IC50	Concentration required to achieve 50% inhibition
IFN	Interferon
IP	Immunoprecipitation
IPTG	Isopropyl- β -thio-galactoside
IR	Ionising radiation
kDa	Kilodalton
LB	Luria Bertani
M	Mitosis
mA	Milli-amperes
MDM2	Mouse double minute 2
MEF	Mouse Embryonic Fibroblast
MRN	Mre11/Nbs1/Rad50
mTOR	Mammalian target of rapamycin
NE	Nuclear extract
NES	Nuclear export signal
NHF	Normal Human Fibroblast
NLS	Nuclear localisation signal
NMD	Nonsense mediated decay
NP40	Nonidet P40

ORF	Open reading frame
PAGE	Polyacrylamide gel electrophoresis
PBS	Phosphate buffered saline
PBST	PBS-Tween 20 (0.01% v/v)
PCNA	Proliferating cell nuclear antigen
PI3-K	Phosphoinositide 3-kinase
PIKK	Phosphoinositide 3-kinase related kinase
PML	Promyelocytic leukaemia
PMSF	Phenylmethanesulphonyl fluoride
Poly(I):poly(C)	Polyinosinic polycytidylic acid
PTC	Premature translation termination codon
Pu	Purine
PUMA	p53 upregulated modulator of apoptosis
Py	Pyrimidine
RLU	Relative light unit
RNA	Ribonucleic acid
SDS	Sodium dodecyl sulfate
Ser	Serine
SH-3	Src homology domain 3
siRNA	Small interfering RNA
SMG	Suppressor with morphogenetic effect on genitalia
Tris	Tris(hydroxymethyl)methylamine
TRRAP	Transformation/translation domain associated protein

Tween 20	Polyoxyethylene sorbitan monolaurate
Ub	Ubiquitin
UV	Ultra violet light
v/v	Volume per volume
w/v	Weight per volume
WAF1	Wild-type p53 activated fragment
WT	Wild Type

ABSTRACT

The p53 tumour-suppressor protein plays a critical role in the cellular response to environmental and intracellular stresses that threaten DNA integrity. Inactivation of p53 represents an important step during carcinogenesis and is associated with genomic instability and tumour development. A key transcriptional target of p53 is the cyclin-dependent kinase inhibitor, p21^{WAF1/CIP1} (hereafter referred to as p21), which mediates p53-dependent G1 arrest. The role of p21 in tumour development remains contentious. Early studies showed that p21 mutations are rare in human cancers however there is a growing list of human carcinomas that have aberrant p21 expression. p21-null animals also have elevated tumour incidence, but the mechanism underlying this is not yet defined.

Our data identifies p21 as a component of a positive feedback loop that maintains the p53 transcriptional response. Three model systems were used to characterise this novel mechanism of p53 regulation. In the human colon carcinoma cell line HCT116 with targeted inactivation of p21, p53 stabilisation is uncoupled from its activity as a transcription factor and shows defects in the p53 response to DNA damage and double stranded RNA, indicating that a common mechanism prevents p53 activation by distinct stresses in the absence of p21. The p53 transcriptional programme in response to cellular damage can be reactivated after complementation of the p21 gene into the HCT116 p21-null cells. In B-cells from mice lacking the p21 gene, a striking loss of the p53-dependent transcription programme was identified using p53-specific microarray screens. Gene dosage effects indicate a progressive loss of p53 function in B-cells heterozygous or homozygous null for p21. Similarly, siRNA to p21 can attenuate the p53-dependent transcription response in normal human fibroblasts. In all three model systems, deletion of the p21 gene results in p53 nuclear export and eliminates the p53 transcriptional response. This data indicates that p53 has evolved a co-ordinated transcription mechanism to control its own function: a positive feedback loop maintained by p21 and a negative feedback loop maintained by MDM2, whose balance controls the specific activity of p53.

CHAPTER 1

INTRODUCTION

1.1 Cancer

Cancer is a genetic disease, resulting from mutations that activate proto-oncogenes and restrain tumour-suppressor genes, leading to the unrelenting clonal expansion of abnormal cells which invade, subvert and erode normal tissues (Evan & Vousden, 2001; Michor et al., 2004; Vogelstein & Kinzler, 2004). Cancer arises by evolutionary processes. Genetic diversity generated by mutagenesis provides the basis for natural selection. Similarly, multiple genetic changes which are followed by clonal selection are required for the generation of tumours (Evan & Vousden, 2001; Albertella, et al., 2005). Epidemiological studies of the kinetics of tumour appearance in human populations indicated that four to six distinct somatic mutations were required to accomplish the process of transformation (Hahn & Weinberg, 2002). Interestingly, it has been proposed that an early event in tumourigenesis is the mutation of a gene involved in the fidelity of DNA replication or efficiency of DNA repair (Loeb *et al.*, 1974). Such a mutation would increase the likelihood of alterations in additional genes involved in genome maintenance, and thus initiate a cascade of mutations throughout the genome that under selective pressure may result in the development of malignant cancer cells.

Ultimately the genetic instability driving tumourigenesis is fuelled by DNA damage and errors made by the DNA repair machinery (Fei & El-Deiry, 2003). Consequently, cells have evolved elaborate mechanisms, including cell cycle checkpoints, to monitor genomic integrity and ensure high fidelity transmission of genetic information (Bartek & Lukas, 2001). A crucial protein in preventing the accumulation of cancer-causing mutations and maintaining genomic stability is the tumour suppressor protein, p53 (Lane, 1992).

1.2 The p53 Tumour Suppressor

1.2.1 Discovery and classification of p53

The p53 protein was originally identified in mouse cells transformed with the small DNA tumour virus, Simian Virus 40 (Lane & Crawford, 1979). The viral T-antigen protein, essential for the initiation and maintenance of the transformed phenotype, was shown to bind to a cellular protein of apparent molecular mass of 53 kDa. This protein was subsequently called p53 (Lane & Crawford, 1979).

The *p53* gene was initially characterised as an oncogene, as over-expression of cloned p53 cDNA resulted in the oncogenic transformation of cells (Jenkins *et al.*, 1985). However, re-evaluation of the original molecular cloning of p53 cDNA revealed that the cDNA was actually an oncogenic mutant form of p53 (Oren & Levine, 1983). In direct contrast, wild-type p53 was subsequently characterised as a tumour suppressor gene. The p53 protein is a stress-activated transcription factor,

whose principal function is to maintain genome stability through regulation of the cell cycle, apoptosis and DNA repair (Lane, 1992).

The importance of p53 in cancer biology is illustrated by the frequency with which p53 function is lost during tumour development, and the scope of mechanisms employed to inactivate p53. Indeed, DNA tumour viruses have evolved their own mechanisms to inactivate p53, thereby facilitating their own replication and maximising transformation potential by preventing cell cycle arrest and increasing genome instability. Viral oncoproteins which sequester p53, include adenovirus E1B (Sarnow *et al.*, 1982), human papillomavirus E6 protein (Scheffner *et al.*, 1990), hepatitis B virus X protein (Wang *et al.*, 1994), human cytomegalovirus IE84 protein (Speir *et al.*, 1994), and Epstein-Barr virus nuclear antigen (Szekely *et al.*, 1993). The significance of p53 as a tumour suppressor is supported by observations that germline mutations of the *p53* gene in humans gives rise to the Li-Fraumeni syndrome, an inherited disorder with a high risk of developing a variety of cancers at an early age (Malkin *et al.*, 1990). Mouse models further support these observations, as mice nullizygous for the *p53* gene developed normally but showed a high incidence of tumour development by six months (Donehower *et al.*, 1992).

In human cancer progression functional inactivation of p53 is a common mechanism (Hupp *et al.*, 2000). Given that different cancers are relatively biologically and pathologically distinct, it is striking that approximately half of all human cancer types from a wide spectrum of tissues carry a *p53* mutation (Levine *et al.*, 1991). The impact of p53 alterations on tumourigenesis is considerably more than the statistics for *p53* gene mutation indicate, as wild-type p53 may be functionally inactivated by other mechanisms, including viral oncogenes and defects

in the p53 activation pathway (Hainut & Hollstein, 2000), signifying that functional p53 may be lost in all human cancers. These data firmly establishes *p53* as a tumour suppressor gene.

1.2.2 Structure of p53

The human *p53* gene has been mapped to the terminal band of the short arm of chromosome 17 (17p13) and spans 20 kb. The gene consists of 11 exons, where the first exon is non-coding and exons 2 – 11 encode the p53 protein (McBride *et al.*, 1986). The *p53* gene has been conserved during evolution and homologues of *p53* have been found in invertebrates such as *Caenorhabditis elegans* (Derry *et al.*, 2001) and *Drosophila melanogaster* (Sogame *et al.*, 2003). Although p53 has not been found in yeast, over-expression of human wild-type p53 inhibits cell division in *Saccharomyces cerevisiae* (Nigro *et al.*, 1992) and *Schizosaccharomyces pombe* (Bischoff *et al.*, 1992), compared to mutant p53 which does not induce a detectable phenotype. These findings and conservation of the p53 gene further highlights its cellular importance.

The human p53 protein consists of 393 amino acids and contains five functional domains (Figure 1.1). At the N-terminus there is a transactivation domain and a proline-rich domain. In the central part of p53 there is a sequence specific DNA-binding domain. And at the C-terminus there is a tetramerisation domain and a regulatory region (Levine, 1997; May & May 1999). The N- and C- terminal regulatory domains also contain heterologous protein docking sites, and

phosphorylation and acetylation sites which are implicated in the modulation of p53 protein-protein interactions (Chène, 2001; Hupp *et al.*, 2000).

Furthermore, phylogenetic characterisation of the p53 protein has shown the existence of five highly conserved sequences suggesting important functional regions that are required for tumour suppression (Soussi *et al.*, 1987; Soussi *et al.*, 1990). These regions are between amino acids 13-23 (BOX-I), 117-142 (BOX-II), 171-181 (BOX-III), 234-250 (BOX-IV) and 270-286 (BOX-V). BOX-I is located in the N-terminus and BOX-II-V are located in the DNA-binding domain (Figure 1.1). BOX II-V regions are frequently mutated in human cancer further indicating the importance of these regions in maintaining p53 function (Soussi & May, 1996).

1.2.2.1 The N-terminal region

The N-terminal region of p53 contains an acidic transactivation domain (amino acids 1-61) (Fields & Jang, 1990), which is representative of a classical activation domain found in transcription factors, such as VP16 (Fields & Jang, 1990). The transactivation domain allows recruitment of the basal transcription machinery, including components of the transcription initiation complex, and is essential for activation of transcription (Lu & Levine, 1995). This domain also interacts with a number of regulatory proteins, such as the negative regulator MDM2, which regulates cellular levels of p53 (Haupt *et al.*, 1997), and the acetyltransferases p300 and CREB binding protein (CBP), which act as co-activators and regulate p53 function via acetylation of its C-terminus (Gu *et al.*, 1997). The proline-rich domain (amino acids 63-97) is composed of five PxxP motifs and displays similarity to Src

homology domain 3 (SH-3) binding proteins which are proposed to play a role in mediating protein-protein interactions in signal transduction pathways (Walker & Levine, 1996). Similarly the proline-rich domain of p53 has been shown to directly interact with p300 to promote DNA-dependent acetylation of p53 and therefore mediate p53 transcriptional activity (Dornan *et al.*, 2003). The N-terminal region is natively unfolded, apart from small regions that exhibit nascent turn or helix formation (Bell *et al.*, 2002). The region with the nascent helix formation extends into a full amphipathic α -helix (amino acids 15-29) upon binding to the hydrophobic cleft of MDM2 (Kussie *et al.*, 1996).

1.2.2.2 The central region

The central region of p53 contains the sequence specific DNA-binding domain (amino acids 102-292) which binds specifically to double-stranded DNA recognition elements present in either the promoter or intron of a target gene (El-Deiry *et al.*, 1992). The consensus recognition element is defined as two repeats of the palindromic sequence 5'-Pu·Pu·Pu·C·W·W·G·Py·Py·Py -3' (Pu is a purine base, Py is pyrimidine base, and W represents A or T), separated by up to 13 base pairs (El-Deiry *et al.*, 1992). The affinity with which p53 binds its response elements varies depending on the sequence. Generally, p53 binds with higher affinity to the recognition elements of genes involved in cell cycle arrest, whereas lower affinity binding sites are found in genes involved in apoptosis (Weinberg *et al.*, 2005).

The DNA-binding domain of p53 is organised into a central β -sandwich of two anti-parallel β -sheets, which provides the basic scaffold for the DNA-binding

surface. This surface is formed by two large loops (L2 comprising of amino acids 164-194 and L3 comprising of residues 237-250) that are stabilised by a tetrahedrally coordinated zinc ion, and a loop-sheet-helix motif (Cho *et al.*, 1994). Removal of the zinc ion substantially destabilises the protein, resulting in local structural perturbation and loss of sequence specific DNA binding (Butler & Loh, 2003). Conserved residues from the loop-sheet-helix motif make specific contacts with the major groove of bound target DNA, and L3 is anchored to the minor groove via arginine-248 (Cho *et al.*, 1994).

The importance of the DNA-binding domain in p53 function is highlighted by the observations that this domain contains four of the five conserved regions, BOX II-V, and that more than 90 % of missense mutations in p53 reside in this domain. The two most frequently altered residues are arginine-248 and arginine-273 which results in defective contacts with the DNA and loss of the ability of p53 to act as a transcription factor. Similarly, additional amino acids are also recurrently mutated including arginine-175, glycine-245, arginine-249 and arginine-282, which results in altered conformation and disruption of the DNA-binding surface, which ultimately impairs p53 function (Cho *et al.*, 1994).

1.2.2.3 The C-terminal region

The C-terminal region of p53 contains the tetramerisation domain (amino acids 325-356) and a negative regulatory region (amino acids 363-393). In undamaged cells p53 is predicted to exist predominantly as monomers (Sakaguchi *et al.*, 1997), and upon binding to DNA containing the consensus recognition element, forms tetramers,

the protein's basic functional unit (Friedman *et al.*, 1993; Kitayner *et al.*, 2006). The tetramerisation domain has been shown to be essential for this function. The structure of this domain contains a β -strand linked to an α -helix by a single residue. Two monomers form a dimer via an anti-parallel β -sheet and an anti-parallel helix/helix interface. The dimers associate across a hydrophobic interface to form a four helix-bundle arranged orthogonally into tetramers (Jeffery *et al.*, 1995). This domain is a secondary site for p53 mutations which promote a conversion from tetrameric to dimeric forms with reduced DNA binding activity, suggesting that p53 activity depends on its conformation (Lomax *et al.*, 1998).

Three nuclear localisation signals (NLS) have been identified in the C-terminus, at amino acids 316-325 (NLS1), 369-375 (NLS2), and 379-384 (NLS3) (Dang & Lee, 1989; Shaulsky *et al.*, 1990a). Mutagenesis of NLS1 fully excluded p53 from the nucleus, whereas alteration of NLS2 and NLS3 leads to both cytoplasmic and nuclear localisation of p53, signifying that NLS1 is the prominent NLS (Shaulsky *et al.*, 1990b). A nuclear export signal (NES) has also been identified at amino acids 340-351 (Stommel *et al.*, 1999). The NES signal would be revealed when p53 is in a monomeric state, yet is buried beneath the surface when it is tetrameric, indicating that the cellular localisation of p53 could be regulated by changes in its quaternary structure (Chène, 2001).

The C-terminus also contains a negative regulatory domain (amino acids 363-393), which maintains the p53 tetramer in an inactive state by allosteric regulation of the DNA-binding domain (Hupp *et al.*, 1992). This model predicts that p53 is maintained in a latent state which precludes DNA binding, until activated by

posttranslational modifications of the C-terminal regulatory domain (Hupp & Lane, 1994), and that this domain is an important regulator of p53 function.

The C-terminal region, similar to the N-terminal region, is largely unstructured in its native state (Bell *et al.*, 2002). Intrinsic disorder is common in proteins at the centre of highly connected protein-protein interaction networks (Dunker *et al.*, 2005), as it facilitates binding and interaction with a large number of diverse target proteins.

1.2.3 Functions of p53

The tumour suppressor p53 functions principally as a transcription factor and can mediate its different downstream functions by regulating the expression of a large number of target genes (Zhao *et al.*, 2000; Laptenko & Prives, 2006). Several signalling pathways are coordinated by p53 including cellular responses to DNA damage, viral infection, oncogene activation, hypoxia, nucleotide depletion, and nutrient deprivation. Activation of p53 initiates various cellular responses including cell-cycle arrest, apoptosis, DNA repair, senescence, differentiation and inhibition of angiogenesis (Rozen & El-Deiry, 2007) (Figure 1.2). In addition p53 has been implicated in metabolism, development, and aging (Vousden & Lane, 2007). Selected functions of p53 will be discussed in more detail.

1.2.3.1 Cell-cycle arrest

The cell-cycle checkpoints are biochemical signalling pathways that sense various types of structural defects in DNA, or in chromosome function, and induce a multifaceted cellular response that activates DNA repair and delays cell cycle progression. When DNA damage is irreparable, checkpoints eliminate such potentially hazardous cells by permanent cell cycle arrest or cell death (Kastan & Bartek, 2004).

The G1/S checkpoint prevents initiation of DNA replication in cells that have damaged DNA. In response to DNA damage, such as DNA double strand breaks induced by ionising radiation, p53 plays a prominent role in mediating the G1/S checkpoint (Kastan *et al.*, 1991). The p53-dependent G1 arrest occurs largely through the transactivation of the *p21^{WAF1/CIP1}* gene (hereafter referred to as p21) (El-Deiry *et al.*, 1993; Dulic *et al.*, 1994). p21 is a potent inhibitor of cyclin dependent kinases (CDK) including cyclin E/CDK2 and cyclin A/CDK2 (Harper *et al.*, 1993). In the G1 phase of the cycle the retinoblastoma protein is hypophosphorylated, and in this state binds to and sequesters the E2F family of transcription factors which promote S phase. Release of active E2F, which then leads to the transcription of genes required for S phase progression, is mediated by sequential phosphorylation of RB by cyclin D/CDK4 and cyclin E/CDK2 (Sherr, 1994; Müller *et al.*, 2001). In response to DNA damage up-regulation of p21 inhibits cyclin E/CDK2, maintaining the RB-E2F complex, and consequently preventing S phase entry and replication of damaged DNA (Harper *et al.*, 1993; Harper *et al.*, 1995). p21 is essential for efficient G1 arrest, as mouse embryonic fibroblasts derived from p21-deficient mice (Deng *et*

al., 1995), and human cells with deletion of p21 by homologous recombination (Waldman *et al.*, 1995), both show impaired DNA-damaged induced G1 arrest.

The G2/M checkpoint prevents the initiation of mitosis in cells that have damaged DNA. G2/M progression is driven by the mitosis-promoting activity of cyclin B/CDK1 kinase, and mitosis is triggered by translocation of cyclin B/CDK1 into the nucleus and activation by dephosphorylation via the CDC25 family of phosphatases (Nurse, 1990). Initiation of the G2 arrest is mediated by phosphorylation of CDC25 by ATM/ATR, CHK1/CHK2, and /or p38, which creates a binding site for the 14-3-3 proteins and this association sequesters CDC25 in the cytoplasm (Kastan & Bartek, 2004). p53 is involved in sustaining G2 arrest, by up-regulation of cell-cycle inhibitors including 14-3-3 σ (Chan *et al.*, 1999), and GADD45 (growth arrest and DNA damage inducible 45 alpha) (Zhan *et al.*, 1999), and down-regulation of CDK1 and cyclin B promoters (Passalaris *et al.*, 1999).

1.2.3.2 Apoptosis

Each cell is under constant surveillance to maintain the integrity of its genome. If a cell is irreparably damaged it is removed in an orderly manner through programmed cell death or apoptosis (Hartwell & Kastan, 1994). There are two major apoptotic pathways in cells that can be activated by p53. One pathway is mediated by transmembrane death receptors of the CD95 (APO-1 or FAS)/TRAIL/tumour-necrosis factor receptor 1 family, whose ligation triggers recruitment and assembly of multi-protein complexes that initiate caspase activation (Walczak & Krammer, 2000). The other pathway is involves the mitochondrion, which acts as an integrating

sensor of death insults by releasing cytochrome c into the cytosol where it triggers caspase activation. Caspases implement cell death by cleaving a variety of intracellular substrates that trigger cell dissolution (Hengartner, 2000).

To date a large number of p53 target genes with pro-apoptotic activity have been identified. They fall into three groups based on their subcellular localisation (Benchimol, 2001). The first group of genes encodes proteins which localise to the cell membrane including *FAS/APO-1*, *KILLER/DR5*, and *PERP*. The second group of genes encodes proteins which localise to the cytoplasm including *PIDD* and *PIGs*. The third group of genes encodes proteins that localise to the mitochondria including *BAX*, *BID*, *NOXA*, *p53AIP1* and *PUMA*. However deletion of many of these apoptotic targets of p53 have little effect on the sensitivity of the cell to stress-induced apoptosis (Moll *et al.*, 2005), and indicated that p53 may induce apoptosis by a transcription-independent mechanism. Subsequent studies have shown that p53-dependent apoptosis is unimpeded by inhibition of transcription or translation (Caelles *et al.*, 1994), and that upon apoptotic stimuli a fraction of induced p53 rapidly translocates to the mitochondria (Marchenko *et al.*, 2000), suggesting that p53 has a transcription-independent role in the mitochondria-mediated apoptotic pathway.

The mitochondrial apoptotic pathway is principally mediated by the family of BCL2-related proteins, with some family members functioning as suppressors of apoptosis and others as promoters of apoptosis. The ultimate vulnerability of cells to diverse apoptotic stimuli is determined by the relative ratio of various pro-apoptotic and anti-apoptotic members of the BCL2 family. For example, BAX and BAK function to promote apoptosis by regulating mitochondrial membrane potential,

whereas anti-apoptotic family members, BCL2 and BCLxL directly bind BAX and BAK, negatively regulating their activity (Cory & Adams, 2002). BCL2 and BCLxL are constitutively anchored at the outer mitochondrial membrane, stabilising the membrane, and inhibiting cytochrome c release. Mitochondrial p53 physically interacts with BCL-2 and BCLxL, liberating BAX and BAK and promoting apoptosis (Mihara *et al.*, 2003). Mitochondrial p53 can also directly bind to BAK, and promote BAK oligomerisation and activation (Leu *et al.*, 2004). Hence mitochondrial p53 induces apoptosis by a dual mechanism of inhibiting anti-apoptotic members and promoting pro-apoptotic members of the BCL2-family.

1.2.3.3 DNA repair

In addition to growth arrest and apoptosis, the ability of p53 to regulate DNA repair after genotoxic stress represents another mechanism by which p53 contributes to maintenance of genome integrity. In eukaryotes, the five main DNA-repair processes are nucleotide excision repair (NER), base-excision repair (BER), mismatch repair (MMR), non-homologous end-joining (NHEJ) and homologous recombination (HR) (Hoeijmakers, 2001). p53 participates in all repair processes by both transcription-dependent and -independent pathways.

NER operates on damaged bases and disrupted base pairings that are caused by ultraviolet light (UV) or oxidative damage, which leads to changes in the structure of the DNA duplex (Hoeijmakers, 2001). Disrupted base pairs are identified, and additional proteins subsequently bind to the DNA to enable repair, including replication protein A, the transcription factor TFIIH sub-complex of RNA

polymerase II, and proliferating cell nuclear antigen (PCNA). p53 can directly interact with replication protein A (Miller *et al.*, 1997; Janus *et al.*, 1999) and TFIIH (Wang *et al.*, 1995) and modulate their activity. p53 also induces expression of GADD45, which can directly bind PCNA (Smith *et al.*, 1996), and xeroderma pigmentosum p48 (Hwang *et al.*, 1999), which recruits TFIIH to sites of DNA damage. In addition p53 mediates chromatin relaxation to allow lesion detection by recruiting p300, which has intrinsic histone acetyltransferase activity (Rubbi & Milner, 2003).

BER repairs apurinic and apyrimidinic sites in DNA. This process is mediated by a DNA glycosylase which removes the damaged base, an endonuclease which processes the abasic site, a DNA polymerase which inserts the new nucleotide, and a DNA ligase which rejoins the DNA strand (Hoeijmakers, 2001). Interestingly, ARE1/REF1 endonuclease associates with p53 and enhances the transcription, growth arrest and apoptotic functions of p53 *in vivo* (Gaiddon *et al.*, 1999), however the consequences of this association are not well defined. In response to reactive oxygen species (Achanta & Huang, 2004) or ionising radiation (Zurer *et al.*, 2004), p53 enhanced the activity of 3-methyladenine DNA glycosylase, which enhanced the removal of damaged bases.

MMR removes mismatched nucleotides and insertions or deletions, which are a consequence of slippage of DNA polymerase during the synthesis of repetitive sequences in replication or recombination (Hoeijmakers, 2001). The MMR process is mediated by the combined action of conserved repair-specific proteins including MLH1 and MSH2. The MMR proteins and p53 have reciprocal effects on each other's function. Stabilisation of MLH1 enhances p53 activation during DNA

damage (Luo *et al.*, 2004), and similarly activation of p53 upregulates *MSH2* gene expression (Scherer *et al.*, 2000). There is an association between p53 mutations and abnormal expression of the *MSH2* gene in a range of different cancers (Saito *et al.*, 2003a). However loss of p53 has little effect on MMR proficient cells, but confers substantial hypersensitivity to the cytotoxic effects of cisplatin on MMR deficient cells, indicating that p53 and MMR may cooperate in response to DNA damage (Lin *et al.*, 2001).

NHEJ is the principal DNA-repair process used throughout the cell cycle to repair DNA double strand breaks in somatic cells. Proteins involved in NHEJ include DNA-PK, XRCC4, and DNA ligase IV (Hoeijmakers, 2001). DNA-PK consists of a catalytic subunit and a regulatory subunit, Ku (a heterodimer of Ku70 and Ku80). DNAPK phosphorylates and activates p53 which leads to increased expression of downstream target genes, including Ku70 (Brown *et al.*, 2000), whose increased expression may promote DSB repair. p53 also has a transcriptional-independent role in NHEJ as wild-type p53 is capable of rejoining DNA with DSBs, *in vitro* and *in vivo* (Tang *et al.*, 1999), and it has also been proposed that p53 can facilitate precise ligation (Lin *et al.*, 2003).

HR uses a homologous double-stranded DNA molecule as a template for the repair of broken DNA to maintain the integrity of the genome (Hoeijmakers, 2001). p53 has been proposed to have a transcriptional-independent role in HR, where p53 specifically binds to the DNA, possibly in combination with other proteins, to check the fidelity of the HR events by specific mismatch recognition in the heteroduplex intermediates (Janz *et al.*, 2002). Hence, p53 contributes to control and efficiency of DNA repair.

1.2.3.4 Senescence

Apoptosis is not the only anti-proliferative response coupled to oncogenic signalling, as there is increasing evidence that senescence provides a barrier to malignant progression (Bartkova *et al.*, 2006). Senescence is characterised as an irreversible growth arrest of cells that remain metabolically active (Campisi, 2001). Senescence can be induced by the erosion of telomeres during cell division (replicative senescence) or in response to oncogene activation, DNA damage or oxidative stress (Lowe *et al.*, 2004). All forms of senescence depend on the DNA damage checkpoint kinase ataxia telangiectasia mutated (ATM) (Bartkova *et al.*, 2006), which in response to DNA DSBs is a potent activator of p53. Similarly, senescence is a p53-dependent process (Rozan & El-Deiry, 2007). However the downstream targets of p53 that induce senescence have not yet been fully clarified. To date, p21 is surprisingly ineffective at maintaining senescence (Pantoja & Serrano, 1999). However another p53 transcriptional target, PAI-1 (plasminogen activator inhibitor-1) is sufficient to induce senescence, and siRNA mediated gene knockdown of PAI-1 enabled cells to bypass p53-induced senescence (Kortlever *et al.*, 2006).

1.2.3.5 Metabolism

Recently, p53 has been implicated in determining the response of cells to nutrient stress and in regulating pathways of glucose usage and energy metabolism. Glycolysis is a metabolic pathway through which glucose is metabolised to provide energy. Under conditions of low glucose, p53 is activated by AMP kinase and

engages a reversible cell cycle checkpoint (Jones *et al.*, 2005). p53 can also inhibit glycolysis through its transcriptional target, TIGAR (Tp53-inducible glycolysis and apoptosis regulator), which lowers the levels of fructose 2,6-bisphosphate, a key glycolytic enzyme that promotes glycolysis (Bensaad *et al.*, 2006). Expression of TIGAR also lowered the amount of reactive oxygen species, and protected cells from apoptosis (Bensaad *et al.*, 2006). Therefore p53 appears to promote cell survival during glucose deprivation.

Expression of p53 also enhances oxidative phosphorylation over glycolysis, by inducing expression of the copper transporter, SCO2 (synthesis of cytochrome c oxidase 2). SCO2 is an assembly factor for the cytochrome c oxidase complex and links p53 to mitochondrial respiration (Matoba *et al.*, 2006).

Cancer cells are characterised by an increase in aerobic glycolysis (Warburg, 1956). Loss of p53 may therefore contribute to the metabolic changes observed in cancer cells, by enabling cells to continue to proliferate in nutrient-poor conditions.

1.2.3.6 Development

Previous studies have indicated that p53 function is not required for normal growth or development (Donehower *et al.*, 1992). However closer analysis of *p53*-null mice revealed that although many mice are normal at birth, some exhibit developmental defects. These mice develop craniofacial abnormalities and show neural tube closure defects, indicating that p53 has a role in neural development (Armstrong *et al.*, 1995). Apoptosis is a crucial event in the development of the nervous system, therefore lack

of p53 may lead to a failure in progenitor cell apoptosis and subsequently, an overproduction of neural tissue and death of the mouse (Miller *et al.*, 2000).

In *Xenopus laevis* embryos, blocking p53 activity impairs further differentiation and the embryos become large, disorganised cellular masses (Wallingford, 1997). Co-operation of p53 and TGF- β in *Xenopus laevis* development has been established, as p53 directly associates with mediators of TGF- β signalling pathway, and regulates expression of meso-endodermal genes (Cordenonsi *et al.*, 2003). Also in zebrafish (*Danio rerio*) p53 has been demonstrated to provide a protective function against a range of early developmental defects that are associated with loss of function mutations in genes as diverse as those involved in DNA synthesis (Plaster *et al.*, 2006), gut development (Chen *et al.*, 2005), and neuronal development (Campbell *et al.*, 2006). These findings imply that p53 may constantly monitor the early developmental process, eliminating defective embryos.

In humans, the Li-Fraumeni syndrome is a heritable condition characterised by *p53* germline mutations. This condition is very rare, with less than four hundred families reported world-wide, and no reports of *p53*-null children born (Olivier *et al.*, 2003). This indicates that in humans *p53*-null mutants are embryonically lethal, and suggests that p53 has a role in embryonic development.

1.2.4 Regulation of p53 transcriptional activity

p53 is a critical cellular protein, and multiple mechanisms have evolved to regulate its activity including co-factors of p53-dependent gene expression, p53 protein stability, post-translational modifications, and subcellular localisation. This plethora

of regulatory mechanisms probably exists both to tightly and rapidly control the activities of p53, and to provide alternative mechanisms for different cell-types and different cellular stresses. The principal function of p53 is as a stress-activated transcription factor, and regulation of p53 transcriptional activity will be discussed in further detail.

1.2.4.1 Co-regulators of p53-dependent gene expression

In eukaryotic cells genomic DNA usually exists in a highly organised chromatin structure, which is not accessible to the general transcription factors and RNA polymerase (Grunstein, 1997). For transcription activation, p53 has been proposed to bind to its consensus recognition element within the promoter of the target gene and facilitate promoter opening. p53 interacts with and recruits histone modification enzymes to the promoter including histone acetyltransferases and/or histone methyltransferases, where they modify histones, forcing the promoter into an open and accessible conformation (Laptenko & Prives, 2007).

p300 and its homologue CBP, are histone acetyltransferases and have been characterised as co-activators of p53-dependent gene expression (Brownell *et al.*, 1996). Initially it was observed that the adenoviral protein E1A bound directly to p300 and repressed p53-activated promoters (Steegenga *et al.*, 1996). Subsequent experiments have shown that p53 transcriptional activity is enhanced by p300/CBP over-expression (Scolnick *et al.*, 1997), and that p300/CBP physically interacts with p53 at the consensus recognition element in the target gene promoter (Lill *et al.*, 1997). Therefore p300/CBP acetylates histones in the vicinity of p53 target

promoters and enhances p53 transcriptional activity. In addition to p300/CBP, three other proteins that are part of a histone acetyltransferase complex, hADA3 (Wang *et al.*, 2001), TRRAP (Ard *et al.*, 2002), and TIP60 (Legube *et al.*, 2004), are involved in regulating p53 transcriptional activity.

An *in vitro* study using the promoter of the *GADD45* gene demonstrated that p53 transcriptional activity is also enhanced by the histone methyltransferases, PRMT1 and CARM1 (An *et al.*, 2004). Interestingly PRMT1 and p300 increase their respective activities reciprocally, and are able to increase p53 transcriptional activity synergistically. However, p300 enhanced histone methylation by CARM1 but CARM1 had no effect on p300 activity (An *et al.*, 2004). Thus the extent of p53 transcriptional activity can be fine-tuned by histone modifications.

Although p53 is a well established activator of transcription, p53 can also suppress transcription of a variety of genes including *MYC*, *Cyclin B*, *VEGF*, *RAD51*, and *BCL2* (Ho *et al.*, 2005; Rozan & El-Deiry, 2007). p53 has been shown to recruit histone deacetylases to target promoters thus altering chromatin structure and preventing transcriptional activators from binding to the promoter. p53 recruitment of histone deacetylases is mediated through the presence of additional protein mediators including mSin3a (Murphy *et al.*, 1999), SnoN (Wilkinson *et al.*, 2005), and p52 (Rocha *et al.*, 2003). This represents a major mechanism of p53-dependent transcriptional repression.

Different cellular stresses may also modulate p53 transcriptional activity by promoting differential interactions with co-regulators. For example, DNA damage induces the interaction of p53 with both the transcriptional co-activator p300 and the transcriptional co-repressor mSin3a, whereas hypoxia predominantly induces the

interaction with mSin3a, but not with p300 (Koumenis *et al.*, 2001). Surprisingly, endoplasmic reticulum stress caused by an accumulation of unfolded proteins, leads to the specific degradation and inactivation of p53 transcriptional activity (Qu *et al.*, 2004).

The specificity of the transcriptional programmes mediated by p53 can be skewed towards a particular cellular outcome by additional protein co-factors. For example, BRCA1 promotes transcription of DNA repair genes and represses expression of pro-apoptotic genes (MacLachlan *et al.*, 2002). MUC1 favours p53-dependent expression of the cell cycle arrest gene, *p21* and inhibits expression of the pro-apoptotic gene *BAX* (Wei *et al.*, 2005). Similarly, HZF is a zinc finger protein that directly interacts with p53 and induces preferential expression of p53-target genes that block the cells cycle, including *p21* and *14-3-3* genes, while simultaneously attenuating expression of pro-apoptotic genes such as *BAX*, *PERP*, *NOXA* and *PUMA* (Das *et al.*, 2007). In contrast, ASPP1 and ASPP2 bind directly to the DNA binding domain of p53 and encourage transcription of pro-apoptotic genes including *BAX* and *PIG-3*, while inhibiting transcription of genes associated with cell cycle arrest including *p21* (Samuels-Lev *et al.*, 2001).

1.2.4.2 Protein stability

p53 is a negative regulator of proliferation, and in unstressed normal cells wild-type p53 protein is maintained at low levels to allow for normal cell growth and development. In unstressed cells p53 is a short-lived protein with a half-life of approximately 20 minutes, in most cell types studied (Maki & Howley, 1997;

Maltzman & Czyzyk, 1984). Degradation of p53 is mediated by the proteasome in an ubiquitin-dependent manner.

MDM2 (murine double minute 2) protein is an essential regulator of p53 and is required to allow survival during normal development (Jones *et al.*, 1995). MDM2 is an ubiquitin ligase, in which the RING domain is indispensable to promote ubiquitination and degradation of target proteins, including p53 (Fang *et al.*, 2000). MDM2, through a hydrophobic pocket domain in its N-terminus, directly binds to the p53 N-terminus, and mediates polyubiquitination and degradation of p53 (Moll & Petrenko, 2003). However the current dogma is under revision. At low levels MDM2 was able to monoubiquitinate p53 leading to nuclear export, but not degradation (Li *et al.*, 2003). At higher levels MDM2 was able to polyubiquitinate p53 leading to its degradation, and was facilitated by p300/CBP (Grossman *et al.*, 2003). It was further proposed that MDM2 can only promote monoubiquitination of p53, and that the binding of p300 to MDM2 is necessary for efficient polyubiquitination, and therefore degradation of p53 to occur (Grossman *et al.*, 2003).

Recent studies have also highlighted several proteins which cooperate with MDM2 in the regulation of p53. The YY1 (Yin Yang 1) transcription factor plays a key role in development and has been shown increase the interaction between p53 and MDM2, and enhance p53 degradation (Gronroos *et al.*, 2004). Similarly, gankyrin promotes increased association of the MDM2-p53 complex to the proteasome, and therefore promotes efficient degradation of p53 and MDM2 (Higashitsuji *et al.*, 2005).

Proline isomerisation of p53 may also influence MDM2 mediated degradation of p53. The proline-rich domain of p53 can be modified by the prolyl-

isomerase (Zacchi *et al.*, 2002), PIN1, changing p53 conformation which may inhibit the p53-MDM2 interaction. The modification of p53 by PIN1 increases the stability of p53 and is required for the transcription of p53 targets including *BAX*, *p21* and *MDM2* (Zheng *et al.*, 2002; Wulf *et al.*, 2002). The importance of the proline-rich domain was highlighted by a transgenic mouse expressing a mutant p53 lacking this domain. The resulting p53 protein lacking the proline-rich domain was more sensitive to MDM2 degradation, and the cells expressing this protein exhibited impaired cell cycle arrest and apoptosis in response to DNA damage (Toledo *et al.*, 2006).

The regulation of p53 stability is further influenced by deubiquitinating enzymes. HAUSP (Herpes virus associated ubiquitin-specific protease) was identified as a novel p53-interacting protein and was shown to deubiquitinate p53, leading to p53 stabilisation and p53-dependent growth suppression (Li *et al.*, 2002). However, HAUSP can also mediate deubiquitination and stabilisation of MDM2 (Li *et al.*, 2004). This modification was recently shown to be influenced by an additional protein, DAXX (death domain-associated protein), which forms a complex with MDM2 and HAUSP, preventing auto-ubiquitination of MDM2 and promoting p53 degradation (Tang *et al.*, 2006b). This further illustrates the intricate and dynamic interactions regulating p53 protein levels.

MDM2 is considered the major p53 E3 ligase. However, other E3 ligases including Pirh2 (Leng *et al.*, 2003), COP-1 (Dornan *et al.*, 2004), CHIP (Esser *et al.*, 2005), and MULE/ARF-BP1 (Chen *et al.*, 2005), can also promote the degradation of p53 under varying conditions. The extent of p53 E3 ligase redundancy, confirms

the importance of tightly regulating p53 stability and function, in regard to cell fitness and survival.

1.2.4.3 Post-translational modifications

Active p53 is subject to a complex and diverse array of covalent post-translational modifications including phosphorylation of serines and/or threonines and acetylation, methylation, ubiquitination, neddylation, and sumoylation of lysines. A series of modifications concurrent on the p53 protein may work in concert to orchestrate a particular cellular response, which are themselves dependent on cell-type and the nature of the cellular stress, further highlighting the complexity of regulating the p53 protein.

1.2.4.3.1 Phosphorylation

In unstressed normal human fibroblast cells, phosphorylation of p53 during cell-cycle progression is transient. During G1 p53 is phosphorylated at serines -9, -15, -20, and -372, whereas phosphorylation at serines -37 and -392 peaks during G2/M. Serine-37 is the only site phosphorylated during S-phase (Bushman *et al.*, 2000). This study illustrates that phosphorylation of p53 is dynamic and transient, which may be predictable under controlled conditions.

In response to stress, phosphorylation of p53 occurs on numerous sites including serines -6, -9, -15, -20, -33, -37, -46, and threonines -18 and -81 in the N-terminal region, serines -315 and -392 in the C-terminal region, and threonines -150,

-155, and serine -149 in the DNA-binding domain. These phosphorylation events are mediated by many different protein kinases that respond to different stresses including, ATM, ATR, CHK1, CHK2, JNK and p38. Significant redundancies are observed in that the same p53 site is often phosphorylated by different protein kinases (Appella & Anderson, 2001; Bode & Dong, 2004).

Generally, phosphorylation of p53 is associated with protein stabilisation and transcriptional activation (Hupp & Lane, 1994; Craig *et al.*, 1999). Due to the magnitude of p53 post-translational modifications, it has been proposed that a distinctive combination of phosphorylated residues may be required for additional modifications, leading to maximal activation of p53 (Bode & Dong, 2004). For example, phosphorylation of p53 at serine-15 occurs rapidly in response to DNA damage and prepares the protein for subsequent modifications, including phosphorylation at threonine-18 and serine-20 by additional kinases (Saito *et al.*, 2003b). Phosphorylations at serine-15, threonine-18 and serine-20 stimulate the recruitment of transcriptional co-activators such as p300/CBP, and enhance p53 transcriptional activity (Saito *et al.*, 2003b). Similarly, phosphorylation of p53 at serine-33, threonine-81, and serine-315 promotes its interaction with the propyl isomerase, PIN1. PIN1 mediates a conformational change in p53 and augments p53 activity (Zheng *et al.*, 2002; Zacchi *et al.*, 2002).

1.2.4.3.2 Lysine modification

The p53 protein is mainly degraded via the ubiquitination pathway in which MDM2 is the E3 ubiquitin ligase. Six residues at the C-terminus of p53 are implicated as

sites for ubiquitination by MDM2 including lysines -370, -372, -373, -381, -382, and -386 (Rodriguez *et al.*, 2000). These lysines can also be modified by acetylation, methylation, sumoylation and neddylation, effecting the p53-MDM2 interaction and p53 protein stability.

p300/CBP serves as a co-activator for p53 by mediating histone acetylation. Interestingly p300/CBP can also directly acetylate p53 at lysine -372, -373, -381, -382, and contribute to p53 stabilisation by blocking MDM2-mediated ubiquitination of p53 at these sites (Gu & Roeder, 1997). Acetylation of these residues also activates and enhances the specific DNA-binding activity of p53 (Gu & Roeder, 1997). Subsequent studies have shown that p53 conformation is altered by the C-terminal acetylation, and leads to increased DNA binding activity (Friedler *et al.*, 2005). Methylation of p53 at lysine-372 by the methyltransferase, SET9, also stabilises p53 in the nucleus and enhances p53 transcriptional activity (Chuikov *et al.*, 2004).

The ubiquitin-like proteins, NEDD8 and SUMO-1 can also be conjugated to p53 and modify its function. Interestingly, MDM2 can function as an E3 ligase for NEDD8 and promote neddylation of p53 at lysines -370, -372, and -373 (Xirodimas *et al.*, 2004). The lysine residues modified by neddylation are also targeted by ubiquitination. Neddylation of p53 corresponds to a decrease in the general transcriptional activity of p53 (Xirodimas *et al.*, 2004). However it has not yet been determined whether neddylation competes with acetylation to enhance ubiquitination and p53 degradation. In contrast, sumoylation of p53 at lysine-386 has been shown to stimulate p53 activity, independent of p53 ubiquitination, by an undetermined mechanism (Gostissa *et al.*, 1999).

1.2.4.3.3 Current controversy

The classical notion that a complex network of post-translational modifications of p53 is important in generating a functional protein is currently under threat. Recent studies indicate that post-translational modifications of p53 only play a minor role in tumour development and are not required for p53 activation.

To address the importance of phosphorylation in stabilisation of p53 protein levels, a series of known stress-induced phosphorylation sites on p53 were mutated, and these mutant forms could still be stabilised (Blattner *et al.*, 1999). Mutation of the thirty C-terminal amino acids of p53, a region predicted to be required for interaction with p300, also failed to prevent damage-induced stabilisation of p53 (Blattner *et al.*, 1999). A mouse model was generated harbouring a mutation at serine-18 (equivalent to serine-15 in humans) to alanine (*S18A*). Homozygous *S18A* mice developed normally and were not tumour prone. Similarly, MEFs derived from these mice did not have defective p53 protein stability, proliferation rate, G1 arrest function after DNA-damage, and suppression of cell immortalisation, suggesting that wild-type p53 function is independent of phosphorylation of serine-15 (Sluss *et al.*, 2004). Further evidence indicating that post-translational modification of p53 is not required for p53 stabilisation and activation was illustrated by using small molecule inhibitors of the p53-MDM2 interaction, called Nutlins. Treatment of cells with Nutlin-1 showed p53 accumulation, followed by an increase in levels of both p21 and MDM2 consistent with activation of the p53 pathway (Vassilev *et al.*, 2004). However in contrast to DNA damage, Nutlin treatment did not induce phosphorylation of p53, but the unphosphorylated form of p53 was equally efficient

at sequence specific DNA-binding and the induction of apoptosis (Thompson *et al.*, 2004).

In addition the importance of C-terminal ubiquitination and acetylation of p53, in regard to protein stabilisation and activation, has also been addressed using mouse models (Krummel *et al.*, 2005). Mice were generated containing mutations of p53 at seven lysines in the C-terminal regulatory domain (lysines -367, -369, -370, -378, -379, -383, and -384 of mouse p53). The mutant mice were viable, and phenotypically normal compared to wild-type mice. Equivalent p53 protein levels of the mutant were observed as compared to wild-type under normal and stressful conditions. The mutant mice also had apoptotic rates comparable to wild-type mice following exposure to ionising radiation or adriamycin (Krummel *et al.*, 2005). These results suggest that the lysine residues in the C-terminal region of p53 are not essential for p53 function and question the importance of ubiquitination and acetylation in the regulation of p53.

However regulation of p53 is likely to consist of a series of modifications that work in concert to achieve a particular functional endpoint, and the effect of an individual modification may be modest. Regulation of p53 is likely to be redundant, for example neddylation or sumoylation of p53 may operate as redundant system for ubiquitination-mediated degradation of p53. Similarly, phosphorylation of p53 at serine-20 may compensate for loss of phosphorylation of p53 at serine-15. Further investigation of p53 regulation will undoubtedly reveal the extent of involvement of post-translational modifications. However it is unlikely and energetically unfavourable that the cell would instigate dynamic post-translational modifications of p53 without functional consequence.

1.2.4.4 Subcellular localisation

The localisation of p53 to the nucleus is essential for its function as a transcription factor (Ginsburg *et al.*, 1991) and as such both the nuclear import and export of p53 are tightly regulated. MDM2 can promote nuclear export of p53 in an ubiquitin-dependent manner (Lohrum *et al.*, 2001). MDM2 does not directly shuttle p53 out of the nucleus, rather monoubiquitination of p53 by MDM2 leads to an unmasking of the nuclear export sequence within the C-terminus of p53 (Gu *et al.*, 2001). Two other ubiquitin ligases also promote cytoplasmic localisation of p53, Cullin 7 (Andrews *et al.*, 2006) and WWP1 (Laine & Ronai, 2007). Neither target p53 for degradation but both promote accumulation of transcriptionally inactive p53 in the cytoplasm.

A novel cytoplasmic protein, PARC (p53-associated, Parkin-like cytoplasmic protein) directly interacts with p53, and serves as a cytoplasmic anchor for p53 in unstressed cells (Nikolaev *et al.*, 2003). Inactivation of endogenous PARC induced p53 nuclear accumulation, while ectopically expressed PARC promoted cytoplasmic retention of p53. Significantly, examination of PARC levels in neuroblastoma cell lines revealed high expression of PARC, consistent with aberrant cytoplasmic localisation of p53 in these cell lines (Nikolaev *et al.*, 2003).

The heat shock protein HSP70 family member, MOT2 is also implicated in p53 cytoplasmic sequestration. MOT2 directly interacts with p53 and abrogates its nuclear translocation (Wadhwa *et al.*, 1999) by binding to the C-terminus of p53 and masking the p53 nuclear localisation signal (Wadhwa *et al.*, 2002). MOT2 has also been identified in p53 aggregates in the cytoplasm of neuroblastoma, glioblastoma,

and breast carcinoma cell lines that show high levels of cytoplasmic p53 (Wadhwa *et al.*, 2002). MOT2 protein has also been shown to mediate p53 mitochondrial localisation (Marchenko *et al.*, 2000).

Another regulator of p53 localisation is glycogen synthase kinase-3 β (GSK-3 β), which binds to p53 in the nucleus and promotes cytoplasmic localisation of p53 in response to ER stress. This effect is induced by phosphorylation of p53 at serine-315 and serine-376 by GSK-3 β (Qu *et al.*, 2004).

In addition to the shuttling of p53 between the nucleus and the cytoplasm, p53 can be recruited to specific sub-nuclear structures. The *PML* (promyelocytic leukaemia) gene is a tumour suppressor originally identified in acute promyelocytic leukaemia patients. PML is an essential component of sub-nuclear structures termed nuclear bodies, which serve as sites where nuclear proteins are post-translationally modified (Pearson *et al.*, 2000). Several p53 post-translational modifications, critical for its function, occur in the PML-bodies, including acetylation of p53 by p300/CBP via the formation of a trimeric p53-PML-p300/CBP complex (Pearson *et al.*, 2000; Boisvert *et al.*, 2001), and phosphorylation of p53 by CHK2 (Louria-Hayon *et al.*, 2003) and HIPK2 (Hofmann *et al.*, 2002). Furthermore, the PML protein is able to sequester MDM2 in the nucleolus, leading to p53 accumulation and activation.

1.2.5 Autoregulatory feedback loops

The regulation of p53 involves multiple autoregulatory feedback loops, where p53-inducible gene products feed back to control or modulate p53 activity. The most prominent autoregulatory feedback loop is between p53 and its major negative

regulator, MDM2. p53 induces expression of MDM2, which in turn inhibits p53 transcriptional activity and promotes p53 degradation. This feedback loop contributes to the negative regulation of p53 activity during normal growth, development, and at the end of a stress response (Lev Bar-Or *et al.*, 2000). Similarly, p53 induces expression of two additional E3 ubiquitin ligases, COP-1 (Dornan *et al.*, 2004) and PIRH-1 (Leng *et al.*, 2003), which also target p53 for proteasome-dependent degradation, resulting in lower p53 activity.

The importance of MDM2 as regulator of p53 activity is further illustrated by the observation that p53 induces the expression of proteins which either directly or indirectly regulate MDM2 including p14/19 ARF, SIAH-1, and PTEN. The p53 - p14/19 ARF feedback loop negatively regulates p53 activity, as p53 represses expression of the *p14/19 ARF* gene, therefore preventing p14/19 ARF-dependent inhibition of MDM2 and accumulation of p53 protein (Honda & Yasuda, 1999) (Figure 1.3A). In addition, the *p14/19 ARF* gene is positively regulated by β -catenin (Damalas *et al.*, 2001). Activated p53 induces expression of the ubiquitin ligase SIAH-1 (Fiucci *et al.*, 2004), which in turn degrades β -catenin, leading to a decrease in p14/19 ARF expression and consequently elevation of MDM2 activity and degradation of p53 (Iwai *et al.*, 2004) (Figure 1.3B).

In contrast, positive autoregulatory feedback loops which promote p53 activation by attenuating MDM2 activity also exist. For example, p53 induces the expression of PTEN. The PTEN protein is a dual lipid and protein phosphatase and its primary target is PIP-3. PIP-3 activates AKT kinase, which subsequently phosphorylates and activates MDM2. Therefore p53-dependent upregulation of

PTEN essentially inhibits MDM2 activation and degradation of p53 (Blanco-Aparicio *et al.*, 2007) (Figure 1.3C).

p53 autoregulatory feedback loops which do not impinge on MDM2 activity are also emerging, for example p53-mediated regulation of p53 phosphorylation. Phosphorylation of p53 at serines -33 and -46 is mediated by the p38 MAP kinase (p38 MAPK). The p38 MAPK is itself activated by phosphorylation, which can be reversed or inactivated by the WIP1 phosphatase. p53 induces expression of the *WIP1* gene, leading to inhibition of p38 MAPK and p53 phosphorylation, thereby forming a negative feedback loop to repress p53 activation (Takekawa *et al.*, 2000) (Figure 1.3D). Another negative feedback loop involves another member of the p53 family of transcription factors. This family includes p53, p63 and p73 that are related by structure and function and have evolved from a common precursor. p53 induces expression of Δ Np73, an amino-terminally truncated version of p73 which lacks the transactivation domain. The Δ Np73 protein can inhibit p53-dependent gene expression by competing for promoter binding sites of p53 target genes, therefore repressing p53 activity (Grob *et al.*, 2001; Kartasheva *et al.*, 2002) (Figure 1.3E).

The p53 response to multiple stress signals is tightly coordinated by an assortment of regulatory mechanisms. Autoregulatory feedback loops intricately manipulate p53 activity to accommodate the cell's needs. The majority of autoregulatory loops identified act through the MDM2 protein to regulate p53, however it is likely that additional p53 downstream effectors will feedback either positively or negatively to fine-tune the p53 response to various cellular stresses. One of the most well established transcriptional targets of p53 is the cyclin dependent

kinase inhibitor, p21. This thesis will explore how p21 contributes to autoregulatory control of the p53 pathway.

1.3 The p21 Cyclin Dependent Kinase Inhibitor

1.3.1 Discovery and characterisation of p21

The discovery of p21 was simultaneously described by six independent groups, exploring distinct cell pathways. Three groups identified p21 by virtue of its interaction with the cell cycle machinery including CDK2 and cyclin D, as a cyclin dependent kinase inhibitor and designated it CIP1 (CDK interacting protein 1) (Harper *et al.*, 1993), CAP20 (CDK2-associated protein-20) (Gu *et al.*, 1993), and p21 (Xiong *et al.*, 1993). p21 was identified in a screen to identify p53 target-genes, and was designated WAF1 (wild-type p53 activated fragment 1) (el-Deiry *et al.*, 1993). p21 was also identified as a protein expressed in senescent fibroblasts and termed SDI1 (senescent cell-derived inhibitor 1) (Noda *et al.*, 1994), and was similarly isolated from differentiating melanocytes and called MDA6 (melanoma differentiation antigen 6) (Jiang *et al.*, 1995).

The human *p21* gene (also referred to as *CDKN1A*) was mapped to 6p21.2 and shown to encode a 21 kDa protein (el-Deiry *et al.*, 1993) involved in cell cycle arrest, apoptosis, and promotion of differentiation and cellular senescence. However, the role of p21 is most well-defined in the p53 pathway, where p21 is a direct transcriptional target of p53, and is strongly induced by DNA damage in cells expressing wild-type p53 (el-Deiry *et al.*, 1994).

1.3.2 Structure of p21

p21 belongs to the Cip/Kip family of cyclin dependent kinase inhibitors comprising of p21, p27^{KIP1}, and p53^{KIP2}. All family members are structurally related, share significant homology in their N-terminal regions, and recognise a broad but not identical range of cyclin/CDK targets. In solution p21 is an unstructured protein possibly enabling it to adopt multiple induced conformations depending on the target protein encountered (Kriwacki *et al.*, 1996). Although the crystal structure of p21 has not been solved, there is data available for the related cyclin dependent kinase inhibitor, p27 (Russo *et al.*, 1996). Upon binding to the cyclin/CDK, the N-terminus of p27 adopts a highly ordered structure with distinct amino acid motifs interacting with the cyclin via a hydrophobic patch on the surface of the cyclin and with the CDK (Russo *et al.*, 1996). There is high degree of similarity between p21 and p27 with regard to the N-terminal region, therefore it is not unreasonable to presume that p21 can bind to and mediate inhibition of cyclin/CDK complexes in a similar manner. Subsequently, biochemical studies have revealed that p21 (Figure 1.4) interacts directly with cyclins through a conserved region near the N-terminus, at amino acids A₁₇CRRLFGP₂₄ in p21 (Chen *et al.*, 1996; Wohlschlegel *et al.*, 2001). This cyclin-binding motif is found in other cyclin/CDK interacting proteins including p27, p57, E2F1 and CDC25A (Adams *et al.*, 1996). p21 has a separate CDK binding site in the N-terminus, at amino acids F₅₃VTETP₅₈ and in conjunction with the 3₁₀ helix, at amino acids P₇₄KLYLP₇₉, contacts the CDK and blocks the ATP binding site, preventing catalytic activity (Chen *et al.*, 1996).

In contrast with the N-terminus, the C-terminus is poorly conserved amongst the CIP/KIP family of cyclin dependent kinase inhibitors, which may reflect distinct roles *in vivo*. The unique C-terminus of p21 associates with the proliferating cell nuclear antigen (PCNA), a subunit of DNA polymerase δ and can inhibit DNA replication (Warbrick *et al.*, 1995). Embedded within the PCNA binding site at amino acids 143-160, is a second cyclin-binding motif at amino acids 153-159, which is not present in p27 or p57 (Chen *et al.*, 1996). A nuclear localisation signal is also located in the C-terminus of p21 (Rodriguez-Vilarrupla *et al.*, 2002).

1.3.3 Functions of p21

p21 is a multifunctional protein and has roles in cell cycle regulation, DNA synthesis, differentiation and regulation of transcription. p21 was principally identified and characterised as a cyclin-dependent kinase inhibitor induced by the p53 tumour suppressor protein, and shown to mediate p53-dependent cell cycle arrest at the G1/S checkpoint by inhibiting the activity of cyclin/CDK2 complexes (detailed in 1.2.3.1). p21 can also be induced by multiple factors independent of p53 including growth factors (Liu *et al.*, 1996a), cytokines (Li *et al.*, 1995), glucocorticoids (Corroyer *et al.*, 1997) and retinoids (Liu *et al.*, 1996b).

Cell cycle progression can also be blocked in S phase by p21. p21 was initially identified as a component of a quaternary complex containing CDK, cyclin and PCNA (Zhang *et al.*, 1993). PCNA plays an essential role in DNA replication and different types of DNA repair including nucleotide excision repair, mismatch repair and base excision repair. Subsequent studies showed that p21 can directly bind

to PCNA via a C-terminal binding site and inhibit DNA synthesis by DNA polymerase δ (Waga *et al.*, 1994; Warbrick *et al.*, 1995). *In vitro* studies have shown that p21 exerts its effect either by inhibiting the loading of the PCNA trimeric complex onto the DNA or the loading of the polymerase δ onto the pre-assembled clamp (Podust *et al.*, 1995). However the effect of p21 on DNA repair via PCNA remains unresolved, as p21 has been demonstrated to reduce (Copper *et al.*, 1999) or to have no effect (Li *et al.*, 1994b) on PCNA-dependent DNA repair.

In contrast to the anti-proliferative functions of p21, p21 also has pro-proliferative and survival roles, as an assembly factor for cyclin D/CDK4 complexes (Cheng *et al.*, 1999). In the cytosol p21 facilitates the assembly of the cyclin D/CDK4 complexes, their subsequent translocation to the nucleus and prevention of their nuclear export (Alt *et al.*, 2002). This results in elevated levels of cyclin D/CDK4 to initiate retinoblastoma protein phosphorylation and promote cell cycle progression.

p21 is also involved in regulation of differentiation, however its effect appears to cell-type dependent. In epithelial cells expression of p21 is induced in post-mitotic cells immediately adjacent to the proliferative compartment, but is decreased in cells further along the differentiation pathway (el-Deiry *et al.*, 1995; Gartel *et al.*, 1996; Ponten *et al.*, 1995). Similarly in cultured epidermal cells at late stages of differentiation, p21 protein levels are decreased by proteasome-dependent degradation of p21 (Di Cunto *et al.*, 1998). Direct over-expression of p21 in these cell lines inhibits differentiation, and this is independent of the N-terminal region of p21 containing the cyclin binding domain (Di Cunto *et al.*, 1998). These data suggest that p21 needs to be inactivated for later stages of differentiation, and is independent

of its function as a cell cycle regulator. In contrast to epithelial cells where p21 is a negative regulator of differentiation (Di Cunto *et al.*, 1998), p21 in retinoic acid induced differentiation of acute promyelocytic leukaemia cells, appears to be a positive regulator of differentiation, where elevated p21 protein levels are associated with differentiation (Casini & Pelicci, 1999). However the mechanism of p21-dependent regulation of differentiation has yet to be resolved.

1.3.4 Regulation of p21

The role of p21 as a mediator of growth suppression and differentiation indicates that p21 protein levels are likely to be delicately balanced. p21 expression has been shown to be mainly regulated at the transcriptional level by both p53-dependent and -independent mechanisms. The p21 promoter contains five p53-binding sites at positions -4001 bp, -3764 bp, -2311 bp, and -1391 bp, and at least one of these sites is required for p53-dependent induction after DNA damage (el-Deiry *et al.*, 1995; Ocker & Schneider-Stock, 2007). Multiple alternative human p21 transcripts have also been identified and shown to be regulated by p53, although the biological significance of these transcripts is yet to be determined (Radhakrishnan *et al.*, 2006). However p21 expression in development occurs independently of p53, as expression of p21 in most tissues of mice nullizygous for *p53* is normal (Macleod *et al.*, 1995). A variety of transcription factors including STATs, E2Fs, AP2, C/EBP α , C/EBP β , BRCA1, c-MYC and MYOD, can regulate p21 transcription independently of p53 through specific *cis*-acting elements in the p21 promoter (Gartel & Tyner, 1999).

p21 protein levels are modulated post-translationally by both ubiquitin-dependent and -independent proteasome mediated degradation. p21 protein degradation has been shown to be mediated by the E3 ubiquitin ligases SCF (SKP1/Cullen/F-box protein related complex) (Bornstein et al., 2003) and APC/C (Anaphase promoting complex) (Amador et al., 2007) in a proteasome dependent manner. Although p21 is degraded by the proteasome, the requirement for ubiquitination prior to degradation remains controversial, since mutation of all lysine residues in p21 did not lead to p21 protein stabilisation (Chen *et al.*, 2004). In addition MDM2 can degrade p21 by facilitating an interaction between p21 and the 20S proteasome, independent of ubiquitination (Zhang *et al.*, 2004).

1.3.5 p21 feedback loops

p21 is primarily upregulated at the transcriptional level by several transcription factors including E2F and STAT3, and down-regulated by c-MYC. A role for p21 is emerging as a regulator of gene expression. p21 contains a nuclear localisation signal and can functionally cooperate with the transcriptional co-activator p300/CBP to enhance NF- κ B target gene expression (Perkins *et al.*, 1997). p21 can also repress transcription when fused to the Gal4 DNA binding domain (Delavaine & La Thangue, 1999). Previous studies indicate that p21 can modulate the transcriptional activity of E2F (Delavaine & La Thangue, 1999), c-MYC (Kitaura *et al.*, 2000), and STAT3 (Coqueret & Gascan, 2000) and reveal that p21 can operate within a feedback network.

The E2F family of transcription factors activate a number of genes responsible for DNA replication and S phase progression. The principal pathway through which p21 mediates G1 arrest is through indirect inhibition of E2F activity. p21 gene expression is induced by E2F-1 and E2F-3 through sequences between -119 bp and +16 bp of the p21 promoter, by a p53-independent mechanism (Gartel *et al.*, 1998; Radhakrishnan *et al.*, 2004). Subsequently p21 can cause specific repression of E2F transcriptional activity independent of RB and inhibition of cyclin/CDK activity. The p21 protein can also regulate numerous protein-protein interactions, and was similarly shown to directly associate with the E2F factor (Delavaine & La Thangue, 1999). Although p21 expression levels were not assessed in this study, it is interesting to speculate that p21 mediates its own expression via an autoregulatory feedback loop involving the E2F transcription factor.

In contrast to E2F transcription factors, c-MYC represses *p21* gene expression in a p53-independent manner (Gartel *et al.*, 2001). *c-MYC* is a proto-oncogene which is rapidly induced in cells following mitogenic stimuli, and is suggested to play an important role in the transition from quiescence to proliferation. c-MYC is a transcription factor and when complexed with MAX recognises the E-box sequence in the target genes to be transactivated. However, p21 transcription is repressed by c-MYC. This involves recruitment of c-MYC directly to the p21 promoter by the DNA-binding protein MIZ-1 (Wu *et al.*, 2003). c-MYC then actively recruits the *de novo* methyltransferase DNMT3a co-repressor to the p21 promoter (Brenner *et al.*, 2005) preventing transcriptional activation of p21. At the protein level p21 can directly bind to the N-terminus of c-MYC and abrogate the c-MYC/MAX complex, subsequently suppressing c-MYC-dependent transcription

(Kitaura *et al.*, 2000). Although it remains to be determined if p21 association with c-MYC is sufficient to alleviate c-MYC repression of p21 transcription, it would provide an additional mechanism of fine-tuning p21 protein levels to the needs of the cell.

The STAT family of transcription factors are cytoplasmic proteins that induce activation of target genes in response to stimulation by cytokines including interleukin 6, the leukaemia inhibitory factor and ciliary neurotrophic factor (Hirano, 1998). These cytokines bind to their respective receptors and activate JAK protein tyrosine kinases, followed by tyrosine phosphorylation of the receptors. This leads to activation and homo- or heterodimerisation of STAT1/3 transcription factors, translocation to the nucleus and transcriptional activation of target genes (Ihle, 1996). The *p21* gene is transcriptionally activated by STAT factors, which recognise a conserved element in the promoter of *p21* and induce p21 expression (Bellido *et al.*, 1998; Matsumura *et al.*, 1997). At the protein level p21 can directly bind to STAT3 and inhibit its transcriptional activity (Coqueret & Gascan, 2000). Therefore cytokine stimulation leads to transcriptional activation of p21 and elevated p21 protein levels, which subsequently repress STAT3 transcriptional activity and p21 expression (Coqueret & Gascan, 2000). This illustrates the operation of a classic feedback mechanism in the regulation of p21.

1.4 Objectives

The activity of the p53 tumour suppressor protein is tightly regulated by multiple mechanisms, to promote p53 function in response to cellular stress or to repress its activity after stress activation to allow normal development and cell proliferation to occur. Autoregulatory feedback loops represent an important mechanism in the regulation of p53 by coordinating the p53 response to the condition of the cell. A well-established downstream effector of the p53 pathway is the cyclin dependent kinase inhibitor, p21. A novel role for p21 is emerging as a regulator of gene expression by interacting with specific transcription factors. The overall aim of this thesis was to investigate and characterise the inter-relationship between p53 and its transcriptional target, p21.

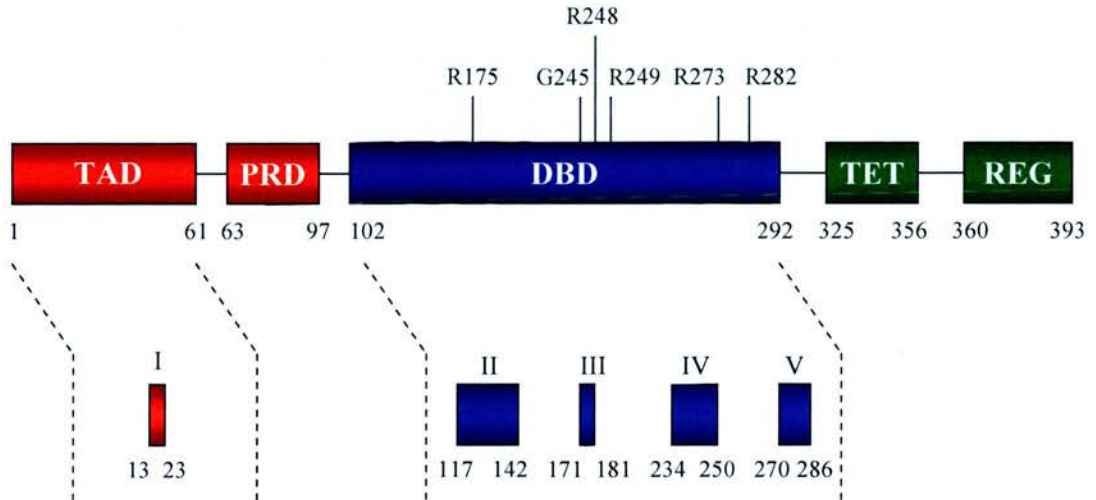


Figure 1.1 Functional domains of the human p53 tumour suppressor protein. The N-terminus (red) contains the transactivation domain (TAD) and the proline-rich domain (PRD). The central region (blue) contains the DNA-binding domain (DBD). The residues most frequently mutated in human cancer are highlighted. The C-terminus (green) contains the tetramerisation domain (TET) and the negative regulatory domain (REG). The corresponding amino acid residues are shown below each domain. The lower panel represents the highly conserved regions termed BOX-I, -II, -III, -IV, and -V with corresponding amino acids shown below each region.

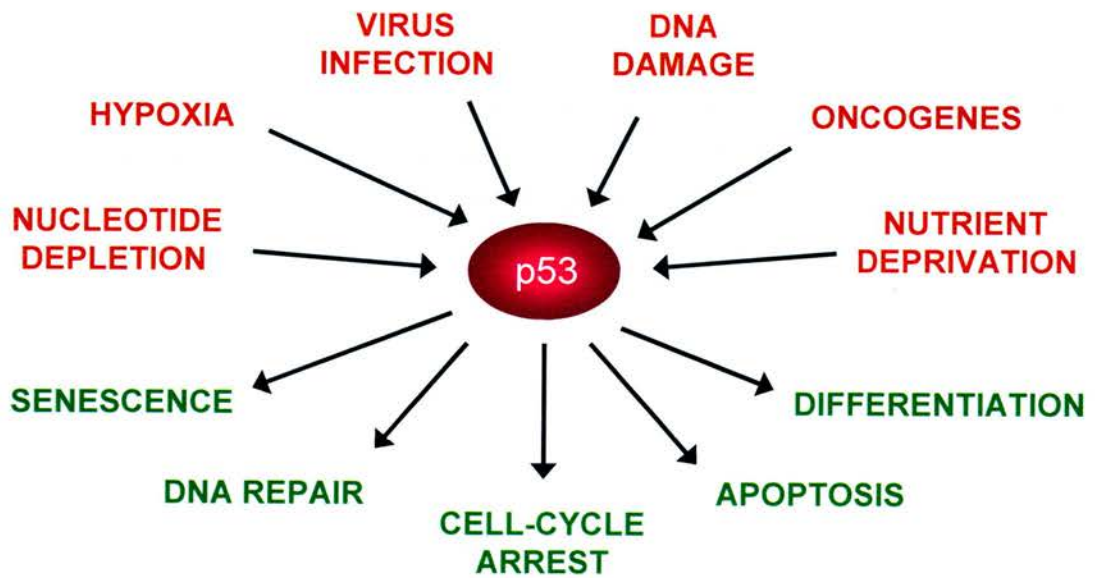


Figure 1.2 The p53 response. Various stress signals (red) induce p53 stabilisation and activation leading to an appropriate cellular response (green).

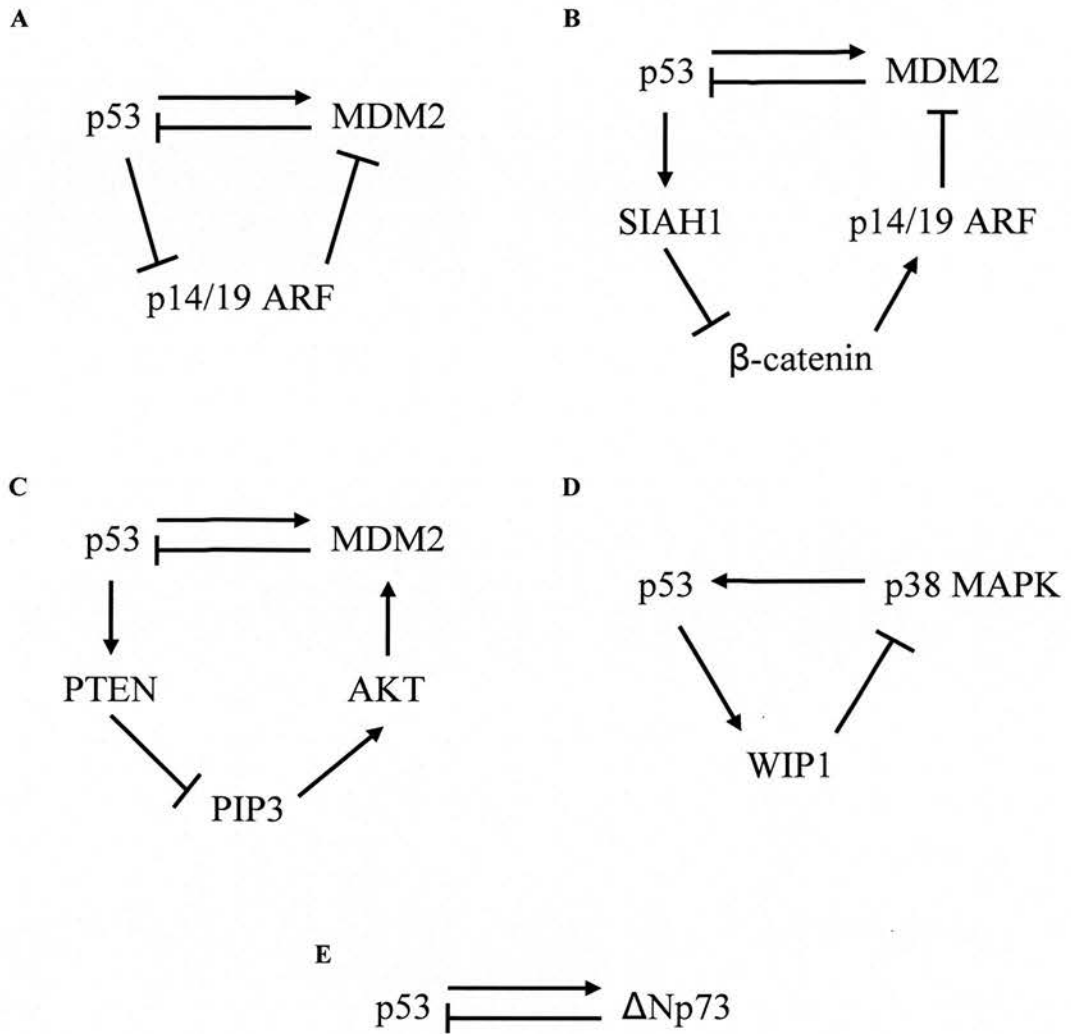


Figure 1.3 Autoregulatory feedback loops modulate p53 activity. (A) p53-MDM2-p14/19ARF loop. (B) p53-SIAH1-βcatenin-p14/19 ARF loop. (C) p53-PTEN-PIP3-AKT loop. (D) p53-WIP1-p38 MAPK loop. (E) p53-ΔNp73 loop. Arrows represent activation. T-shaped lines represent inhibition.

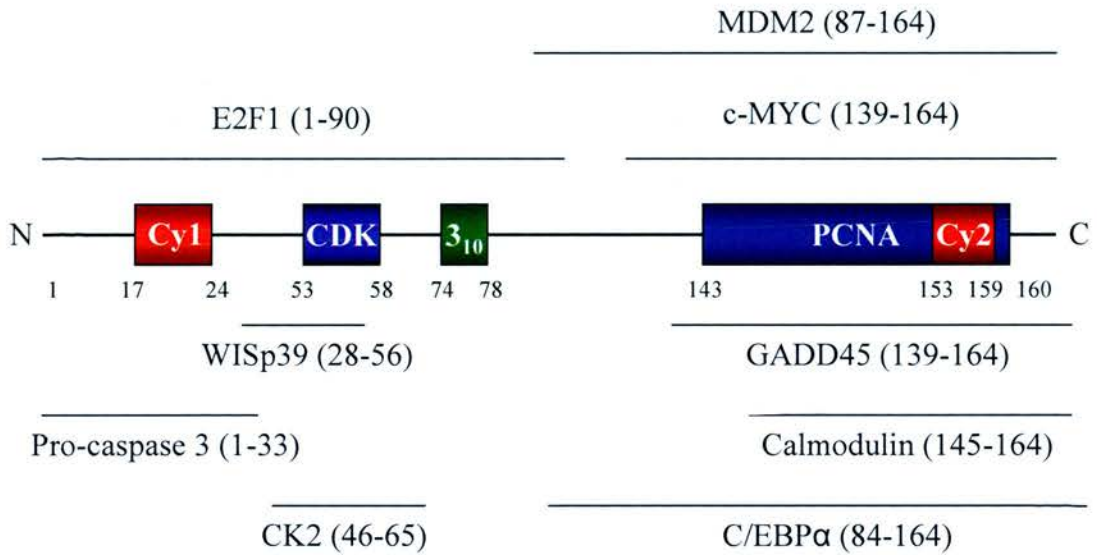


Figure 1.4 Human p21 protein and its direct protein-protein interactions. The major interaction motifs are represented in boxes; Cy1 (red) – cyclin binding site 1; CDK (purple) – cyclin-dependent kinase interaction domain; 3₁₀ (green) – 3₁₀ helix involved in CDK binding; PCNA (blue) – proliferative cell nuclear antigen binding site; Cy2 (red) – cyclin binding site 2. The corresponding amino acid residues are shown below each domain. p21 interacts with a variety of proteins, a selection are illustrated above and corresponding amino acids are shown in brackets. MDM2, E2F1 and c-MYC interactions with p21 are further discussed in the text and are shown above the map of human p21.

CHAPTER 2

MATERIALS AND METHODS

2.1 General Reagents

All chemicals and reagents were supplied by Sigma unless otherwise stated. All tissue culture reagents including foetal bovine serum (FBS), Dulbecco's modified eagle's medium (D-MEM), McCoy's 5A medium, penicillin-streptomycin solution, trypsin-EDTA solution and Lipofectamine™2000 were supplied by Invitrogen unless otherwise stated.

2.2 Equipment

Irradiation treatment of cells was carried out in a Faxitron® cabinet X-ray system, 43855D (Faxitron X-ray Corporation). A Fluroskan (Ascent FL), PowerwaveXS™ microplate reader (Bio-Tek), and an Envision fluorescence detector (Perkin Elmer) were used to read 96-well plates. RNA concentrations were measured using a NanoDrop® spectrophotometer. SDS PAGE was carried out using Biorad Protean II mini-gel system. Coomassie stained gels were dried using a gel drier (MGD-5040, VWR International). X-ray films were developed using a Mediphot 937 developer. Microarray hybridisations were carried out in a hybridisation oven (Hybridiser H8-ID, Techne). Sorvall RC-5C plus and Eppendorf 5415R were used for all centrifugations.

2.3 Antibodies

2.3.1 Primary antibodies

All primary antibodies used are detailed in Table 2.1, including the final dilution used for immunoblotting and the size of the protein bands detected.

2.3.2 Secondary antibodies

Goat Anti Mouse IgG (Pierce); Rabbit Anti Mouse IgG (DakoCytomation); Swine Anti Rabbit IgG (DakoCytomation). All secondary antibodies are conjugated to horse radish peroxidase.

2.4 Plasmids

Generally vectors used for transfection of mammalian cell lines were pcDNA3.1 (Invitrogen) including full length p21 used for transient transfection and p21 truncations (kindly provided by M. Scott). This vector contains a multiple cloning site, an ampicillin resistance gene and a strong mammalian CMV promoter upstream of the multiple cloning site. For stable transfection of p21, full length p21 was previously cloned into pIRESpuro2 vector (Clontech) (kindly provided by A. Ingram). This vector contains a puromycin resistance gene and a CMV promoter upstream of the multiple cloning site.

Target	kDa	Clonality	Supplier	Dilution
ATM (5C2)	370	Mouse Monoclonal	Abcam	1:500
Phosho-ATMser1981	370	Mouse Monoclonal	Upstate	1:500
β - actin	42	Mouse Monoclonal	Abcam	1:2000
BAX (N-20)	23	Rabbit Polyclonal	Santa Cruz	1:1000
CHK1 (G-4)	56	Mouse Monoclonal	Santa Cruz	1:1000
CHK2 (A-12)	66	Mouse Monoclonal	Santa Cruz	1:500
Phospho-CHK2thr68	66	Rabbit Polyclonal	Santa Cruz	1:500
DAPK1	160	Mouse Monoclonal	BD	1:1000
E2F-1 (C-20)	60	Rabbit Polyclonal	Santa Cruz	1:1000
GADD34	90	Goat Polyclonal	Abcam	1:500
IRF-1	48	Mouse Monoclonal	BD	1:1000
MDM2 (2A9)	90	Mouse Monoclonal	Moravian Biotechnology	1:1000
MDM2 (2A10)	90	Mouse Monoclonal	Moravian Biotechnology	1:1000
MDM2 (4B2)	90	Mouse Monoclonal	Moravian Biotechnology	1:1000
p21 (Ab-1)	21	Mouse Monoclonal	Oncogene	1:1000
p53 (DO1)	53	Mouse Monoclonal	Moravian Biotechnology	1:1000
p53 (DO12)	53	Mouse Monoclonal	Moravian Biotechnology	1:1000
p53 (19.1)	53	Mouse Monoclonal	Moravian Biotechnology	1:1000
p53 (PAb 240)	53	Mouse Monoclonal	Moravian Biotechnology	see 2.15
p53 (PAb 1620)	53	Mouse Monoclonal	Moravian Biotechnology	see 2.15
p53 (CM-1)	53	Rabbit Polyclonal	Moravian Biotechnology	see 2.15
p53 (CM-5)	53	Rabbit Polyclonal	Moravian Biotechnology	1:1000
Phospho-p53ser15	53	Mouse Monoclonal	Cell Signaling	1:1000
Phospho-p53ser15	53	Rabbit Polyclonal	Cell Signaling	1:1000

Table 2.1 Details of primary antibodies.

2.5 Sterilisation

Flame sterilisation was employed when sterile conditions were required for bacterial work. Equipment and broth were sterilised using the autoclave. All tissue culture work was carried out in a sterile laminar flow hood.

2.6 Molecular Biology Methods

2.6.1 Bacterial growth media and culture conditions

Bacterial cultures were grown in an appropriate volume of Luria Bertani (LB) media (1 % (w/v) bacto - tryptone, 0.5% (w/v) bacto – yeast extract, 1 % (w/v) NaCl, adjusted to pH 7.5) containing a selective antibiotic if required, at a final concentration of 100 µg/ml. Inoculated cultures were incubated in sterile flasks four times the culture volume to allow aeration, for ~8 hr at 37 °C with rotation at 225 rpm.

Agar plates were prepared using LB media containing 1.5 % (w/v) bacto-agar. LB agar was liquefied by heating in a microwave oven. When the agar was hand-warm it was poured into 90 mm diameter Petri dishes (Sterilin) and left to cool. If antibiotic selection was required, the antibiotic was added to the agar immediately before pouring. The culture dishes were stored at 4 °C for no longer than one month. Prior to use the plates were dried at 37 °C for 1 hr.

2.6.2 Storage of bacterial stocks

For short – term storage, bacterial colonies were stored at 4 °C, on inverted parafilm-sealed agar plates of LB medium containing the appropriate antibiotics.

For long-term storage, glycerol stocks were made of bacterial cultures. 875 µl bacterial overnight culture was added to 125 µl sterile glycerol (80 %) in a cryotube (Nunc), vortexed to mix, snap frozen in liquid nitrogen and stored at -70 °C.

2.6.3 Preparation of competent cells

An aliquot of the required bacterial stock was thawed on ice, 5 µl was added to 5 ml LB, and incubated overnight at 37 °C with rotation at 225 rpm. The overnight culture was diluted 1:200 in 100 ml LB and incubated at 37 °C for approximately 2 hr until an O.D_{600nm} of between 0.3 and 0.6 was reached. Cells were spun at 4000 g for 20 min at 4 °C, resuspended in 15 ml transformation buffer 1 (100 mM RbCl, 79 mM MnCl₂, 30 mM Potassium Acetate pH 7.5, 13.5 mM CaCl, 15 % (v/v) Glycerol, adjusted to pH 5.8) and incubated on ice for 1 hr. Cells were spun at 4000 g for 5 mins at 4 °C to produce a fluffy white pellet, which was resuspended in 4 ml transformation buffer 2 (10 mM MOPS pH 6.8, 10 mM RbCl, 13.5 mM CaCl₂, 15% (v/v) Glycerol, adjusted to pH 6.8). After incubation on ice for 15 min, the cells were aliquoted (100 µl) into sterile microcentrifuge tubes, snap frozen in liquid nitrogen and stored at -70 °C.

2.6.4 Transformation of *E.coli* competent cells with plasmid DNA

The DH5 α competent strain of *E. coli* was used to transform all recombinant plasmid DNA. The competent cells were gently thawed and the plasmid DNA was added (up to 40 ng). The tube was gently tapped and left on ice for 30 min. The cells were then heat shocked at 42 °C for 90 sec, replaced on ice for 2 min, 500 μ l LB medium was then added, and shaken at 37 °C for 1 hr. The resulting suspension was spread to dryness on selective agar plates and incubated at 37 °C for 16 hr.

2.6.5 Amplification of plasmid DNA

A single colony of transformed bacteria was picked and used to inoculate a starter culture of 5 ml LB containing selective antibiotic at a final concentration of 100 μ g/ml. The culture was incubated at 37 °C at 225 rpm for 4-8 hr in a 15 ml sterile tube.

2.6.6 Purification of plasmid DNA

Plasmid DNA was isolated using Qiagen[®] plasmid DNA Mini and Maxi Kits. For a Mini prep (Qiagen) the starter culture was used directly. For a Maxi prep (Qiagen) the starter culture was diluted 1:500 into selective LB media (250 ml, overnight). The cells were harvested by centrifugation and plasmid DNA purified according to the manufacturer's instructions. The Mini prep yields 5-10 μ g of DNA depending on plasmid copy number. The Maxi prep yields up to 500 μ g of DNA depending on the

plasmid copy number. Plasmid DNA was resuspended in nuclease-free dH₂O and stored at -20 °C.

2.6.7 Quantification of DNA Concentration

The concentration of plasmid DNA was determined by spectrophotometry at 260 nm using the PowerwaveXS™ Microplate Spectrophotometer (Bio-Tek). Plasmid DNA was diluted 1:100 and 100 µl volumes were added to wells of a 96-well UV-Star™ Plate (Greiner), using 100 µl dH₂O as a blank control. DNA concentrations were calculated based on the observation that 50 µg/ml DNA gives an OD_{260nm} of 1.

2.6.8 Agarose gel electrophoresis

Plasmid DNA was resolved and analysed by agarose gel electrophoresis. Agarose gels were prepared by adding agarose to TAE buffer (0.4 M Tris-HCl pH 8.0, 0.2 M Sodium Acetate, 0.02 M EDTA pH 8.0) to a final concentration of 1 % and heating until dissolved. The solution was cooled to 55 °C and ethidium bromide was added to a final concentration of 0.5 µg/ml. The gel was then poured into a casting mould and allowed to set at room temperature. Prior to loading onto the gel DNA samples were diluted 1:4 into DNA sample loading buffer (40 % (v/v) Glycerol, 50 mM EDTA, 0.1 % (w/v) Bromophenol Blue). The gel was then immersed in TAE buffer and DNA samples were subjected to electrophoresis at 100V for 1 hr before visualising plasmid DNA bands under a UV transilluminator.

2.7 Cell Culture

2.7.1 Human cell lines

All human cell lines were maintained in a humidified incubator (Hera) at 37 °C.

Cell Line	Source	Medium	% CO ₂	p53 Status
A375	Melanoma	D-MEM	5	Wild Type
HCT116 WT	Colorectal carcinoma	McCoy's 5A	10	Wild Type
HCT116 p21 ^{-/-}	Colorectal carcinoma	McCoy's 5A	10	Wild Type
HCT116 p53 ^{-/-}	Colorectal carcinoma	McCoy's 5A	10	Inactive
NHF	Normal fibroblast	HepesBSS	10	Wild Type

Table 2.2 Human cell lines and culture conditions

The isogenic cell panel HCT116 WT, p21^{-/-} and p53^{-/-} was a kind gift from B. Vogelstein (John Hopkins University).

2.7.1.1 Cell maintenance

2.7.1.1.1 Subculturing

Cells were maintained in sterile 10 cm diameter culture dishes. When cells were confluent the medium was discarded, and cells washed with sterile PBS (10 ml /10

cm culture dish), followed by the addition of trypsin-EDTA solution (1 ml/ 10 cm culture dish). The cells were incubated at 37 °C for 5 – 10 min until the cells start to detach from the culture dish. Trypsinised cells were then diluted 10-fold with fresh medium and seeded into fresh plates with fresh medium at the desired cell density. Cells were counted using a haemocytometer.

2.7.1.1.2 Cell storage and recovery

For long-term storage, cells were kept in liquid nitrogen. To prepare cells for storage, 80 % confluent cells were trypsinised and collected by centrifugation at 200 g for 5 min. The supernatant was discarded and the cell pellet from a 10 cm diameter culture dish was gently resuspended in 3 ml freezing media (50% (v/v) Tissue culture media (depending on cell line), 40 % (v/v) FBS, 10% (v/v) DMSO), and transferred to cryotubes (Nunc) at 1 ml/ tube. The cells were frozen slowly in Nalgene™ Cryo 1 °C freezing containers overnight at -70 °C and then transferred to liquid nitrogen.

To recover the cells from frozen stock, one tube was rapidly thawed at 37 °C, resuspended in 10 ml fresh medium and cells were collected by centrifugation at 200 g for 5 min to remove DMSO. The cell pellet was resuspended in fresh medium and transferred to a culture dish. The medium was changed the following day and the cells were left to grow until confluent before subculturing.

2.7.2 Harvesting adherent cells

All human cell lines used are adherent cells. To harvest, cells were washed on ice with chilled PBS, scraped in 1 ml ice-cold PBS and sedimented by centrifugation at 1000 g for 3 min at 4 °C. Supernatant was discarded and cell pellets were snap frozen in liquid nitrogen and stored at -70 °C.

2.7.3 Mouse cells

p21 homozygous (*Cdkn1a* *-/-*) heterozygous (*Cdkn1a* *+/-*) and wild type (*Cdkn1a* *+/+*) mice were a kind gift from B. Wardlaw (Roslin Institute, Midlothian UK). The homozygous mice mating system was purchased from The Jackson Laboratory, JAX[®] Mice strain name: B6; 129S2-*Cdkn1a*^{*tm1Tyj*}/J.

2.7.3.1 Extraction of B-cells from mouse spleen

The isolation of B cells from mice spleens was achieved using the QuadroMACS[™] separation system (Miltenyi Biotec). This involves magnetically labelling the biological material of interest with MACS[®] Microbeads and passing the material through a MACS[®] separation column which is placed in the strong permanent magnet of the QuadroMACS[™] separation unit. The magnetically labelled material is maintained in the column and separated from the unlabelled material. Removal of the column from the magnetic field allows the retained fraction to be eluted.

Spleens were removed from mice and stored at 4 °C in IMDM media (Invitrogen) supplemented with 5 % FCS and 50 µM 2-mercaptoethanol, until processed. Each spleen was macerated with a fine syringe needle and cells were flushed out by repeatedly injecting media into the spleen. Generally, $\sim 1 \times 10^8$ cells per spleen were obtained. Cells were centrifuged at 300 g for 10 min at 4 °C. The cell pellet was resuspended in 900 µl separation buffer (2 mM EDTA, 0.5 % BSA in PBS pH 7.2) and 100 µl CD45R mouse MACS[®] Microbeads (Miltenyi Biotec), and incubated for 15 min at 4 °C. The CD45R antigen is expressed on B lymphocytes throughout their development and is commonly used as a pan-specific B cell marker. Therefore the microbeads should magnetically label only CD45R+ cells allowing magnetic cell sorting. Cells were washed with 10 ml separation buffer and resuspended in 500 µl separation buffer. A MACS[®] LS separation column (Miltenyi Biotec) was placed in the QuadroMACS[™] separation unit (Miltenyi Biotec) and washed with 3 ml separation buffer. The cell suspension was applied to the column and the column was washed three times with 3 ml separation buffer. The column was then removed from the magnetic field and B-cells were flushed out with 5 ml separation buffer into a clean falcon tube. Cells were collected by centrifugation at 200 g for 5 min at room temperature, resuspended in culture media and seeded at a cell density of 0.5×10^6 cells/ml. Cells were treated (see 2.8) 24 hr after seeding.

2.7.3.2 Harvesting suspension cells

Mouse B-cells are suspension cells. To harvest, all cells were transferred to a 15 ml falcon tube and spun at 1000 g for 5 min at 4 °C. The cell pellet was washed in 1 ml

ice-cold PBS and transferred to a microcentrifuge tube. The cell pellet was collected by centrifugation at 2,300 g for 5 min at 4 °C. Cell pellets were snap frozen in liquid nitrogen and stored at -70 °C.

2.8 Manipulation of Mammalian Cells

2.8.1 Transient transfection

Cells were seeded into 6 cm diameter culture dishes at a density of 8×10^5 cells/ml and grown for 24 hr. The liposome-mediate method of transfection was carried out using Lipofectamine™2000 (Invitrogen) based on the manufacturer's recommendations. The quantity of DNA transfected is indicated in each experiment and the amount of DNA normalised with empty vector DNA (pcDNA3.1, Invitrogen) as required. Generally, 5 µl Lipofectamine™2000 was added to 200 µl serum-free medium and incubated for 5 min at room temperature. Plasmid DNA was similarly diluted in 200 µl serum-free medium. The diluted Lipofectamine™2000 was then added to the diluted DNA and incubated for 20 min at room temperature to allow DNA/ Lipofectamine™2000 complexes to form. The resulting mixture was then added to each plate, and cells were incubated for a further 24 or 48 hr before harvesting (2.7.2) and analysis.

2.8.2 Stable transfection

Cells were seeded into 10 cm diameter culture dishes at a low cell density of 1×10^6 cells/ml and grown for 24 hr. Cells were transfected with $1\mu\text{g}$ of DNA as described in 2.8.1. In the construction of the p21 stable cell lines, HCT116 p21^{-/-} cells were transfected with pIRESpuro2 vector (Clontech) expressing full length p21 and puromycin-N-acetyl-transferase. After 24 hr incubation at 37 °C, cells containing the plasmid were selected for by the addition of puromycin (Calbiochem). Fresh medium containing 5 $\mu\text{g}/\text{ml}$ puromycin was added after a majority of cells died. Individual colonies were grown up and picked using small squares of sterile blotting paper (2 mm x 2mm) soaked in trypsin to detach individual colonies, and each clone was transferred to an individual well of a 24 well plate. Clones were expanded under selection conditions. To confirm that the cells were expressing p21, immunoblotting was carried out.

2.8.3 RNA interference mediated gene knockdown

Small interfering RNA (siRNA) mediated gene knock-down was achieved by transfecting siRNAs (Dharmacon) into cells using Lipofectamine™2000 (Invitrogen) in accordance with the manufacturer's recommendations (as previously detailed in section 2.8.1). p21 siRNA, MDM2 siRNA and control siRNA (*SMART*pool™ Dharmacon) were used at a final concentration of 33 nM. After transfection cells were incubated at 37 °C in 5 % CO₂ for 24 – 48 hr, harvested and analysed by immunoblotting.

2.8.4 Gene reporter assays

2.8.4.1 Cell transfection and lysis

Cells were seeded into 6-well plates, and incubated until ~70 % confluency was obtained before being transfected with 1 μg pGL3p21-Luc and 1 μg pCMV β -Gal DNA (as previously detailed in 2.8.1). Cells were incubated for 24 hr at 37 °C. Cells were then treated and lysed at stated time points. To lyse, cells were washed twice in ice-cold PBS and lysed in 70 μl 5x Reporter Lysis Buffer (Promega) on ice for 10 min. The cells were scraped and spun at 15,000 g for 2 min at 4 °C. The supernatant was transferred to a fresh microcentrifuge tube and snap frozen in liquid nitrogen.

2.8.4.2 Luciferase assay

For the Luciferase assay, the lysates (20 μl) from 2.8.4.1 were aliquoted into a white Microlite2TM 96-well ELISA plate (CoStar; Corning Inc.) on ice. 50 μl of Luciferase SubstrateTM from the Luciferase Assay SystemsTM (Promega) kit was added to each well of the Microlite2 plate, and allowed to reach room temperature. Luciferase activity was quantified using a luminometer (Fluoroskan Ascent FL).

2.8.4.3 β -Galactosidase assay

For the β -Galactosidase assay, the lysates (20 μl) from 2.8.4.1 were aliquoted into a clear 96-well plate at room temperature, and 20 μl of β -Galactosidase 2x assay buffer

(Promega) was added and incubated for 20 min at 37 °C. β -Galactosidase activity was quantified using a PowerwaveXSTM Microplate Spectrophotometer (Bio-Tek) at a wavelength of 405 nm. The results were normalised to account for variation in transfection efficiency, by dividing the Luciferase readout by the β -galactosidase readout to give relative light units.

2.8.5 Genotoxic or drug treatment of mammalian cells

Cells were grown to 70 % confluency before treating with indicated drug or stress. If cells were incubated for longer than 24 hr, culture medium was replenished 24 hr prior to treatment to ensure mitogen levels were consistently high. Following treatments cells were cultured for the indicated time and harvested as described in 2.7.2.

2.8.5.1 IR treatment

Cells were irradiated in culture medium using a Faxitron[®] cabinet X-ray system, 43855D (Faxitron X-ray Corporation), at a central dose rate of 2 Gy/min. Cells were irradiated at the stated doses and harvested at the stated time points.

2.8.5.2 Treatment with inhibitors

Table 2.3 details the inhibitors used. The stated concentration of drug, or solvent only (vehicle control), was added to cells in culture medium, and cells were harvested at the stated time points.

Drug	Target	Solvent	Stock Conc	Final Conc
KU-55933	ATM	DMSO	10 mM	10 μ M
NU-7441	DNAPK	DMSO	10 mM	1 μ M
Wortmannin	PIKK family	DMSO	20 mM	10 μ M
Nutlin-3	MDM2	DMSO	45 mM	10 μ M

Table 2.3 Details of Inhibitors of Cellular Targets

2.8.5.3 Cyclohexamide treatment

Cyclohexamide is an antibiotic produced by *Streptomyces griseus*, and in eukaryotic cells it causes inhibition of protein synthesis leading to cell growth arrest and cell death. Cyclohexamide was used to determine the half-life of short lived proteins. Cyclohexamide was dissolved in DMSO at a stock concentration of 100 mg/ml and added directly into the culture media at a final concentration of 30 μ g/ml. Cells were harvested at 0 hr, 0.5 hr, 1 hr, 2 hr, 4 hr after treatment.

2.8.5.4 Poly(I).poly(C) treatment

Polyinosinic polycytidylic acid (poly(I).poly(C)) (Sigma) was dissolved in 0.5 M Hepes pH 7.5 at a stock concentration of 25 mg/ml. The stated concentration was added to cells in culture medium, and cells were harvested at the stated time points.

2.9 Recovery and Detection of Protein

2.9.1 Urea lysis

All manipulations were performed on ice. Twice the pellet volume of chilled urea lysis buffer (7 M urea, 0.1 M DTT, 0.05 % Triton X-100, 25 mM NaCl, 20 mM Hepes pH 7.5) was added to the frozen cell pellet, and cells were agitated by pipetting until no solid particles could be observed, then incubated on ice for 30 min. Extracts were clarified by centrifugation at 10,000 g for 10 min at 4 °C. The supernatant was snap frozen in liquid nitrogen and stored at -70 °C. Protein concentration of the lysates was determined by Bradford Assay (2.9.3).

2.9.2 Protein precipitation

Trichloroacetic acid (TCA) was used to precipitate protein and concentrate protein samples using the following method. 2 % deoxycholate (DOC) was added to the samples to a final concentration of 0.02 % and incubated at room temperature for 15 min. 24 % TCA was added to a final concentration of 8 % and incubated on ice for 1

hr. The precipitated proteins were pelleted by centrifugation at 13,000 *g* for 10 min at 4 °C. The supernatant was removed and the pellet washed with 200 µl ice cold acetone to remove residual TCA. The protein pellet was air dried for 1 – 2 min before resuspending in either urea lysis buffer or 4 x SDS sample buffer (4 % SDS, 250 mM Tris-HCl pH 6.8, 10 mM EDTA, 0.2 M DTT, 1% Bromophenol blue).

2.9.3 Bradford assay

Biorad protein assay dye reagent concentrate was diluted 1 in 5 in distilled water. 1 µl diluted protein sample was added to 200 µl of this solution in a clear 96-well plate and mixed. The absorbance at 595 nm was measured and the protein concentration was determined from a standard curve generated from known concentrations of BSA.

2.9.4 SDS polyacrylamide gel electrophoresis (SDS PAGE)

Proteins were resolved on the basis of their molecular weight by SDS PAGE. Different percentage acrylamide gels were poured according to the size of the protein of interest, for example 6% acrylamide gels were used for high molecular weight proteins (ATM - 370 kDa) and 15% acrylamide gels were used for low molecular weight proteins (p21 – 21 kDa). The polyacrylamide gels were prepared and assembled using Biorad Protean II mini-gel system. The resolving gel (6 - 15 % Acrylamide, 390 mM Tris-HCl pH 8.8, 0.1 % SDS, 0.1 % Ammonium peroxidisulphate, polymerisation was initiated by adding 0.08 % TEMED) was overlaid with 80 % isopropanol_(aq) to remove air bubbles, and allowed to set at room

temperature. The isopropanol was removed and the stacking gel (5 % Acrylamide, 123 mM Tris-HCl pH 6.8, 0.1 % SDS, 0.1 % Ammonium peroxodisulphate, 0.1 % TEMED) was applied, 10- or 15- well loading combs were inserted and the gel was allowed to set at room temperature. Gels were immersed in SDS-PAGE Running Buffer (192 mM Glycine, 25 mM Tris, 0.1 % (w/v) SDS) prior to protein sample loading.

Protein samples were prepared by adding an appropriate volume of 4 x SDS sample buffer to cell lysates. Prior to loading all samples were heated to 95 °C for 3 min to denature the proteins. Protein samples were loaded into wells in the stacking gel and subjected to electrophoresis at 180 V until the dye front had run from bottom of the resolving gel. A low or high molecular weight pre-stained marker (4 µl, Biorad) was also added to gauge size of the protein bands. Resolved proteins were visualised by immunoblotting (2.9.5) or coomassie staining (2.9.6).

2.9.5 Immunoblotting

Proteins resolved by SDS-PAGE were transferred onto Hybond-C nitrocellulose membrane (Amersham Pharmacia Biotech) in transfer buffer (192 mM Glycine, 25 mM Tris, 20 % (v/v) Methanol) at either 300 mA for 1 hr or 30 mA overnight. Nitrocellulose membranes were ink stained (0.4 % ink (Pelikan) /PBS) to ensure equal loading. Non-specific antibody binding was blocked by incubating membranes in 5 % milk/ 1 % β-glycerophosphate/ PBST for 1 hr at room temperature. β-glycerophosphate is a serine/threonine phosphatase inhibitor and is critical for the retention of p53 serine-15 phosphorylation. Membranes were probed with primary

antibody (see Table 1.1 for working concentration) for 3 hr at room temperature or overnight at 4 °C. Membranes were washed once in PBST. Specific antibody binding was detected by incubating membranes for 1 hr at room temperature with a secondary horseradish peroxidase (HRP) conjugated antibody diluted 1:1000 in 5 % milk/ 1% β -glycerophosphate/ PBST. Following three 15 min washes in PBST, membranes were treated with ECL chemiluminescent detection system (2 ml /blot, 1:1 ratio ECL I : ECL II) and protein bands were visualized by exposure to X-ray film (Kodak).

2.9.6 Coomassie staining

Following SDS-PAGE, resolved proteins were coomassie stained. Protein staining of polyacrylamide gels was achieved by a 30 min incubation with Coomassie blue solution (45 % Methanol, 10 % Acetic acid, 0.1 % w/v Coomassie Blue R250) . Gels were destained by incubating with destain 1 (5 % (v/v) Methanol, 7 % (v/v) Acetic acid) until bands became visible and background staining was removed. For rapid destaining, destain 2 (50 % (v/v) Methanol, 10 % (v/v) Acetic acid) was used. Gels were dried onto 3 mm chromatography paper (Whatman[®], Schleicher & Schuell Biosciences) using a gel drier (MGD-5040, VWR International).

2.10 Subcellular Proteome Extraction

The ProteoExtract[®] Subcellular Proteome Extraction Kit (Calbiochem[®]), here after referred to as S-PEK, was used to extract proteins from mammalian cells according

to their subcellular localisation. The kit was used in accordance with the manufacturer's recommendations. All extraction buffers contain protease inhibitors and all steps were carried out at 4 °C unless stated. All fractions were stored at -70 °C and analysed by immunoblotting (see 2.9.5).

2.10.1 Adherent cells

For adherent tissue culture cells including HCT116 and NHF, cells were treated at 70 % confluency. Growth medium was carefully removed and cells were washed twice with 2 ml ice cold Wash Buffer for 5 min. Next 1 ml Extraction Buffer 1 was added to the cell monolayer and incubated for 10 min with gentle agitation. Extraction Buffer 1 was removed from the cell monolayer and transferred to a microcentrifuge tube and labelled fraction 1 (F1). Similarly, 1 ml Extraction Buffer 2 was added to the cell monolayer and incubated for 30 min with gentle agitation. This fraction was removed and transferred to a microcentrifuge tube and labelled fraction 2 (F2). 500 µl Extraction Buffer 3 containing Benzonase[®] nuclease, was added to the cell monolayer and incubated for 10 min with gentle agitation. Extraction Buffer 3 was transferred to a microcentrifuge tube and labelled fraction 3 (F3). Finally, 500 µl Extraction Buffer 4 was added to the cell monolayer at room temperature. All residual cell structures were solubilised. The resulting extract was transferred to a microcentrifuge tube and labelled fraction 4 (F4).

2.10.2 Suspension cells

For suspension cells including mice B-cells, cells were seeded at 4×10^6 cells in 10 cm plates. Cells were pelleted by centrifugation at 300 g for 10 min. The pellet was then washed twice with 2 ml cold Wash Buffer for 5 min with gentle agitation provided by a rotary shaker. 1 ml Extraction Buffer 1 was added to the cell pellet. The pellet was resuspended by gently flicking the tube and then incubated for 10 min with gentle agitation. Insoluble material was then pelleted by centrifugation at 1000 g for 10 min. The resulting supernatant was transferred to a microcentrifuge tube and labelled fraction 1 (F1). Similarly, 1 ml Extraction Buffer 2 was added to the cell pellet. The pellet was resuspended by gently flicking the tube and then incubated for 30 min with gentle agitation. Insoluble material was then pelleted by centrifugation at 6000 g for 10 min. The soluble fraction was transferred to a microcentrifuge tube and labelled fraction 2 (F2). Next, 500 μ l Extraction Buffer 3 containing Benzonase[®] nuclease and added to the cell pellet. The pellet was resuspended by pipetting up and down, and then incubated for 10 min with gentle agitation. Insoluble material was then pelleted by centrifugation at 6800 g for 10 min. The resulting supernatant was transferred to a microcentrifuge tube and labelled fraction 3 (F3). Finally, 500 μ l Extraction Buffer 4 was added to the cell pellet at room temperature. All residual particles were resuspended by pipetting up and down. The resulting extract was transferred to a clean tube and labelled fraction 4 (F4).

2.11 Cell Fractionation and Nuclease Digestion

Cells were also fractionated by the method of Gilbert & Allan (2001). 5×10^6 cells were seeded in 15 cm diameter culture dishes and grown until 80 % confluent. Cells were trypsinised and the cell pellet resuspended in 5 ml NBA (85 mM KCl, 5.5 % (w/v) sucrose, 10 mM Tris-HCl pH 7.5, 0.2 mM EDTA, 0.5 mM spermidine, 250 μ M PMSF). An equal amount of NBB (85 mM KCl, 5.5 % (w/v) sucrose, 10 mM Tris-HCl pH 7.5, 0.2 mM EDTA, 0.5 mM spermidine, 250 μ M PMSF, 0.1 % (v/v) NP40) was added and the cells were incubated on ice for 3 min. A sample was taken of total cellular extract, mixed with an equal volume of SDS sample buffer and stored at -20°C . The nuclei were pelleted by centrifugation at 360 g for 4 min at 4°C . Nuclei were resuspended in NBR (85 mM KCl, 5.5 % (w/v) sucrose, 10 mM Tris-HCl pH 7.5, 1.5 mM CaCl_2 , 3 mM MgCl_2 , 250 μ M PMSF) and digested with 8-14 units of micrococcal nuclease (Worthington) per 20 A_{260} units of nuclei for 10 min on ice in the presence of 100 $\mu\text{g/ml}$ RNaseA. The reaction was stopped by adding 10 mM EDTA. The nuclei were washed, resuspended in TEEP₂₀ (10 mM Tris-HCl pH 8.0, 1 mM EDTA, 1 mM EGTA, 250 μ M PMSF, 20 mM NaCl) and incubated at 4°C overnight. Nuclear debris was removed leaving soluble chromatin in the supernatant by centrifugation at 12,000 g for 5 min at 4°C . A sample of both the insoluble nuclear fraction and the soluble chromatin containing fraction was removed, mixed with an equal amount of SDS sample buffer and stored at -20°C . All fractions were resolved by SDS PAGE (2.9.4) and analysed by immunoblotting (2.9.5).

2.12 Proteasome Activity Assay

Active proteasomes were obtained from cells by the method of Araya *et al.* (2002). Harvested cells were lysed with proteasome lysis buffer (20 mM Tris-HCl pH 7.2, 0.1 mM EDTA, 1 mM 2-mercaptoethanol, 5 mM ATP, 20 % glycerol, and 0.04 % NP40) by repeated pipetting, followed by a 20 min incubation on ice. Cell lysates were centrifuged at 16,000 g at 4 °C for 10 min.

Proteasome activity was analysed using a 20S Proteasome Assay Kit (Calbiochem[®]) in accordance with the manufacturer's recommendations. The 20S activity is measured by monitoring the release of free AMC (7-amino 4-methylcoumarin) from the fluorogenic proteasome specific peptide Suc-Leu-Leu-Val-Tyr-AMC. The rate of AMC release is measured by fluorescence spectroscopy. Cell lysates (final concentration 0.02 mg/ml) were diluted in 190 µl SDS activated Reaction Buffer, added to a white Microlite2[™] 96-well ELISA plate (CoStar; Corning Inc.) and equilibrated to 37 °C. The reaction was initiated by adding 10 µl of the fluorogenic peptide solution to each well. The intensity of fluorescence of each reaction was measured over time by fluorescence spectroscopy (excitation max: ~380 nm; emission max: ~460 nm) using an Envision fluorescence detector (Perkin Elmer).

2.13 ATM Kinase Assay

2.13.1 Nuclear extraction

Nuclear extract from frozen cell pellets were prepared using the method of Gooarzi & Lees-Miller (2004). Frozen cell pellets were lysed in twice the cell volume of low salt buffer (10 mM Hepes pH 7.4, 25 mM KCl, 10 mM NaCl, 1 mM MgCl₂, 0.1 mM EDTA) and centrifuged at 10,000 g for 15 min at 4 °C. The resulting supernatant was discarded. The pellet was gently extracted with one fifth the original cell pellet volume of high salt buffer (50 mM Tris-HCl pH 8, 5 % Glycerol, 1 mM EDTA, 10 mM MgCl₂, 400 mM KCl) and centrifuged at 10,000 g for 15 min at 4 °C. The resulting nuclear extract was removed and stored on ice. The remaining pellet was further extracted with one tenth the original cell pellet volume of high salt buffer and centrifuged at 10,000 g for 15 min at 4 °C. The resulting supernatant was added to the nuclear extract and stored on ice. The protein concentration of the nuclear extract was determined by Bradford assay (see 2.9.3).

2.13.2 Immunoprecipitation of ATM

To immunoprecipitate ATM from nuclear extracts, 0.5 mg of nuclear extract was mixed with 1 µl anti-ATM antiserum (mouse monoclonal (α -536), KuDOS) and an equal volume of 250 mM IP buffer (250 mM KCl, 25 mM Hepes pH 7.4, 10 % Glycerol, 2 mM MgCl₂, 0.5 mM EDTA, 0.1 mM Na₃VO₄, 0.1 % NP40) and incubated for 2 hr at 4 °C with rotation. Prior to addition to the IP mix 20 µl protein

A-sepharose beads (Sigma) were washed three times with 500 μ l 250 mM IP buffer. Beads were collected by centrifugation at 1000 *g* for 2 min at 4 °C, added to the IP mix and incubated for a further 2 hr at 4 °C with rotation. The beads were washed four times with 500 μ l 250 mM IP buffer and twice with 500 μ l ATM Kinase buffer (50 mM Hepes pH 7.5, 150 mM NaCl, 4 mM MnCl₂, 6 mM MgCl₂, 10 % Glycerol, 1 mM DTT, 0.1 mM Na₃VO₄) before being resuspended in 16 μ l ATM kinase buffer.

2.13.3 Immunochemical detection of kinase activity

ATM kinase activity was monitored by immunochemical detection of a phospho-substrate, GST-p53N66 fragment (N-terminal 66 amino acids of p53 fused to GST; ~34 kDa) and as a negative control GST-p53N66 (S15A) mutant fragment. The immunoprecipitated ATM was mixed with 2 μ l substrate (concentration 1 μ g/ μ l) and 4 μ l ATM kinase buffer. The reaction was initiated by adding ATP to a final concentration of 500 μ M. The reaction was carried out in a 96-well plate and incubated at 30 °C for 30 mins with vigorous shaking. The reaction was stopped by adding 10 μ l 4 x SDS sample buffer. The reactions were resolved on a 12 % acrylamide gel (see 2.9.4), immunoblotted (see 2.9.5) and probed for p53 serine-15 phosphorylation using a rabbit polyclonal antibody (Cell Signalling) to avoid IgG heavy and light chain contamination of the blot.

2.13.4 Radioactive detection of kinase activity

ATM kinase activity was also detected by radiolabelling the substrate with [$\gamma^{32}\text{P}$] ATP. GST-N66p53 fusion protein and the negative control GST-p53N66 (S15A) mutant fragment were used as substrates. The immunoprecipitated ATM was mixed with 2 μl substrate (concentration 1 $\mu\text{g}/\mu\text{l}$) and 4 μl ATM kinase buffer. The reaction was initiated by adding 1 μl ATP (1:50 dilution of [$\gamma^{32}\text{P}$] ATP (3000 Ci/mmol) in 2 mM ATP). Reactions were incubated in 1.5 ml microcentrifuge tubes at 30 °C for 30 mins with vigorous shaking, and stopped by adding 10 μl 4 x SDS sample buffer. Reaction products were resolved by SDS-PAGE (see 2.9.4). Gels were dried and exposed to a storage phosphor screen (Amersham) overnight, and [$\gamma^{32}\text{P}$] ATP incorporation was detected via a phosphoimager (Storm 840, Amersham Biosciences).

2.14 Co-immunoprecipitation assay

For the purpose of immunoprecipitation, cells were seeded at 5×10^6 in 15 cm dishes and harvested at 80 % confluency. Frozen cell pellets were lysed in 2 x cell pellet volume NP40 lysis buffer (1 % NP40, 25 mM Hepes pH 7.6, 400 mM KCl, 200 μM Na_3VO_4), incubated on ice for 30 min and centrifuged at 13,000 g for 10 min. The lysate were stored at -70 °C.

To avoid IgG light chain and heavy chain masking of immunoblots, the antibodies were cross-linked to Protein A-sepharose beads. 100 μl Protein A-sepharose beads were washed in 10 ml PBS for 5 min. 2 μg of antibody was mixed

with 10 ml PBS and used to resuspend the beads. The mix was incubated overnight at 4 °C with rotation to allow the antibody to bind to the beads. The beads were collected by centrifuging at 1000 g for 5 min at 4 °C. The beads were resuspended in 10 ml 0.2 M sodium borate pH 9.0 and 25 mM dimethyl pimelimidate hydrochloride (Sigma) and incubated for 30 min at room temperature to crosslink the antibody to the beads. The cross-linking reaction was quenched by washing twice (once for 30 min, once for 2 hr) with 10 ml 0.1 M ethanolamine. The beads were then washed twice with 10 ml PBS and resuspended in 90 µl PBS to 50 % slurry. The cross-linked beads were stored at 4 °C.

To immunoprecipitate the desired protein from cell lysate, 2 mg of cell lysate was mixed with an equal volume of wash buffer (150 mM KCl, 25 mM Hepes pH 7.4, 1 mM EDTA, 200 µM Na₃VO₄) and 30 µl of cross-linked Protein A-sepharose beads, and incubated overnight at 4 °C with rotation. The beads were washed four times with 500 µl wash buffer and bound proteins were eluted by resuspending the beads in 30µl 4 x SDS sample buffer. The samples were resolved by SDS-PAGE (2.9.4) and immunoblotted (2.9.5) for the desired protein and protein binding partners which may have co-immunoprecipitated.

2.15 Antibody Capture ELISA

Different conformations of native p53 were detected using p53 conformation specific antibodies in an ELISA format. Frozen cell pellets were lysed in NP40 lysis buffer 2 (50 mM Tris-HCl pH 7.4, 1 mM EDTA pH 7.4, 150 mM NaCl, 1 % NP40, 10 % glycerol). A six-point dilution series of the lysates and BSA negative control were

generated and stored at -70 °C. A white Microlite2™ 96-well ELISA plate (CoStar; Corning Inc.) was coated with affinity purified monoclonal antibodies for p53, DO1 (200 ng/well), DO12 (2000 ng/well), PAb1620 (200 ng/well) and PAb240 (1000 ng/well) in 50 µl 0.1 M sodium borate pH 9.0, overnight at 4 °C. The plate was washed three times with 200 µl/well PBST (0.05 % v/v) to remove unbound antibodies. Non-reactive sites were blocked with 200 µl/well 3 % (w/v) BSA/PBST for 1 hr at 4 °C. The six-point dilution series of cell lysates and BSA negative control were thawed and 50 µl of each concentration was added to an appropriate well, and incubated for 1 hr at 4 °C. The plate was washed five times with 200 µl/well PBST (0.05 % v/v) to remove unbound proteins. Captured p53 protein was detected by incubating with 50 µl/well anti-p53 polyclonal antibody CM1 diluted 1:2000 in 3 % (w/v) BSA/PBST for 1 hr at 4 °C. The plate was washed five times with 200 µl/well PBST (0.05 % v/v). 50 µl/well HRP-coupled anti-rabbit antibody diluted 1:2000 in 3 % (w/v) BSA/PBST was added and incubated for 1 hr at 4 °C. The amount of CM1 captured on the ELISA plate was detected by ECL chemiluminescent detection system (1:1 ratio ECL I : ECL II) and the chemiluminescence produced was detected by a luminometer (Fluoroskan, Ascent FL).

2.16 DNA Microarray

The OligoGEArray® System from SuperArray is a gene expression profiling system. Here the Oligo GEArray® p53 Signalling Pathway Microarray for human and mouse was used to profile the expression of 113 genes related to p53 mediated signal transduction. The system was used according to the manufacturer's instructions.

2.16.1 Total RNA isolation

Total RNA was isolated from cells using the RNeasy kit (Qiagen) according to the manufacturer's instructions. $\sim 1 \times 10^7$ cells were harvested and the cells were lysed with denaturing RLT buffer (Qiagen). The sample was homogenised with QIAshredder spin column (Qiagen) to shear genomic DNA and reduce viscosity of lysate. An equal volume of ethanol was added to the lysate, this was directly applied to the RNeasy spin column for absorption of RNA to the silica-gel based membrane. Contaminants were removed by washing and centrifugation. RNA was eluted from the column with 30 μ l water. RNA concentration was determined using a NanoDrop® spectrophotometer.

2.16.2 cRNA target labelling

TrueLabelling-AMP™ 2.0 (SuperArray) is designed to amplify and label antisense RNA for hybridisation to Oligo GEArray® and was used according to the manufacturer's instructions. cDNA was synthesised from total RNA, and used as the template for cRNA synthesis in the presence of biotinylated-UTP, leading to the incorporating biotin labelled uridine into the newly synthesised cRNA.

The cRNA was purified using the SuperArray ArrayGrade™ cRNA cleanup kit, according to the manufacturer's instructions. A denaturing buffer was added to the cRNA synthesis reaction mix, followed by an equal volume of ethanol and the sample was loaded on to a spin column. Contaminants were removed by washing and

centrifugation. cRNA was eluted from the column with 50 µl 10 mM Tris pH 8.0, and concentration was determined using a NanoDrop® spectrophotometer.

2.16.3 Array hybridisation and detection

The cRNA was hybridised to the array following the Oligo GEArray® HybTube Protocol (option 1). The array membranes were individually supplied in a 5 ml plastic tube for easy use in a roller bottle hybridisation oven. The array membrane was pre-wet with deionised water. GEArray Hybridisation Solution (SuperArray) was warmed to 60 °C, added to the membrane and incubated for 2 hr at 60 °C in a hybridisation oven with slow agitation. 3 µg biotin labelled cRNA target was mixed with GEArray Hybridisation Solution, added to the membrane, and allowed to hybridise overnight at 60 °C with slow rotation. The membrane was repeatedly washed, then cooled to room temperature. To prevent non-specific binding, the membrane was blocked with GEArray Blocking Solution Q (SuperArray) for 40 min with continuous rotation at room temperature. The blocking solution was discarded and membrane was incubated with alkaline phosphatase-conjugated streptavidin. The membrane was repeatedly washed, before being incubated with CDP-Star chemiluminescent substrate (SuperArray). Excess CDP-Star solution was removed from the membrane and array image was acquired by exposure to X-ray film (Kodak).

2.16.4 Image and data analysis

The resulting images were scanned and saved as 16 bit TIFF files. The images were uploaded into the GEMArray Expression Analysis Suite programme (<http://geasuite.superarray.com>) which was used to convert the fluorescent intensity of the probe into values representing gene expression, and allow data analysis of the microarray results.

REGULATION OF p53 PROTEIN LEVELS AND
TRANSCRIPTIONAL ACTIVITY IS p21-DEPENDENT

3.1 Introduction

The p53 tumour suppressor protein is a central component in the cellular response to environmental and intracellular stresses that threaten DNA integrity, and loss of p53 is associated with genomic instability and tumour development (Ashcroft *et al.*, 1999; Vogelstein & Kinzler, 2004; Zhou & Elledge, 2000; Ziyaie *et al.*, 2000). This is supported by the observations that p53 is mutated in over 50% of all human cancers (Levine, 1997; Ziyaie *et al.*, 2000) and that p53-deficient mice are highly susceptible to the spontaneous development of a wide range of tumours (Attardi & Jacks, 1999).

Upon exposure to DNA damage, p53 is post-translationally modified in a site-specific manner leading to rapid elevation of p53 protein levels, principally through stabilisation, and accumulation of active p53 in the nucleus (Ashcroft *et al.*, 2000). The principal function of p53 in response to cellular stress is as a transcription factor that binds with high affinity to specific sequences in the regulatory region of p53-responsive genes, including effectors of cell cycle (*p21*, *14-3-3 σ* , *GADD45*) (el-Deiry *et al.*, 1993; Hermeking *et al.*, 1997), of apoptosis (*BAX*, *KILLER/DR5*, *APO-*

1/FAS, AIP1, PUMA, NOXA, PIG3) (Vousden, 2000) and of DNA repair (*p53R2*) (Seemann & Hainaut, 2005).

Several p53 target genes also play a role in the regulation of p53 through autoregulatory feedback loops, fine-tuning p53 activity and linking p53 to other signal transduction pathways in the cell (Harris & Levine, 2005). The best characterised regulatory partner of p53 is the E3 ligase, MDM2, which mediates both ubiquitination and proteasome-dependent degradation of p53 (Haupt *et al.*, 1997). The *MDM2* gene is itself transcriptionally activated by p53 and the two proteins function within an autoregulatory loop, whereby p53 positively regulates MDM2 expression while MDM2 negatively regulates p53 levels and activity (Harris & Levine, 2005; Haupt *et al.*, 1997; Meek, 2004).

The cyclin-dependent kinase inhibitor, p21^{WAF1/CIP1} (referred to hereafter as p21) has been well characterised as a critical downstream effector in DNA damage induced p53-dependent growth arrest in mammalian cells (Abraham, 2001; el-Deiry *et al.*, 1994; el-Deiry *et al.*, 1993). Several studies have reported additional roles for p21, including a regulatory function in differentiation (Dotto, 2000), protecting cells from p53-induced apoptosis (Javelaud & Besançon, 2002), and control of stem cell self-renewal in both the keratinocyte and hematopoietic systems (Dotto, 2000). Importantly, p21 has been shown to function as a highly specific regulator of gene expression (Perkins, 2002). However, as p21 lacks DNA binding motifs and detectable affinity for DNA, it is likely that p21 functions as a transcriptional co-factor. In particular, p21 directly binds to and inhibits the transcriptional activities of E2F (Delavaine & La Thangue, 1999), c-Myc (Kitaura *et al.*, 2000) and STAT-3 (Coqueret & Gascan, 2000). In contrast, p21 can also induce gene expression through

stimulating the activity of the transcriptional co-activator proteins p300 and CBP (Snowden *et al.*, 2000), and by enhancing NF- κ B- (Perkins *et al.*, 1997) and ER α -mediated transcription (Fritah *et al.*, 2005).

The importance of p21 in tumourigenesis is highlighted by the susceptibility of p21-null mice to develop spontaneous tumours at an average age of 16 months, whereas wild-type mice remain tumour free beyond two years (Martin-Caballero *et al.*, 2001). Also a growing number of clinical studies show that under-expression of p21 protein is indicative of low survival rates and is a negative prognostic marker in different malignancies, including lung (Komiya *et al.*, 1997), breast (Wakasugi *et al.*, 1997), bladder (Stein *et al.*, 1998), ovarian (Anttila *et al.*, 1999), and anal carcinomas (Holm *et al.*, 2001).

In this chapter, the role of p21 in tumour progression has been investigated using isogenic derivatives of the HCT116 colorectal cancer cell line. Substantial defects in the basal, and damage-induced p53 pathways were observed in the absence of p21, suggesting that p21 regulates p53 via a novel feedback loop and that p21 is an essential transcriptional co-factor of the p53 response.

3.2 Results

3.2.1 Basal p53 levels, half-life and transcriptional activity are affected by loss of p21

HCT116 colon carcinoma cells containing wild-type p53 and wild-type p21 (HCT116 WT), and the isogenic derivative, HCT116 p21^{-/-}, which has targeted

inactivation of the *p21* gene (Bunz *et al.*, 1998), were used to evaluate the consequences of p21 deficiency on p53 regulation. In normal cells, p53 is present at extremely low levels as the protein is rapidly degraded following synthesis (Ashcroft & Vousden, 1999). Initial observations highlighted that in unstressed cells p53 protein was expressed at a higher level in HCT116 p21^{-/-} cells than in the HCT116 WT cells (Figure 3.1A). The level of p53 protein was determined by visual assessment to be approximately 5-fold greater in p21^{-/-} cells than in the HCT116 parental cells (Figure 3.1A). To confirm that accumulation of p53 in p21^{-/-} cells was specific and that loss of p21 did not cause a global increase in protein expression, whole cell lysates derived from WT and p21^{-/-} cells were resolved by SDS-PAGE and cellular proteins were stained with Coomassie (Figure 3.1B). Both cell lines had similar protein banding patterns and intensities, consistent with them being isogenic, and containing no gross defect in protein expression.

Accumulation of p53 protein in p21^{-/-} cells could be caused by increased *p53* gene expression, increased stabilisation of p53 protein, or decreased degradation of p53. To determine whether the high level of p53 protein was caused by increased stabilisation, the half-life of p53 was determined using an inhibitor of protein synthesis, cyclohexamide. Cyclohexamide was added to WT and p21^{-/-} cells at a final concentration of 30 µg/ml and cells were harvested over the indicated time course. In WT cells p53 was rapidly degraded, whereby p53 protein levels decreased by 50 % by approximately 30 minutes. There after the rate of p53 degradation decreases leaving a low basal level of p53 protein detectable after 4 hours. Whereas in p21^{-/-} cells p53 was very stable with a half-life extending beyond 4 hours (Figure 3.2A, carried out by M. Scott), indicating that the high basal level of p53 in p21^{-/-}

cells may be due to a reduced turn-over of p53. To establish that p53 accumulation in p21^{-/-} cells was not due to impaired proteasome activity, active proteasomes were purified from WT and p21^{-/-} cells, and 20S proteasome activity was measured by monitoring the release of AMC (7-amino-4-methylcoumarin) from a 20S specific fluorogenic peptide. Proteasome activity in p21^{-/-} cells was similar to that of WT cells (Figure 3.2B). These findings suggest that the high basal level of p53 observed in p21^{-/-} cells is due to a specific increase in p53 protein stabilisation rather than decreased proteasome activity and p53 degradation.

p53 activity is principally governed by controlling the stability of the p53 protein, and induction of the p53 response is closely associated with increased p53 stabilisation. Specific transcriptional activity of p53 was determined by a gene reporter assay, whereby the p53-specific p21 promoter is fused to the luciferase gene. p53 induction causes activation of the p21 promoter and increased luciferase expression. p53 activity was measured by determining luciferase production standardised to β Gal production (Relative Light Units; R.L.U.). The level of p21 luciferase reporter activity was measured in lysates of WT, p21^{-/-} and as a negative control, the isogenic derivative p53^{-/-} cells. Figure 3.3 shows a graph of relative p53 transcriptional activity in WT, p21^{-/-} and p53^{-/-} cells. Surprisingly, p53 activity in p21^{-/-} cells was approximately 4-fold lower than that observed in WT lysates, indicating that p53 is transcriptionally inactive in the p21^{-/-} cells. In support of this, the level of reporter activity in p21^{-/-} cells was similar to that seen in the p53^{-/-} cells. This data demonstrates that the increase in p53 stabilisation observed in the p21^{-/-} cells is not associated with the predicted increase in p53 activity, and signifies that in

the absence of p21, p53 stability is uncoupled from the transcriptional activity of the protein.

3.2.2 p53 stress responses are not induced in p21^{-/-} cells

Basal transcriptional activity of p53 is decreased in p21^{-/-} cells (Figure 3.3). To determine whether p53 transcriptional activity in p21^{-/-} cells could be induced by cellular stresses, HCT116 WT and p21^{-/-} cells were exposed to double stranded RNA (dsRNA) and ionising radiation (IR) to examine the p53 viral and DNA damage response, respectively.

Polyinosinic polycytidylic acid (poly(I).poly(C)) is a synthetic viral-like dsRNA that stimulates antiviral activities of the innate immune system and can be used to mimic viral infections *in vitro* (Fortier *et al.*, 2004). Poly(I).poly(C) is also a potent inducer of interferon (IFN)- α and $-\beta$ *in vitro* and *in vivo* (Trapman, 1979), which have been shown to induce transcription of the p53 gene, contributing to tumour suppression and antiviral defence (Takaoka *et al.*, 2003). However, the p53 response to viral infection is relatively novel and undefined. To examine the p53 response to viral infection HCT116 WT and p21^{-/-} cells were treated with poly(I).poly(C) and harvested over an 8 hour time course (Figure 3.4). Immunoblot analysis of WT cells showed p53 protein levels and phosphorylation of p53 at serine-15, a marker of p53 activity, were maximal at approximately 2 hours post-treatment (Figure 3.4A), whereas in p21^{-/-} cells there was a high basal level of p53 protein and surprisingly a high basal level of p53 serine-15 phosphorylation, neither of which

were induced further by poly(I).poly(C) treatment (Figure 3.4A). These data indicate defects in p53 activation in the absence of p21.

The consequences of p53 activation are mostly mediated through enhanced expression of specific target genes. It was previously shown that p21, IRF-1 and GADD34 are induced in a p53-dependent manner, following poly(I).poly(C) treatment (Mirijam Eckert, unpublished data). Therefore, induction of these p53 targets, were examined as markers of p53 transcriptional activity (Figure 3.4A). In the WT cells, p21, IRF-1 and GADD34 proteins were progressively induced following poly(I).poly(C) treatment. However in the absence of p21, both IRF-1 and GADD34 failed to be up-regulated and could not be detected by immunoblotting (Figure 3.4A), suggesting that stress-activated p53 transcriptional activity is significantly attenuated in the absence of p21. This was confirmed by p21 luciferase reporter assay of poly(I).poly(C) treated WT and p21^{-/-} cells (Figure 3.4B). In WT cells p53 transcriptional activity peaked 2 hours after treatment. In contrast, p53 activity was not induced in response to poly(I).poly(C) in p21^{-/-} cells (Figure 3.4B). In untreated cells basal p53 activity was 3-fold higher in WT cells than in p21^{-/-} cells. Following poly(I).poly(C) treatment at 2 hours, p53 activity was 8-fold higher in WT cells than in corresponding p21^{-/-} cells (Figure 3.4B). This data reiterates the importance of p21 for p53-dependent transcription in response to dsRNA, and signifies that p21 is required for the p53 viral response pathway.

The relatively novel and uncharacterised p53 viral response does not completely overlap with the p53 response to DNA damage (Mirijam Eckert, unpublished data). Therefore to further characterise the extent at which p21 is required for the p53 response to different cellular stresses, the DNA damage response

induced by ionising radiation was also analysed. HCT116 WT and p21^{-/-} cells were irradiated with 7 Gy IR and harvested over an 8 hour time course. Similar results were obtained to those of the poly(I).poly(C) treated cells. In the WT cells p53 levels peaked at 2 hours post-irradiation and phosphorylation of p53 at serine-15 increased gradually peaking at 6 hours post-irradiation. In contrast the p21^{-/-} cells showed high basal levels of p53 and phosphorylation of p53 at serine-15, which were not further induced by IR (Figure 3.5A), indicating defects in p53 activation.

In response to IR, p53-dependent induction of p21, MDM2 and pro-apoptotic protein BAX (Miyashita & Reed, 1995), have been well characterised. In WT cells MDM2 and p21 increased gradually after irradiation, and both peaked at 6 hours (Figure 3.5A). However MDM2 induction was not observed in the p21^{-/-} cells (Figure 3.5A), indicating that p21 is required for p53-dependent transcription in response to IR induced DNA damage. Unlike the other p53 targets examined, WT cells had a high basal level of BAX which was not further induced by IR. This adaptation is likely to be HCT116-specific as other cell lines show induction of BAX in response to IR (Miyashita & Reed, 1995; Coates *et al.*, 2003). However, interestingly in the p21^{-/-} cells BAX could not be detected even after IR treatment (Figure 3.5A), indicating that basal BAX levels are p21-dependent.

The requirement of p21 for activation of p53 in response to IR was further confirmed by a p21 luciferase reporter assay (Figure 3.5C). In WT cells p53 activity peaked at 6 hours after IR treatment, where as in p21^{-/-} cells p53 activity was not activated after irradiation. Highlighting that p53 is transcriptionally inactive in the p21^{-/-} cells in response to IR (Figure 3.5C) and that p21 is necessary for the p53-dependent response to both viral infection and DNA damage.

In the absence of p21 there is a high basal level of phosphorylation of p53 at serine-15 (Figure 3.5A). In response to genotoxic stress the serine-15 site is targeted by members of the PIKK family of protein kinases, principally ATM and ATR (Banin *et al.*, 1998; Canman & Lim, 1998). Phosphorylation of the serine-15 site has also been proposed to play a role in p53 stabilisation by reducing the interaction between p53 and its E3 ligase MDM2 (Ashcroft *et al.* 1999). Another specific target site of ATM is CHK2 threonine-68 (Matsuoka *et al.*, 2000). Therefore levels of CHK2 and phosphorylation of CHK2 at threonine-68 were also examined following IR treatment (Figure 3.5B). In both WT and p21^{-/-} cells total CHK2 protein levels remained unchanged in response to IR. However in WT cells, phosphorylation of CHK2 at threonine-68 was induced by irradiation and peaked at 4 hours after treatment. In contrast, there was a high basal level of CHK2 threonine-68 phosphorylation which was not altered by IR in the p21^{-/-} cells (Figure 3.5B), similar to the high level of p53 serine-15 phosphorylation also observed in these cells (Figure 3.5A). As ATM phosphorylates both p53 at serine-15 and CHK2 at threonine-68 and both proteins are constitutively phosphorylated in p21^{-/-} cells, this preliminary data suggests that p21 regulates a p53 serine-15 kinase and that the prime candidate is ATM.

3.2.3 p21 regulates basal p53 levels and activity

HCT116 cells are mismatch repair deficient as a result of silencing hMLH1 expression, and are therefore prone to genetic alteration (Hayward *et al.* 2005). HCT116 p21^{-/-} cells may have accumulated additional genetic modifications leading

to inactivation of p53. To confirm that p21 is a genuine p53 regulator, the p21^{-/-} phenotype was reconstituted in the WT cells using p21 siRNA mediated gene knockdown to reduce endogenous p21 protein levels. WT cells were treated with p21 siRNA, and p21 protein levels in WT cells were reduced to a level comparable to that of the p21^{-/-} cells 48 hours after treatment (Figure 3.6). Reduction of p21 was accompanied by an increase in p53 levels and phosphorylation of p53 at serine-15 compared to the control siRNA at 48 hours after treatment (Figure 3.6), highlighting that the p21^{-/-} phenotype can indeed be reconstituted in the WT cells by reduction of p21 protein levels only. This data suggests that p21 protein levels do influence and regulate p53 protein levels and phosphorylation of p53 at serine-15.

Conversely, the WT phenotype was aimed to be reconstituted in p21^{-/-} cells. Initially p21^{-/-} cells were transiently transfected with increasing amounts of p21 DNA and harvested 24 hours after transfection (Figure 3.7A). p53 levels and phosphorylation of p53 at serine-15 remained unchanged despite increasing p21 protein levels. However, basal p53 transcriptional activity was recovered in a p21 dependent manner (Figure 3.7B). Recovery of p53 transcriptional activity peaked at 50 ng p21 DNA, and showed a 5-fold increase over the empty vector control (Figure 3.7B). These findings signify that p21 can reinstate p53 transcriptional activity and that p21 is a bona fide regulator of p53.

3.2.4 Reintroduction of p21 into p21^{-/-} cells rescues the p53 stress response

Transient transfection of p21 DNA into p21^{-/-} cells had no effect on p53 protein levels (Figure 3.7A). These cells were harvested 24 hours after transfection,

indicating that this time frame may not have been sufficient for reintroduction of p21 to be effective. Therefore p21 was stably reintroduced into p21^{-/-} cells. Pooled colonies were tested for p21 expression. Clones 2 and 3 were stably expressing a low level of p21 and showed a corresponding reduction in levels of p53 and phosphorylation of p53 at serine-15, compared to clone 1 which did not express p21 and had a high level of p53 and p53 serine-15 phosphorylation (Figure 3.8). Therefore stable reintroduction of p21 into p21^{-/-} cells was sufficient to reduce p53 protein levels and phosphorylation of p53 at serine-15 to levels comparable to those observed in the WT cells (Figure 3.8), and further confirms that p21 is a novel p53 regulator.

As previously shown, the p53 stress response to dsRNA (Figure 3.4A) and IR (Figure 3.5A) is abated in p21^{-/-} cells. To determine if stable reintroduction of p21 is sufficient to restore the p53 stress response pathway in response to dsRNA and IR, clone 2 cells stably expressing p21 were compared to p21^{-/-} cells under different stress conditions. Initially, the p53 viral response was analysed by treating p21^{-/-} cells and clone 2 cells with 50 µg/ml poly(I).poly(C), harvesting at the indicated time points and immunoblotting for p53 induced proteins (Figure 3.9). As previously observed, in p21^{-/-} cells there was a high basal level of p53 and p53 serine-15 phosphorylation which was not further induced by poly(I).poly(C) treatment (Figure 3.9). In striking contrast, clone 2 cells had a low basal level of p53 and p53 serine-15 phosphorylation which were progressively induced in response to poly(I).poly(C). Therefore re-introduction of p21 can re-establish p53 induction by viral stress. Markers of p53 transcriptional activity, IRF-1 and GADD34, were also analysed by immunoblotting. In the p21^{-/-} cells, p53-dependent induction of IRF-1 and GADD34

was not detected, but in clone 2 cells progressive induction of IRF-1 and GADD34 was restored (Figure 3.9). These findings show that stable reintroduction of p21 into p21^{-/-} cells can restore p53 induction, accompanied by induction of p53 transcriptional targets in response to poly(I).poly(C), and signifies that p21 is a regulator of p53 transcriptional activity.

The p53 viral response induced by dsRNA was again compared to the DNA damage response induced by IR. HCT116 p21^{-/-} and clone 2 cells were irradiated at 7 Gy, harvested at the indicated time points and analysed by immunoblotting (Figure 3.10). In the p21^{-/-} cells there was a high basal level of p53 and phosphorylation of p53 at serine-15 which was not altered by IR, whereas clone 2 cells had a low basal level of p53 and phosphorylation of p53 at serine-15 which was progressively induced by IR (Figure 3.10). MDM2 was not detectable in the p21^{-/-} cells, but in clone 2 cells MDM2 induction after IR treatment was restored (Figure 3.10), indicating that p53 transcriptional activity was also restored by stable expression of p21. However, the best characterised transcriptional targets of p53 in response to IR are p21 and BAX. Monitoring p21 levels as a marker of p53 transcriptional activity was not feasible as p21 in the clone 2 cells is under the control of a CMV promoter which is not induced by p53, and therefore not representative of p53 activity. As previously shown (Figure 3.5A), there is a high basal level of BAX in the WT cells which is not induced by IR, whereas BAX is not detectable in p21^{-/-} cells (Figure 3.5A). Here, stable reintroduction of p21 into p21^{-/-} cells restored the high basal level of BAX (Figure 3.10) to levels comparable to those previously observed in the WT cells (Figure 3.5A). In summary, reintroduction of p21 into p21^{-/-} cells can restore basal WT levels of p53, phosphorylation of p53 at serine-15 and BAX, and in

response to IR can restore p53 stabilisation, induction of MDM2, and phosphorylation of p53 at serine-15.

Stable reintroduction of p21 back into the p21^{-/-} cells restored both the p53 viral and DNA damage response, signifying the importance of p21 in the p53 response pathway.

3.2.5 The C-terminus of p21 is not required for p53 reactivation

Reintroduction of full length p21 into p21^{-/-} cells was sufficient to reactivate p53 transcriptional activity. To determine the domain of p21 required for this p53 regulation, different p21 forms were stably transfected into p21^{-/-} cells. The forms used were; p21¹⁻¹⁵⁵ C-terminal truncation which lacks the second cyclin binding domain; p21¹⁻¹³³ C-terminal truncation which lacks the second cyclin binding domain, the PCNA binding domain, and the nuclear localisation signal (Dotto, 2000); and p21^{S146A} point mutation where serine-146 is mutated to alanine, to block phosphorylation. Phosphorylation of the serine-146 site, alters the half-life of p21 (Scott *et al.*, 2002; Li *et al.*, 2002a), is sufficient to inhibit the interaction of p21 with PCNA (Scott *et al.*, 2000), and is targeted by protein kinase C ζ (Scott *et al.*, 2002). Clones were selected in duplicate, termed A and B, and full-length p21 was used as a positive control (Figure 3.11). p21 protein levels were detected by immunoblotting with a N-terminal antibody which recognises the Ab-1 epitope at 58-77 aa. p21 was detected in p21^{-/-} cells transfected with full-length p21 and p21^{S146A} mutant, but not the C-terminal truncations as they resolve at a lower molecular weight and could not be detected by immunoblotting, therefore introducing a degree of uncertainty into the

interpretation of the experiment. p53 levels and phosphorylation of p53 at serine-15 were marginally affected by the different forms of p21, although WT and p21^{-/-} samples were run on different gels to clones A and B preventing conclusive comparisons. However the increase in BAX levels appeared to be the more sensitive assay for determining successful p21 expression. The A clones did not show an increase in BAX levels, whereas the B clones all showed increased BAX levels compared to p21^{-/-} cells (Figure 3.11), which may indicate that p53 activity has been restored, and that the C-terminus of p21 including the serine-146 phospho-site, is not required for p53 reactivation.

3.3 Discussion

Normal cells challenged with stresses such as genetic insults, trigger a variety of intracellular programmes that lead to either, cell growth, senescence or apoptosis (Abraham, 2001). One of the major mechanisms involved in these stress responses is p53-dependent induction of the cyclin-dependent kinase inhibitor p21 (Bakkenist & Kastan, 2004). To date, p21 has been characterised as a downstream effector of the p53 response. The data presented here demonstrates a novel role for p21 as a requisite co-factor of p53 transcriptional activity in HCT116 cells.

In the absence of p21 there is a high basal level of p53 which is phosphorylated at serine-15 (Figure 3.3). ATM phosphorylates p53 at serine-15 (Banin *et al.*, 1998) and CHK2 at threonine-68 (Matsuoka *et al.*, 2000) in response to damage. In p21^{-/-} cells both proteins are phosphorylated in the absence of damage (Figure 3.5), suggesting that loss of p21 may cause constitutive activation of the

ATM kinase. p53 serine-15 phosphorylation is associated with p53 stabilisation and biochemical activation (Canman *et al.*, 1998), by reducing the interaction between p53 and the E3 ubiquitin ligase MDM2. ATM also directly phosphorylates MDM2 at serine-395, and this blocks degradation of p53 and prevents MDM2-mediated nuclear export of p53 (Khosravi *et al.*, 1999). Constitutive activation of ATM could therefore lead to a high basal level of p53 and p53 serine-15 phosphorylation, markers of p53 transcriptional activity. However, the data presented here shows that although basal levels of p53 are high in p21^{-/-} cells, p53 is inactive as a transcription factor. p53 inactivation may occur in tumour cells lacking p21, as an adaptive response to compensate for high basal levels of p53, which would essentially shut the cell down by causing growth arrest or apoptosis. Stable reintroduction of p21 into p21^{-/-} cells can however restore p53 transcriptional activity, indicating that the relationship between p53 and p21 is more intricate.

The p53 protein plays an essential role in tumour suppression by modulating cellular functions such as gene transcription, DNA synthesis, DNA repair, cell cycle arrest, senescence and apoptosis (Larkin & Jackson, 1999). This is highlighted by the observation that p53 is mutated in over 50% of all human cancers (Ziyaie *et al.*, 2000) and that mice lacking p53 are highly susceptible to spontaneous tumour development (Donehower *et al.*, 1992; Harvey *et al.*, 1993; Purdie *et al.*, 1994). In normal cells p53 is maintained at a very low level within the cell, as over-expression of p53 would lead to cell growth arrest and apoptosis of healthy cells eventually impairing the entire organism. Correspondingly, p53 activity is tightly regulated by several feedback loops. Central to the control of p53 activity is the p53-MDM2 feedback loop (Chen *et al.*, 1994; Wu *et al.*, 1993) where p53 activation stimulates

up-regulation of the p53 target gene *MDM2* and accumulation of MDM2 protein then leads to p53 degradation. In this chapter, an additional feedback loop has been described, where a p53 target gene p21, is required for p53 activation. This model compliments the p53-MDM2 feedback loop, in that MDM2 drives p53 degradation and p21 drives p53 activation (Figure 3.12).

The role of p53 as a tumour suppressor is well established while the role of p21 in carcinogenesis remains controversial. Mouse models lacking the p21 gene were initially reported to remain tumour free until at least 7 months of age (Deng *et al.*, 1995). However, Martin-Caballero *et al.* (2001) went on to show that p21^{-/-} mice do develop spontaneous tumours at an average age of 16 months whereas control animals remain tumour free for over 2 years. In addition, loss of p21 accelerates tumourigenesis in Rb-haploinsufficient (Brugarolas *et al.*, 1998), p18Ink4c-deficient (Franklin *et al.*, 2000), APC-haploinsufficient (Yang *et al.*, 2001) and v-Ha-ras (Adnane *et al.*, 2000) transgenic backgrounds. The data presented here provides a mechanism whereby p21 inactivation could accelerate tumourigenesis via the inactivation of p53, indicating that p21 may function as a tumour suppressor protein.

In human cancer, early studies concluded that p21 mutations are exceedingly rare, which is in striking contrast to p53 (Shiohara *et al.*, 1994). However as p21 expression is one of the most prominent markers for the functional activity of p53, many clinical studies have analysed p21 expression in different types of human cancer. p21 expression was initially concluded to have no prognostic value (Shiohara *et al.*, 1994; Ito *et al.*, 1996; Elledge & Allred, 1998; Lipponen *et al.*, 1998), but a growing list of studies now show that loss of p21 correlates with tumour progression and negative prognosis in a range of different malignancies, including lung (Komiya

et al., 1997), breast (Wakasugi *et al.*, 1997), bladder (Stein *et al.*, 1998), ovarian (Anttila *et al.*, 1999), cervical (Lu *et al.*, 1998), head and neck (Kapranos *et al.*, 2001), and anal carcinomas (Holm *et al.*, 2001). Previously these studies have assumed that such correlations are strongest when the absence of p21 is seen along with the expression of p53, as an indicator of loss of p53 function. However, in human breast carcinoma there is an inverse relationship between p21 and p53 expression; where low p21 expression is associated with p53 over-expression, and this is significantly related to low histology grade and lymph-node metastasis (Jiang *et al.*, 1997). Similarly, in epithelial ovarian cancer, patients with tumours expressing no or low p21 protein but that were positive for p53 had a notably higher risk of recurrent disease, and were more prone to treatment failures (Anttila *et al.*, 1999). Also low p21 expression is confined to advanced stage of tumour development (Anttila *et al.*, 1999). A similar observation was made in gastric cancer, where patients with p21-negative tumours usually had a metastatic disease (Ogawa *et al.*, 1997). In the context of the data presented in this chapter, p21 negative tumours maybe associated with poor prognosis because not only are these tumours p21-null but they also lack functional p53 and are essentially p53-null.

Earlier clinical studies which concluded that low p21 expression is an artefact of mutated p53 should be re-evaluated, as evidence presented here indicates that down-regulation of p21 expression may be a mechanism employed by cancer cells to functionally inactivate p53. For example, ovarian tumours frequently show loss of heterozygosity in chromosomal segment 6p, where the p21 gene is located (Wan *et al.*, 1996), which could lead to inactivation of p53 and subsequent tumour progression. Similarly, malignant melanomas represent only 3-5% of total skin

cancers, but they are very aggressive and rapidly produce metastasis yet rarely accumulate p53 mutations (Papp *et al.*, 1996). A recent study reported that p21 protein is degraded after low but not high doses of UV irradiation (Bendjennat *et al.*, 2003). UV degradation of p21, by our model, would lead to functionally inactive p53, and provide an alternative mechanism of p53 inactivation, and may explain why p53 mutations are rarely observed in melanomas caused by UV damage.

In this study an isogenic cell model was used, which has wild type p53 but lacks p21. Our findings demonstrate that in the absence of p21, p53 is functionally inactive as a transcription factor, but upon reintroduction of p21 into the p21^{-/-} cells p53 transcriptional activity is recovered (Figure 3.8). Further to this, the C-terminus of p21 is not required for p53 reactivation as the p21¹⁻¹³³ truncated form may also be able to recover p53 activity. The C-terminus of p21 contains the PCNA binding domain, the nuclear localisation domain and the threonine-145 and serine-146 phosphorylation sites. As the nuclear localisation site of p21 is not required for p53 activity, this suggests that p21 may have cytoplasmic functions which ensure correct activation and function of p53.

p21 has been shown to be much more than a cyclin-dependent kinase inhibitor, it has roles in differentiation (El-Deiry *et al.*, 1995), apoptosis (Sohn *et al.*, 2006), and DNA synthesis (Chen *et al.*, 1995). The data presented in this chapter, further extends the role of p21 as a transcriptional co-activator. The p21 protein often has different and conflicting roles depending on cell context. Here, a novel p53 autoregulatory feedback loop is described where p21 is required for p53 transcriptional activity. This data contributes to evidence that p21 is a tumour suppressor protein. Although the effect of p21 on tumour-cell phenotype remains

unclear, this evidence highlights the significance of p21 in p53 regulation and human cancer.

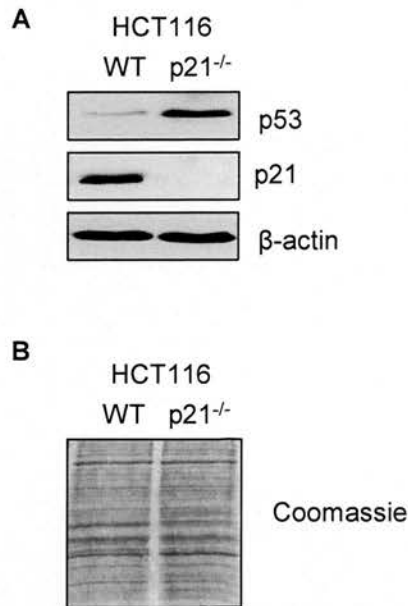


Figure 3.1 p53 protein levels are aberrant in the absence of p21. (A) p53 protein levels are higher in HCT116 p21^{-/-} cells compared to WT cells. HCT116 WT and p21^{-/-} cells were lysed in urea lysis buffer. Whole cell lysates were resolved by SDS-PAGE. p53 and p21 were detected by immunoblotting with anti-p53 (DO1) and anti-p21 (ab-1) respectively. β-actin was used as a loading control. 10 μg total protein was loaded per lane. (B) Loss of p21 does not cause a global defect in protein levels. Urea cell lysates of WT and p21^{-/-} cells were separated by SDS-PAGE and proteins were detected by Coomassie staining, to show non-specific protein banding pattern.

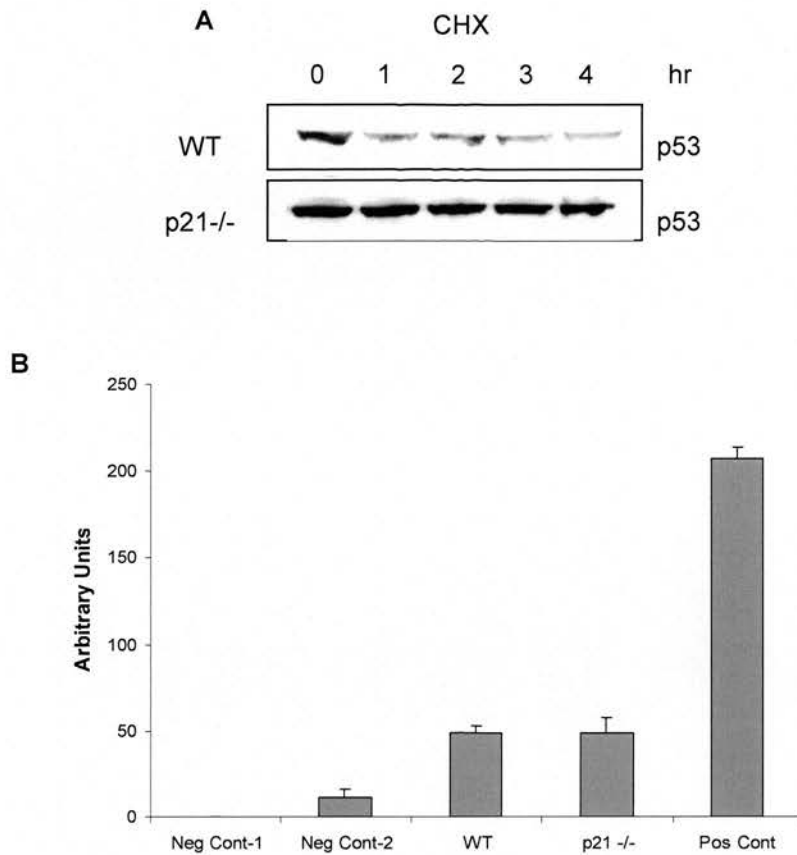


Figure 3.2 High basal level of p53 in the HCT116 p21^{-/-} cells is due to increased stabilisation (A) The half-life of endogenous p53 is extended in the absence of p21. Urea lysates were prepared from HCT116 WT and p21^{-/-} cells at 0, 1, 2, 3 and 4 hr after addition of 30 µg/ml cyclohexamide (CHX). p53 was detected by immunoblotting. (Figure 3.2A was kindly provided by M. Scott). **(B)** Proteasome activity is unaffected in p21^{-/-} cells. The 20s proteasome activity of HCT116 WT and p21^{-/-} cells was determined by monitoring the release of a fluorophore AMC (7-amino-4-methylcoumarin) from a proteasome specific peptide, using a 20s Proteasome Assay Kit (Calbiochem).

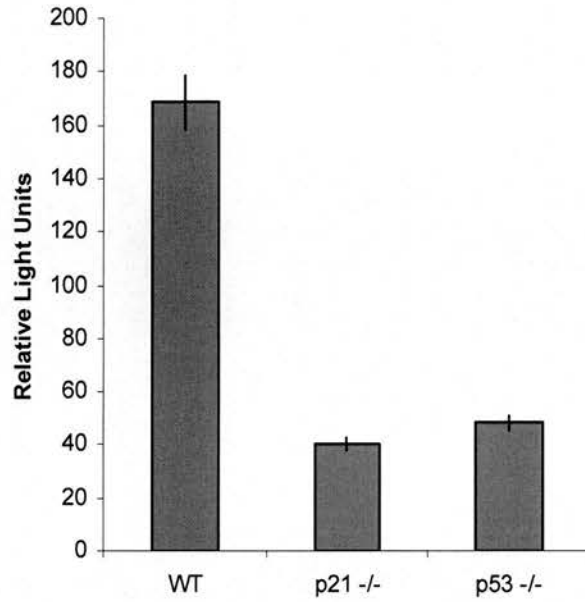


Figure 3.3 p53 transcriptional activity is uncoupled from p53 protein stabilisation in p21^{-/-} cells. Specific transcriptional activity of p53 is reduced in p21^{-/-} cells. The human *p21* promoter fused to luciferase (1 μ g) was introduced into HCT116 WT, p21^{-/-} and p53^{-/-} cells together with 1 μ g pCMV- β gal reporter. Cells were harvested 24 hr after transfection and lysed with 5x Reporter Lysis Buffer (Promega). Luciferase activity was detected by a luminometer. p53-dependent activity (relative light units) is expressed as a ratio of p21-Luciferase activity to the internal transfection control β -gal (Figure was kindly provided by M.Scott).

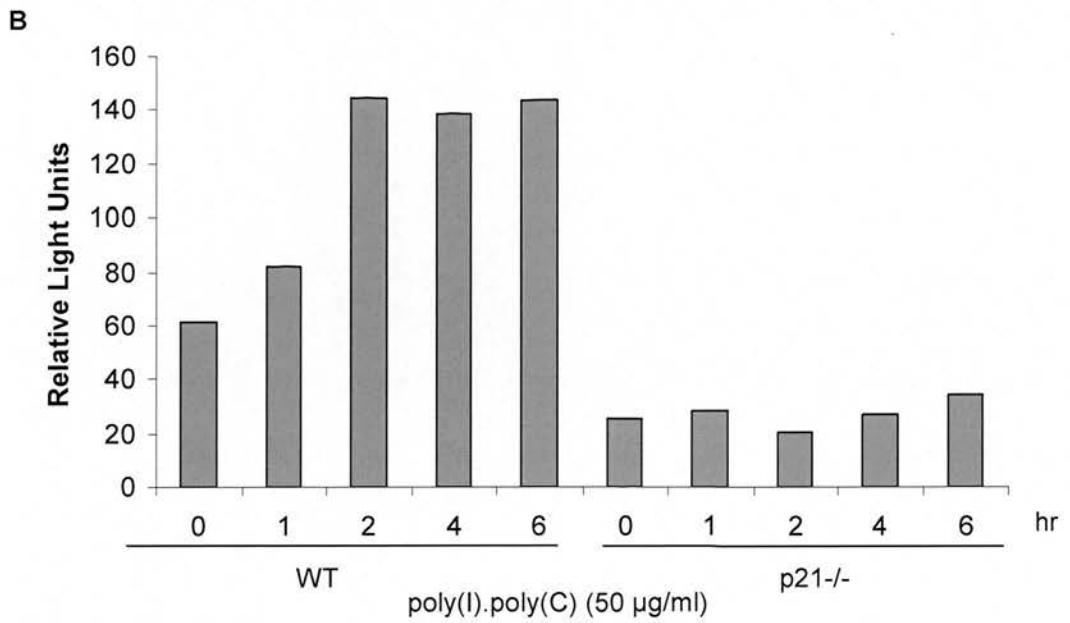
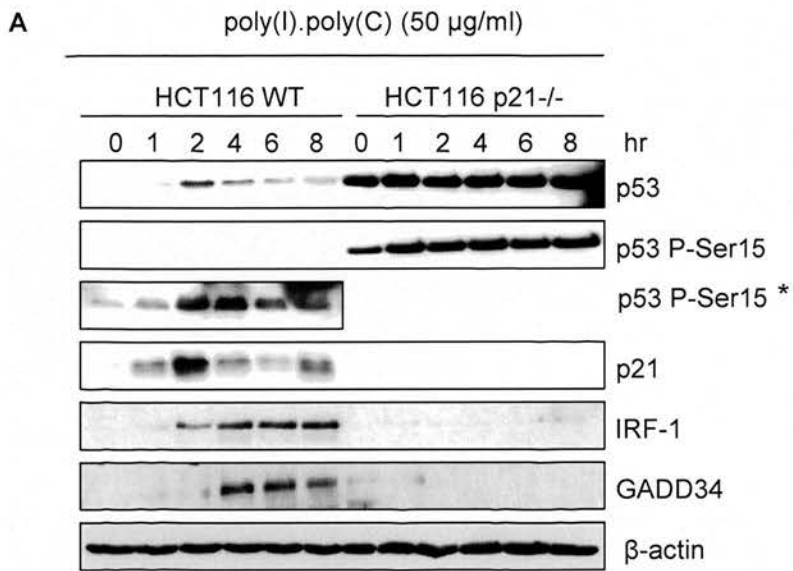


Figure 3.4 The p53 viral response is suppressed in p21^{-/-} cells. (A) HCT116 WT and p21^{-/-} cells were treated with 50 µg/ml poly(I).poly(C) and harvested at the stated time points. Cells were lysed with urea lysis buffer. Whole cell lysates were resolved by SDS-PAGE. p53, p53 serine-15 phosphorylation, p21, IRF-1 and GADD34 were detected by immunoblotting. β-actin was used a loading control. 10 µg protein was loaded per lane. * 30 µg protein was loaded per lane. **(B)** p53 transcriptional activity in response to poly(I).poly(C) was monitored by a *p21*-Luciferase reporter assay. HCT116 WT and p21^{-/-} cells were transiently transfected with 1 µg *p21*-Luciferase and 1 µg pCMV-βgal reporter and treated with 50 µg/ml poly(I).poly(C) 24 hr after transfection. Cells were harvested at the time points indicated and lysed with 5x Reporter Lysis Buffer (Promega). Luciferase activity was detected by a luminometer. p53-dependent activity (relative light units) is expressed as a ratio of *p21*-Luciferase activity to the internal transfection control β-gal.

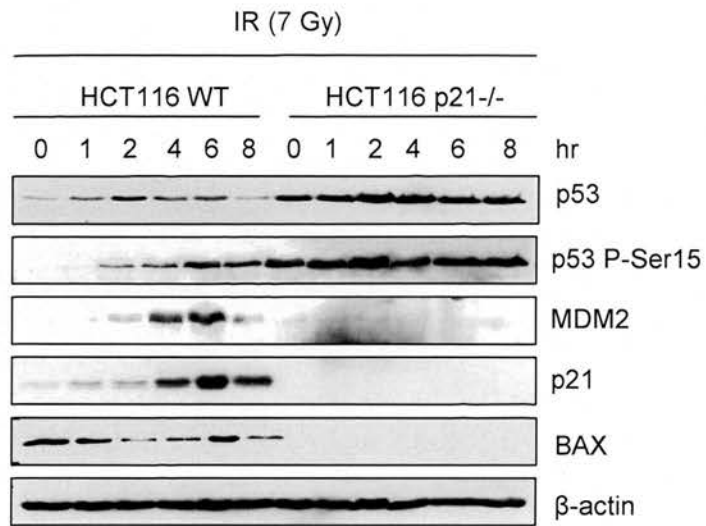
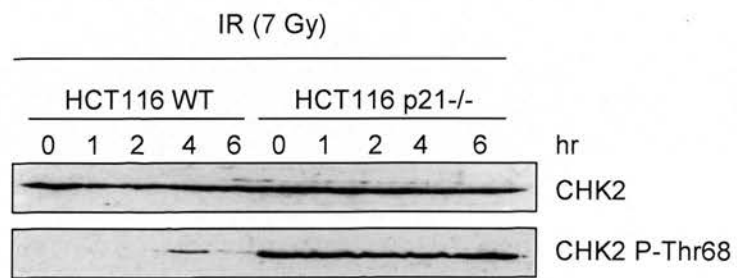
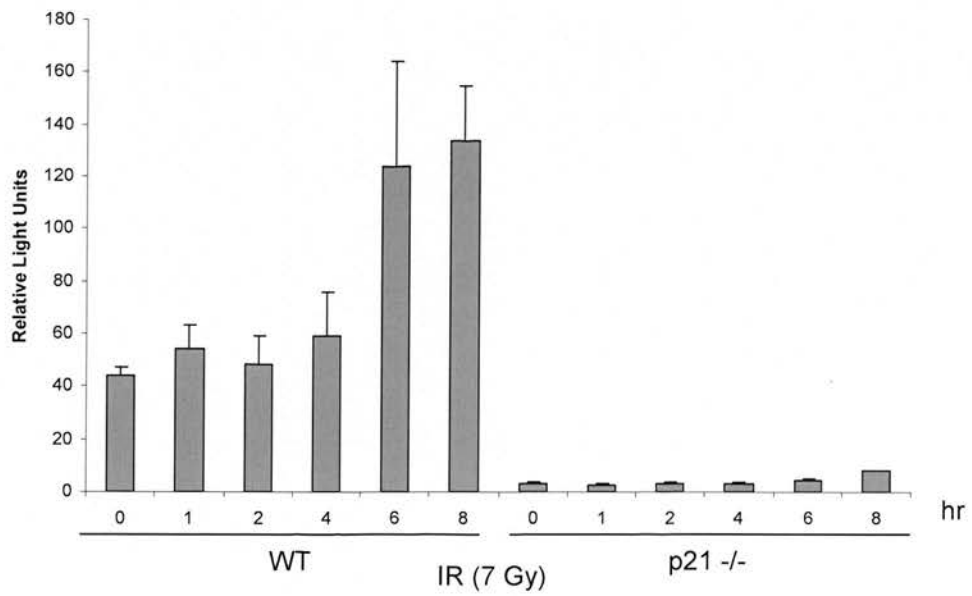
A**B****C**

Figure 3.5 The p53 DNA damage response is suppressed in p21^{-/-} cells. (A) HCT116 WT and p21^{-/-} cells were treated with 7 Gy of ionising radiation (IR) and harvested at the stated time points. Cells were lysed with urea lysis buffer. Whole cell lysates were resolved by SDS-PAGE. p53, p53 serine-15 phosphorylation, MDM2, p21 and BAX were detected by immunoblotting. β -actin was used as a loading control. 20 μ g protein was loaded per lane. (B) CHK2 and CHK2 threonine-68 phosphorylation was detected following exposure to IR by immunoblotting. 30 μ g of protein was loaded per lane. (C) p53 transcriptional activity in response to IR was monitored by a *p21*-Luciferase reporter assay. HCT116 WT and p21^{-/-} cells were transiently transfected with 1 μ g *p21*-Luciferase and 1 μ g pCMV- β gal reporter and treated with 7 Gy IR 24 hr post-transfection. Cells were harvested at the time points indicated and lysed with 5x Reporter Lysis Buffer (Promega). Luciferase activity was detected by a luminometer. p53-dependent activity (relative light units) is expressed as a ratio of p21-luciferase activity to the internal transfection control β -gal.

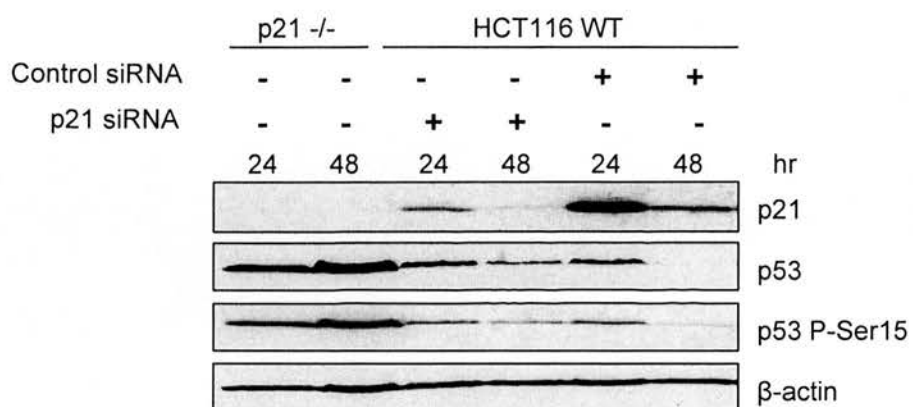


Figure 3.6 Basal p53 protein levels are p21-dependent. HCT116 WT cells were transfected with either p21 siRNA or control siRNA and were harvested at 24 and 48 hr post-transfection. Cell pellets were lysed with urea lysis buffer. Whole cell lysates were resolved by SDS-PAGE. p21, p53, and p53 serine-15 phosphorylation were detected by immunoblotting. β-actin was included as a loading control. 10 μg protein was loaded per lane.

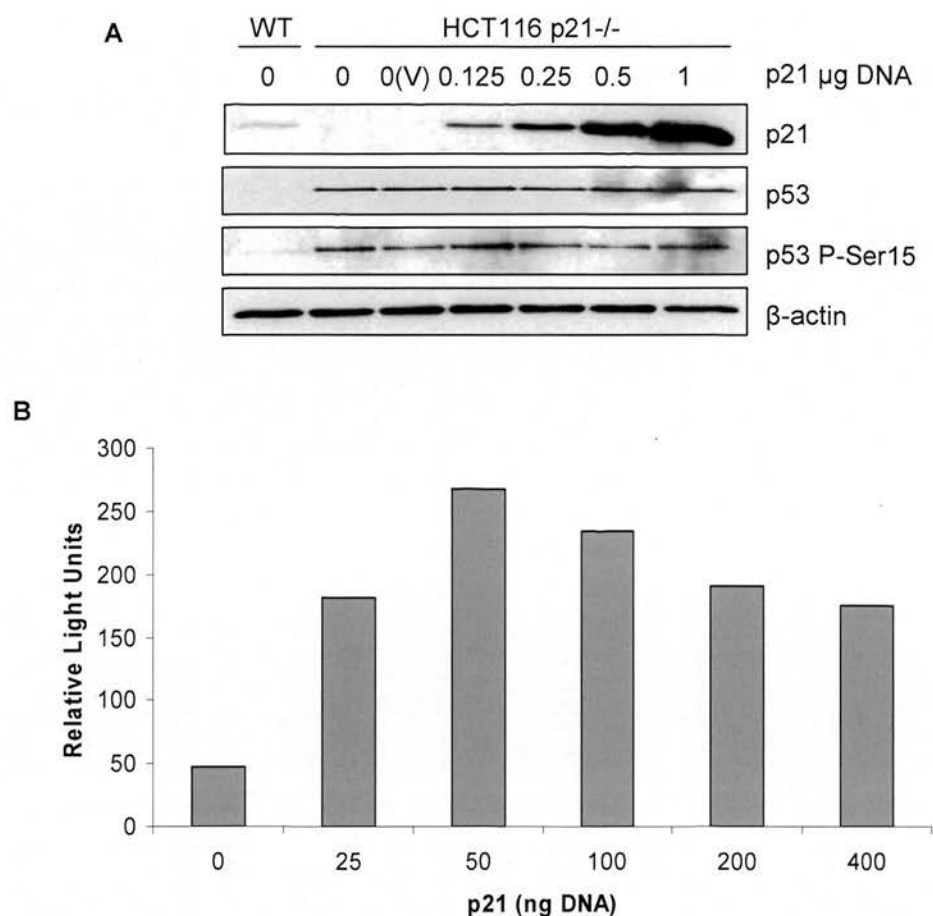


Figure 3.7 Transient transfection of p21 can partially recover p53 activity yet has no effect on p53 protein levels. (A) Over-expression of *p21* in HCT116 p21^{-/-} cells did not suppress p53 protein levels. Increasing amounts of the plasmid containing full-length p21 was transiently transfected into p21^{-/-} cells. Cells were harvested 24 hr after transfection, and lysed with urea lysis buffer. Whole cell lysates were resolved by SDS-PAGE. p21, p53, and p53 serine-15 phosphorylation were detected by immunoblotting. β -actin was used as a loading control. 10 μ g of protein was loaded per lane. Lanes were loaded as follows: WT untransfected control, 0 μ g; p21^{-/-} untransfected control, 0 μ g; p21^{-/-} vehicle control transfected with 1 μ g empty pcDNA3.1 vector, 0(V) μ g; p21^{-/-} 0.125 μ g; p21^{-/-} 0.25 μ g; p21^{-/-} 0.5 μ g; and p21^{-/-} 1 μ g. **(B)** p21-dependent recovery of p53 activity. HCT116 p21^{-/-} cells were co-transfected with increasing amounts of the *p21* gene as indicated and fixed levels of *p21*-Luciferase (1 μ g) and pCMV- β gal (1 μ g), and cells were harvested 24 hr post-transfection and analysed for p53 activity. p53-dependent transactivation activity is represented as relative light units (figure 3.7B was kindly provided by M.Scott).

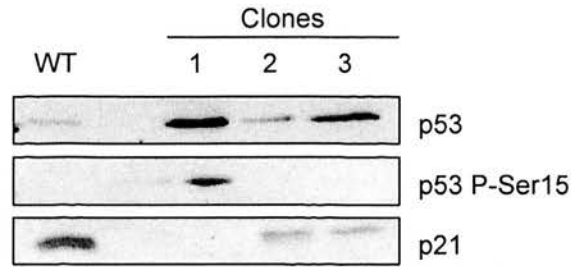


Figure 3.8 Stable reintroduction of p21 into HCT116 p21^{-/-} cells restores basal levels of p53 and phosphorylation of p53 at serine-15. HCT116 p21^{-/-} cells were transfected with 1 μ g pIRESpuro2 vector expressing full length p21. 24 hours post-transfection, cells containing the plasmid were selected for by the addition of puromycin. Pooled clones were expanded and permanently maintained under selection conditions. To confirm that the clones were expressing p21, immunoblotting was carried out. Cells were harvested at ~70 % confluency and lysed in urea lysis buffer. Whole cell lysates were resolved by SDS-PAGE. p21, p53 and p53 serine-15 phosphorylation was detected by immunoblotting. 10 μ g of protein was loaded per lane Clone 2 cells were used for further experiments.

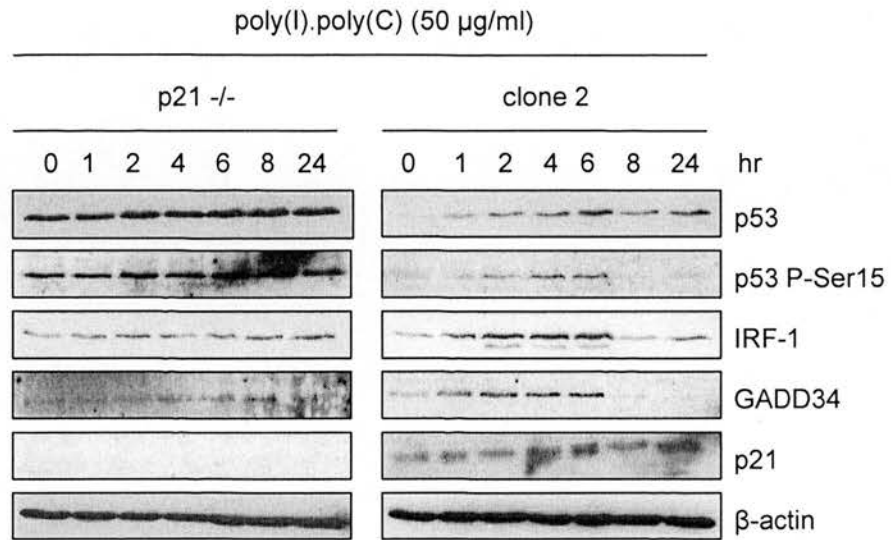


Figure 3.9 Stable reintroduction of p21 into HCT116 p21^{-/-} cells restores the p53 viral response. Clone 2 cells which stably express full length p21 and HCT116 p21^{-/-} were treated with 50 µg/ml poly(I).poly(C) and harvested at the indicated time points. Cells were lysed with urea lysis buffer. Whole cell lysates were resolved by SDS-PAGE. p53, p53 serine15 phosphorylation, IRF-1, GADD34 and p21 were detected by immunoblotting. β-actin was used as a loading control. 20 µg of protein was loaded per lane.

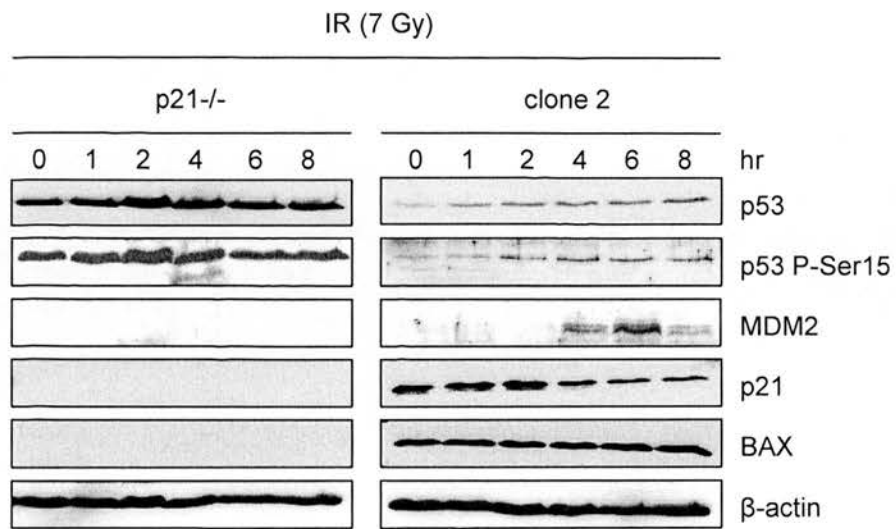


Figure 3.10 Stable reintroduction of p21 into HCT116 p21^{-/-} cells restores the p53 DNA damage response. Clone 2 cells which stably express full length p21 and HCT116 p21^{-/-} were treated with 7 Gy of IR and harvested at the indicated time points. Cells were lysed with urea lysis buffer. Whole cell lysates were resolved by SDS-PAGE. p53, p53 serine-15 phosphorylation, MDM2, p21, and BAX were detected by immunoblotting. β-actin was used as a loading control. 20 μg of protein was loaded per lane.

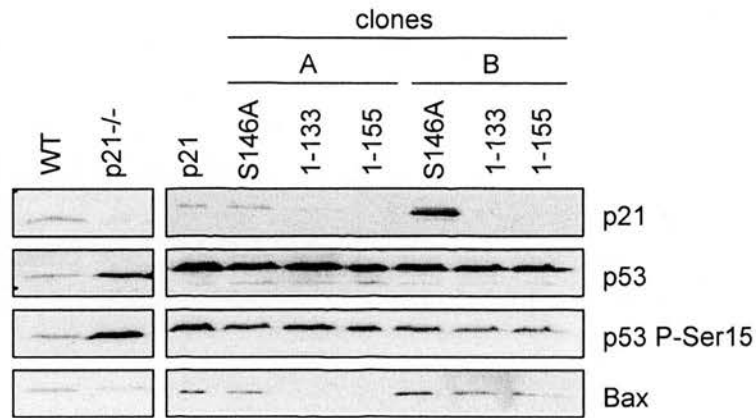


Figure 3.11 The C-terminus of p21 is not required for recovery of p53 activity. (A) HCT116 p21^{-/-} cells were co-transfected with 1 μ g empty pIRESpuro2 vector and 1 μ g of pcDNA3.1 containing either full-length p21, p21 serine 146 to alanine (S146A) mutant, p21 1-133 truncation or p21 1-155 truncation. Successfully transfected cells were selected with puromycin. Clones were selected in duplicate and termed A and B. Whole cell lysates were resolved by SDS-PAGE and immunoblotting was used to detect p21, p53, p53 serine-15 phosphorylation and BAX. 20 μ g of protein was loaded per lane.

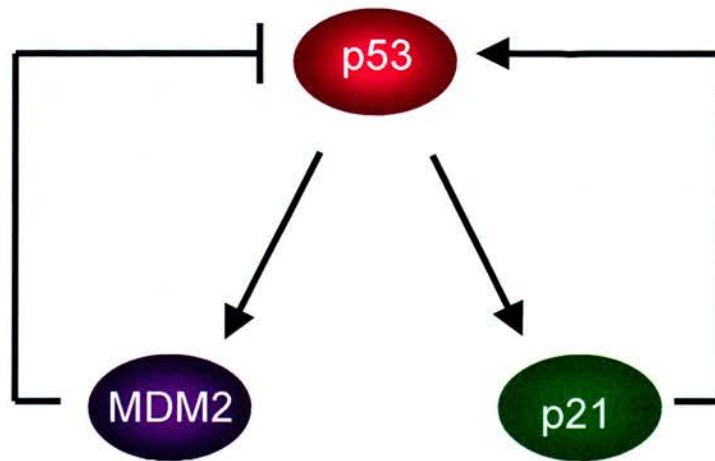


Figure 3.12 A model of p53 regulation by autoregulatory feedback loops. p53 up-regulates *MDM2* expression, MDM2 then negatively feeds back to p53 and drives its degradation. p53 up-regulates *p21* expression, p21 then positively feeds back to p53 and drives its activation. Inhibition represented by T-shaped lines. Activation represented by arrows.

LOSS OF p21 CAUSES ABERRANT LOCALISATION OF p53 AND
REPRESSES EXPRESSION OF p53 TARGET GENES IN
THREE MODEL SYSTEMS

4.1 Introduction

DNA microarrays have become an established technique in monitoring the expression of thousands of genes simultaneously (Manning *et al.*, 2007). Within an organism, every cell with a nucleus has the same genome but only a minority of genes are expressed in quantities large enough to have an effect. Gene expression is a highly complex and tightly regulated process that governs development, tumour progression, and also allows the cell to respond to the environment inside and outside the cell (Plomin & Schalkwyk, 2007; Rhodes & Chinnaiyan, 2005). Using microarray technology changes in transcription rate of nearly all genes in a particular tissue or cell type, can be measured in disease states, during development, and in response to intentional experimental perturbation, such as gene disruption and drug treatments (Rhodes & Chinnaiyan, 2005; Stoughton, 2005). The resulting gene expression profiles can help illuminate mechanisms of disease, predict disease progression, assign function to previously un-annotated genes, group genes into functional pathways and predict activities of new compounds (Stoughton, 2005). Although the principal use of microarray technology is gene-expression profiling, the

technology is being applied to additional processes including: genome-wide epigenetic analysis; protein-DNA interactions by on-chip chromatin immunoprecipitation; and detailed analysis of genomic DNA with respect to sequence, structure, copy number and SNP regions (Hoheisel, 2006; Stoughton, 2005). For the purpose of this chapter, discussion of microarray technology will focus on gene expression profiling.

Microarrays detect DNA by taking advantage of the complementarity of the DNA duplex, whereby short single-stranded segments of DNA are hybridised to their complements (Plomin & Schalkwyk, 2007; Manning *et al.*, 2007). Microarrays are miniature devices containing thousands of DNA sequences, which act as gene-specific probes, immobilised on a solid support (nylon, glass, or silicon) in a highly parallel format (Draghici *et al.*, 2006; Manning *et al.*, 2007). Microarrays can be categorised as cDNA arrays, using probes constructed with PCR products up to a few thousand base pairs; or oligonucleotide arrays, using either short (25-30mer) or long (60-70mer) oligonucleotide probes. Probes can either be contact-spotted, ink-jet deposited, or directly synthesised onto the solid support (Draghici *et al.*, 2006). A microarray study is a multi-step process and the aim commonly is to look at differences in the expression of specific genes across samples. RNA isolated from tissues or cells comprises a complex mixture of different RNA transcripts. The abundance of individual transcripts in the mixture is a reflection of the expression levels of the corresponding genes. RNA is reverse transcribed into complementary DNA (cDNA), labelled with a radioactive, fluorescent or chemiluminescent tag, and hybridised to the microarray. The intensity of the signal produced by each bound probe indicates the relative abundance of that transcript in the sample and is a

measure of the expression level of the corresponding gene. The intensity readings from the image of the microarray are background adjusted, processed and analysed (Plomin & Schalkwyk, 2007; Stoughton, 2005; Manning *et al.*, 2007).

Reliability issues in microarray analysis can arise from the affinity of the probe to its target transcript under the hybridisation conditions, steric effects of labels, insufficient measurement replication, detection of low-abundance transcripts, and errors in background subtraction (Draghici *et al.*, 2006). Modern microarrays are increasingly commercially produced leading to optimisation and characterisation of probes, and the steric effect of labels on transcripts. Much information is contained in the behaviour of low-abundance transcripts whose brightness is not much above the background level, therefore negative control spots containing the average sequence properties of the other probes but avoiding homology to any expected sequences in the sample, can be important in subtracting background offsets. Similarly it is equally important to have a positive subset of transcripts which are not different between two samples (Draghici *et al.*, 2006; Stoughton, 2005).

A limitation of microarray technology is that although changes in mRNA provide an insight into which genes are transcriptionally active, this does not automatically translate into changes in protein levels which are arguably more directly related to cell function than mRNA messages (Stoughton, 2005; Manning *et al.*, 2007). Generally gene expression is responsive to the cellular and extra-cellular environment, and there is a tight connection between the function of a gene product and its expression pattern. Hence, regulation of gene expression controls when and where the protein is made and in what quantity, indicating that generally mRNA levels are surrogates for corresponding protein levels (Brown & Botstein, 1999).

The tumour suppressor function of p53 is due mainly to its activity as a transcription factor (Levine, 1997). The transcriptional program regulated by p53 has previously been analysed using oligonucleotide arrays (Zhao *et al.*, 2000; Kannan *et al.*, 2001). Zhao *et al.* (2000) used a human colon cell line, EB-1, carrying a wild-type p53 gene under the control of an inducible metallothionein promoter to screen for p53-regulated genes. Of 6,000 genes examined for p53 regulatory responses, they found 107 induced and 54 repressed genes. Similarly, Kannan *et al.* (2001) used a temperature sensitive p53 (ts p53Val135) expressed in the human lung cancer cell line H1299, to analyse the p53 mediated transcriptional profile. The temperature sensitive p53 protein changes from a mutant to wild-type conformation by a temperature switch from 37 °C to 32 °C. Of 7,070 genes analysed, 259 genes were up-regulated and 125 genes were down regulated. However, inhibition of protein synthesis by cyclohexamide, resulted in a reduction of p53-regulated transcripts to 38 up-regulated and 24 down-regulated. This supports the argument that many of the identified p53 regulated genes are indirect targets (Kannan *et al.* 2001). In both studies, the probes of the microarrays were randomly selected from the human genome, therefore indicating that p53 may regulate 2-4% of all human genes.

A recent study by Rahman-Roblick *et al.* (2007) was the first to investigate p53-dependent expression at the protein level. They investigated the effect of p53 activation on the proteome using 2D gel electrophoresis and mass spectrometry analysis of mitogen-C treated HCT116 wild-type cells. Approximately 5,800 protein spots were separated, and 2% showed p53-dependent changes in expression (Rahman-Roblick *et al.*, 2007). This result is consistent with previous DNA microarray data (Zhao *et al.*, 2000; Kannan *et al.*, 2001), and indicates that the

number of proteins regulated by p53 are approximately equal to the number of p53-regulated genes.

In this chapter, commercially available oligonucleotide microarrays designed to profile the gene expression of 113 genes involved in p53 pathways (SuperArray), were used to investigate the effect of p21 on the transcriptional program regulated by p53. Three model systems were used: HCT116 isogenic cell panel; normal human fibroblast (NHF) cells with specific siRNA-targeted disruption of the *p21* gene; and B-cells from mice lacking the *p21* gene. In all three model systems, deletion of the *p21* gene resulted in p53 nuclear exclusion and eliminated the p53 transcriptional response.

4.2 Results

4.2.1 Loss of p21 influences the cellular localisation of endogenous p53

In the previous chapter, data was presented showing that loss of p21 in the HCT116 colon carcinoma cell line has an adverse effect on p53 transcriptional activity, whereby p53 stabilisation is uncoupled from its activity as a transcription factor and shows defects in the p53 response to DNA damage and double stranded RNA. Subsequently, complementation of the *p21* gene into the HCT116 p21^{-/-} cells was sufficient to reactivate the p53 transcriptional programme in response to cellular damage.

Localisation of p53 to the nucleus is essential for its function as a transcription factor (Ginsburg *et al.*, 1991). Therefore the subcellular localisation of

p53 in the absence of p21 was examined. Proteins from HCT116 WT and p21^{-/-} cells were differentially extracted according to their subcellular localisation, and analysed by immunoblotting (Figure 4.1). In WT cells, a small amount of p53 was detected in the nucleus and no phosphorylation of p53 at serine-15 could be detected (Figure 4.1A). In striking contrast, in p21^{-/-} cells a higher level of p53 protein was detected and predominately localised to the cytoplasm and membranes/organelles (Figure 4.1A). A relatively small proportion of p53 was also localised to the nucleus (Figure 4.1A). However, all phosphorylated p53 at serine-15 was localised to the cytoplasm and membranes/organelles (Figure 4.1A). These observations indicate that p21 may enhance nuclear retention of p53 and subsequent transcriptional activity.

p53 serine-15 and CHK2 threonine-68 are specific target sites for the ATM kinase, and high phosphorylation levels have been observed for both proteins in the absence of p21 (Figure 3.4A and B). As p53 was mislocalised in p21^{-/-} cells, cellular localisation of additional ATM targets that are involved in the p53 pathway were examined (Figure 4.1A). Loss of p21 had no effect on the subcellular localisation of MDM2 and CHK1, whereas CHK2 and E2F1 were partially mislocalised (Figure 4.1A). In WT cells CHK2 was localised to the cytoplasm and membranes/organelles, compared to the p21^{-/-} cells where CHK2 was cytoplasmic. E2F1 in WT cells was predominately nuclear, where as in p21^{-/-} cells a small proportion of endogenous E2F1 was cytoplasmic. Neither CHK2 nor E2F1 mislocalisation was as striking as that of p53, but highlights that subcellular localisation of other proteins in addition to p53 are altered by loss of p21.

DAPK-1 is a serine/threonine protein kinase that functions as a component of an oncogene activated checkpoint that activates p53 activity, and promotes apoptosis

(Raveh *et al.*, 2001). In addition p21 has been characterised as a DAPK-1 substrate *in vitro* (Fraser & Hupp, 2007). Surprisingly, DAPK-1 protein was not detected in p21^{-/-} cells, whereas in WT cells DAPK-1 was localised mainly to membranes/organelles, and to a lesser extent the nucleus (Figure 4.1A).

To confirm that this subcellular fractionation method yields distinct fractions, proteins from each fraction were resolved by SDS-PAGE and analysed by Coomassie staining. The protein expression patterns from each fraction are clearly distinct and confirm the validity of the technique (Figure 4.1B). Further validation should be made by extracting proteins bands unique to each fraction and analysing by mass spectrometry to identify proteins representative of each fraction.

To further confirm the status of p53 localisation in the HCT116 p21^{-/-} cells, an alternative method (Gilbert & Allan, 2001) was used to fractionate cells involving nuclear extraction and nuclease digestion. This technique separates the insoluble nuclear debris from the soluble nuclear fraction containing chromatin. Transcriptionally active p53 should be associated with chromatin. In WT cells there is approximately 4-fold less total cellular p53 than the p21^{-/-} cells (Figure 4.1C, lane E), and the majority of p53 in WT cells was associated with the soluble nuclear fraction containing chromatin (Figure 4.1C, lane SN) and was not detected in the insoluble nuclear fraction (Figure 4.1C, lane P). In contrast, in the p21^{-/-} cells, there was a high level of p53 protein detected in the total cellular extract but barely detectable amounts in either nuclear fraction (Figure 4.1C), consistent with p53 being predominantly cytoplasmic (Figure 4.1A). This data indicates that in WT cells p53 is chromatin associated and may be active as a transcription factor due to its correct cellular localisation, whereas in the absence of p21, p53 is not localised to the

nucleus and may not be active as a transcription factor due its atypical cytoplasmic location.

4.2.2 Reintroduction of p21 restores p53 nuclear localisation

As previously shown, stable reintroduction of p21 into HCT116 p21^{-/-} cells was sufficient to restore p53 transcriptional activity in response to both dsRNA (Figure 3.9) and IR (Figure 3.10). To confirm that restoration of p53 activity was due to a restoration of p53 nuclear localisation, proteins from HCT116 WT, p21^{-/-}, and clone 2 cells stably expressing p21 (Figure 3.7) were differentially extracted according to their subcellular localisation, and analysed by immunoblotting (Figure 4.2A). In WT cells p53 was confined to the nuclear fraction, whereas in p21^{-/-} cells p53 was localised to the cytoplasm, membranes/organelles and the nuclear fraction. However, stable reintroduction of p21 into the p21^{-/-} cells, as represented by clone 2 cells, was sufficient to restore p53 nuclear localisation (Figure 4.2A). This data confirms that p21 regulates p53 transcriptional activity (Figure 3.9) by controlling its subcellular localisation (Figure 4.2A). Similarly, CHK2 localisation pattern was also restored (Figure 4.2A). In WT cells CHK2 was localised to the cytoplasm and membranes/organelles, whereas in p21^{-/-} cells CHK2 was confined to the cytoplasm. In clone 2 cells CHK2 localisation was restored to that of WT cells. Therefore p21 may regulate additional targets to p53 by controlling their subcellular localisation.

The C-terminus of p21 has been shown not to be required for reactivation of p53 transcriptional activity (Figure 3.11). Here full-length p21 and p21¹⁻¹³³ clones (HCT116 p21^{-/-} cells stably expressing full-length p21 and p21¹⁻¹³³ C-terminal

truncation, respectively) were compared to HCT116 p21^{-/-} and WT cells in respect to p53 subcellular localisation. For simplicity's sake only cytoplasmic (F1) and nuclear fractions (F3) are shown (Figure 4.2B). In p21^{-/-} cells, p53 was detected in both the cytoplasm and the nucleus, whereas in WT cells p53 was confined to the nuclear fraction. Stable expression of full-length p21 and p21¹⁻¹³³ C-terminal truncation was sufficient to restore p53 nuclear localisation (Figure 4.2B), indicating that the C-terminus of p21 is not required for the restoration of p53 nuclear localisation. In WT cells E2F1 was localised to the nucleus but mislocalised in p21^{-/-} cells to the cytoplasm. Stable expression of full-length p21 and p21¹⁻¹³³ C-terminal truncation was also sufficient to restore E2F1 nuclear localisation (Figure 4.2B). These results indicate that p21 may regulate additional targets to p53 by controlling their subcellular localisation, and that the C-terminus of p21 is not required for this function.

Overall, stable reintroduction of p21 into p21^{-/-} cells is sufficient to restore p53 activity and nuclear localisation, and the nuclear retention of p53 is independent of the C-terminus of p21. These observations demonstrate that p21 is an essential regulator of the p53 pathway by controlling its subcellular localisation.

4.2.3 Aberrant localisation of p53 is not associated with unfolding

p53 is a conformationally flexible protein, which has been shown to be partially unstructured in its native conformation (Bell *et al.*, 2002). An allosteric model has been proposed where native p53 protein is partially unfolded, and the equilibrium between partially-folded states can modulate p53 conformation and activity (Bell *et*

al., 2002; Lane & Hupp, 2003). Furthermore, most cancer-derived p53 mutants are thermodynamically unstable and in an unfolded conformation (Bullock & Firsht, 2001). The extent of folding and unfolding of wild-type or mutant p53 can be quantified by the use of monoclonal antibodies specific for epitopes confined to each respective conformation. Previously, Shimizu *et al.* (2006) showed that in H1299 cells transfected with wild-type p53, the ratio of folded to unfolded wild-type p53 is approximately 9:1, indicating that 10 % of wild-type p53 is in the unfolded conformation.

In HCT116 WT cells p53 was progressively ubiquitinated in response to DNA damage induced by IR (Figure 4.3A). Higher molecular weight bands detected by over-exposure of an anti-p53 (DO1) immunoblot, have previously been characterised as ubiquitinated forms of p53 (Lohrum *et al.*, 2001; Wallace *et al.*, 2006). In the p21^{-/-} cells, the p53 ubiquitination ladder was not detected. This may be expected as polyubiquitination of p53 is proposed to take place in the nucleus (Brooks & Gu, 2004), and in the absence of p21, the majority of p53 is confined to the cytoplasm. However, strikingly in p21^{-/-} cells, and absent in WT cells, a ladder of p53 lower molecular weight adducts was detected approximately 2 hours after irradiation (Figure 4.3A). This suggests that p53 from p21^{-/-} cells, which is re-localised to the cytoplasm, may be unfolded, and therefore more prone to proteolytic degradation.

An antibody capture ELISA was used to quantify the levels of unfolded and folded p53 in HCT116 WT, p21^{-/-}, and clone 2 cells. BSA was used as a negative control. Cell lysates were incubated in ELISA wells coated with monoclonal antibodies: DO1 specific for total p53; PAb1620 specific for folded p53; DO12

specific for unfolded p53; or PAb240 specific for unfolded p53. Following capture of the respective conformational variants of p53, all captured p53 was detected using a polyclonal antibody, CM1. The capture profiles for each monoclonal p53 antibody used in each cell line, demonstrates that there is no detectable difference between cell lines, with the majority of p53 detected in the folded conformation, as detected by PAb1620 (Figure 4.3B). Direct comparison of p53 in the PAb1620 folded conformation to the PAb240 unfolded conformation, shows that the ratio of folded to unfolded p53 is approximately 50:1, for WT, p21^{-/-} and clone 2 cells (Figure 4.3C). However, there is a detectable difference in all cell lines used between DO1 and PAb1620 captured p53 (Figure 4.3B). If we assume that p53 is either folded or unfolded, and have shown by PAb240 and DO12 detection that the amount of unfolded p53 is negligible (Figure 4.3B), then the amount of p53 captured by DO1 should be approximately equal the amount of p53 captured by PAb1620. However, in all cell lines used, the ratio of total p53 detected by DO1 to folded p53 detected by PAb1620 is approximately 1.5:1, which indicates that approximately 67 % of p53 is in the folded conformation. We can speculate that the unaccounted for p53 is in a partially folded conformation in which both the PAb1620 and PAb240 epitopes are masked.

This data shows that in response to DNA damage induced by IR, p53 in the p21^{-/-} cells is more prone to proteolytic degradation but this is probably due to cytoplasmic re-localisation rather than protein unfolding. Here we show that in undamaged cells, p53 conformation is unaffected by the absence of p21.

4.2.4 p53 localisation is independent of DNA damage

DNA damage induced by IR has been shown to promote activation of p53-dependent gene expression (Figure 3.5A). To determine the effect of DNA damage on p53 subcellular localisation, HCT116 WT and p21^{-/-} cells were treated with 7 Gy IR and harvested after 4 hours (Figure 4.4). Proteins were extracted according to their subcellular localisation from each sample and analysed by immunoblotting. In un-irradiated WT cells, p53 was weakly detected in the nuclear fraction. In response to IR p53 protein levels increased by approximately 4-fold, yet remained confined to the nucleus. In p21^{-/-} cells p53 was mainly localised to the cytoplasm and membranes/organelles, with a small pool of p53 localised to the nucleus. In response to IR, both p53 levels and subcellular localisation were unchanged in the p21^{-/-} cells (Figure 4.4). This supports the observation that in p21^{-/-} cells the p53 response to IR is inactive (Figure 3.5A).

4.2.5 Microarray analysis of the HCT116 isogenic cell panel

Loss of p21 in the HCT116 cell line results in repression of p53 transcriptional activity basally (Figure 3.3) and in response to cellular stresses including dsRNA (Figure 3.4) and IR (Figure 3.5). Luciferase reporter assays and detection of specific p53 targets by immunoblotting were used to determine the status of p53 transcriptional activity. Here oligonucleotide microarrays, designed to profile gene expression of 113 genes involved in the p53 pathway (SuperArray), were used to assess the global effect of loss of p21 in the HCT116 cell line in response to IR.

HCT116 WT, p21^{-/-} and p53^{-/-} cells were irradiated with 7 Gy IR and incubated for 4 hours. p53^{-/-} cells were included as a control to determine which genes included on the microarray are regulated by p53, and which genes are expressed independent of p53 in the HCT116 cell line. Cell line variations in gene expression are very common, including p53 specific targets, with often conflicting data in the literature. Total RNA was isolated from all cell lines, before and after irradiation, reverse transcribed into cDNA, labelled with biotin and hybridised to the oligonucleotide arrays (Oligo GEArray[®] DNA Microarray, Human p53 Signalling Pathway, SuperArray). The raw image of each microarray (Figure 4.5) provides an overview of the expression pattern in each cell line, and the effect of IR. Table 4.1 details which genes were expressed in each cell line and in response to IR, as determined by visual observation. No speculation of fold changes has been inferred here, and genes not expressed in all samples have been omitted. From a visual assessment of the raw images of non-irradiated WT, p21^{-/-} and p53^{-/-} cells (Figure 4.5), it appears that approximately a third more genes were expressed in WT cells compared to p21^{-/-} and p53^{-/-} cells. The expression patterns observed in p21^{-/-} and p53^{-/-} cells were very similar, with 21 and 20 genes expressed, respectively (Table 4.1). However, within this there are subtle differences such as, the pro-apoptotic genes *BAK1* and *DAPK-1* were expressed in p21^{-/-} cells but not in p53^{-/-} cells, suggesting that p21^{-/-} cells may more readily undergo apoptosis than p53^{-/-} cells, *PTEN* was expressed in p21^{-/-} cells but not in p53^{-/-} cells, and *ATM* and *CDKN1A* were expressed in p53^{-/-} cells but not in p21^{-/-} cells (Table 4.1). These findings indicate that loss of p21 causes a global loss of p53 activity similar to having targeted inactivation of the *p53* gene.

In response to IR, in WT cells there was an increase in gene expression of a majority of genes (Figure 4.5). In p53^{-/-} cells, there was very little observed difference in the expression pattern of irradiated cells compared with non-irradiated control (Figure 4.5), indicating that p53 is required for IR induced induction of p53 targets genes included on the microarray. The only genes expressed in response to IR in p53^{-/-} cells were *BAK1* and *PTEN* (Table 4.1). These genes were also expressed in non-irradiated p21^{-/-} cells, indicating that in the HCT116 cell line, expression of *BAK1* and *PTEN* is p53-independent. Irradiation of p21^{-/-} cells caused a decrease in general gene expression, 21 genes were expressed in non-irradiated control cells compared to 4 genes in irradiated samples. The 4 genes expressed in irradiated p21^{-/-} cells were *BAK1*, *BCL2*, *CDK7* and *CDKN2A* (Table 4.1). The overall decrease in gene expression and over-expression of *BAK1* may indicate that p21^{-/-} cells were unable to cope with this degree of damage, and were undergoing apoptosis.

The microarray images (Figure 4.5) were analysed using the GEM Expressions Analysis Suite software (SuperArray). Each image was fitted to a grid (manually or automatically) to define areas of individual spots. Averages of signal intensities and background noise of individually defined areas were calculated. Accurate control of starting RNA samples can be difficult and lead to discrepancies in chemiluminescent signal intensities between two probes. Therefore normalisation of signals between samples was achieved using selected normalisation control spots (Figure 4.5, indicated by red arrows), including house-keeping genes, which were considered to be expressed consistently under most circumstances. The GEM Expressions Analysis Suite software determines the normalised spot brightness of each gene by dividing the raw spot brightness of each gene by the average brightness

of the selected normalisation control spots. After normalisation and background correction, chemiluminescent signal intensities representative of mRNA levels, were expressed as relative units. Table 4.2 details differences in gene expression between samples as fold changes, calculated by determining the ratio of gene intensities between indicated samples. There is no standard criterion for the selection of differentially expressed genes, in regard to which values are significant. Therefore a cut-off value has been applied, where 1.5-fold change in gene expression in the test sample compared with the reference is defined as a significant induction or repression.

Individual genes were analysed in more detail (Figure 4.5, highlighted by a red box) by graphical representation of transcript levels (Figure 4.6). Generally, expression of a majority of genes was disrupted in p21^{-/-} and p53^{-/-} cells compared to WT cells, and are not induced by IR. Expression profiles of *CDK4*, *JUN* and *STAT1* represent the general trend (Figure 4.6). *CDK4* was expressed in non-irradiated WT cells, and in response to IR expression was enhanced approximately 2-fold (Figure 4.6, Table 4.2). In p21^{-/-} and p53^{-/-} cells *CDK4* was not expressed, even after irradiation. A similar expression profile is shown for *JUN*. In p21^{-/-} and p53^{-/-} cells, *STAT1* was expressed approximately 2-fold lower than in WT cells. In response to IR, *STAT1* expression remained unchanged in WT and p53^{-/-} cells, yet in p21^{-/-} cells *STAT1* expression was diminished. *MDM2* showed a similar expression profile to that of *STAT1*, in that *MDM2* is expressed in p21^{-/-} and p53^{-/-} cells but at levels approximately 1.5-fold lower than WT cells (Figure 4.6, Table 4.2).

Previously, high phosphorylation levels of specific ATM targets have been observed in the absence of p21 (Figure 3.4A, B). Microarray analysis shows that

ATM was expressed in WT cells, with minimal change in expression in response to IR. In p53^{-/-} cells there was a 2-fold reduction of *ATM* expression compared to WT cells, which was also unaffected by IR. Unexpectedly, *ATM* expression was not detected in p21^{-/-} cells, although mRNA levels may not directly reflect protein levels (Figure 4.6).

Particularly interesting in the microarray analysis were the genes that did not fit the general trend. In the non-irradiated cells, the only gene expressed at a higher level in p21^{-/-} cells than WT cells, was *DAPK-1*, by approximately 4-fold (Figure 4.6, Table 4.2). In response to IR, *DAPK-1* expression was increased in WT cells but decreased in p21^{-/-} cells. *DAPK-1* expression was not detected in p53^{-/-} cells. Although *DAPK-1* mRNA expression was elevated in p21^{-/-} cells, this may not translate to protein levels, as DAPK-1 protein could not be detected by immunoblotting (Figure 4.1A). In irradiated samples, the only gene up-regulated in p21^{-/-} cells compared to WT cells was *BAK1*, which was elevated by approximately 2-fold. *BAK1* expression was unchanged in the p53^{-/-} cells. BAK1 has a role in promoting apoptosis (Moll *et al.*, 2006), indicating that in response to damage, p21^{-/-} cells may undergo apoptosis more readily than WT or p53^{-/-} cells.

To provide an overall impression of the effect of loss of p21 on gene expression of proposed p53 target genes, cluster analysis of the microarray data was performed using the clustergram data analysis tool included in the GEM Expressions Analysis Suite software (SuperArray). The program clusters genes with similar expression profiles together, where genes that are more similar are joined to the right, and genes less similar are joined further to the left (Figure 4.7). Clustergram analysis of gene expression is presented for basal gene expression in the

HCT116 isogenic cell panel (Figure 4.7A) and in response to IR (Figure 4.7B). In Figure 4.7A colour coding of gene expression was according to each gene in all the samples, therefore expression levels of the same gene across all the samples can be compared, however expression levels of different genes in the same sample are not relative to one another. This analysis provides a clear picture of which individual genes are expressed in which sample but does not provide information regarding extent of expression in context with other genes. Here, basal expression of p53 target genes was clearly diminished in p21^{-/-} cells compared to WT cells. In Figure 4.7B clustergram analysis of gene expression levels is presented for all cell lines in response to IR. In contrast to Figure 4.7A, the extent of gene expression was colour coded according to all the values in all the samples, therefore enabling expression levels of all genes to be compared across all samples. This provides an overview of gene expression in cellular context, however this method is less sensitive and genes expressed at lower levels in a sample can be under represented. The clustergram analysis confirms that in response to IR in WT cells there was an increase in general gene expression, irradiation of p21^{-/-} cells further decreased p53-dependent gene expression, and irradiation of p53^{-/-} cells had generally no effect on gene expression (Figure 4.7B). Microarray analysis has shown that in the HCT116 cell line, loss of p21 causes inhibition of p53 transcriptional activity towards its targets indiscriminately, and is akin to inactivation of both copies of the *p53* gene.

4.2.6 The p21-null phenotype characterised in a cancer cell model applies to normal human cells

The work presented so far has used an isogenic cancer cell line panel, with targeted inactivation of the *p21* gene. The data has shown that in the HCT116 cancer cell line, p53 transcriptional activity and subcellular localisation are dependent on p21. To determine if p21-dependent regulation of p53 is a common mechanism or cell-type specific, levels of p21 were reduced in a normal cell model. Normal human fibroblast (here after referred to as NHF) cells derived from human skin (PromoCell), have previously been used to characterise regulation of p53 serine-15 phosphorylation (Tibbetts *et al.*, 1999). Here, p21 levels in NHF cells were reduced using p21 siRNA-mediated gene knockdown. NHF cells were treated with either p21 or control siRNA, and harvested 48 hours after transfection. Protein levels were assessed by immunoblotting (Figure 4.8). p21 siRNA successfully reduced p21 protein levels compared to control. Although minimum change in p53 protein levels and phosphorylation of p53 at serine-15 could be detected, there was a detectable change in BAX protein levels. BAX levels decreased in the absence of p21, compared to control siRNA treated cells (Figure 4.8). Previously BAX levels were found to be associated with p21 levels in HCT116 cells (Figure 3.5A; Figure 3.10; Figure 3.11), and may be a more sensitive marker of p21-deficiency than p53 levels.

The subcellular localisation of p53 was subsequently examined in NHF cells with reduced levels of p21. NHF cells were transfected with p21 or control siRNA and incubated for 48 hours, all proteins were differentially extracted according to their subcellular localisation, and analysed by immunoblotting (Figure 4.9). In p21

siRNA treated NHF cells p53 subcellular localisation was deviant compared to control siRNA NHF cells. In control cells, p53 was localised to the nucleus, whereas in p21 siRNA treated NHF cells p53 was localised to both the cytoplasm and the nucleus (Figure 4.9). This data indicates that p21-dependent regulation of p53 subcellular localisation is a general mechanism, not specific to the HCT116 cell line. In NHF cells, the difference in p53 levels and localisation are not as striking as the HCT116 cell model (Figure 4.1A), but it must be taken into account that the NHF cells were transiently transfected with p21 siRNA, as opposed to HCT116 p21^{-/-} cells which stably support inactivation of the p21 gene and have adapted accordingly.

MDM2 and CHK1 subcellular localisation were unaffected in NHF cells treated with p21 siRNA compared to control siRNA treated NHF cells (Figure 4.9). However, E2F1 localisation was marginally affected. In control siRNA treated cells E2F1 was nuclear, whereas in p21 siRNA treated cells, E2F1 was partially mislocalised to the cytoplasm (Figure 4.9). These observations are consistent with findings in the HCT116 cell model (Figure 4.1).

4.2.7 Microarray analysis of normal human fibroblast cells shows that loss of p21 suppresses p53-dependent gene expression

NHF cells treated with p21 siRNA show defects in p53 subcellular localisation, where approximately a quarter of total p53 is mislocalised from the nucleus to the cytoplasm compared to control siRNA treated NHF cells (Figure 4.9). In the HCT116 model mislocalisation of p53 is associated with loss of p53 transcriptional activity (Figure 4.7). Therefore to determine the effect of loss of p21 on p53

transcriptional activity in NHF cells, oligonucleotide microarrays, designed to profile gene expression of 113 genes involved in the p53 pathway (Oligo GEArray[®] DNA Microarray, Human p53 Signalling Pathway, SuperArray), were used. The DNA damage response induced by IR was also examined.

NHF cells were treated with p21 siRNA or control siRNA, incubated for 48 hours, irradiated with 5 Gy IR and harvested after further 4 hour incubation. Oligonucleotide microarrays were prepared as previously detailed (Materials & Methods 2.17). The raw image of each microarray provides an overview of the expression pattern of each siRNA treatment, and the effect of IR (Figure 4.10). Table 4.3 details which genes are expressed in each treatment and in response to IR, as determined by visual observation. No speculation of fold changes has been inferred here, and genes not expressed in all samples have been omitted. From a visual assessment of the raw images of non-irradiated NHF cells treated with p21 siRNA or control siRNA (Figure 4.10), loss of p21 caused a dramatic loss of p53-dependent gene expression. In control siRNA treated cells, 52 genes are expressed, compared to p21 siRNA treated cells, where only 7 genes are weakly detected (Table 4.3). This could highlight the importance of p21 in p53-dependent gene expression, but may also indicate that loss of p21 in NHF cells is causing a crisis resulting in a global reduction of gene expression, as housekeeping genes including β -actin, were also affected. This was not observed in HCT116 cells, where the level of gene expression of housekeeping genes were unaffected by loss of p21 (Figure 4.6). In response to irradiation, gene expression in p21 siRNA treated NHF cells showed some degree of recovery (Figure 4.10) with 56 genes expressed compared to only 7 genes detected in non-irradiated p21 siRNA treated NHF cells (Table 4.3). p21 siRNA treatment does

not cause complete loss of p21, and p53 redistribution to the cytoplasm is not as pronounced as in the HCT116 model. Therefore partial recovery of p53 activity was not surprising. In control siRNA treated cells, 60 genes were expressed in the irradiated sample, compared to 52 genes in non-irradiated sample. Although only 8 genes were additionally expressed in response to IR (Table 4.3), there was an increase in expression of genes previously detected at a low level in non-irradiated samples (Figure 4.10).

Microarrays were analysed as previously described in 4.2.5, where each signal was normalised to control spots (Figure 4.10, indicated by red arrows) and background corrected. Table 4.4 details differences in gene expression between samples as fold changes, calculated by determining the ratio of gene intensities between indicated samples. A cut-off value has been applied as before, where 1.5-fold change in gene expression in the test sample compared with the reference is defined as a significant induction or repression.

The expression profiles of selected individual genes were analysed in more detail (Figure 4.10, highlighted by a red box), by graphical representation of transcript levels (Figure 4.11). The general trend is illustrated by the expression profile of *ATM*, *BAX*, *CDK4*, *JUN* and *MDM2* (Figure 4.11), where each gene was expressed in control siRNA treated cells, and following DNA damage gene expression was enhanced by approximately 2-3-fold induction. In p21 siRNA treated NHF cells *ATM*, *BAX*, *CDK4*, *JUN* and *MDM2* were not expressed basally, but following DNA damage gene expression was induced. Gene expression was significantly lower in irradiated p21 siRNA treated cells compared to irradiated control siRNA treated cells, for example, *ATM*, *BAX*, *CDK4*, *JUN* and *MDM2*

expression levels were 9-fold, 4-fold, 3-fold, 4-fold, and 2-fold lower respectively, compared to irradiated control cells (Table 4.4). This data confirms that loss of p21 in NHF cells has an adverse effect on p53-dependent gene expression.

Graphical representation of 20 representative genes further illustrates the general trend where the expression of a majority of genes was disrupted in p21 siRNA treated NHF cells compared to control cells (Figure 4.12A). Irradiation stimulated a partial recovery of gene expression in p21 siRNA treated cells (Figure 4.12B), but expression levels were still significantly lower than that of control irradiated cells (Figure 4.12C). This data highlights the significance of p21 in p53-dependent gene expression.

Similar to the HCT116 model system, the two genes which diverge from the general trend in NHF cells treated with p21 siRNA were *BAK1* and *DAPK-1*. In non-irradiated p21 siRNA treated NHF cells a majority of genes were not expressed, except for *BAK1*, which was expressed approximately 2-fold more than in control siRNA treated cells. In response to IR, *BAK1* expression levels decreased to a level comparable to non-irradiated control cells. In contrast, *DAPK-1* was expressed at approximately 10-fold lower in non-irradiated p21 siRNA treated NHF cells than non-irradiated control cells. *DAPK-1* expression was induced in both p21 siRNA and control siRNA treated cells following irradiation, showing approximately 12-fold and 2-fold induction respectively. There was no significant difference in *DAPK-1* expression levels between the irradiated samples (Figure 4.11, Table 4.4). This indicates that cells lacking p21 may readily undergo apoptosis, due to increased expression of pro-apoptotic genes.

Interestingly *HSP90* was included as a control gene on the microarray, but in p21 siRNA treated NHF cells, expression of *HSP90* was elevated 2-fold compared to control cells. Irradiation of p21 siRNA treated NHF cells returned *HSP90* expression levels to those comparable to control cells. This was not observed in HCT116 cell model, where *HSP90* expression levels were consistent across cell lines.

As before, cluster analysis was performed (Figure 4.13). The extent of gene expression was colour coded according to all values in all the samples, allowing all four expression profiles to be clearly compared. As previously observed, a majority of genes were expressed in NHF cells treated with control siRNA, and a sub-set of genes were further expressed in response to irradiation. In contrast, in NHF cells treated with p21 siRNA, there was an overall suppression of gene expression except for expression of *BAK1*. Irradiation of these cells induced gene expression in a majority of genes, but to a much lower extent of that seen in control cells. Therefore in a normal cell model, loss of p21 can cause loss of p53-dependent gene expression.

4.2.8 p21-dependent regulation of p53 subcellular localisation is evolutionarily conserved

To determine if p21-dependent regulation of p53 subcellular localisation and transcriptional activity is evolutionarily conserved, a transgenic mouse model was employed. B-cells were selected as the model of choice, because mice homozygous for p53 mutated at serine-23 (equivalent of human serine-20), show defects in p53 stability and activity, and predominantly die from B-cell lineage tumours (MacPherson *et al.* 2004). Therefore B-cells may be more sensitive to alterations in

p53 status than other cell lines. B-cells give rise to antibody producing cells after infection, and are easily extractable using the B-cell specific marker, CD45 (Hardy *et al.* 2007). B-cells were extracted from p21 nullizygous (p21^{-/-}) and wild type (p21^{+/+}, referred to hereafter as WT) mice spleens. Proteins were differentially extracted according to their subcellular localisation, and analysed by immunoblotting (Figure 4.14). p53 subcellular localisation was atypical in the absence of p21 in the mouse model. In the p21^{-/-} B-cells, p53 was localised mainly to the cytoplasm with a small proportion localised to the nucleus, whereas in WT B-cells, all detectable p53 was localised to the nucleus (Figure 4.14). Thus, p21-dependent regulation of p53 localisation is conserved in mice, and may indicate a common mechanism of p53 regulation.

4.2.9 The mouse model illustrates that p53 activity is p21 gene dose dependent

In both HCT116 and NHF cells, loss of p21 caused suppression of p53-dependent gene expression as determined by p53 specific microarray analysis. In the NHF cells knock-down of p21 was not complete, and partial recovery of p53 activity was observed after stress, indicating that p53 activity may depend on p21 dose. In the mouse model system, this can be tested using B-cells extracted from p21 nullizygous (p21^{-/-}), heterozygous (p21^{+/-}) and wild-type (p21^{+/+}) mice. Mouse oligonucleotide microarrays (Oligo GEArray[®] DNA Microarray, Mouse p53 Signaling Pathway, SuperArray) detailing the expression of genes involved in the p53 pathway, were prepared as previously detailed (Materials & Methods 2.17). The raw image of each microarray provides an overview of the expression pattern of each genotype (Figure

4.15). Table 4.5 details which genes are expressed in each genotype, as determined by visual observation. No speculation of fold changes has been inferred here, and genes not expressed in all samples have been omitted. From a visual assessment of the raw microarray images (Figure 4.15), the decrease in p53-dependent gene expression caused by loss of p21, was *p21* gene dosage-dependent. Loss of one *p21* allele caused a 21% decrease in the number of p53-dependent genes expressed compared to WT B-cells. Loss of both *p21* alleles caused a 68% decrease in the number of genes expressed compared to WT B-cells (Table 4.5), indicating that in the mouse model system p53 activity depends on p21 dose.

Microarrays were analysed as previously described in 4.2.5, where each signal was normalised to control spots (Figure 4.15, indicated by red arrows) and background corrected. Differences in gene expression between samples are represented as fold changes (Table 4.6), calculated by determining the ratio of gene intensities between indicated samples. A cut-off value of 1.5-fold change has been applied as before.

The expression profiles of selected individual genes were analysed in more detail (Figure 4.15, highlighted by a red box) by graphical representation of transcript levels (Figure 4.16). The general trend is illustrated by the expression profile of *Bax*, *Caspase-2*, *Jun*, *Mdm2* and *Perp* (Figure 4.16), whereby gene expression was highest in WT B-cells, reduced in p21^{+/-} B-cells, and further reduced in p21^{-/-} cells. The extent of inhibition of gene expression depends on the gene. In the expression profile of *Bax*, *Bax* transcript levels were highest in WT B-cells, were reduced in p21^{+/-} B-cells, and were significantly reduced by approximately 17-fold in p21^{-/-} B-cells (Figure 4.16, Table 4.6). For *Caspase-2*, gene expression was

reduced in p21^{+/-} and p21^{-/-} B-cells compared to WT B-cells by approximately 2-fold and 9-fold respectively (Figure 4.16, Table 4.6). For *Mdm2*, the change in expression was more pronounced whereby expression in p21^{+/-} B-cells was repressed by 9-fold compared to WT B-cells, and in p21^{-/-} B-cells *Mdm2* expression could not be detected (Figure 4.16, Table 4.6). The general trend was observed for all expressed genes, as detected by the microarray, except for *Birc5*, *Ciao1*, *Gadd45a*, and *Pycard*. These genes were expressed in all genotypes and expression was not significantly changed by loss of p21. Expression profiles for *Birc5* and *Pycard* are shown (Figure 4.16). Previous data from the HCT116 model system showed that *GADD45* and *PYCARD* were expressed in p53^{-/-} cells and may be expressed independently of p53 (Figure 4.7A). Expression of housekeeping genes, as illustrated by the expression profile of *HSP90* (Figure 4.16) were also unaffected across genotypes.

The general trend of gene expression and correlation to genotype can be clearly observed by graphical representation of randomly selected genes. The data is presented as a bar graph (Figure 4.17A) to allow analysis of individual genes of interest not previously mentioned, including *ATM* and *Bak1*, whose expression profiles fit the general trend. *DAPK-1* was not expressed in any genotype and is therefore omitted. The data is also presented as a line graph, which clearly shows the gradual decrease in p53-dependent gene expression caused by loss of each *p21* allele (Figure 4.1B).

To further classify gene expression profiles, cluster analysis was performed as before (Figure 4.18). The extent of gene expression was colour coded according to all the values in all the samples, enabling expression levels of all genes to be

compared across all samples. This further showed that all detected genes were expressed in WT B-cells, loss of one allele of *p21* caused an overall decrease in gene expression, and loss of both *p21* alleles caused a further decrease in gene expression, with many genes no longer detected. The microarray analysis clearly illustrates that p53-dependent gene expression is regulated by p21 in a gene dose dependent manner.

4.3 Discussion

Previously, p21 was identified and characterised as a novel co-factor of p53 transcriptional activity in the HCT116 cell line (Chapter 3). This chapter focuses on the mechanism of p21-dependent regulation of p53 and the effect of loss of p21 on p53-dependent gene expression profiles, as measured by p53 pathway specific DNA microarrays. To confirm that p21-dependent regulation of p53 extends beyond the HCT116 cancer cell model, NHF cells treated transiently with p21 siRNA, and a transgenic mouse model with targeted inactivation of the *p21* gene, were used. In all three model systems, we show that loss of p21 causes aberrant subcellular localisation of p53 and global loss of p53-dependent gene expression.

4.3.1 p21-dependent regulation of p53 subcellular localisation

Nuclear localisation of p53 is essential for its growth suppressing activity (Shaulsky *et al.* 1991; Moll *et al.* 1996), and re-localisation of p53 to cytoplasm represents a mutation independent mechanism utilised by malignancies to inactivate wild-type p53 (Moll *et al.* 1995). Primary human tumours which exhibit aberrant cytoplasmic

sequestration of p53 and lack of response to DNA damage include inflammatory breast cancer (Moll *et al.* 1992), undifferentiated neuroblastoma (Moll *et al.* 1995), retinoblastoma (Schlamp *et al.* 1997) and colorectal carcinoma (Bosari *et al.* 1995). Constitutive cytoplasmic localisation of p53 in these tumour types is associated with poor response to chemotherapy, tumour metastasis and poor long-term patient survival (Bosari *et al.* 1995; Moll *et al.* 1995; Schlamp *et al.* 1997). The specific mechanisms governing abnormal cytoplasmic localisation of p53 are not well defined. However, Ostermeyer *et al.* (1996) showed that the C-terminal domain of cytoplasmic p53 from undifferentiated neuroblastoma cells is masked. The C-terminus (amino acids 300-393) of p53 harbours one major and two minor nuclear localisation signals (NLS) (Dang & Lee, 1989; Shaulsky *et al.*, 1990a), which mediates p53 import into the nucleus in response to DNA damage (el-Deiry *et al.* 1992; Jimenez *et al.* 1999). Furthermore, in undifferentiated neuroblastoma cells, stable expression of a p53 C-terminal peptide encompassing all three NLSs was sufficient to restore p53 nuclear localisation (Ostermeyer *et al.* 1996). To date, the source of p53 C-terminal masking and the genetic alterations responsible for this phenotype in undifferentiated neuroblastoma cells has yet to be resolved. Here, we show in three model systems including normal human cells, that loss of p21 can cause a similar phenotype to that observed in the indicated primary tumours (Zaika *et al.* 1999), where high levels of wild type p53 protein accumulates in the cytoplasm in the absence of stress. Although the mechanism of how p21 governs p53 subcellular localisation remains elusive, p53 in HCT116 p21^{-/-} cells is correctly folded (Figure 4.2) therefore C-terminal masking is unlikely.

Interestingly, Crook *et al.* (1998) characterised a Burkitt lymphoma derived cell line DG75. These cells express a constitutively high level of p53, an extremely low level of p21, and no detectable BAX. Furthermore, in DG75 cells transcription of p53 target genes was not induced by cisplatin treatment, and p53 was exclusively localised to the cytoplasm. Crook *et al.* (1998) found that DG75 cells contain one wild-type p53 allele and a mis-sense mutation in the second allele, causing substitution of an arginine residue at amino acid position 283 to histidine (referred to hereafter as Arg283His), and proposed that Arg283His is responsible for p53 mislocalisation in this cell line. From *in vitro* studies, Crook *et al.* (1998) propose that Arg283His binds DNA and transactivates p53 target genes, and is essentially wild type. Transformation of Arg283His into rat embryonic fibroblast cells and the p53-null human cell line SAOS-2 shows a gradual shift of p53 from the nucleus to the cytoplasm over a 60 hour time course, and shows a corresponding decline in p53 activity. Crook *et al.* (1998) speculate that Arg283His heterodimerises with wild-type p53, and acts as chaperone to export p53 out of the nucleus. However, Crook *et al.* (1998) fail to show that removal of Arg283His mutation by, for example siRNA mediated gene knockdown, restored nuclear localisation of p53 and therefore definitive proof that Arg283His causes p53 cytoplasmic accumulation. In light of the research presented in this chapter, where loss of p21 causes aberrant localisation of p53 and subsequent restoration of p21 can restore p53 nuclear localisation, the study by Crook *et al.* (1998) can be re-evaluated. Crook *et al.* (1998) show that *in vitro* Arg283His did demonstrate reduced DNA binding capabilities compared to wild-type p53. This is not surprising considering that the mutation is within the H2 α -helix which makes contact with the phosphate backbone in the major groove of the

consensus DNA sequence (Cho *et al.* 1994). Therefore the findings in rat embryonic fibroblast cells and SAOS-2 cells where initial transformation with Arg283His shows nuclear localisation, then subsequent accumulation in the cytoplasm by 60 hr, may indicate that basal expression of the p21 gene is being reduced leading to a gradual increase in cytoplasmic localisation of p53, and inactivation of p53 transcriptional activity. Hence, we propose that expression of Arg283His induces a decrease in steady state p53-dependent gene expression, leading to a loss of p21, which in turn causes mislocalisation and inactivation of p53. Therefore, Burkitt lymphoma derived DG75 cells have evolved a novel mechanism of inactivating both copies of p53 to enhance tumour progression.

However, the mechanism governing p21-dependent regulation of p53 subcellular localisation remains to be determined. We have shown that p21¹⁻¹³³ truncation, which lacks the NLS, can restore p53 subcellular localisation therefore p21 may have a cytoplasmic function in the regulation of p53. Indeed in the HCT116 WT cells p21 has been shown to localise to the cytoplasm (Figure 4.1A). In speculation, cytoplasmic p21 could block p53 interaction with a nuclear export protein or cytoplasmic anchor leading to p53 nuclear localisation. This would correspond with evidence from the mouse B-cell model, showing that p53 transcriptional activity is p21 dose dependent, whereby p21 could displace p53 in a dose dependent manner from potential cytoplasmic binding partners, allowing p53 nuclear accumulation and activation.

The loss of p21 also affected the subcellular localisation of additional targets to p53, including CHK2 and E2F1 (Figure 4.1A), indicating that p21 may impinge on a general localisation mechanism. The microtubule cytoskeleton and associated

molecular motor proteins, such as dynein, contribute to the subcellular localisation of a range of cargo proteins (Vale & Milligan, 2000; Roth *et al.*, 2007). Interestingly, p53 is associated with cellular microtubules and the microtubule based motor protein dynein, and has been proposed to utilise this system to translocate from the cytoplasm to the nucleus (Giannakakou *et al.*, 2000). Disruption of the microtubule network or impaired function of a microtubule associated protein, by loss of p21 may disrupt the subcellular localisation of a subset of proteins.

In normal cells under non-stressed conditions, p53 shuttles between the nucleus and the cytoplasm. Nuclear p53 is only detected in cells at the G1/S transition, and cytoplasmic p53 is associated with S-phase cells (Shaulsky *et al.*, 1990b). Strikingly, expression levels of p21 are highest at the G1/S transition when p53 is nuclear and lowest at the S-phase of cell cycle when p53 is cytoplasmic (Li *et al.*, 1994a). In response to stress, the shuttle is biased towards p53 nuclear accumulation. The work presented here was carried out in asynchronous populations of cells, where nuclear p53 was predominately located in control cells, and cytoplasmic p53 is detected in cells lacking p21. However, future studies involving synchronised cell populations and cell cycle analysis may show that in normal cells p21 plays an important role in coordinating the cell cycle and p53 transcriptional activity via its subcellular localisation.

4.3.2 Loss of p21 causes a global decrease in p53-dependent gene expression

p53-dependent gene expression was assessed using p53 specific DNA microarrays, profiling the expression of genes involved in p53 signalling pathways. Loss of p21

and aberrant localisation of p53 was shown to be associated with an over-all decrease in p53-dependent gene expression in the HCT116 cancer cell model, the NHF model and the transgenic mouse model. The decrease in gene expression was not as pronounced in HCT116 p21^{-/-} cells as compared to the other models, however this maybe expected as HCT116 p21^{-/-} cells stably support inactivation of the p21 gene and may have adapted alternative strategies to ensure cell survival. Indeed, NHF cells treated with p21 siRNA showed an 86% decrease in number of genes expressed compared to control siRNA treated cells, except for *HSP90*, whose expression was increased 2-fold compared to control cells. The *HSP90* gene encodes a molecular chaperone, and has been implicated as a facilitator of tumour progression by stabilising conformations of mutant proteins (Zhang & Burrows, 2004; Calderwood *et al.*, 2006). To speculate, initial loss of p21 may constitute as a micro-environmental stress, similar to the unfolded protein response activated by a potentially toxic accumulation of mis-folded proteins in the endoplasmic reticulum (Feldman *et al.*, 2005). This response involves a reduction in the global rates of transcription and protein synthesis, but causes a robust increase in molecular chaperones, which assist in protein re-folding and undesirably, stabilising conformations of mutant proteins (Feldman *et al.*, 2005; Calderwood *et al.*, 2006). Therefore elevation of HSP90 protein levels may provide a mechanism akin to natural selection in overcoming normal cell defences, to oncogenic transformation (Zhang & Burrows, 2004; Calderwood *et al.*, 2006). siRNA mediated gene knockdown of p21 in NHF cells is only transient, where as loss of p21 in HCT116 and mouse B-cells is due to stable inactivation of the p21 gene. Therefore cells from

these model systems have previously adapted to loss of p21, and *HSP90* expression levels have reduced accordingly.

A remarkable finding was illustrated by the transgenic mouse model, where p53-dependent gene expression was decreased by the loss of one allele of *p21*, and then further decreased by loss of both *p21* alleles (Figure 4.17). This data indicates that p53 activity is fine-tuned to levels of p21 and provides insight into the sensitivity of this feedback loop, and is an indication of its cellular importance. In comparison, the MDM2-p53 negative feedback loop, consisting of p53 transactivation of *MDM2* and MDM2-mediated ubiquitination and degradation of p53, is predicted to set up an oscillator with p53 and MDM2 levels increasing and decreasing with time and out of phase in the cell (Lev Bar-Or *et al.*, 2000). Similarly, oscillations of p21 levels, as observed during the cell cycle (Li *et al.*, 1994a), may be sufficient to regulate p53 activity. Cell and mouse models with *p21* gene expression under inducible control will prove invaluable in further dissecting this novel feedback loop in regards to p21 levels (See chapter 6 for future directions).

Previously, Lohr *et al.* (2003) reported that increased expression of p21 is necessary for negative regulation of gene expression by p53. Genes down regulated by p53 include *BRCA1* (MacLachlan *et al.*, 2000), *CDC25C* (Badie *et al.*, 2000), *Cyclin B1* (Badie *et al.*, 2000), and *Survivin* (Hoffman *et al.*, 2002). Lohr *et al.* (2003) speculate that p53 reduces the expression of certain genes indirectly by enhancing the expression of *p21*. Elevated p21 protein levels would cause inactivation of cyclin-dependent kinases, leading to hypo-phosphorylation of Rb and subsequent conversion of E2F transcriptional activators to transcriptional repressors. Taken in context with the data presented in this chapter, p21 may regulate both

positive and negative p53-dependent transcription, enabling p21 to fully orchestrate the p53 response to cellular damage.

4.3.3 p21 and apoptosis

The Microarray analysis of HCT116 and NHF cells showed that two genes which consistently diverged from the general trend were *BAK1* and *DAPK-1*. Both genes have roles in promoting cell death. BAK1 is similar to BAX, in that in response to pro-apoptotic stimuli, BAK1 effects the permeabilisation of the mitochondrial membrane, allowing proteins in the mitochondrial inter-membrane space, such as cytochrome *c*, to escape into the cytosol where they can induce caspase activation and cell death (Antignani & Youle, 2006). DAPK-1 has roles in both, apoptotic and autophagic cell death, whereby over-expression of DAPK-1 leads to pronounced death associated cellular changes including membrane blebbing, cell rounding, detachment from extracellular matrix, and the formation of autophagic vesicles (Bialik & Kimchi, 2006). The mechanisms of DAPK-1 mediated cell death are yet to be determined, although DAPK-1 catalytic activity is required (Bialik & Kimchi, 2006), and has been associated with p53-dependent apoptotic cell death (Raveh *et al.* 2001).

An emerging function of p21 is as a modulator of apoptosis (Gartel & Tyner, 2002). Deciphering the role of p21 in apoptosis is complicated as a number of studies have shown that p21 can assume both pro- and anti-apoptotic functions depending on cell type and cellular context (Liu *et al.*, 2003). Overall, the evidence in favour of an

anti-apoptotic role for p21 outweighs the evidence suggesting p21 has apoptosis promoting abilities.

Wu et al. (2002) showed that p21 can induce apoptosis, by over-expressing p21 in human ovarian cancer cells with mutant p53. p21 induced apoptosis caused no detectable activation of *BAX* and *BCL-2* genes, while significant differential expression of those genes preceded p53-induced apoptosis, suggesting that p21 induces apoptosis through a distinct apoptosis pathway. Similar results were obtained in a papillary serous endometrial carcinoma cell line (Ramondetta *et al.*, 2000) and human cervical cancer cells (Taso *et al.*, 1999).

p21 can also act as an inhibitor of apoptosis in a variety of systems, dramatically limiting the effectiveness of anticancer agents (Gartel & Tyner, 2002). The mechanism of how a cell chooses between apoptosis and p21-dependent cell cycle arrest after DNA damage is not yet defined, but often high levels of p21 expression mediate cell cycle arrest and protect from apoptosis. For example, Martinez *et al.* (2002) show that doxorubicin treatment of human prostate cancer with wild-type p53, strongly induced p53 expression while p21 expression was increased at low doses and decreased at high doses. Doxorubicin induced apoptosis occurred in parallel with p21 down-regulation, and knock-down of p21 using anti-sense oligonucleotides efficiently sensitised prostate cells to doxorubicin (Martinez *et al.*, 2002). This indicates that p21 may regulate apoptosis, by inhibiting apoptosis when a low degree of DNA damage has occurred, allowing cells to repair the damage. Upon a high degree of cellular damage, a decrease in p21 expression may induce apoptosis in an attempt to eliminate the damaged cells. Similarly, differential apoptotic effects were observed in the human HCT116 cell line expressing wild-type

p53, following treatment with the anti-cancer drug camptothecin (Han *et al.*, 2002). Camptothecin induces topoisomerase I mediated DNA damage. Low doses of camptothecin induced apoptosis in HCT116 p21^{-/-} cells compared to growth arrest in WT cells. High doses of same drug induced apoptosis independent of p21 status (Han *et al.* 2002). This suggests that p21 is capable of blocking apoptosis and inducing growth arrest in cells with a low degree of damage. In general, p21 status of cancer cells may be important to consider prior to treatment. RKO human colorectal carcinoma cells express low levels of p21 and normally undergo apoptosis in response to prostaglandin A₂ (Gorospe *et al.*, 1996a). In contrast NIH 3T3 cells (Hitomi *et al.*, 1996) and MCF-7 cells (Gorospe *et al.*, 1996a) express high levels of p21 and undergo G1 arrest in response to prostaglandin A₂. Hence, levels of p21 may be a central factor in determining the cellular response to different drugs.

The molecular mechanisms by which p21 can prevent cells from undergoing apoptosis remain to be elucidated. p21 is capable of interacting with several proteins which may contribute to its anti-apoptotic functions. These include binding to procaspase-3 and blocking its processing and activation (Suzuki *et al.*, 1998; Tang *et al.*, 2006a), inhibition of key apoptosis regulatory proteins such as stress activated protein kinase (SAPK) (Shim *et al.*, 1996), and apoptosis signal-regulating kinase 1 (ASK1) (Dotto, 2002), and inhibition of apoptosis-stimulating transcription factors, Myc, E2F1 (Roninson, 2002) and as we have presented here, p53. Javelaud & Besançon (2002) have presented an alternative mechanism, where inactivation of p21 in HCT116 cells exhibits inhibitory effects on apoptosis induced by enhancement of p53 expression at the post-transcriptional level. This correlated with an elevated expression of p14/19ARF, an inhibitor of the ubiquitin ligase activity of MDM2.

This suggests that enhanced sensitivity of HCT116 p21^{-/-} cells to anti-tumour agents may result from a stabilisation and activation of wild-type p53, leading to enhanced BAX expression and apoptosis. The results presented by Javelaud & Besançon (2002) are in stark contrast to our own, where we show that loss of p21 in HCT116 cells causes transcriptional inactivation of p53 and low expression levels of BAX. Importantly, we show that reconstitution of p21 into HCT116 p21^{-/-} cells restores p53 transcriptional activity and BAX levels (Figure 3.10). The study by Javelaud & Besançon (2002) is also contradictory of studies where loss of p21 sensitised cells to apoptosis in a p53-null background (Gorospe *et al.*, 1996b; Han *et al.*, 2002; Marches *et al.*, 1999; Mahyar-Roemer & Roemer, 2001; Wang *et al.*, 1999).

The microarray analysis of HCT116 and NHF cells presented here, implicates the pro-apoptotic genes *BAK1* and *DAPK-1* in p21-mediated inhibition of apoptosis. In HCT116 cells loss of p21 caused an increased expression of *DAPK-1* in non-irradiated cells (Figure 4.6), however immunoblot analysis could not detect DAPK-1 protein in p21^{-/-} cells (Figure 4.1). This may indicate that p21^{-/-} cells have adapted a survival mechanism to compensate for high *DAPK-1* expression levels by preventing DAPK-1 protein translation. In response to irradiation in HCT116 cells (Figure 4.6) and in NHF cells (Figure 4.11), *BAK1* expression is increased compared to control cells. HCT116 p21^{-/-} cells have also been shown to undergo extensive cytochrome *c* release, mitochondrial membrane depolarisation, and caspase activation in response to damage (Le *et al.*, 2005). These observations taken together indicate that p21 could mediate sensitivity of the mitochondria to pro-apoptotic signals by regulating *BAK1* expression. Therefore loss of p21 may sensitise cells to DNA-damage induced apoptosis due to increased expression of the pro-apoptotic gene *BAK1*. The pro-

apoptotic role of p21 inactivation could result in increased apoptosis, and may partially explain, given that loss of p21 causes inactivation of p53, why p21-null mice are less tumour prone than p53-null mice (Martin-Caballero *et al.*, 2001) and why mutation of p21 is rarely observed in human tumours (Shiohara *et al.*, 1994).

In this chapter, exciting and novel data has been presented indicating that loss of p21 mediates transcriptional inactivation of p53 via aberrant subcellular localisation of p53 from the nucleus to the cytoplasm; has a global effect on p53-target gene expression; and that p53-dependent gene expression is gene dose-dependent on p21.

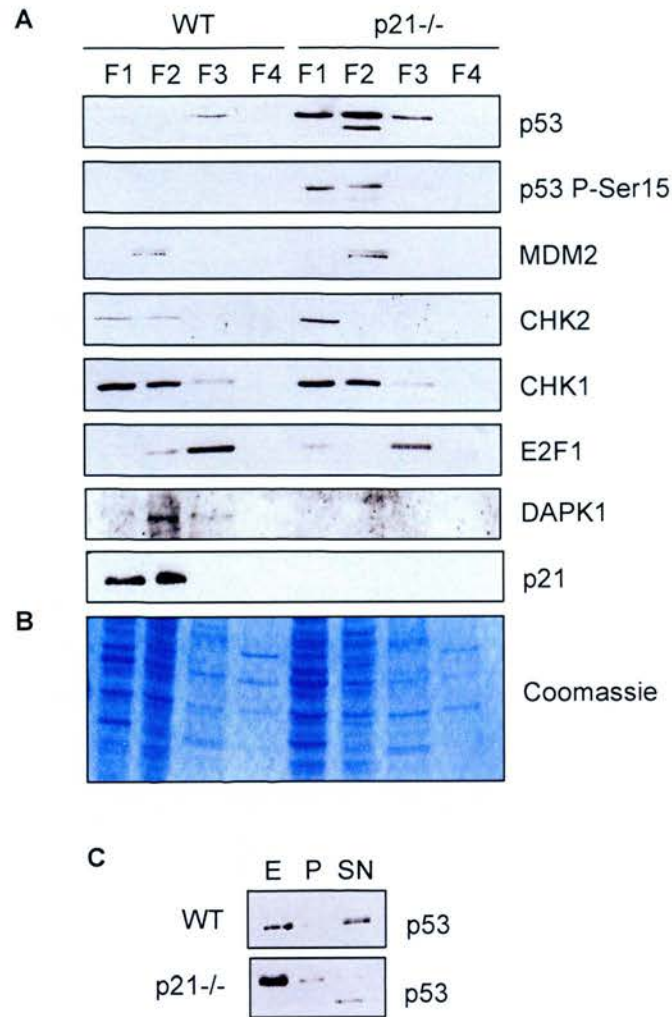


Figure 4.1 Loss of p21 is associated with mislocalisation of p53. (A) Subcellular fractionation of HCT116 p21^{-/-} cells show defects in p53 localisation. Proteins from HCT116 WT and p21^{-/-} cells were extracted according to their subcellular localisation: F1– Cytosol; F2– Membrane/organelle; F3– Nucleus; F4– Cytoskeleton (ProteoExtract[®] Subcellular Proteome Extraction Kit (S-PEK), Calbiochem[®]). Proteins from each fraction were resolved by SDS-PAGE and analysed by immunoblotting for p53; p53 serine-15 phosphorylation; MDM2; CHK2; CHK1; E2F1; DAPK1 and p21. 10 µg protein was loaded per lane. (B) Protein expression patterns from each fraction are clearly distinct. Proteins from each fraction were resolved by SDS-PAGE and analysed by coomassie staining. 5 µg protein was loaded per lane. (C) In the absence of p21, p53 is predominantly cytoplasmic. HCT116 WT and p21^{-/-} cells were fractionated by the method of Gilbert and Allan (2001). E – total cellular extract; P- insoluble nuclear fraction; SN- soluble nuclear fraction. p53 protein levels were detected by immunoblotting. 10 µg protein was loaded per lane.

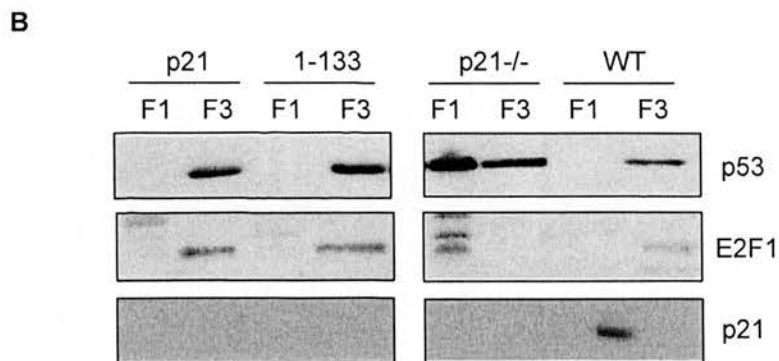
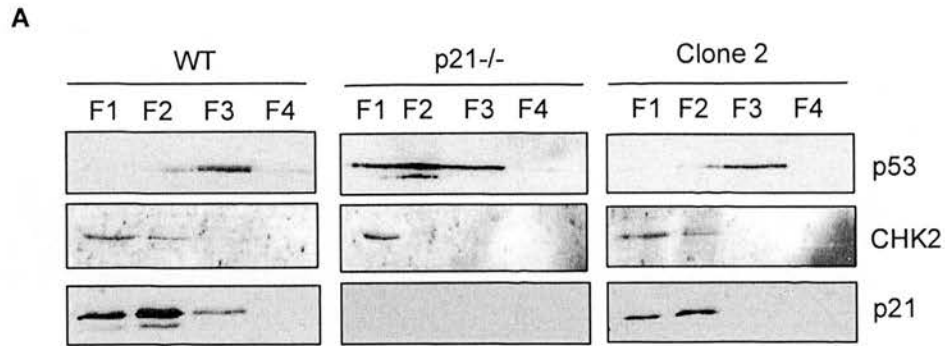
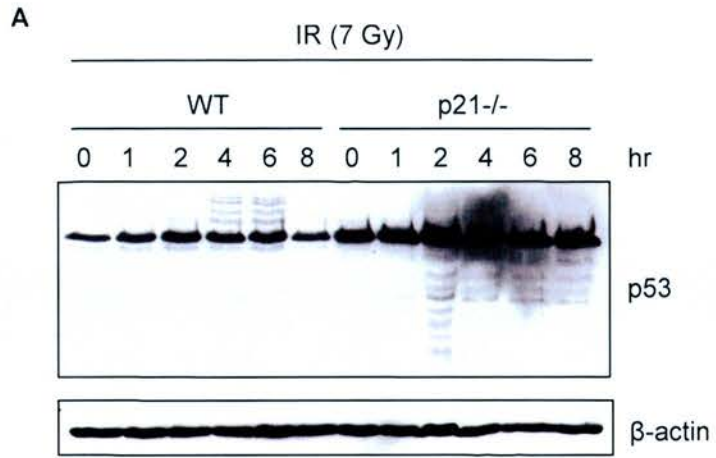
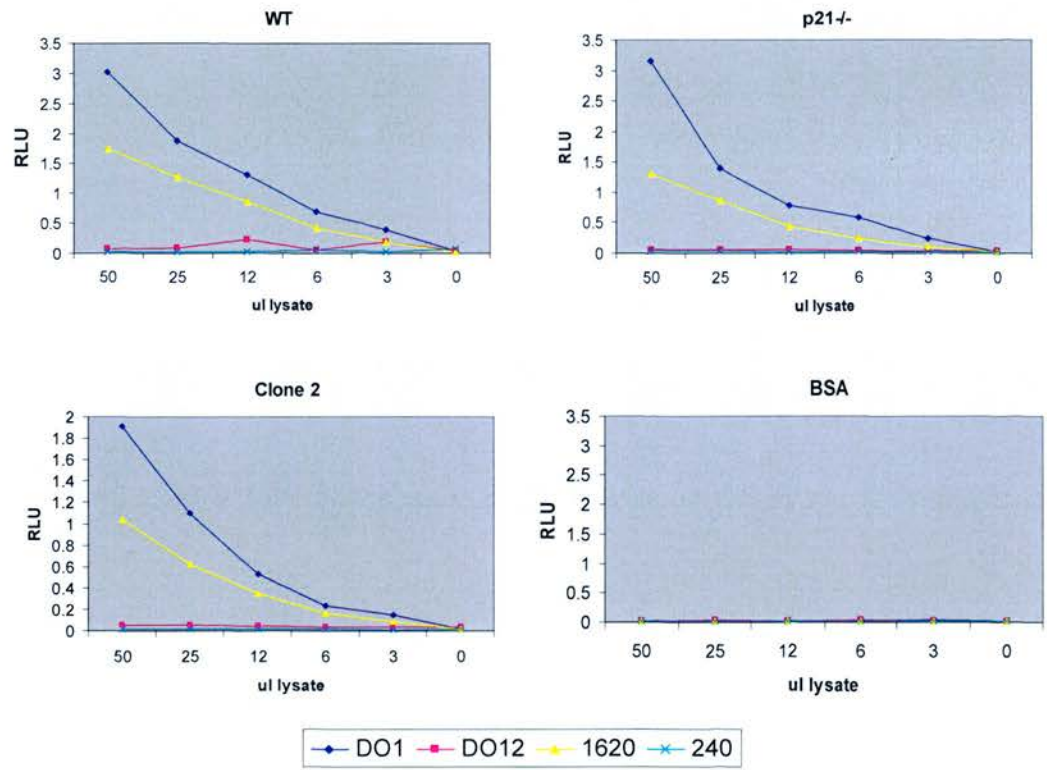


Figure 4.2 p53 nuclear localisation is p21-dependent. (A) Stable reintroduction of p21 into p21^{-/-} cells is sufficient to restore p53 subcellular localisation. Proteins from HCT116 WT, p21^{-/-} and Clone 2 cells were extracted according to their subcellular localisation: F1– Cytosol; F2– Membrane/organelle; F3– Nucleus; F4- Cytoskeleton (S-PEK, Calbiochem®). Proteins from each fraction were resolved by SDS-PAGE and analysed by immunoblotting for p53; CHK2; and p21. 10 µg protein was loaded per lane. (B) The C-terminus of p21 is not required for recovery of p53 localisation. Proteins from HCT116 WT, p21^{-/-} and p21^{-/-} cells stably expressing either full length p21 (p21) or p21 1-133 truncation (1-133), were extracted according to their subcellular localisation, as before. Proteins from the F1 and the F3 fractions were separated by SDS-PAGE and analysed by immunoblotting for p53, E2F1, and p21. 10 µg protein was loaded per lane.



B



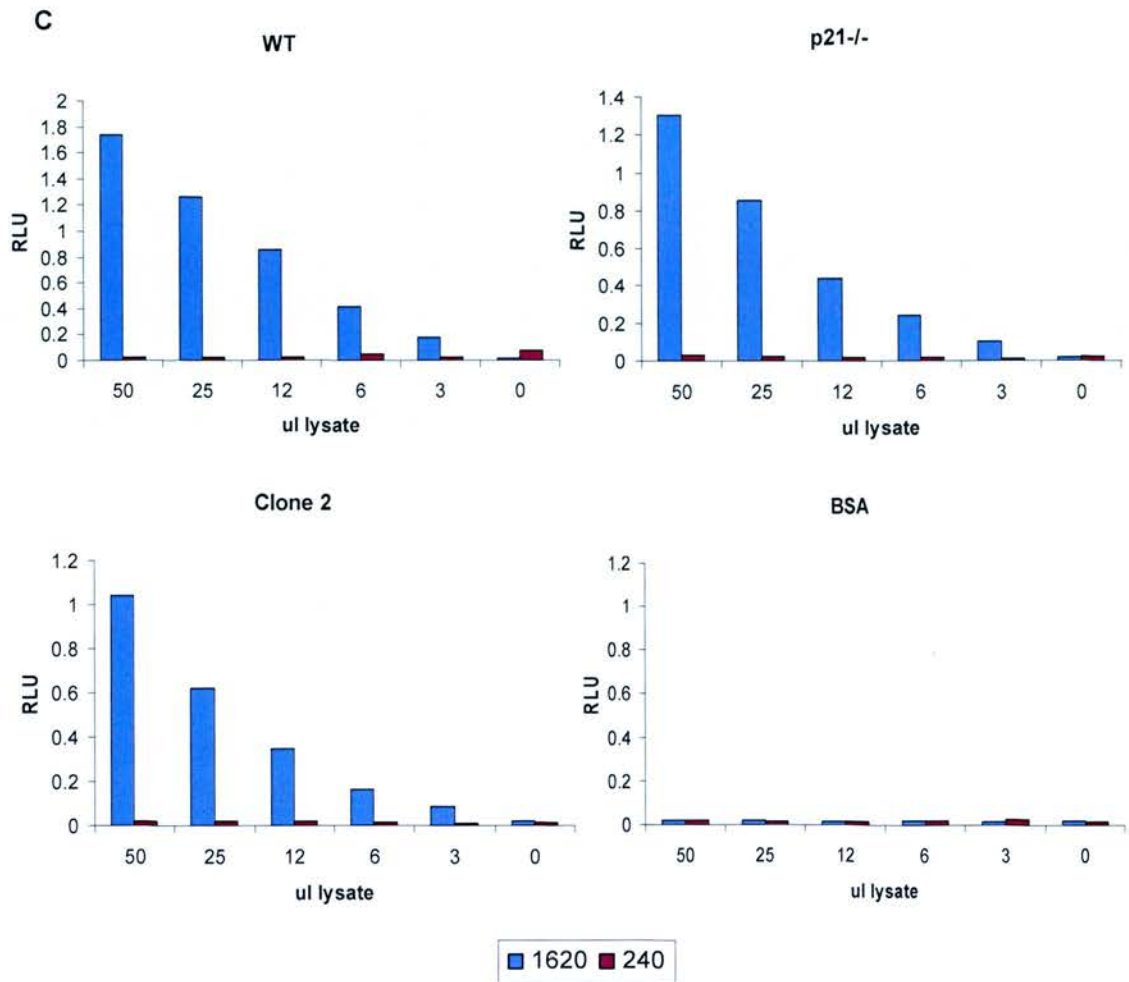


Figure 4.3 Mislocalised p53 is not unfolded in the absence of p21. (A) Loss of p21 is associated with loss of damaged induced p53 ubiquitination and accumulation of lower molecular-weight adducts. HCT116 WT and p21^{-/-} cells were irradiated at 7 Gy and harvested over the indicated time course. Whole cell urea lysates were analysed by immunoblotting for p53 with anti-p53 (DO1). β -actin was used as a loading control. 10 μ g protein was loaded per lane. (B) and (C) Antibody-capture ELISA using p53 conformation sensitive antibodies shows the extent of p53 unfolding in cells. Cell lysates were prepared as described in materials and methods (2.16). p53 proteins in lysates were captured by monoclonal antibodies DO1, DO12, PAb1620 and PAb240 coated onto ELISA wells, followed by polyclonal antibody CM1 incubation and ECL[®] detection. The data are represented as luminescence in relative light units (RLU) as a function of the monoclonal antibody used to capture p53. (C) shows a comparison between PAb1620 which detects folded p53 and PAb240 which detects unfolded p53.

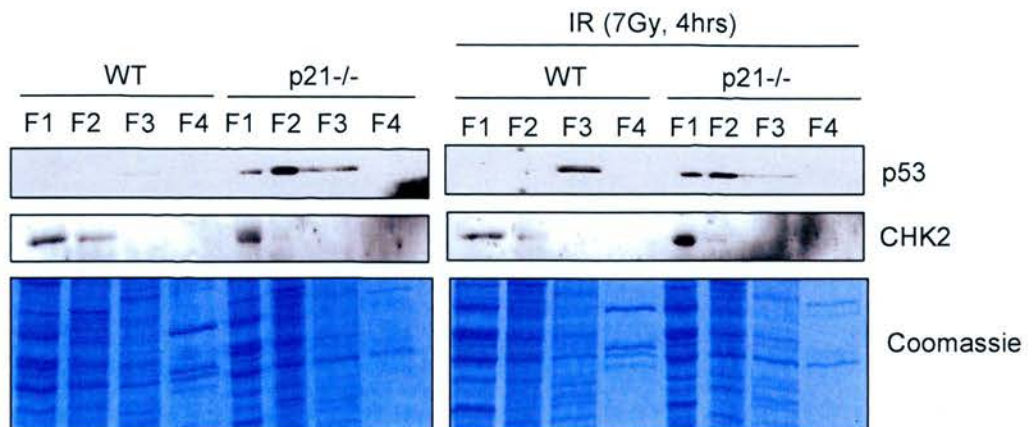


Figure 4.4 p53 localisation is not DNA damage-dependent. HCT116 WT and p21^{-/-} cells were irradiated with 7 Gy and incubated for 4 hr, before all proteins were extracted according to their subcellular localisation: F1– Cytosol; F2– Membrane/organelle; F3– Nucleus; F4– Cytoskeleton (S-PEK, Calbiochem®). Proteins from each fraction were resolved by SDS-PAGE and analysed by immunoblotting for p53 and CHK2. 10 µg protein was loaded per lane. Coomassie staining (5 µg protein was loaded per lane) confirmed that protein expression patterns from each fraction are distinct.

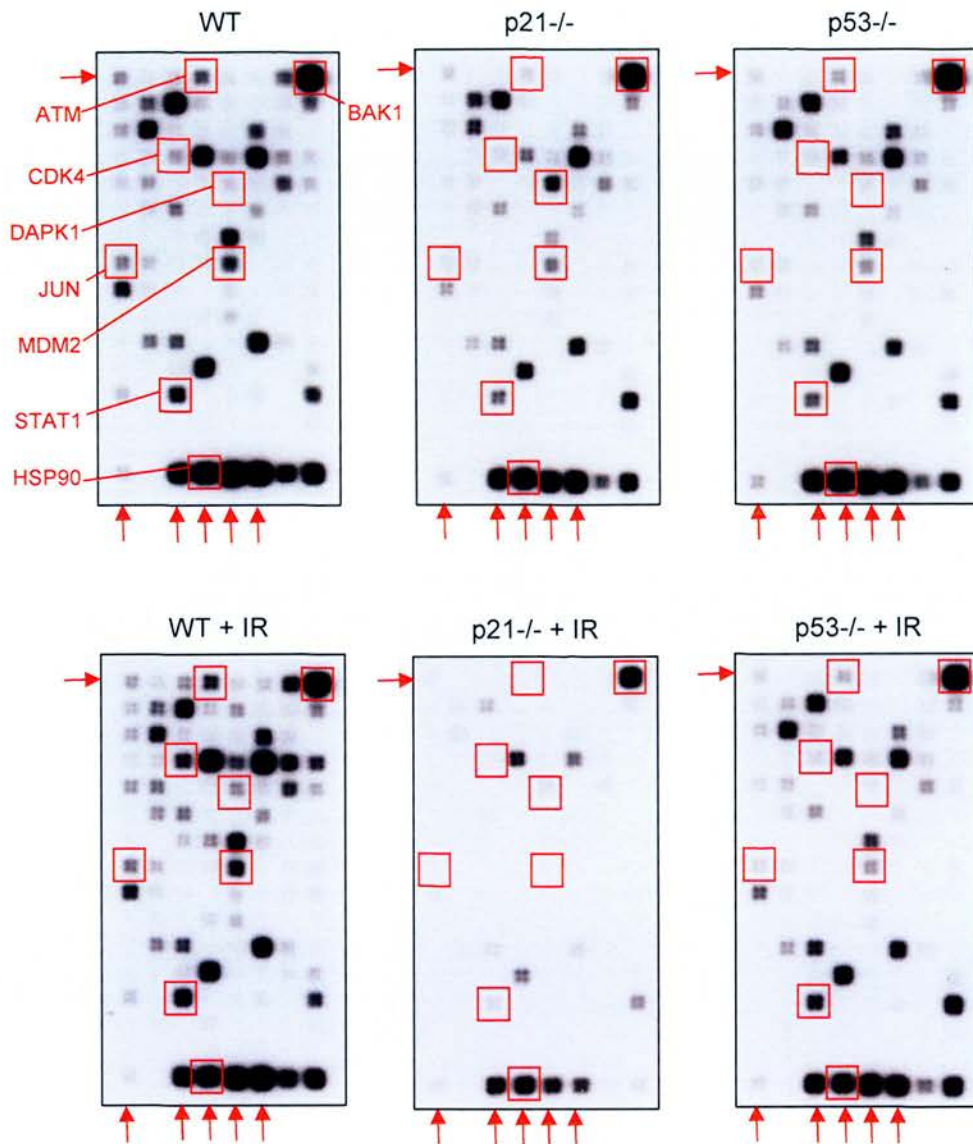


Figure 4.5 Analysis of gene expression alterations in the absence of p21. HCT116 WT, p21^{-/-} and as a negative control p53^{-/-} cells were irradiated with 7 Gy and incubated for 4 hr to activate expression of p53-target genes. DNA microarrays, profiling the gene expression of 113 genes related to p53-mediated signal transduction (OligoGEArray[®] System, SuperArray), were used (as detailed in materials and methods, 2.17) to indicate the extent of p53 activation in the absence of p21 and in response to IR. Normalisation genes are indicated by red arrows. The genes analysed further are indicated by red boxes.

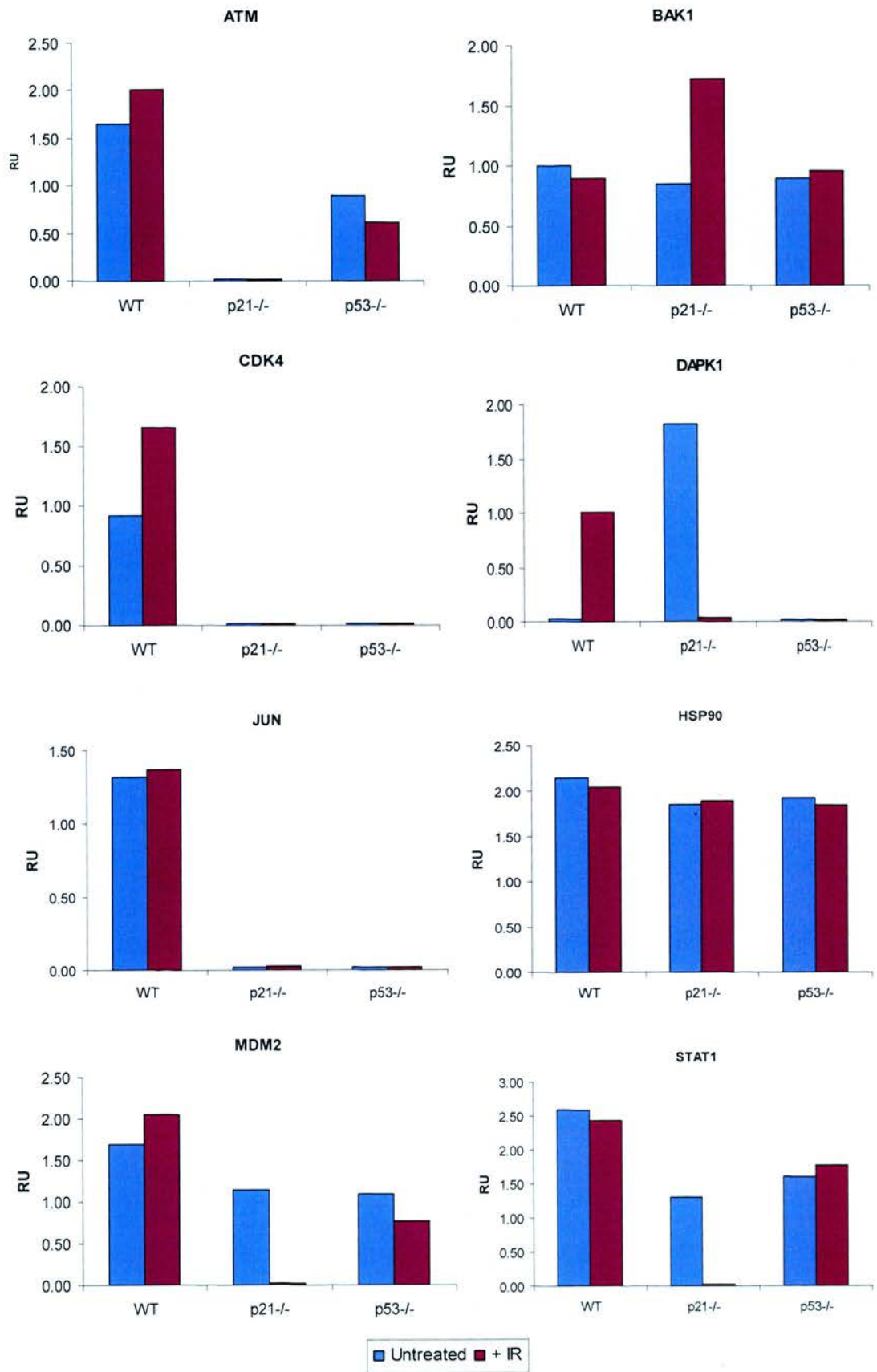


Figure 4.6 Graphical representation of microarray results of selected genes indicates aberrant basal and IR-induced gene expression in the absence of p21. Genes selected to be analysed in more detail included: genes representing the overall trend (see figure 4.7) including *CDK4*, *JUN* and *STAT1*; genes divergent from the overall trend including *BAK1* and *DAPK1*; genes of interest due to previous data including *ATM* and *MDM2*; and as a positive control *HSP90*. mRNA levels are indicated by relative units (RU) and were determined by fluorescence intensity normalised to background intensity of microarray membranes.

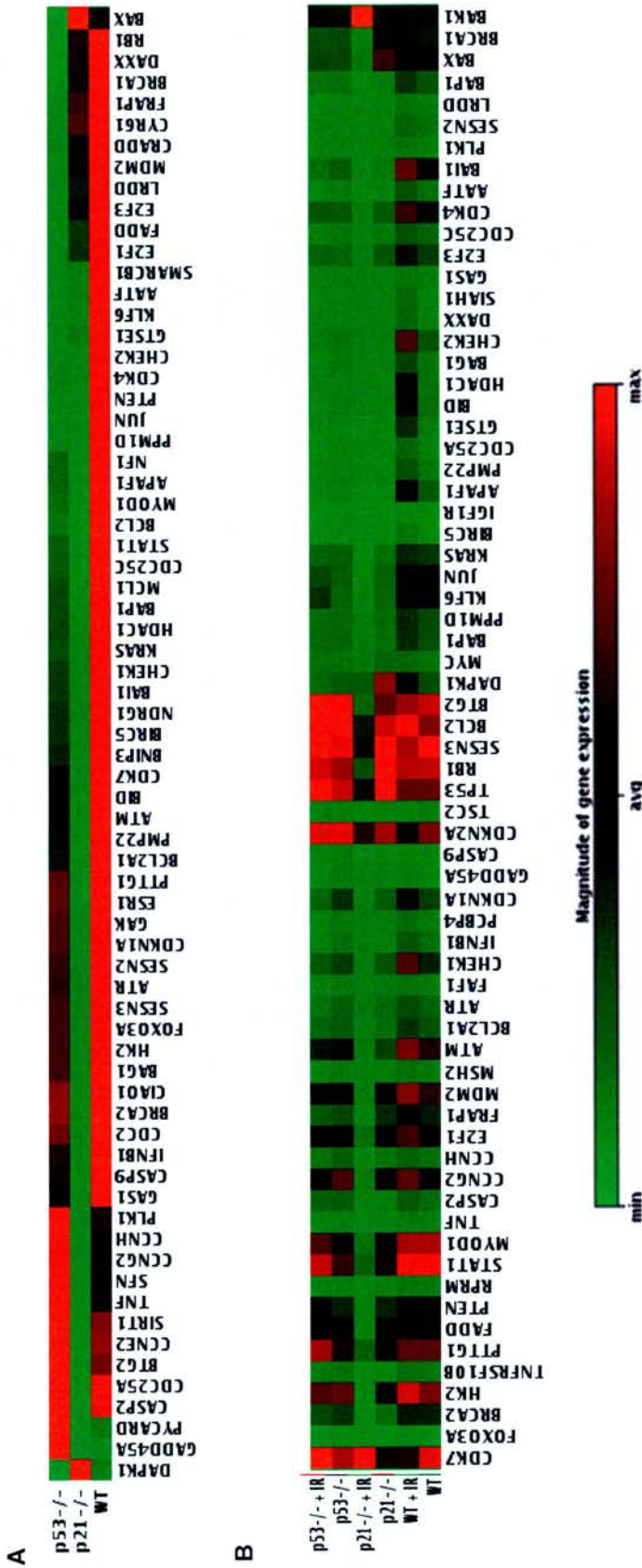


Figure 4.7 Gene expression profiles show an overall decrease in p53 target gene expression in the absence of p21. (A) Basal gene expression of HCT116 p21-/- cells is lower than both HCT116 WT and p53-/- cells. Colours were assigned according to the value of the gene in all samples, whereby expression of each gene is not comparable to other genes in the same sample, but is comparable to the same gene in different samples. (B) IR-induced gene expression is decreased in the absence of p21. Microarrays were analysed using the clustergram data analysis tool of the GEArray Expression Analysis Suite programme (SuperArray). Colours were assigned according to all the values in all the samples, whereby expression of each gene is relative to another in the sample, and across samples. The colour represents the magnitude of gene expression on a scale of green (lowest) to red (highest).

Symbol	HCT116					
	WT	WT + IR	p21 ^{-/-}	p21 ^{-/-} + IR	p53 ^{-/-}	p53 ^{-/-} + IR
Apoptosis						
APAF1		x				
BAK1	x	x	x	x	x	x
BAX	x	x	x			x
BCL2	x	x	x	x	x	x
BID		x				
DAPK1		x	x			
FADD	x	x	x		x	x
HDAC1		x				
TP53	x	x	x		x	x
Cell Cycle						
ATM	x	x			x	x
BRCA1	x	x	x		x	x
BRCA2	x	x				
CCNG2	x	x	x		x	x
CDK4	x	x				
CDK7	x	x	x	x	x	x
CDKN1A	x	x			x	
CDKN2A	x	x	x	x	x	x
CHEK1	x	x				
CHEK2		x				
E2F1	x	x	x		x	x
FRAP1	x	x				
HK2	x	x	x		x	x
PTEN	x	x	x			x
RB1	x	x	x		x	x
SESN3	x	x	x		x	x
STAT1	x	x	x		x	x
TP53	x	x	x		x	x
Cell Growth, proliferation and differentiation						
BAI1	x	x				
BTG2	x	x	x		x	x
CIAO1		x				
ESR1		x				
JUN	x	x				
KLF6	x	x				
MDM2	x	x	x		x	x
MYOD1	x	x	x		x	x
PTTG1	x	x	x		x	x
Control						
ACTB	x	x	x	x	x	x
HSP90	x	x	x	x	x	x
RPS27A	x	x				

x - Gene expression detected by visual assessment

Table 4.1 Genes expressed in HCT116 isogenic cell panel in response to IR

Symbol	HCT116					
	p21 ^{-/-} Vs WT	p53 ^{-/-} Vs WT	WT + IR Vs WT	p21 ^{-/-} + IR Vs p21 ^{-/-}	p53 ^{-/-} + IR Vs p53 ^{-/-}	p21 ^{-/-} + IR Vs WT + IR
Apoptosis						
<i>AAPF1</i>	▲◊	●◊	◊	■▲	◊●	■
<i>BAK1</i>				+2.03		+1.80
<i>BAX</i>		●		■	●	■
<i>BCL2</i>				-3.57		-3.45
<i>BID</i>	▲◊	●◊	◊	■▲	◊●	■
<i>DAPK1</i>	+4.12	●◊	◊	■	◊●	■
<i>FADD</i>	-1.64	-1.56		■		■
<i>HDAC1</i>	▲◊	●◊	◊	■▲	◊●	■
Cell Cycle						
<i>ATM</i>	▲	-1.85		■▲		■
<i>BRCA1</i>		-1.81		■		■
<i>BRCA2</i>	▲	●		■▲	◊●	■
<i>CCNG2</i>	-1.54			■	-1.75	■
<i>CDK4</i>	▲	●	+1.81	■▲	◊●	■
<i>CDK7</i>	-1.92		-1.64			■
<i>CDKN1A</i>	▲		+1.78	■▲	◊	■
<i>CDKN2A</i>			-1.59	-1.67		-1.61
<i>CHEK1</i>	▲	●	+2.33	■▲	◊●	■
<i>CHEK2</i>	▲◊	●	◊	■▲	◊●	■
<i>E2F1</i>				■		■
<i>FRAP1</i>	▲	●		■▲	◊●	■
<i>HK2</i>	-2.44			■		■
<i>PTEN</i>	-2.63	●		■	●	■
<i>RB1</i>				■		■
<i>SESN3</i>				■		■
<i>STAT1</i>	-2.00	-1.61		■		■
<i>TP53</i>				■		■
Cell Growth, proliferation and differentiation						
<i>BAI1</i>	▲	●	+1.89	■▲	◊●	■
<i>BTG2</i>	-1.54			■		■
<i>CIAO1</i>	▲◊	●◊	◊	■▲	◊●	■
<i>ESR1</i>	▲◊	●◊	◊	■▲	◊●	■
<i>JUN</i>	▲	●		■▲	◊●	■
<i>KLF6</i>	▲	●		■▲	◊●	■
<i>MDM2</i>		-1.56		■		■
<i>MYOD1</i>	-2.63	-2.00		■		■
<i>PTTG1</i>	-1.59			■		■
Control						
<i>ACTB</i>	2.33	1.70				
<i>HSP90</i>						
<i>RPS27A</i>	-2.56	-2.27		■		■

▲ Absent in p21^{-/-} ● Absent in p53^{-/-} ◊ Absent in WT ■ Absent in p21^{-/-} + IR ◊ Absent in p53^{-/-} + IR

Table 4.2 Ratio of gene expression between HCT116 isogenic cells in response to IR

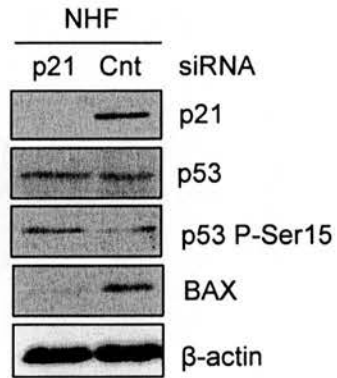


Figure 4.8 In normal human fibroblast cells basal levels of BAX protein are reduced by p21 siRNA mediated gene knockdown. Normal human fibroblast (NHF) cells were transfected with either 1 μ g p21 siRNA or control (Cnt) siRNA and harvested after 48 hr. p21, p53, p53 serine-15 phosphorylation, and BAX were detected by immunoblotting. β -actin was included as a loading control. 10 μ g protein was loaded per lane.

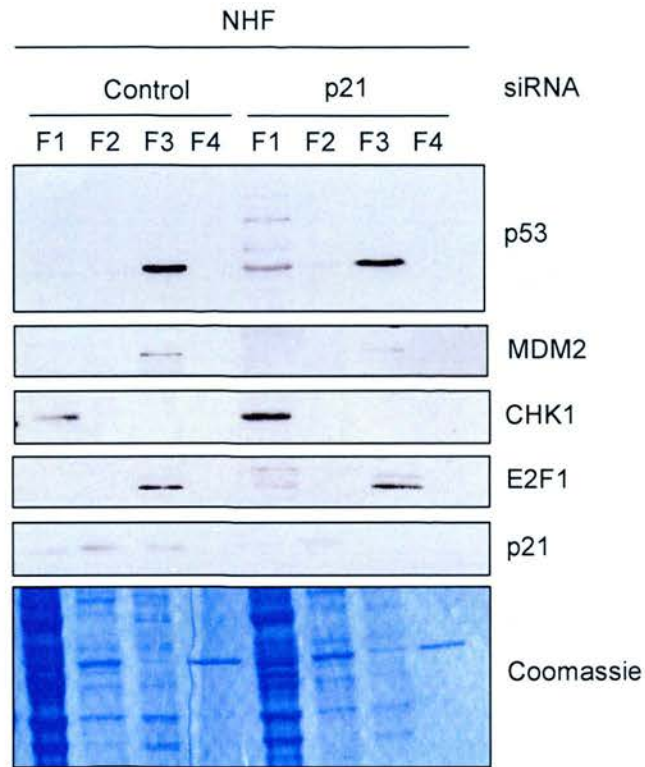


Figure 4.9 p53 subcellular localisation is p21-dependent in NHF cells. NHF cells were transfected with either 1 μg p21 siRNA or control siRNA and after 48 hr, all proteins were extracted according to their subcellular localisation: F1– Cytosol; F2– Membrane/organelle; F3– Nucleus; F4- Cytoskeleton (S-PEK, Calbiochem®). Proteins from each fraction were resolved by SDS-PAGE and analysed by immunoblotting for p53, MDM2, CHK1, E2F1, and p21. 10 μg protein was loaded per lane. Coomassie staining confirmed that protein expression patterns from each fraction are distinct. 5 μg protein was loaded per lane.

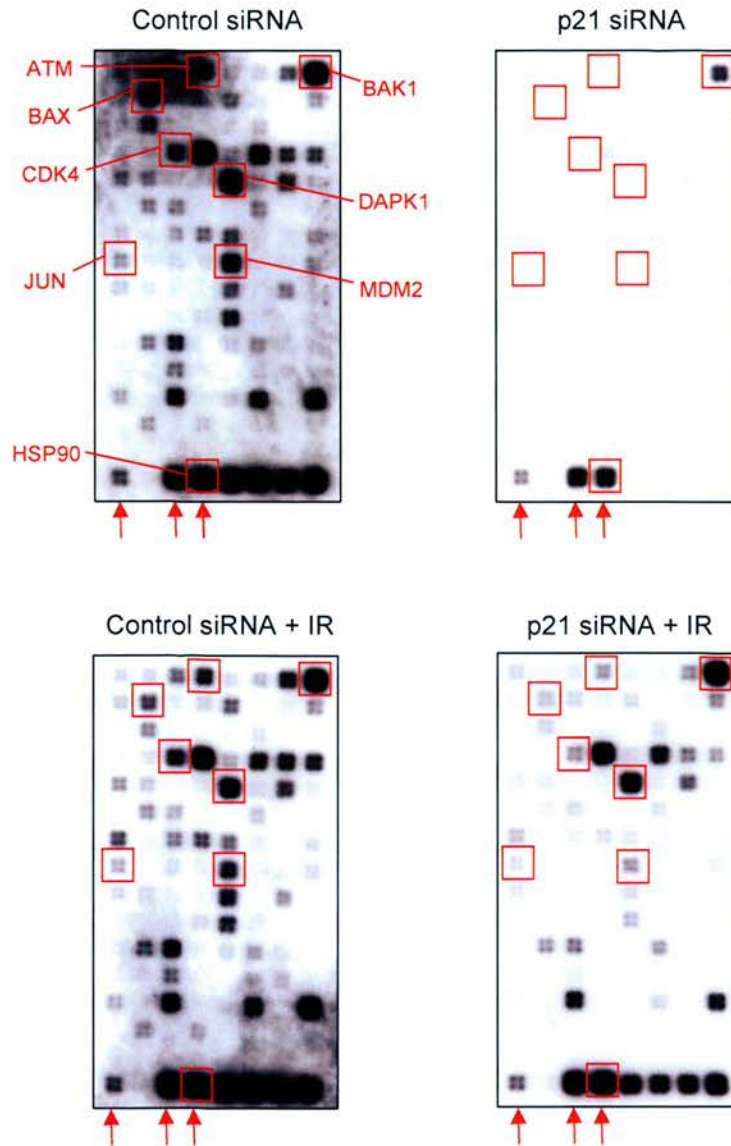


Figure 4.10 Reduction of p21 protein levels in NHF cells causes defects in basal and IR induced p53-dependent gene expression. NHF cells were transfected with either 1 μ g p21 siRNA or control siRNA. After 48 hr cells were irradiated at 5Gy and incubated for a further 4 hr prior to harvesting. DNA microarrays, profiling the gene expression of 113 genes related to p53-mediated signal transduction pathways (OligoGEArray® System, SuperArray), were used (as detailed in materials and methods, 2.17) to indicate the extent of p53 activation in the absence of p21 and in response to IR. Normalisation genes are indicated by red arrows. The genes analysed further are indicated by red boxes.

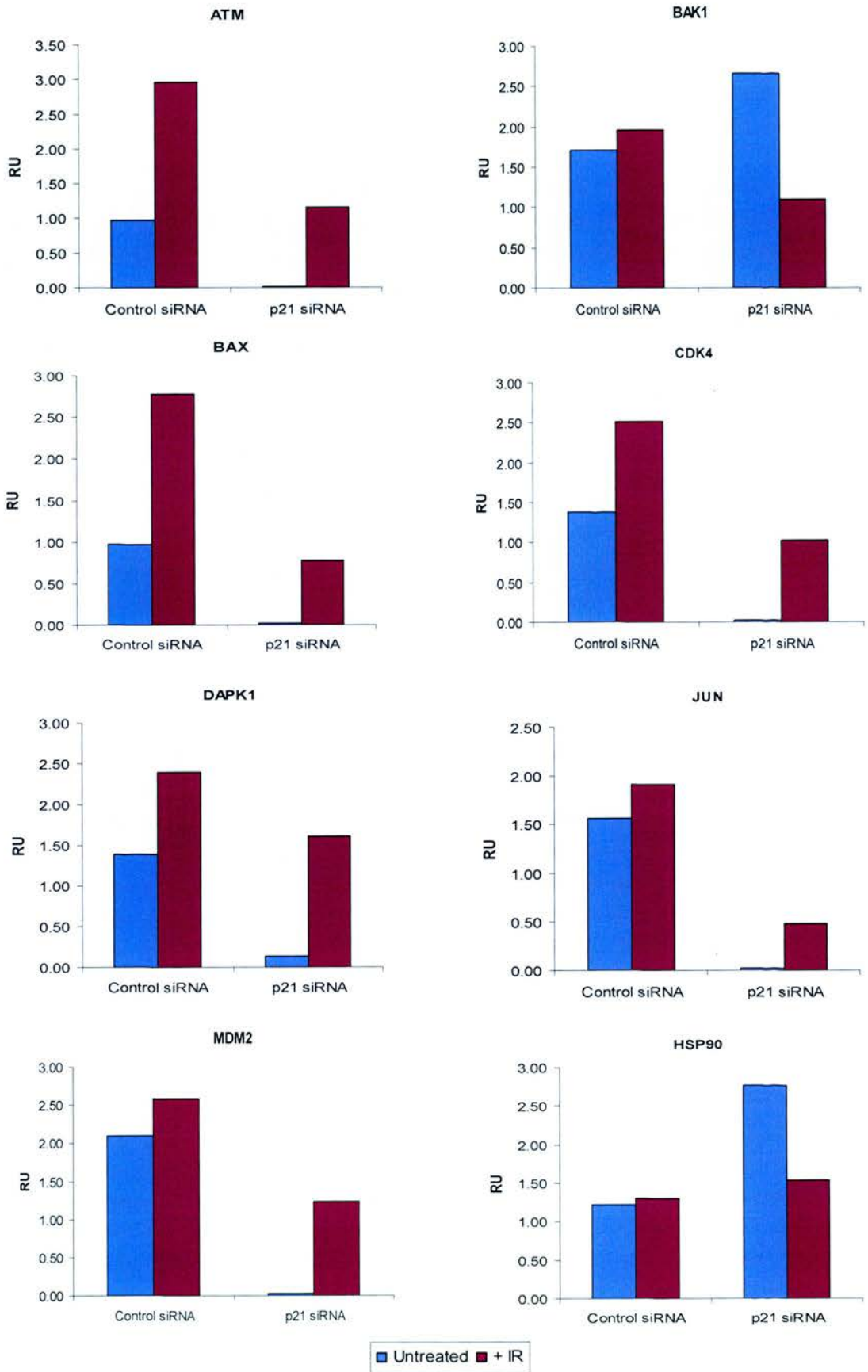
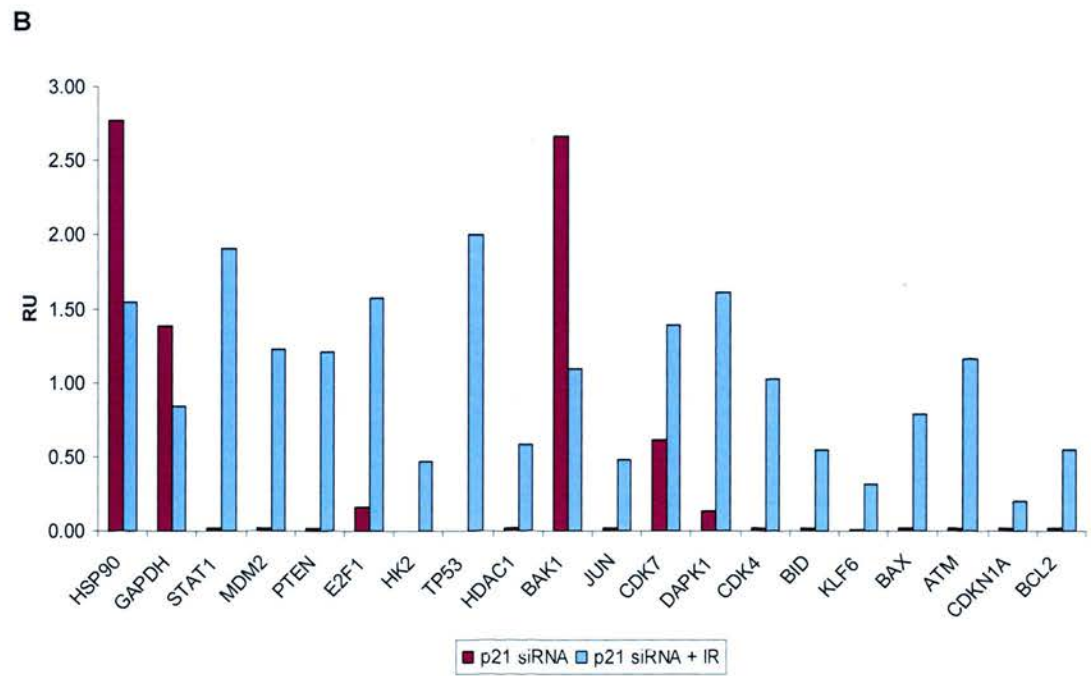
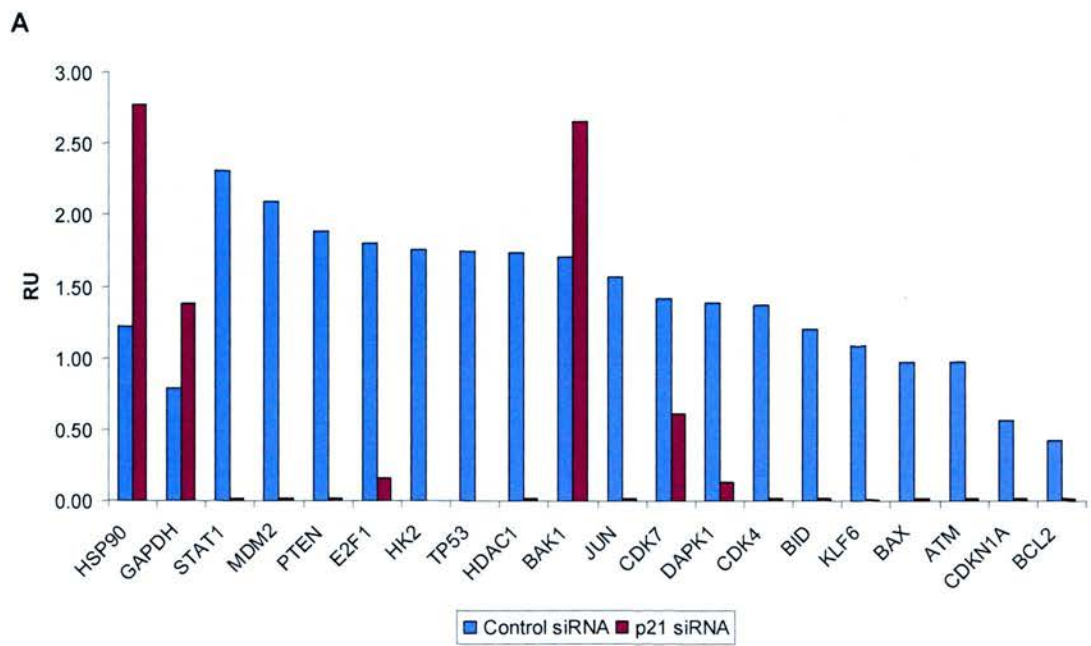


Figure 4.11 Microarray analysis of individual genes indicates aberrant basal and IR-induced gene expression in the absence of p21 in NHF cells. Genes selected to be analysed in more detail included: genes representing the overall trend (see figure 4.13) including *CDK4* and *JUN*; genes divergent from the overall trend including *BAK1* and *DAPK1*; genes of interest due to previous data including *ATM*, *BAX* and *MDM2*; and as a positive control *HSP90*. mRNA levels are indicated by relative units (RU) and were determined by fluorescence intensity normalised to background intensity of microarray membranes.



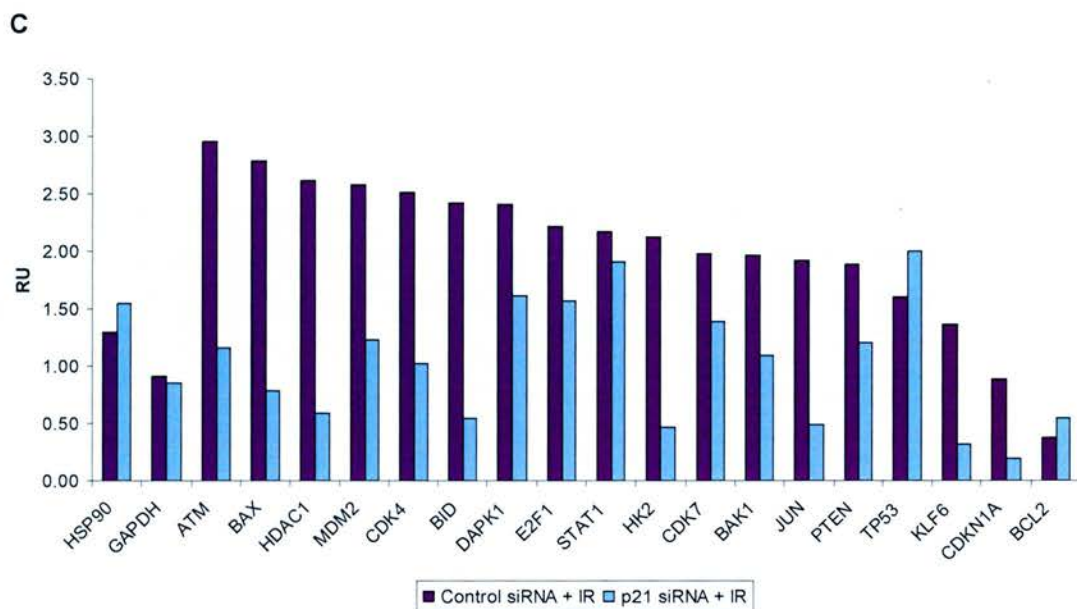


Figure 4.12 Graphical representation of NHF microarray results shows a general reduction of gene expression in the absence of p21 and partial recovery in response to IR. (A) Bar graph comparing gene expression levels of control siRNA- to p21 siRNA- treated NHF cells. **(B)** Bar graph comparing gene expression levels of p21 siRNA- to irradiated p21 siRNA- treated NHF cells. **(C)** Bar graph comparing gene expression levels of irradiated control siRNA- treated cells to irradiated p21 siRNA treated- NHF cells. mRNA levels are indicated by relative units (RU) and were determined by fluorescence intensity normalised to background intensity of microarray membranes.

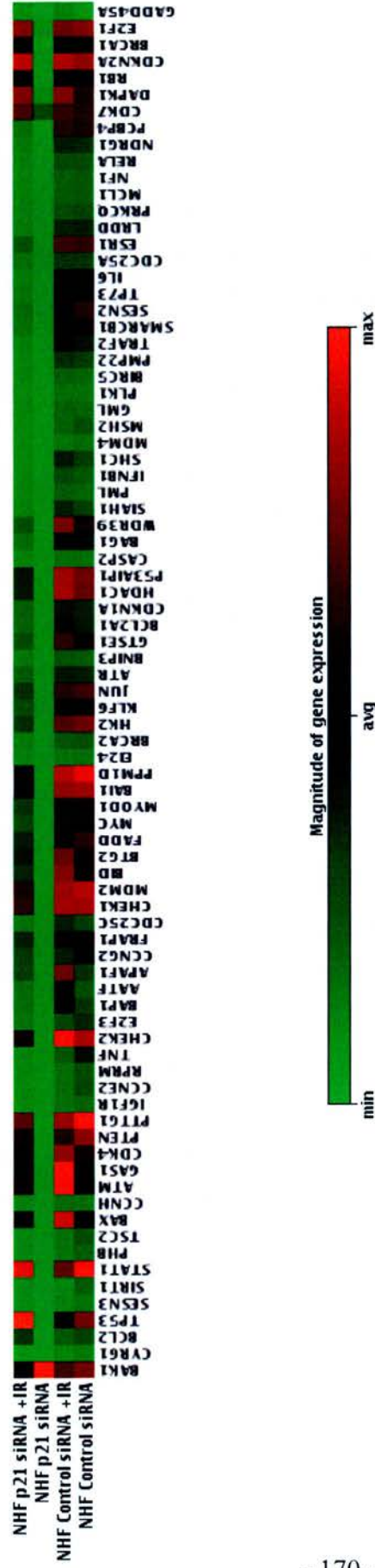


Figure 4.13 NHF gene expression profiles show an overall decrease in basal and IR-induced p53 target gene expression in the absence of p21. Microarrays were analysed using clustergram data analysis tool of the GEArray Expression Analysis Suite programme (SuperArray). The colour coding was assigned according to all values of all samples, whereby expression of each gene is relative to another, as well as across samples. The colour represents the magnitude of gene expression on a scale of green (lowest) to red (highest).

Symbol	NHF			
	Control siRNA	Control siRNA + IR	p21 siRNA	p21 siRNA + IR
Apoptosis				
AATF	X	X		X
APAF1	X	X		X
BAG1		X		X
BAK1	X	X	X	X
BAX	X	X		X
BCL2	X			X
BCL2A1	X	X		X
BID	X	X		X
BNIP3				X
CASP2				X
CRADD	X			
DAPK1	X	X	X	X
DAXX	X	X		X
FADD	X	X		X
HDAC1	X	X		X
LRDD		X		
P53AIP1	X	X		X
PCBP4	X	X		X
PPP1R13L		X		
SIAH1		X	X	
SIRT1	X			
SNCA		X		
TNF		X		
TNFRSF10B	X	X		X
TP73	X	X		X
TP73L		X		
TRAF2		X		
Cell Cycle				
ATM	X	X		X
ATR	X			X
BRCA1	X	X		X
BRCA2	X			X
CCNG2				X
CCNH				X
CDC25A	X			X
CDK4	X	X		X
CDK7	X	X	X	X
CDKN1A	X	X		X
CDKN2A	X	X		X
CHEK1	X	X		X
CHEK2	X	X		X
E2F1	X	X	X	X
E2F3	X			X
FRAP1	X	X		X
GAS1		X		X
GTSE1	X	X		X
HK2	X	X		X
MYC	X	X		X
PLK1		X		
PPM1D	X	X		X
PTEN	X	X		X
RB1	X	X		X
SESN1		X		
SESN2	X	X		X
SMARCB1		X		X
STAT1	X	X	X	X
TP53	X	X		X
TSC1		X		
TSC2		X		
Cell Growth, proliferation and differentiation				
BAI1	X	X		X
BAP1	X	X		X
BTG2	X	X		X
CDC25C	X			X
CIAO1	X	X		X
CYR61	X		X	
KLF6	X	X		X
ESR1	X	X		X
IL6	X			
JUN	X	X		X
MDM2	X	X		X
MYOD1				X
NDRG1		X		
PML		X		
PMP22		X		
PTTG1	X	X		X
SHC1		X		
Control				
HSP90	X	X	X	X
RPS27A	X	X	X	X

X - Gene expression detected by visual assessment

Table 4.3 Genes expressed in NHF cells in response to p21 siRNA and IR

Symbol	NHF			
	p21 siRNA Vs Cnt siRNA	Cnt siRNA + IR Vs Cnt siRNA	p21 siRNA + IR Vs p21 siRNA	p21 siRNA +IR Vs Cnt siRNA + IR
Apoptosis				
AATF	▲	+4.99	▲	-9.09
APAF1	▲	+5.91	▲	-6.67
BAG1	▲	+1.86	▲	-10.0
BAK1	+1.76		-2.44	-1.79
BAX	▲	+2.85	▲	-3.57
BCL2	▲		▲	
BCL2A1	▲	+1.61	▲	-5.0
BID	▲	+2.01	▲	-4.35
BNIP3	▲		▲	○
CASP2	▲	+3.52	▲	
CRADD	▲	-14.29	▲	
DAPK1	-10.0	+1.73	+11.85	
DAXX	▲		▲	-7.14
FADD	▲		▲	-2.44
HDAC1	▲	+1.50	▲	-4.55
LRDD	▲		▲	○
P53AIP1	▲		▲	-4.17
PCBP4	▲		▲	-12.5
PPP1R13L	▲		▲	○
SIAH1	-25.0	◊		○
SIRT1	▲		▲	
SNCA	▲		▲	
TNF	▲	-2.27	▲	○
TNFRSF10B	▲		▲	-2.70
TP73	▲		▲	-16.67
TP73L	▲		▲	
TRAF2	▲	○	▲	○
Cell Cycle				
ATM	▲	+3.04	▲	-2.56
ATR	▲	*	▲	○
BRCA1	▲		▲	
BRCA2	▲	*	▲	○
CCNG2	▲	*	▲	○
CCNH	▲	*	▲	○
CDC25A	▲		▲	
CDK4	▲	+1.83	▲	-2.44
CDK7	-2.32		+2.28	
CDKN1A	▲	+1.56	▲	-4.55
CDKN2A	▲		▲	
CHEK1	▲		▲	-2.0
CHEK2	▲		▲	-2.50
E2F1	-11.11		+9.76	
E2F3	▲	■	▲	○
FRAP1	▲		▲	-2.27
GAS1	▲	+4.08	▲	-3.45
GTSE1	▲	+1.56	▲	-6.67
HK2	▲		▲	-4.55
MYC	▲		▲	-2.70
PLK1	▲		▲	
PPM1D	▲		▲	-2.70
PTEN	▲		▲	-1.56
RB1	▲		▲	
SESN1	▲	+5.98	▲	○
SESN2	▲		▲	-10.0
SMARCB1	▲		▲	-12.5
STAT1	-100.0		+101.38	
TP53	▲		▲	
TSC1	▲		▲	
TSC2	▲		▲	
Cell Growth, proliferation and differentiation				
BAI1	▲		▲	-2.56
BAP1	▲	+3.72	▲	-11.1
BTG2	▲	+1.83	▲	-3.45
CDC25C	▲	■	▲	○
CIAO1	▲		▲	
CYR61	-16.67	■	▲	
KLF6	▲		▲	-4.35
ESR1	▲		▲	-7.69
IL6	▲	■	▲	
JUN	▲		▲	-4.0
MDM2	▲		▲	-2.08
MYOD1	▲	■	▲	○
NDRG1	▲		▲	○
PML	▲	+1.88	▲	
PMP22	▲	+1.60	▲	○
PTTG1	▲		▲	-1.75
SHC1	▲	◊	▲	○
Control				
HSP90	+1.76			
RPS27A				

▲ Absent in p21 siRNA ◊ Absent in Control siRNA ■ Absent in Control siRNA + IR ○ Absent in p21 siRNA + IR

Table 4.4 Ratio of gene expression between NHF cells treated with either control or p21 siRNA and with or without IR

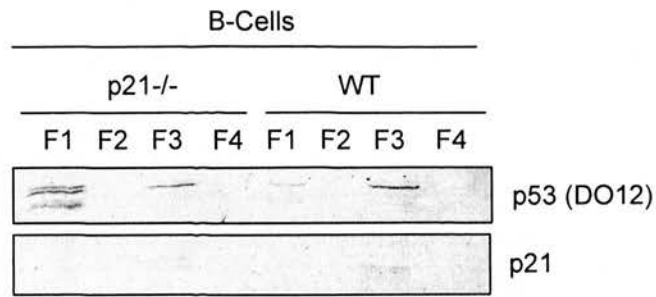


Figure 4.14 B-cells extracted from p21^{-/-} mice contain mislocalised p53 compared to WT counterparts. B-cells were extracted from WT and p21^{-/-} mice (as described in materials and methods 2.10), and incubated for 24 hr. Proteins were extracted according to their subcellular localisation: F1– Cytosol; F2– Membrane/organelle; F3– Nucleus; F4- Cytoskeleton (S-PEK, Calbiochem®). Proteins from each fraction were resolved by SDS-PAGE and analysed by immunoblotting for p53 and p21. 10 µg protein was loaded per lane.

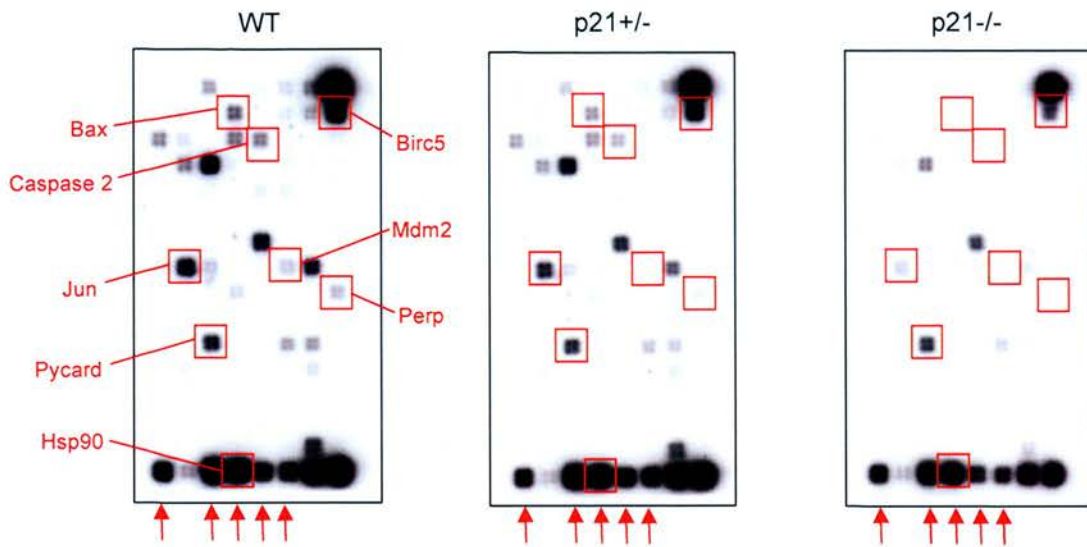


Figure 4.15 Microarray analysis of B-cells extracted from WT, p21^{+/-} and p21^{-/-} mice show that p53-dependent gene expression is affected by p21 gene dosage. B-cells were extracted from WT, p21^{+/-} and p21^{-/-} mice (as described in materials and methods 2.10), and incubated for 24 hr. DNA microarrays, profiling the gene expression of 113 genes related to p53-mediated signal transduction pathways (OligoGEArray® System, SuperArray), were used (as detailed in materials and methods, 2.17) to indicate the extent of p53 activation in the absence of p21. Normalisation genes are indicated by red arrows. The genes analysed further are indicated by red boxes.

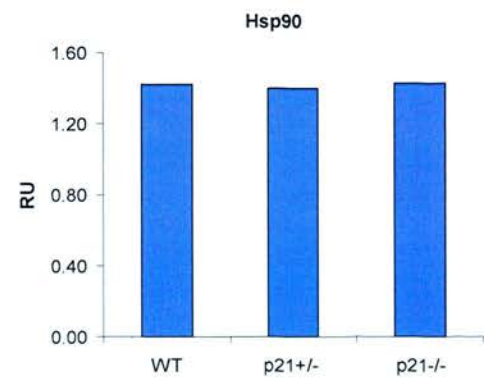
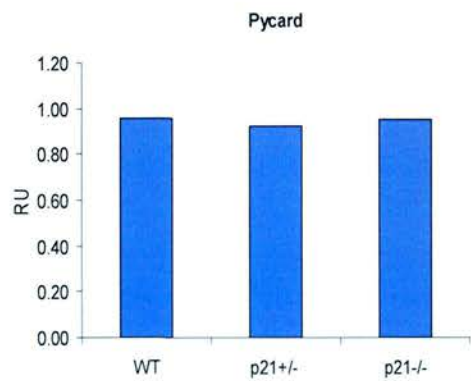
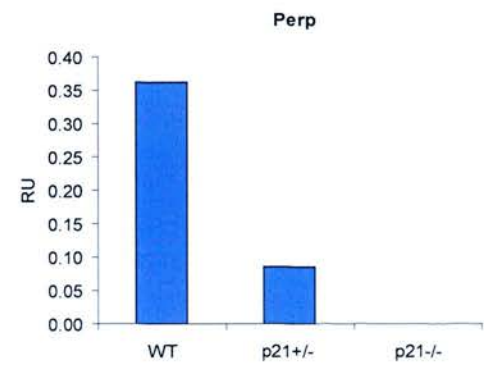
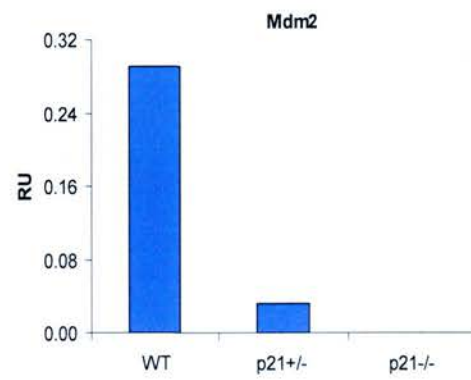
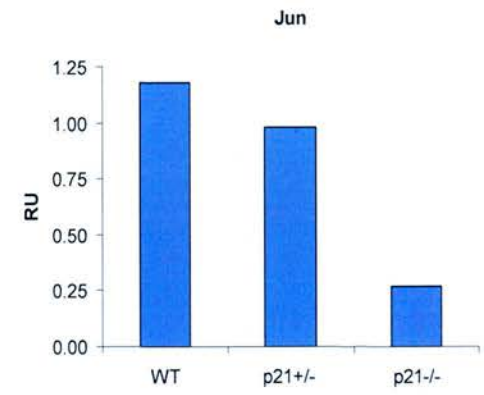
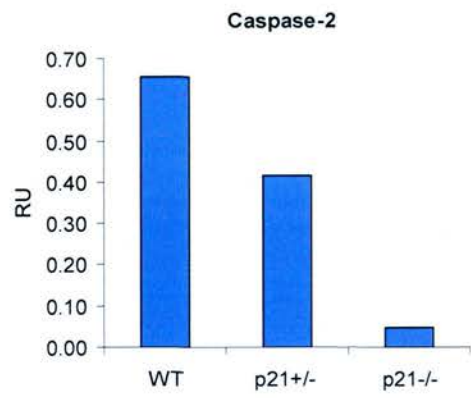
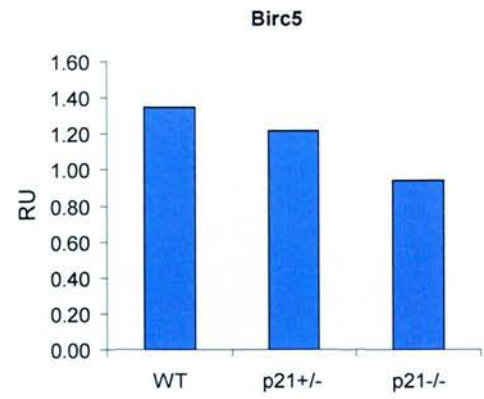
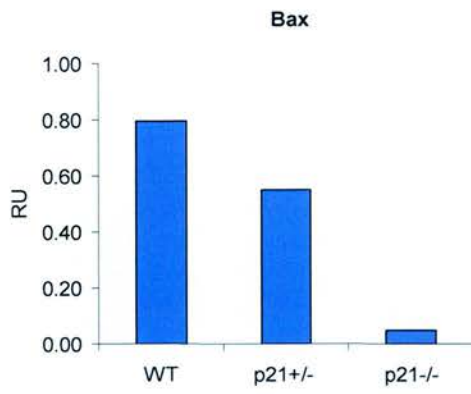


Figure 4.16 Graphical representation of microarray results of selected genes indicates p21 gene dosage effects. Genes selected to be analysed in more detail included: genes representing the overall trend (see figure 4.18) including, *Bax*, *Caspase-2*, *Jun*, *Mdm2* and *Perp*; genes divergent from the overall trend *Bir5* and *Pycard*; and as a positive control *HSP90*. mRNA levels are indicated by relative units (RU) and were determined by fluorescence intensity normalised to background intensity of microarray membranes.

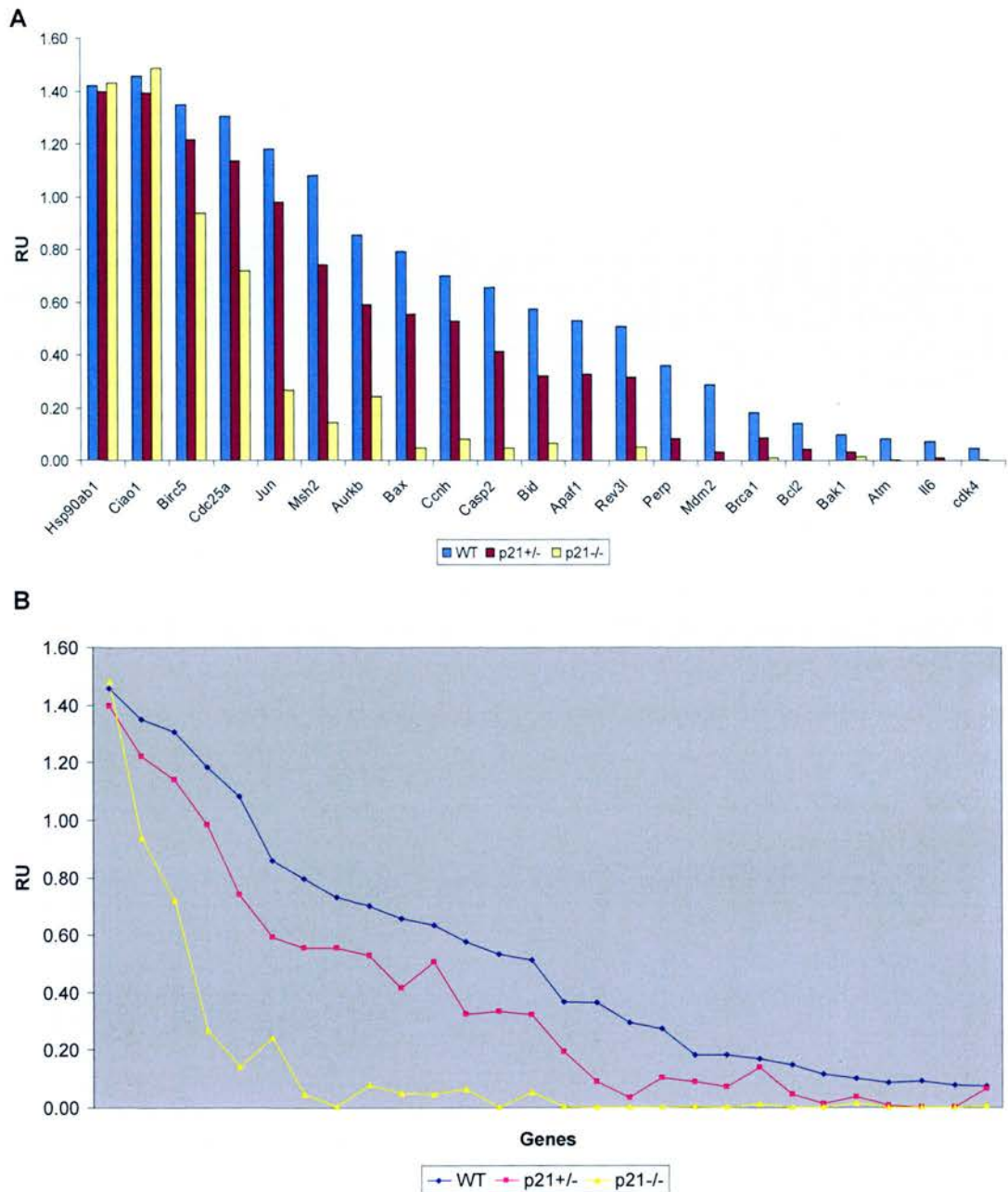


Figure 4.17 p53-dependent gene expression is affected by p21 gene dosage. **(A)** Bar graph representation of microarray results comparing gene expression of B-cells extracted from WT, p21^{+/-} and p21^{-/-} mice. **(B)** Line graph representation of microarray results comparing gene expression of B-cells extracted from WT, p21^{+/-} and p21^{-/-} mice. mRNA levels are indicated by relative units (RU) and were determined by fluorescence intensity normalised to background intensity of microarray membranes.

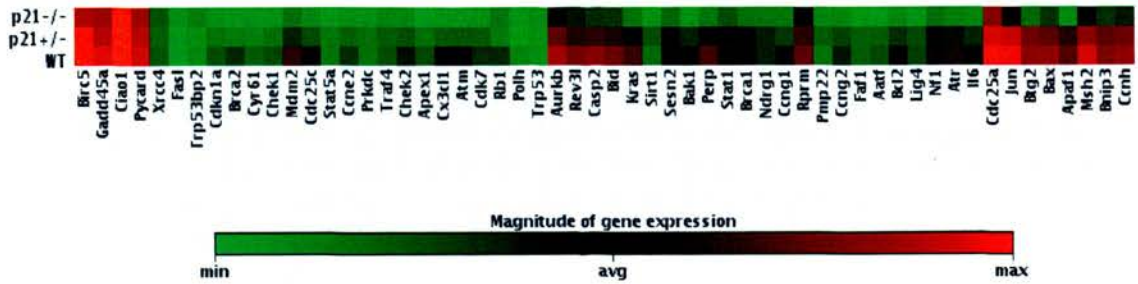


Figure 4.18 Gene expression profiles of B-cells extracted from WT, p21^{+/-} and p21^{-/-} mice show an overall decrease in basal p53 target gene expression in the absence of p21. Microarrays were analysed using the clustergram data analysis tool of the GEArray Expression Analysis Suite programme (SuperArray). The colour coding was assigned according to all the values of all samples, whereby expression of each gene is relative to another, as well as across genotypes. The colour represents the magnitude of gene expression on a scale of green (lowest) to red (highest).

Symbol	Mouse B-Cells		
	WT	p21+/-	p21-/-
Apoptosis			
<i>Apaf1</i>	x	x	
<i>Bak1</i>	x	x	x
<i>Bax</i>	x	x	x
<i>Bbc3</i>	x		
<i>Bcl2</i>	x	x	
<i>Bid</i>	x	x	x
<i>Birc5</i>	x	x	x
<i>Bnip3</i>	x	x	x
<i>Casp2</i>	x	x	
<i>Foxo3a</i>	x		
<i>Perp</i>	x	x	
<i>Pycard</i>	x	x	x
<i>Rela</i>	x		
<i>Sirt1</i>		x	
<i>Tnf</i>		x	
Cell Cycle			
<i>Atm</i>	x	x	
<i>Atr</i>	x	x	
<i>Aurkb</i>	x	x	
<i>Brca1</i>	x	x	
<i>Ccng2</i>	x	x	
<i>Ccnh</i>	x	x	x
<i>Cdc25a</i>	x		x
<i>Cdk4</i>	x	x	
<i>Cdk7</i>	x		
<i>Cdkn1a</i>	x		
<i>Chek2</i>	x		
<i>Gadd45a</i>	x	x	x
<i>Kras</i>	x	x	
<i>Msh2</i>	x	x	x
<i>Pmp22</i>		x	
<i>Reprimo</i>	x	x	x
<i>Sesn2</i>	x	x	
<i>Stat1</i>	x	x	
Cell Growth, proliferation and differentiation			
<i>Btg2</i>	x	x	
<i>Cdc25c</i>	x		
<i>Ciao1</i>	x	x	x
<i>Cx3cl1</i>	x		
<i>Il6</i>	x	x	
<i>Jun</i>	x	x	x
<i>Mdm2</i>	x	x	
<i>Myod1</i>	x		
<i>Ndr1</i>	x	x	
<i>Nf1</i>	x	x	
<i>Pttg1</i>	x		
DNA Repair			
<i>Lig4</i>	x		
<i>Rev3l</i>	x	x	x
Control			
<i>B2m</i>	x	x	x
<i>Hsp90</i>	x	x	x
<i>Ppia</i>	x	x	x
<i>Rps27a</i>	x	x	x

x - Gene expression detected by visual assessment

Table 4.5 Genes expressed in B-cells extracted from transgenic mice either wild-type, heterozygous, or nullizygous for the *p21* gene

Symbol	Mouse B-Cells		
	p21+/- Vs WT	p21-/- Vs WT	p21-/- Vs p21+/-
Apoptosis			
<i>Apaf1</i>	-1.62	▲	▲
<i>Bak1</i>	-2.86	-7.14	-2.43
<i>Bax</i>		-16.67	-11.11
<i>Bbc3</i>	•	▲	•▲
<i>Bcl2</i>	-3.33	▲	▲
<i>Bid</i>	-1.79	-9.1	-5.0
<i>Birc5</i>			
<i>Bnip3</i>		-14.28	-11.11
<i>Casp2</i>	-1.59	-14.29	-8.33
<i>Foxo3a</i>	•	▲	•▲
<i>Perp</i>	-4.17	▲	▲
<i>Pycard</i>			
<i>Rela</i>	•	▲	•▲
<i>Sirt1</i>	◇	▲	▲
<i>Tnf</i>	+5.40	▲	▲
Cell Cycle			
<i>Atm</i>	-16.67	▲	▲
<i>Atr</i>	-2.63	▲	▲
<i>Aurkb</i>		▲	▲
<i>Brca1</i>	-2.08	▲	▲
<i>Ccng2</i>	-7.70	▲	▲
<i>Ccnh</i>		-9.10	-6.67
<i>Cdc25a</i>	•	-1.81	-1.59
<i>Cdk4</i>	-16.67	▲	▲
<i>Cdk7</i>	•	▲	▲
<i>Cdkn1a</i>	•	▲	•▲
<i>Chek2</i>	•	▲	•▲
<i>Gadd45a</i>			
<i>Kras</i>	-1.89	▲	▲
<i>Msh2</i>		-7.69	-5.26
<i>Pmp22</i>	◇	▲	▲
<i>Reprimo</i>		-1.72	
<i>Sesn2</i>		▲	▲
<i>Stat1</i>		▲	▲
Cell Growth, proliferation and differentiation			
<i>Btg2</i>		▲	▲
<i>Cdc25c</i>	•	▲	▲
<i>Ciao1</i>			
<i>Cx3cl1</i>	•	▲	▲
<i>Il6</i>	-6.67	▲	▲
<i>Jun</i>		-4.35	-3.7
<i>Mdm2</i>	-9.09	▲	▲
<i>Myod1</i>	•	▲	▲
<i>Ndrp1</i>		▲	▲
<i>Nf1</i>	-2.63	▲	▲
<i>Pttg1</i>	•	▲	▲
DNA Repair			
<i>Lig4</i>	•	▲	▲
<i>Rev3l</i>	-1.59	-10	-6.25
Control			
<i>B2m</i>			
<i>Hsp90</i>			
<i>Ppia</i>			
<i>Rps27a</i>			

◇ Absent in WT • Absent in p21+/- ▲ Absent in p21-/-

Table 4.6 Ratio of gene expression in B-cells extracted from transgenic mice either wild-type, heterozygous, or nullizygous for the *p21* gene

A GENETIC INTERACTION BETWEEN ATM AND p21
MAINTAINS p53 NUCLEAR LOCALISATION

5.1 Introduction

ATM kinase plays a central role in regulating the cellular response to DNA damage through the phosphorylation of proteins involved in cell cycle checkpoints and DNA repair. The *ATM* gene is defective in the autosomal recessive disorder Ataxia Telangiectasia, a disease characterised by neurodegeneration, immunodeficiency, growth retardation and cancer susceptibility. Cellular features of Ataxia Telangiectasia include hypersensitivity to agents that cause DNA double strand breaks and a decreased capacity to activate the G1, S, and G2 cell cycle checkpoints (Canman & Lim, 1998; Lavin & Shiloh, 1997).

ATM is predominantly a nuclear protein (Andegeko *et al.*, 2005; Lakin *et al.*, 1996), and is recruited to sites of DNA damage, leading to activation of DNA damage response pathways (Falck *et al.*, 2005). Consistent with ATM's role as a primary transducer of the DNA damage response, northern blot analysis showed that *ATM* is ubiquitously expressed in all human tissues (Chen & Lee, 1996), and ATM steady-state protein levels do not significantly vary during the cell cycle or in response to IR (Chan *et al.*, 1998; Larkin *et al.* 1996; Gately *et al.*, 1998). The lack of observable changes in ATM is in marked contrast to the changes in p53 and other

proteins, which are induced in response to DNA damage. Although ATM is constitutively expressed through out the cell cycle, ATM kinase activity increases approximately 3-fold following cellular exposure to IR (Canman *et al.*, 1998). Exposure of cells to IR causes a rapid autophosphorylation of ATM on serine-1981, and leads to dissociation of inactive ATM homodimers to generate catalytically active monomers (Bakkenist & Kastan, 2003). ATM activation has also been shown to depend on two additional ATM autophosphorylation sites, serine-367 and serine-1893 (Kozlov *et al.* 2006), and acetylation mediated by Tip60 histone acetyltransferase (Sun *et al.*, 2005). Similarly, two protein phosphatases have been implicated in ATM regulation, protein phosphatase 2A mediated dephosphorylation inhibits ATM activation (Goodarzi *et al.*, 2004), whereas protein phosphatase 5 interacts with ATM in a DNA damage inducible fashion and contributes to ATM activation (Ali *et al.*, 2004). This illustrates that ATM is highly regulated by a repertoire of post-translational modifications, and regulation of ATM may involve yet uncharacterised interactions with additional proteins.

Activation of ATM results in phosphorylation of a plethora of downstream targets. Some of these proteins are direct targets of ATM, for example ATM directly phosphorylates p53 at serine-15 (Canman *et al.*, 1998) and histone H2AX at serine-139 (Rogakou *et al.*, 1998). Other proteins may be phosphorylated indirectly, through ATM-mediated regulation of additional protein kinases, such as CHK1 and CHK2. Recently, a large scale proteomic analysis of proteins phosphorylated in response DNA damage on consensus sites recognised by ATM, revealed an incredible 700 human proteins are potentially targeted by ATM (Matsuoka *et al.*, 2007).

An important target of ATM is p53, and phosphorylation of p53 at serine-15 is frequently used as an indicator of ATM kinase activity. ATM phosphorylates p53 directly at serine-15 in response to IR (Canman *et al.*, 1998; Banin *et al.*, 1998; Sciliciano *et al.*, 1997). This contributes primarily to enhancing the activity of p53 as a transcription factor (Ashcroft *et al.* 1999; Dumaz & Meek, 1999). ATM also regulates the phosphorylation of p53 at serine-20, by activating an intermediate serine/threonine protein kinase, CHK2. CHK2 is phosphorylated by ATM at threonine-68 in response to IR (Matsuoka *et al.*, 2000). ATM and CHK2 therefore cooperate to ensure optimal stabilisation and activation of p53 by reducing the interaction of p53 with MDM2, as MDM2 docks to the N-terminal region of p53 (amino acids 18-23) and targets it for proteasome-mediated degradation (Haupt *et al.*, 1997; Kubbutat *et al.*, 1997). ATM-dependent phosphorylation of MDM2 at serine-395 (Khosravi *et al.* 1999) may also contribute to p53 stabilisation by decreasing the ability of MDM2 to shuttle p53 from the nucleus to the cytoplasm (Maya *et al.*, 2001). In addition, phosphorylation of p53 at serine-15 has been shown to recruit the transcriptional co-activator p300 and to stabilise the p53/p300 complex (Dumaz & Meek, 1999). p300 acetylates p53 at lysine-373 and lysine-382, activating p53-sequence specific DNA binding. p300 and MDM2 bind to overlapping sites in the N-terminus of p53, therefore phosphorylation of this region may regulate the activity of p53 by influencing the steady state binding of these molecules (Lakin & Jackson, 1999; Dornan & Hupp, 2000). Hence, ATM-mediated activation and stabilisation of p53 protein is achieved by several different ATM-dependent mechanisms, and the existence of additional ATM targets in this pathway is not unlikely.

Specific inhibition of ATM by a small molecule compound would enable further dissection of the ATM signalling pathway. ATM is a member of the phosphatidylinositol-3-kinase like kinase (PIKK) family of serine/threonine protein kinases (Shiloh, 2003). The mammalian members of this family include, ATM, ATR, hSMG-1, mTOR, and DNA-PK. The PIKK protein kinases are conserved from yeast to mammals, and respond to various stresses by phosphorylation of substrates in the appropriate pathways (Abraham, 2004a). All members of the PIKK family are classically inhibited by two small molecule inhibitors, wortmannin and caffeine (Sarkaria *et al.* 1998; Sarkaria *et al.*, 1999).

Wortmannin (Figure 5.1A) is a sterol-like fungal metabolite, which competes with ATP for binding to the kinase domain. Once inserted into the binding cleft, wortmannin undergoes nucleophilic attack by a conserved lysine residue in the catalytic domain of the PIKK, resulting in the formation of a covalent bond (Wymann *et al.* 1996; Price & Youmell, 1996). Wortmannin is therefore a potent irreversible inhibitor of ATM (IC_{50} 150 nM), DNA-PK (IC_{50} 16 nM), and hSMG-1 (IC_{50} 80 nM), and to a lesser extent ATR (IC_{50} 1.8 μ M) (Sarkaria *et al.* 1998). Caffeine (Figure 5.1B) is a purine analogue, and competes with ATP to inhibit the phosphotransferase activities of PIKKs. Caffeine inhibits the protein kinase activities of ATM, ATR, hSMG-1, and mTOR with IC_{50} values ranging from 0.2 to 1 mM, although DNA-PK activity seemed to be relatively resistant to caffeine (IC_{50} 10 mM) (Sarkaria *et al.*, 1999; Yamashita A. *et al.*, 2001). Wortmannin and caffeine have previously been used at the cellular and molecular level to study the PIKK family. However interpretation of these results has proved difficult due to the non-specific nature of these drugs.

Identification and characterisation of a specific inhibitor of ATM (Hickson *et al.* 2004) has provided a novel molecular tool in a new era of ATM research, including classifying the role ATM plays in HIV-1 replication (Lau *et al.*, 2005). Hickson *et al.* (2004) through screening a small molecule compound library developed for the PIKK family identified an ATP competitive inhibitor, 2-morpholin-4-yl-6-thianthren-1-yl-pyran-4-one (KU-55933) (Figure 5.1C) that inhibits ATM with an IC_{50} of 13 nM. KU-55933 was shown to be specific with respect to other members of the PIKK family. The cellular activity of KU-55933 was illustrated in the human osteosarcoma cell line, U2OS. KU-55933 had a dose dependent effect, inhibiting ATM-dependent phosphorylation of p53 at serine-15 with an estimated cellular IC_{50} of 300 nM. However this has not been shown in other cell lines which may exhibit varying sensitivity to the drug.

In this chapter, KU-55933 was utilised as a specific and cellularly active ATM inhibitor to elucidate the role of ATM in p21-dependent regulation of p53.

5.2 Results

5.2.1 Elevated phosphorylation of p53 at serine-15 is abated by specific inhibition of ATM

To determine the effectiveness of KU-55933 as a specific ATM inhibitor in the HCT116 cell line, HCT116 WT cells were treated with increasing concentrations of KU-55933, irradiated at 7 Gy and harvested after 4 hours (Figure 5.2). The phosphorylation status of p53 at serine-15 and CHK2 at threonine-68 were used as

markers of ATM activity. KU-55933 had a dose dependent effect, inhibiting ATM-dependent phosphorylation of p53 at serine-15 and CHK2 at threonine-68 with an estimated cellular IC_{50} of 300 nM and 100 nM, respectively. These values are comparable to those found for U2OS cells (Hickson *et al.* 2004). KU-55933 also had a dose dependent effect on phosphorylation of ATM at serine-1981 (Figure 5.2), which confirms that phosphorylation of ATM at serine-1981 in response to IR is ATM-dependent. CHK2 is a very stable protein and has a half-life longer than 6 hours (Bartek *et al.*, 2001), consistently CHK2 protein levels remained constant with increasing doses of KU-55933. In contrast p53 is a relatively unstable protein with a half-life of approximately 30 minutes (Figure 3.2A). Phosphorylation of p53 at serine-15 is associated with stabilisation of p53 protein (Siliciano *et al.*, 1997). Interestingly, inhibition of ATM did not cause the expected decrease in p53 levels associated with dephosphorylation of p53, indicating that KU-55933 mediated ATM inhibition may uncouple p53 phosphorylation and protein levels. This data indicates that additional factors maybe involved in p53 stabilisation. In the HCT116 cell line ATM kinase activity, as analysed by immunoblotting of ATM targets in response to IR, was effectively inhibited using KU-55933 at a concentration of 10 μ M. This concentration was therefore selected for use in further experiments to inhibit ATM kinase activity.

As previously shown, p53 serine-15 phosphorylation levels are elevated in HCT116 p21^{-/-} cells compared to WT cells (Figure 3.4A) and in response to cellular stress are not further induced (Figure 3.5A). This indicates that p21 negatively regulates a p53 serine-15 kinase whereby loss of p21 facilitates constitutive activation of the kinase and enhances phosphorylation of p53 at serine-15. CHK2

threonine-68 phosphorylation levels are also elevated in the p21^{-/-} cells compared to WT cells (Figure 3.5B), as CHK2 threonine-68 is a specific ATM target, this data suggests that ATM may be the active p53 serine-15 kinase in p21^{-/-} cells. The specific ATM inhibitor, KU-55933 was used a molecular tool to dissect the role of ATM in p21-dependent p53 serine-15 phosphorylation. HCT116 WT and p21^{-/-} cells were incubated with 10 μ M KU-55933 for 0 hour, 14 hours and 24 hours (Figure 5.3). In WT cells p53 and CHK2 protein levels were not affected by ATM inhibition and neither p53 serine-15 nor CHK2 threonine-68 phosphorylation could be detected. In p21^{-/-} cells, both p53 and p53 serine-15 phosphorylation levels were elevated compared to WT cells. In p21^{-/-} cells p53 protein levels were unchanged by ATM inhibition, whereas levels of p53 serine-15 phosphorylation were significantly attenuated although not fully reduced, after 24 hours incubation with KU-55933 (Figure 5.3). Similarly, levels of CHK2 phosphorylation at threonine-68 were elevated in p21^{-/-} cells compared to WT cells at 0 hour and 14 hours. Following 24 hours incubation with KU-55933, CHK2 threonine-68 phosphorylation levels were diminished (Figure 5.3). Phosphorylation of p53 at serine-15 and CHK2 at threonine-68 are specific ATM targets. In the absence of p21, phosphorylation of both proteins at ATM targets sites are elevated, specific inhibition of ATM by KU-55933 confirmed that phosphorylation of these sites are ATM-dependent. This data suggests that ATM activity is influenced by p21 levels and that ATM is constitutively active in the absence of p21.

Phosphorylation of ATM at serine-1981 is associated with ATM activation, and has been proposed to be an autophosphorylation site (Bakkenist & Kastan, 2004). However, ATM and ATR have similar consensus phosphorylation motifs and target

common substrates, although CHK1 at serine-317 and CHK2 at threonine-68 are specific ATR and ATM substrates, respectively (Jazayeri *et al.*, 2006). In response to UV treatment and replication fork stalling, phosphorylation of ATM at serine-1981 and ATM activation is ATR-dependent, and phosphorylation of ATM at serine-1981 has been shown to be targeted by ATR *in vitro* (Stiff *et al.*, 2006). Here, we show that p21^{-/-} cells contain elevated levels of ATM and ATM serine-1981 phosphorylation compared to WT cells (Figure 5.3). Phosphorylation of ATM was unaffected by ATM inhibition mediated by KU-55933 and suggests that in p21^{-/-} cells phosphorylation of ATM at serine-1981 is ATM-independent (Figure 5.3). Therefore ATM appears to be the principal p53 serine-15 kinase active in p21^{-/-} cells however additional kinases may be active which are able to target ATM at serine-1981 and p53 at serine-15 but not CHK2 at threonine-68. This data indicates that p21-dependent regulation of p53 serine-15 phosphorylation is predominantly mediated by ATM, but supplementary kinases, such as ATR, may be involved.

5.2.2 *In vitro* ATM kinase activity is unaffected by loss of p21

In the absence of p21 and exogenous cellular stress, ATM appears to be constitutively active as a p53 serine-15 and CHK2 threonine-68 kinase. Previously, specific inhibition of ATM in HCT116 p21^{-/-} cells by a specific small molecule inhibitor was shown to reduce p53 serine-15 and CHK2 threonine-68 phosphorylation to levels comparable to WT cells (Figure 5.3). This data indicates that *in vivo* ATM is more active in the absence of p21. To assess specific ATM kinase activity *in vitro*, ATM was initially immunoprecipitated from the nuclear

extracts of HCT116 WT and p21^{-/-} cells. To confirm that the immunoprecipitation of ATM had been successful, samples were analysed by immunoblotting (Figure 5.4A). WT and p21^{-/-} nuclear extracts contained approximately equal amounts of immunoprecipitated ATM (Figure 5.4A). Previously, immunoblotting of WT and p21^{-/-} whole cell extracts has shown that p21^{-/-} cells contain more ATM than WT cells (Figure 5.3). This apparent difference in immunoblots suggests that WT and p21^{-/-} cells contain the same quantity of nuclear ATM, but that p21^{-/-} cells may contain more cytoplasmic ATM than WT cells.

Specific kinase activity of immunoprecipitated ATM from WT, p21^{-/-} and as a positive control HeLa nuclear extracts, was measured by immunochemical detection of a phospho-substrate (Figure 5.4B) or radiolabelling the substrate with [γ -³²P] ATP (Figure 5.4C). The substrates used in both experiments were N-terminal 66 amino acids of p53 fused to GST (GST-p53N66), and as a negative control GST-p53N66 fragment with serine-15 mutated to alanine (GST-p53N66-S15A). Immunochemical detection of GST-p53N66 with a p53 serine-15 phosphorylation specific antibody showed no difference in p53 serine-15 phosphorylation between WT and p21^{-/-} cells (Figure 5.4B). As expected the negative control, GST-p53N66-S15A, was not detected. ATM immunoprecipitated from HeLa nuclear extract appeared more active than that of WT cells (Figure 5.4B). Similar results were obtained by radiolabelling the substrate with [γ -³²P] ATP (Figure 5.4C). To fully confirm that ATM is specifically immunoprecipitated from the cell lysates and is responsible for the specific phosphorylation of the substrate, an additional negative control should have been included, consisting of ATM immunoprecipitated from

ATM-null cells. Therefore specific ATM activity can only be presumed to be assayed here and requires further confirmation.

In contrast to *in vivo* data, no difference in presumed ATM kinase activity could be detected *in vitro* between WT and p21^{-/-} cells. Here, ATM was immunoprecipitated from nuclear extracts as ATM is principally characterised as a nuclear protein (Goodarzi & Lees-Miller, 2003). However, previous papers have shown that small amounts of ATM can be localized to the cytoplasm (Lim *et al.*, 1998; Barlow *et al.*, 2000; Wu *et al.*, 2006), and our data indicates that there may be more cytoplasmic ATM in HCT116 p21^{-/-} cells compared to WT cells. In speculation, different pools of ATM within cells maybe influenced by different factors depending on its subcellular localisation. Cytoplasmic ATM may interact with cytoplasmic p21, which maintains ATM in a readily activated state. Therefore in the absence of p21, p53 could be shuttled out of the nucleus and phosphorylated at serine-15 by a small cytoplasmic pool of active ATM. This is supported by subcellular fractionation data which showed that phosphorylated p53 at serine-15 in the p21^{-/-} cells is localised to the cytoplasm and membranes/organelles, and not detected in the nucleus (Figure 4.1).

5.2.3 Specific inhibition of ATM disrupts cellular localisation of endogenous p53

Previous data shows that loss of p21 in three model systems caused aberrant cellular localisation of endogenous p53 (Chapter 4). In control cells p53 is strictly nuclear, whereas loss of p21 causes p53 redistribution to both the cytoplasm and the nucleus. To assess the role of ATM in p53 localisation, HCT116 WT and p21^{-/-} cells were

treated with 10 μ M KU-55933 and incubated for 24 hours. Proteins were differentially extracted according to their subcellular localisation, and analysed by immunoblotting (Figure 5.5A). Surprisingly, specific inhibition of ATM in WT cells caused mislocalisation of endogenous p53, to the same extent as direct loss of p21. In DMSO treated WT cells (0 μ M, Figure 5.5A) p53 was localised to the nucleus, consistent with previous observations (Figure 4.1). In contrast, in WT cells treated with KU-55933 p53 was localised to the cytoplasm, membranes/organelles and nucleus (Figure 5.5A). Interestingly, p21 levels were also elevated in WT cells treated with KU-55933 compared to DMSO treated WT cells, indicating that inhibition of ATM may be stimulating an endogenous cellular stress response (Figure 5.5A). In untreated p21^{-/-} cells, p53 was localised to the cytoplasm, membranes/organelles and nucleus (Figure 5.5A), which corresponds with previous observations (Figure 4.1). Inhibition of ATM in p21^{-/-} cells slightly increased p53 protein levels but had no effect on p53 localisation (Figure 5.5A).

To confirm that this result is specific to ATM inhibition, HCT116 WT and p21^{-/-} cells were also treated with a specific small molecule inhibitor of DNA-PK, NU-7441 (Leahy *et al.*, 2004). DNA-PK is a member of the PIKK family and has a role in DNA double strand break repair (Izzard *et al.*, 1999). WT and p21^{-/-} cells were treated with 1 μ M NU-7441 and incubated for 24 hours. Proteins were differentially extracted according to their subcellular localisation, and analysed by immunoblotting (Figure 5.5B). In WT cells p53 was localised to the nucleus, and localisation was unaffected by DNA-PK inhibition. p21 protein levels were elevated in response to DNA-PK inhibition, similar to ATM inhibition, and may indicate the activation of a general stress response to small molecule inhibition of cellular targets.

In p21^{-/-} cells, DNA-PK inhibition had no effect on the subcellular localisation of p53.

Direct inhibition of ATM kinase activity in HCT116 WT cells results in the same p53 localisation phenotype as observed in p21^{-/-} cells, yet has no effect on p53 localisation in p21^{-/-} cells. This data indicates that a genetic interaction between ATM and p21 exists, and that both are mutually required to ensure nuclear localisation of p53.

5.2.4 Lack of evidence that ATM and p21 physically interact

Previously, we have shown that p21 regulates ATM activity, and provided evidence that ATM and p21 genetically interact to maintain p53 nuclear localisation. To establish if ATM and p21 physically interact, co-immunoprecipitation assays were carried out (Figure 5.6). As earlier results indicate that ATM and p21 may have cytoplasmic roles, ATM and p21 were immunoprecipitated from whole cell lysates of HCT116 WT and p21^{-/-} cells, as opposed to nuclear extracts. ATM immunoprecipitated from HeLa nuclear extract has been characterised (Goodarzi & Less-Miller, 2004), and was used here as a control for ATM immunoprecipitation. As a negative control, an equal volume of cell lysate was replaced with NP40 lysis buffer (Blank, Figure 5.6), and provided a control for IgG light chain contamination in the p21 immunoblot. Immunoprecipitation samples were analysed by immunoblotting. ATM was successfully immunoprecipitated from HeLa nuclear extract, WT and p21^{-/-} whole cell lysates, however co-eluting p21 was unable to be detected in these samples (Figure 5.6). In the parallel experiment, p21 was

immunoprecipitated from HeLa nuclear extract, WT and p21^{-/-} whole cell lysates. p21 was only immunoprecipitated from WT cells, and no co-eluting ATM could be detected (Figure 5.6). This data indicates that ATM and p21 do not physically interact.

5.2.5 ATM inhibition of normal human cells mimics loss of p21 by causing p53 mislocalisation

Loss of p21 in NHF cells by p21 siRNA mediated gene knockdown, revealed that p53 nuclear localisation is p21-dependent (Figure 4.9). In HCT116 cells, through the use of specific inhibitors, p53 nuclear localisation also depends on ATM kinase activity (Figure 5.5A) yet not DNA-PK activity (figure 5.5B). To assess the role of ATM, DNA-PK and MDM2 in p53 localisation in normal cells, NHF cells were treated with DMSO (vehicle control), 10 μ M KU-55933 (ATM inhibitor), 1 μ M NU-7441 (DNA-PK inhibitor) or 10 μ M nutlin-3 (p53-MDM2 interaction inhibitor), and incubated for 24 hours. Proteins were extracted according to their subcellular localisation and analysed by immunoblotting for p53, E2F1, and p21 (Figure 5.7). E2F1 was included here to determine if ATM inhibition has a similar effect on E2F1 localisation as loss of p21. Previously, in NHF cells treated with p21 siRNA, E2F1 was partially mislocalised to the cytoplasm, compared to control cells where E2F1 was nuclear (Figure 4.9). Here, NHF cells were treated with DMSO as a vehicle control, and p53 and E2F1 were shown to be nuclear (Figure 5.7). Specific inhibition of ATM by KU-55933 caused aberrant p53 subcellular localisation compared to DMSO treated NHF cells (Figure 5.7). In DMSO treated NHF cells, p53 was

localised to the nucleus, whereas in KU-55933 treated NHF cells p53 was localised to both the cytoplasm and the nucleus (Figure 5.7). This is in agreement with previous observations in p21 siRNA treated NHF cells (Figure 4.9). Similarly, inhibition of ATM caused E2F1 to be partially mislocalised to the cytoplasm compared to DMSO treated control cells (Figure 5.7). These results are specific to ATM inhibition, as specific inhibition of DNA-PK by NU-7441 had no effect on p53 or E2F1 localisation compared to DMSO treated control cells (Figure 5.7). This data indicates that inhibition of ATM can mimic p21 siRNA mediated gene knockdown in NHF cells, with respect to p53 and E2F1 localisation.

MDM2 is a key negative regulator of p53, which binds and targets p53 for proteasomal degradation (Harris & Levine, 2005). Nutlin-3 fits into the hydrophobic pocket of MDM2 and competes with p53 binding to MDM2, therefore disrupting the p53-MDM2 interaction and inducing expression of p53 regulated genes (Vassilev *et al.*, 2004). Here, inhibition of the p53-MDM2 interaction by nutlin-3 induced a large increase in p53 protein levels (Figure 5.7). Nutlin-3 treatment also altered p53 subcellular localisation, where a majority of p53 was localised to the nucleus, and to a lesser extent the cytoplasm and membranes/organelles. However, in the presence of Nutlin-3 E2F1 levels were unchanged and maintained nuclear localisation (Figure 5.7). p21 levels were elevated compared to DMSO treated control cells, reflecting an increase in p53-dependent gene expression induced by nutlin-3 treatment (Figure 5.7). The redistribution of p53 in nutlin-3 treated cells is probably due to the substantial increase in the p53 protein level which has saturated the nucleus, and therefore excess p53 has been deployed to additional subcellular locations. However,

it is not inconceivable that MDM2 is involved in ATM/p21 regulation of p53 localisation, and warrants further investigation.

5.2.6 p53 subcellular localisation is MDM2-independent

To assess the role of MDM2 in p21-dependent p53 localisation, p21 and MDM2 protein levels were decreased by siRNA mediated gene knockdown. NHF cells were treated with control siRNA, p21 siRNA, MDM2 siRNA, or a combination of p21 and MDM2 siRNA, and the effect on p53 subcellular localisation was analysed by immunoblotting for p53, p21, and MDM2 (Figure 5.8). In control siRNA treated NHF cells, p53 was localised to the nucleus, and p21 and MDM2 were localised to the cytoplasm. siRNA mediated gene knockdown of p21 caused a significant reduction in the p21 protein level and alteration of p53 subcellular localisation compared to control siRNA treated NHF cells. In p21 siRNA treated NHF cells p53 was mislocalised to the cytoplasm and the nucleus, compared to control siRNA treated cells where p53 is confined to the nucleus (Figure 5.8). In contrast, MDM2 siRNA mediated gene knockdown had no effect on p53 nuclear localisation, or p21 levels. In combined siRNA mediated gene knockdown of both p21 and MDM2, loss of MDM2 did not rescue the aberrant p53 localisation phenotype associated with loss of p21 (Figure 5.8). This data indicates that loss of MDM2 does not effect p53 localisation, and that MDM2 does not impinge on ATM/p21 regulation of p53 subcellular localisation.

5.3 Discussion

5.3.1 Evidence of a genetic interaction between ATM and p21

Lymphoblasts derived from patients suffering from Ataxia Telangiectasia express a chronically high level of p21, which suggests a genetic interaction between ATM and p21 (Beamish *et al.*, 1996). *Atm*-deficient mice recapitulate most of the ataxia telangiectasia phenotype, and similarly mouse embryonic fibroblasts derived from *Atm*-deficient mice show elevated levels of p21 (Xu *et al.*, 1998). *Atm*-deficient mouse fibroblasts grown in culture show proliferative defects and enhanced senescence, these effects are correlated with increased levels of p21 (Xu & Baltimore, 1996; Westpal *et al.*, 1997). Genetic deletion of *p21* in an *Atm*-deficient mouse can rescue cells from senescence and overcome growth arrest seen in *Atm*-null fibroblasts, indicating that p21 is a downstream effector of ATM-mediated growth regulation and cellular senescence (Wang *et al.*, 1997; Xu *et al.*, 1998). Loss of p21 in *Atm*-deficient mice also delays onset of lymphoma and increases radiation sensitivity by inducing an apoptotic response (Wang *et al.*, 1997). However, Shen *et al.* (2005) provided a detailed analysis of the tumour spectrum observed in *Atm*^{-/-}*p21*^{-/-} mice, including sarcomas, myeloid, leukaemia, hepatomas and teratomas. These tumours were not observed in either *Atm*^{-/-} or *p21*^{-/-} mice, but the tumour spectrum was strikingly similar to those observed in *p53*^{-/-} mice. In this chapter, data has been presented indicating that p21 and ATM may cooperate to maintain p53 nuclear localisation and subsequently p53 transcriptional activity. Therefore the observation

that *Atm*^{-/-} *p21*^{-/-} mice develop similar tumours to *p53*^{-/-} mice further corroborates our data.

ATM may act upstream of p21 by regulating basal p21 expression in a p53-independent manner, via histone acetylation-mediated gene expression (Ju & Muller, 2003). In eukaryotic cells, DNA combines with core histones and other chromosomal proteins to form chromatin, where the nucleosome core particle is composed of a 146 base pairs of DNA wrapped around a histone octamer (consisting of a H3-H3-H4-H4 tetramer and two H2A-H2B dimers). The nucleosomes, connected by linker DNA and stabilised by histone H1, are further packaged into higher order structures (Luger *et al*, 1997; Akey & Luger, 2003). The presence of histones on DNA limits the access of non-histone DNA-binding proteins and thereby represses transcription. There is a strong electrostatic interaction between the negatively charged phosphate groups of DNA and the positively charged lysine and arginine residues of histone proteins (Stanley *et al.*, 2001). Therefore dynamic changes in chromatin structure can be mediated by post-translational modifications of histones for example, acetylation of N-terminal tails of histone core proteins neutralises the positive charge of basic histones and weaken histone-DNA interactions thus making nucleosomes more accessible (Kuo & Allis, 1998). Consequently, histone acetyltransferases (HAT), which catalyse the addition of acetyl groups to lysine residues of proteins, activate transcription (Grunstein, 1997), and histone deacetylases (HDAC), which remove acetyl groups, facilitate a closed chromatin structure and repression of gene expression (Laherty *et al.*, 1997). Inhibitors of HDACs, including butyrate, vorinostat and trichostatin A, induce growth arrest and apoptosis, and are therefore of therapeutic value (Ocker & Schneider-Stock, 2007). Chromatin becomes more

accessible to transcription factors with HDAC inhibition resulting in the activation of 2% of all genes (Van Lint *et al.*, 1996), including increased expression of p21 in a p53-independent manner (Huang *et al.*, 2000). Ju & Muller (2003) subsequently showed that HDAC inhibitor activation of p21 expression requires ATM however the nature of the requirement is unknown. Therefore functional ATM is required for histone acetylation-dependent *p21* gene expression. Although this is in stark contrast to the studies showing that p21 protein levels are elevated in cells derived from ataxia telangiectasia patients and *Atm*-deficient mice (Beamish *et al.*, 1996; Xu *et al.*, 1998), Xu *et al.* (1998) found that despite elevated p21 protein levels, p21 mRNA is significantly lower in the *Atm*^{-/-} MEFs compared to that of *Atm*^{+/+} MEFs.

In the context of our findings, ATM could regulate histone acetylation-dependent *p21* gene expression in undamaged cells, maintaining low basal expression of p21 independent of p53. Upon cellular stress, p53-dependent p21 expression mechanisms predominate, leading to enhanced p21 expression. The low basal level of p21 protein maintained by ATM may be essential in regulating p53 subcellular localisation, whereby inhibition or loss of ATM would lead to decreased expression of p21 and loss of functional p53. Therefore ATM may be a master regulator of the DNA damage response, by not only initiating signalling cascades immediately after damage, but by priming the cell before damage, via coordination of key components of the DNA damage response pathway, in anticipation of threats to genome integrity.

5.3.2 Induced ATM kinase activity is associated with loss of p21

In vivo evidence has been presented indicating that in the absence of p21, ATM kinase activity is enhanced (Figure 5.3). Although *in vitro* studies could not confirm that nuclear ATM kinase activity is altered by loss of p21 (Figure 5.4), we can speculate that cytoplasmic ATM kinase activity is increased. We have previously shown that reintroduction of the p21¹⁻¹³³ truncation, which lacks the C-terminus NLS, into p21^{-/-} cells is sufficient to restore p53 nuclear localisation (Figure 4.2B), indicating a cytoplasmic function of p21 in the regulation of p53 localisation. Therefore cytoplasmic ATM and p21 may interact, either directly or indirectly, to modify each others function, by an as yet undefined mechanism. Alternatively, ATM activation may be a secondary effect caused by defective p21-mediated genome stability. Loss of p21 has been associated with DNA re-replication (Chang *et al.*, 2000) and DNA damaged cells lacking p21, arrest in a G2-like state, but then undergo additional S-phases without intervening mitoses, and as such acquire grossly deformed, polyploid nuclei and subsequently die by apoptosis (Waldman *et al.*, 1996). Subsequent studies utilised cell systems with inducible p21 expression and showed that cells released from a p21-induced G2 arrest resulted in DNA re-replication in a small proportion of cells (Bates *et al.*, 1998; Chang *et al.*, 2000). Regulation of DNA replication ensures that origins of replication that have fired once in S-phase do not fire a second time within the same cell cycle, and therefore prevents re-replication of segments of the genome (Dutta & Bell, 1997). S-phase CDK2 activity is necessary for the firing of origins, however an increased level of Cyclin A and associated CDK2 activity has been shown to promote DNA re-

replication (Vaziri *et al.*, 2003). Induction of re-replication is sufficient to activate the ATM/ATR-mediated DNA damage response pathway, leading to activation of p53 and increased expression of p21 (Vaziri *et al.*, 2003). p21 is a potent inhibitor of Cyclin A-CDK2 and therefore protects the cell from DNA re-replication (Vaziri *et al.*, 2003). Loss of p21 would facilitate re-replication, leading to the propagation of aneuploid cells. As previously discussed, loss of p21 may sensitise cells to undergo apoptosis in response to DNA damage (4.3.3), and DNA re-replication may be sufficient to activate this process. In cells lacking p21, DNA re-replication may represent a persistent form of endogenous cellular stress capable of activating ATM, and therefore may account for elevated ATM kinase activity observed in HCT116 p21^{-/-} cells. In addition, Shen *et al.* (2005) demonstrated that Atm^{-/-} p21^{-/-} mouse embryonic fibroblasts exhibit increased chromosomal instability, by chromatid breaks and aneuploidy, compared to Atm^{-/-} or p21^{-/-} cells. This data suggests that Atm and p21 cooperate to suppress aneuploidy development and subsequent tumorigenesis.

Generally, the related protein kinases, ATM and ATR, are considered to work independently of one another. However, a degree of cellular crosstalk between ATM and ATR pathways is being gradually revealed. In *Xenopus laevis* egg extracts, Atm and Atr were both shown to be required to prevent DSB accumulation during DNA replication by promoting the restart of collapsed replication forks (Trenz *et al.*, 2006). In human cells, ATM is required for ATR function in response to DSBs, and ATM regulation of ATR occurs in a cell-cycle dependent manner (Jazayeri *et al.*, 2006). In contrast, ATR has been shown to regulate ATM phosphorylation and activation in response to UV treatment or replication fork stalling (Stiff *et al.*, 2006). Furthermore

certain substrates of ATM and ATR overlap, for example, p53 serine-15 and BRCA-1 serine-1423 are common targets. However CHK2-threonine-68 is exclusively targeted by ATM (Abraham, 2001; Jazayeri *et al.*, 2006). In response to IR, ATM is rapidly activated and phosphorylates p53 at serine-15, while ATR activation occurs more slowly and is involved in maintaining p53 serine-15 phosphorylation (Canman *et al.*, 1998; Tibbetts *et al.*, 1999). Here, data has been presented showing that ATM kinase activity is activated in HCT116 p21^{-/-} cells compared to WT cells, as specific inhibition of ATM completely blocked elevated CHK2 threonine-68 phosphorylation and significantly decreased elevated levels of p53 serine-15 phosphorylation observed in p21^{-/-} cells (Figure 5.3). However, a small amount of residual p53 serine-15 phosphorylation persists following ATM inhibition, and ATM serine-1981 phosphorylation is unaffected, suggesting up-regulation of an additional kinase. ATR is the prime candidate due to its functional similarity to ATM, and its ability to target p53 serine-15 (Canman *et al.*, 1998; Tibbetts *et al.*, 1999) and ATM serine-1981 (Stiff *et al.*, 2006), but not CHK2 threonine-68 (Jazayeri *et al.*, 2006). In speculation, loss of p21 may permit DNA re-replication, which persistently activates ATM, in a similar manner as IR, eventually leading ATR activation which contributes to phosphorylation of p53 at serine-15. Hence ATM is the principal kinase activated by loss of p21, yet may be supported to a lesser extent by ATR.

5.3.3 ATM/p21 regulation of p53 localisation is independent of MDM2

MDM2 is an important negative regulator of p53, by targeting it for ubiquitination and proteasomal degradation (Harris & Levine, 2005). MDM2 also has a role in p53

nuclear export, as MDM2-dependent degradation of p53 occurs mainly in the cytoplasm. Although the mechanism of MDM2-dependent p53 nuclear export has not been clearly defined, evidence favours the model in which MDM2 ubiquitination of p53 unmask the p53 NES resulting in nuclear export (Stommel *et al.*, 1999; Lohrum, *et al.*, 2001). Therefore in light of our research, p21 may mediate p53 nuclear import, and MDM2 ubiquitination of p53 controls nuclear export, and the equilibrium between these systems may serve to coordinate p53 subcellular localisation to the cell's requirements. However, no cross talk between p21 and MDM2 could be identified. Where siRNA mediated gene knockdown of MDM2 and p21 had no effect on loss of p21-mediated aberrant p53 subcellular localisation (Figure 5.8). This data indicates that p21 regulation of p53 subcellular localisation is independent of MDM2.

In this chapter, specific small molecule inhibitors of ATM have enabled dissection of the role of ATM in the novel p21 feedback loop that regulates p53. We have shown that ATM kinase activity *in vivo* is elevated in cells lacking p21, and speculate that this may be caused by DNA re-replication. Surprisingly, a genetic interaction between ATM and p21 was uncovered, and illustrates that ATM and p21 cooperate to ensure functional p53 by maintaining its nuclear localisation.

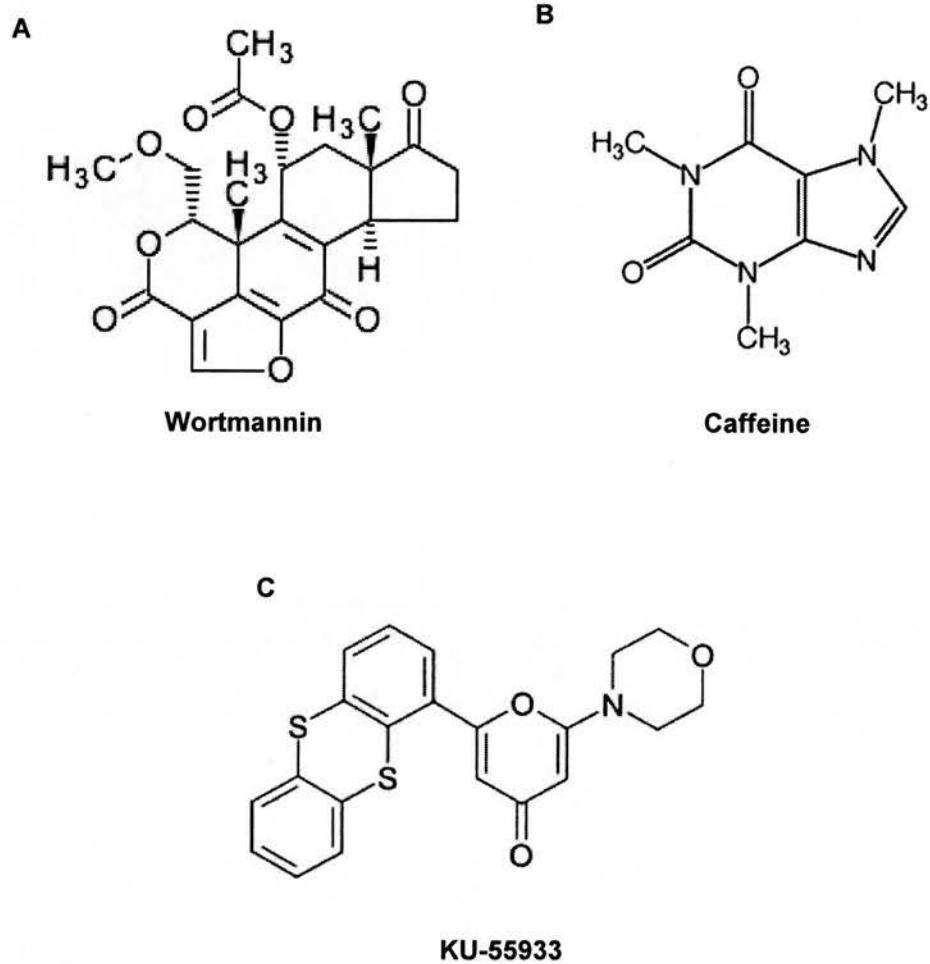


Figure 5.1 Chemical Structures of ATM inhibitors. (A) Wortmannin (adapted from Wymann *et al.*, 1996). **(B)** Caffeine. **(C)** 2-morpholin-4-yl-6-thianthren-1-yl-pyran-4-one (KU-55933) (Hickson *et al.*, 2004).

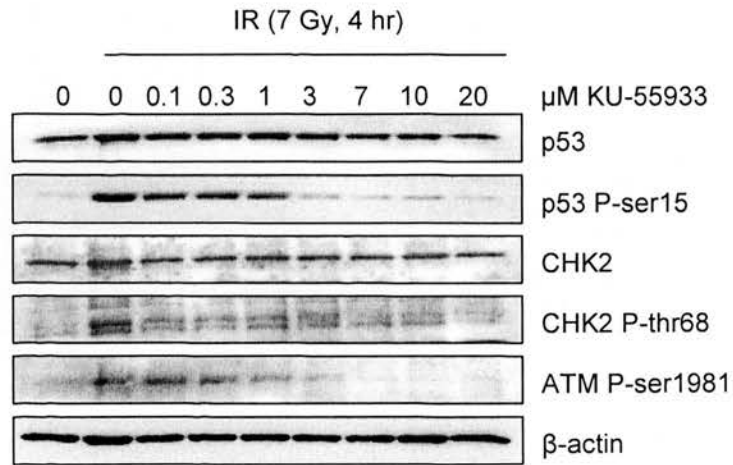


Figure 5.2 Small molecule inhibition of ATM leads to a dose dependent decrease in ATM substrate phosphorylation. HCT116 WT cells were treated with increasing concentrations of the specific ATM inhibitor, KU-55933, prior to irradiation with 7 Gy. Cells were harvested 4hr after irradiation. Urea lysates were resolved by SDS-PAGE and analysed by immunoblotting for p53; p53 serine-15 phosphorylation; CHK2; CHK2 threonine-68 phosphorylation and ATM serine-1981 phosphorylation. β -actin was included as a loading control. 30 μ g protein loaded per lane.

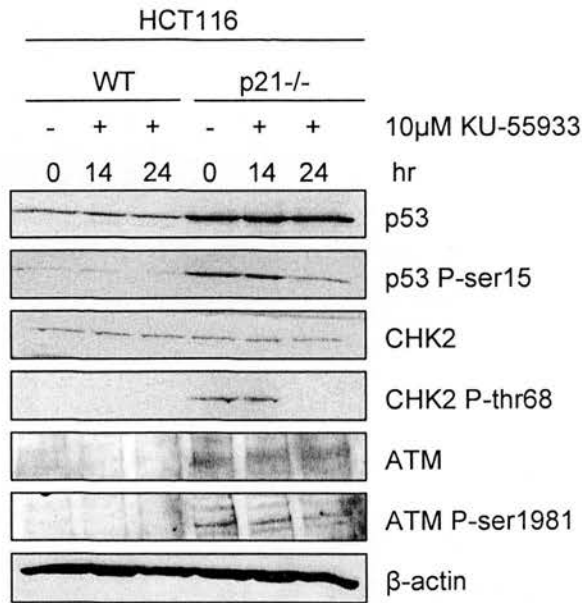


Figure 5.3 Specific inhibition of ATM decreases the elevated p53 serine-15 and CHK2 threonine-68 phosphorylation levels that are induced by loss of p21. HCT116 WT and p21^{-/-} cells were incubated with KU-55933 for 0 hr, 14 hr and 24 hr. Whole cell lysates were resolved by SDS-PAGE and analysed by immunoblotting for p53; p53 serine-15 phosphorylation; CHK2; CHK2 threonine-68; ATM and ATM serine-1981. β -actin was included as a loading control. 30 μ g protein loaded per lane.

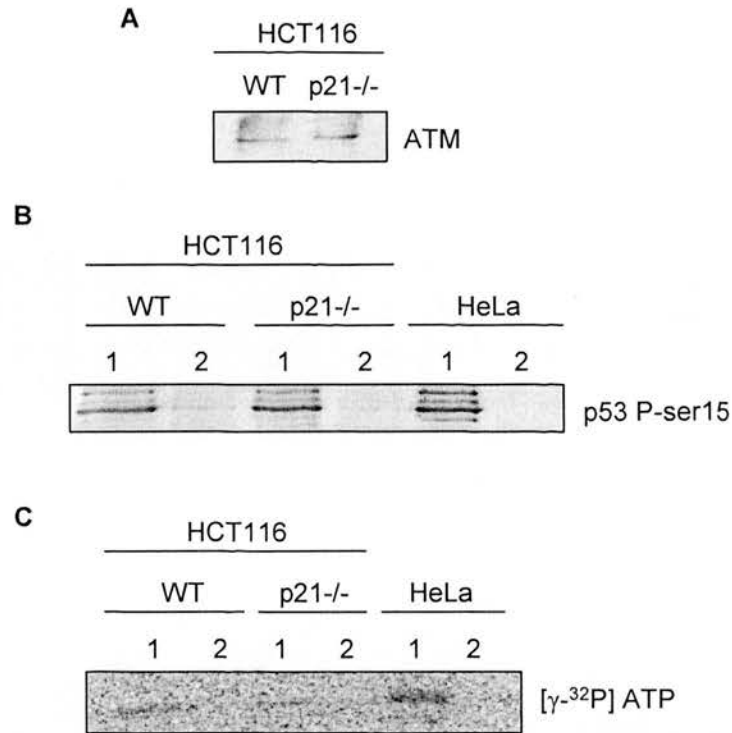


Figure 5.4 ATM kinase activity is not affected by loss of p21 as measured by *in vitro* kinase assays. ATM was immunoprecipitated from the nuclear extract of HCT116 WT, p21^{-/-} and HeLa cells. **(A)** Immunoblot analysis of extracted ATM from HCT116 WT and p21^{-/-} cells. **(B)** Immunochemical detection of ATM kinase activity showed no difference between HCT116 WT, p21^{-/-} and HeLa cells. ATM kinase activity was monitored by immunochemical detection of a phospho-substrate, GST-p53N66 fragment (N-terminal 66 amino acids of p53 fused to GST; ~34 kDa) (Lane 1) and as a negative control GST-p53N66-S15A mutant fragment (Lane 2). Kinase reactions containing cold ATP and 2 μ g substrate were assembled in the presence of immunoprecipitated ATM and incubated for 30 min at 30 °C. The reaction products were resolved by SDS-PAGE and transferred to nitrocellulose. Phosphorylation of p53 at serine-15 was detected by immunoblotting. **(C)** Radioactive detection of ATM kinase activity showed no difference between HCT116 WT and p21^{-/-} cells. ATM kinase activity was detected by radiolabelling the substrate with [γ ³²P]ATP. GST-N66p53 fusion protein (Lane 1) and the negative control GST-p53N66-S15A mutant fragment (Lane 2) were used as substrates. Kinase reactions containing [γ ³²P]ATP and 2 μ g substrate were assembled in the presence of immunoprecipitated ATM and incubated for 30 min at 30 °C. The reaction products were resolved by SDS-PAGE and [γ ³²P]ATP incorporation was visualised by autoradiography.

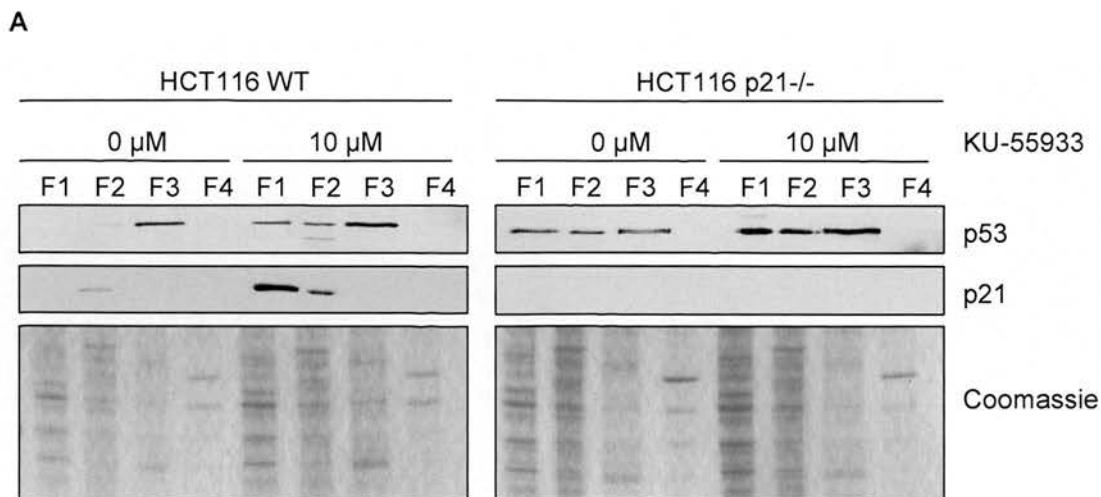


Figure 5.5 Specific ATM inhibition mimics the p21^{-/-} phenotype. (A) Specific inhibition of ATM causes mislocalisation of p53. HCT116 WT and p21^{-/-} cells were incubated with either DMSO (0 μ M) as a vehicle control or KU-55933 (10 μ M) for 24 hr. Proteins were extracted according to their subcellular localisation: F1- cytosol; F2- membranes/organelles; F3- nucleus; F4- cytoskeleton (S-PEK, Calbiochem®). Proteins from each fraction were resolved by SDS-PAGE and analysed by immunoblotting for p53 and p21. 10 μ g protein was loaded per lane. Coomassie staining confirmed that protein expression profiles from each fraction were distinct. 5 μ g protein was loaded per lane. **(B)** Specific inhibition of DNA-PK does not affect p53 localisation. HCT116 WT and p21^{-/-} cells were incubated with either DMSO (0 μ M) as a vehicle control or Nu-7441 (1 μ M) for 24 hr. Proteins were extracted according to their subcellular localisation: F1- cytosol; F2- membranes/organelles; F3- nucleus; F4- cytoskeleton (S-PEK, Calbiochem®). Proteins from each fraction were resolved by SDS-PAGE and analysed by immunoblotting for p53 and p21. 10 μ g protein was loaded per lane.

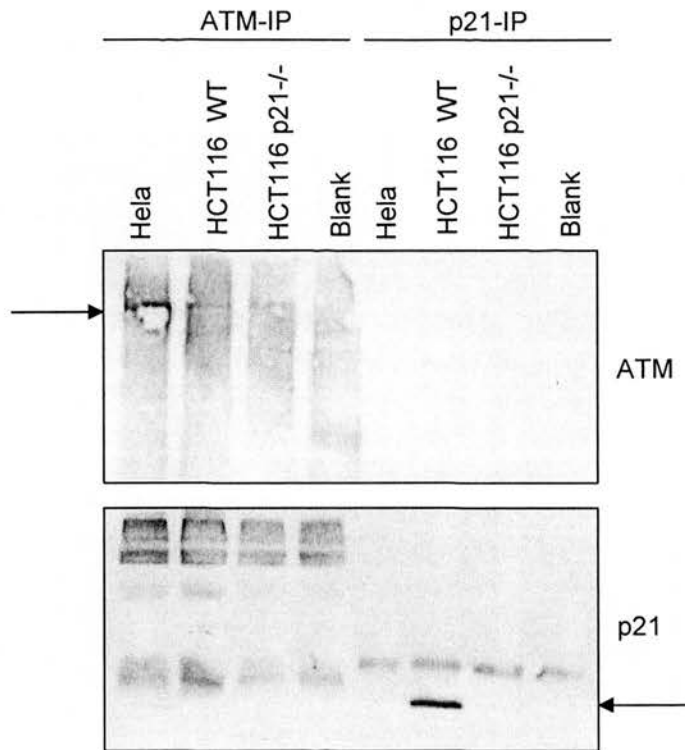


Figure 5.6 Endogenous ATM and p21 do not co-immunoprecipitate. ATM and p21 were immunoprecipitated from HeLa nuclear extract, HCT116 WT whole cell lysate and HCT116 p21^{-/-} whole cell lysate, with anti-ATM monoclonal antibody (α -536, KuDOS) and with anti-p21 monoclonal antibody (Ab-1, Oncogene), respectively. Blank control, cell lysate is replaced with an equal volume of NP40 lysis buffer. Reactions were resolved by SDS-PAGE and analysed by immunoblotting for ATM and p21. Arrows indicate protein bands correlating to immunoprecipitated protein of interest.

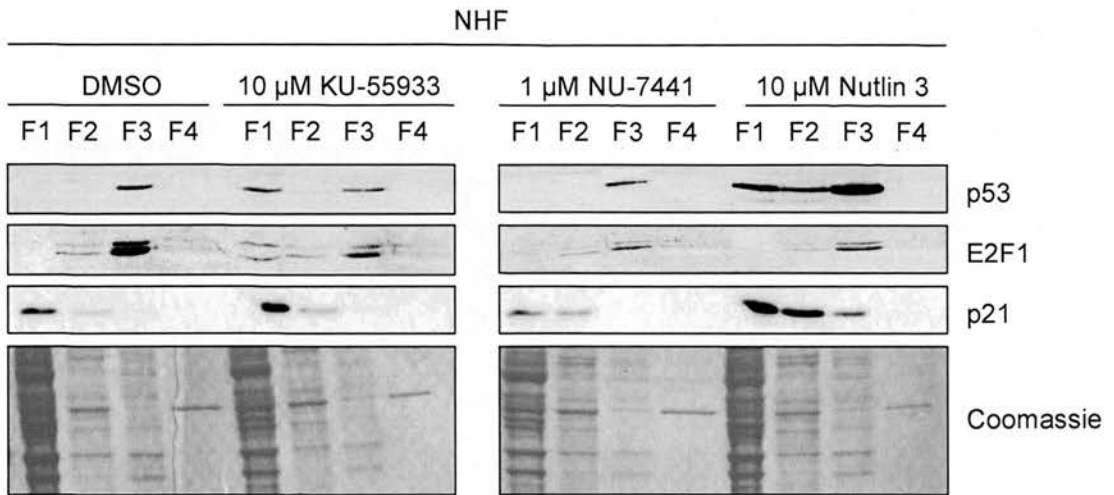


Figure 5.7 p53 nuclear localisation is ATM-dependent in NHF cells. NHF cells were incubated for 24 hr with either DMSO as a vehicle control; specific ATM inhibitor, KU-55933 (10 μ M); specific DNA-PK inhibitor, NU-7441 (1 μ M); or MDM2 inhibitor, Nutlin-3 (10 μ M). Proteins were extracted according to their subcellular localisation: F1- cytosol; F2- membranes/organelles; F3- nucleus; F4- cytoskeleton (S-PEK, Calbiochem®). Proteins from each fraction were resolved by SDS-PAGE and analysed by immunoblotting for p53, E2F1 and p21. 10 μ g protein was loaded per lane. Coomassie staining confirmed that protein expression profiles from each fraction were distinct. 5 μ g protein was loaded per lane.

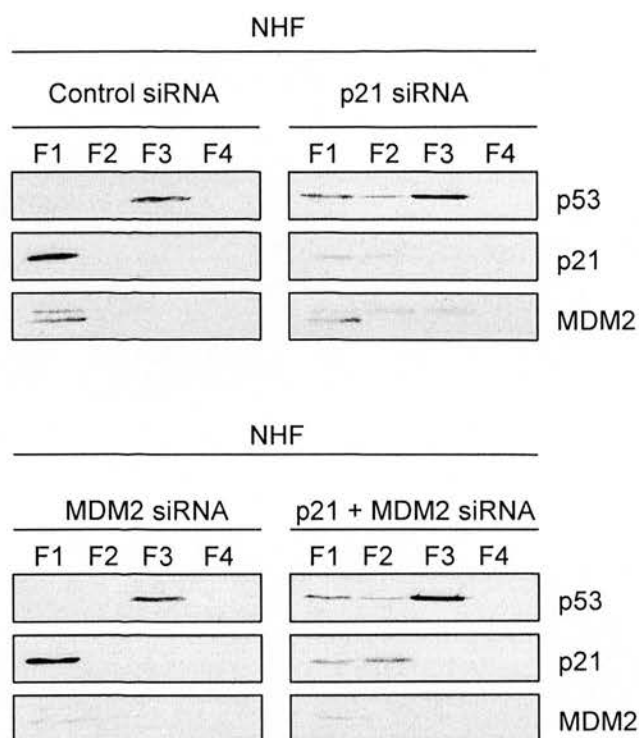


Figure 5.8 MDM2 is not required for p21-dependent localisation of p53. NHF cells were transfected and incubated for 24 hr with either control siRNA; p21 siRNA; MDM2 siRNA; or both p21 and MDM2 siRNA. Proteins were extracted according to their subcellular localisation: F1- cytosol; F2- membranes/organelles; F3- nucleus; F4- cytoskeleton (S-PEK, Calbiochem®). Proteins from each fraction were resolved by SDS-PAGE and analysed by immunoblotting for p53, MDM2 and p21. 10 µg protein was loaded per lane.

CONCLUSIONS AND FUTURE PERSPECTIVES

6.1 Regulation of p53 transcriptional activity by p21

The p53 tumour suppressor protein is a key regulator of a range of processes involved in the prevention of cancer formation, including cell cycle arrest, DNA repair and apoptosis (Lane, 1992). The regulation of p53 functions is tightly controlled through several mechanisms including p53 transcription and translation, protein stability, post-translational modifications, and subcellular localisation (Hayon & Haupt, 2002). In this study, p21 has been identified as a novel regulator of p53 transcriptional activity. p21 regulates p53 subcellular localisation and is required for global p53-dependent gene expression. Loss of p21 is associated with increased cytoplasmic localisation of p53 and a dramatic decrease in p53 transcriptional activity. We propose that p21 is an essential co-factor of the p53 pathway.

6.1.1 Mechanism of p21-dependent regulation of p53 localisation

In this study p21 has been identified as a novel regulator of p53 subcellular localisation (Figure 4.1). We have shown that reconstitution of p21 into HCT116 p21^{-/-} cells restores p53 nuclear localisation (Figure 4.2), as yet a mechanism has not been identified. The p53 negative regulator MDM2 is required for efficient export of

p53 from the nucleus to the cytoplasm (Lohrum *et al.*, 2001). Interestingly, MDM2 has also been identified as a negative regulator of p21, whereby increased expression of MDM2 decreases p21 protein stability (Zhang *et al.*, 2004). In the context of our data, the following model can be proposed, whereby MDM2 drives p53 nuclear export and p21 drives p53 nuclear import (Figure 6.1). Basal levels of p21 may maintain p53 nuclear localisation, such that it is poised for responding to damage. In response to damage, p53 activation would lead to increased levels of MDM2 protein which drives p21 degradation and p53 nuclear export. In this model, ATM may function as a master regulator, cooperating with p21 to sustain p53 activation and gene expression, and inhibiting MDM2-p53 interaction by phosphorylation of MDM2 at serine-395 and p53 at serine-15. However, we were unable to substantiate this model. Targeted inactivation of MDM2 by siRNA mediated gene knockdown had no effect on p53 subcellular localisation in cells lacking p21 (Figure 5.8). Nevertheless, more rigorous testing of this model may provide evidence for or against the model, for example, over-expression of MDM2 in wild-type cells may cause degradation of p21 and aberrant localisation of p53.

Further investigation should focus on identifying the mechanism by which p21 regulates p53 localisation. To determine if p53 is actively exported from the nucleus in the absence of p21, cells lacking p21 could be treated with inhibitors of nuclear export, such as leptomycin-B. Leptomycin-B is a potent, specific inhibitor of the nuclear export factor, CRM-1, and inhibits NES-dependent protein export from the nucleus. Therefore if loss of p21 induces active exportation of p53 from the nucleus, leptomycin-B treatment of cells lacking p21 should restore nuclear

localisation. Alternatively, if p53 is sequestered in the cytoplasm prior to nuclear import, leptomycin-B treatment would have no effect on p53 localisation.

As previously discussed (4.3.1), the C-terminus of p21 is not required for restoration of p53 nuclear localisation. The C-terminus of p21 contains the PCNA binding site and the NLS (Dotto, 2000). Therefore p21 may have cytoplasmic functions in the regulation of p53. p53 is synthesised in the cytoplasm and must be transported to the nucleus to exert its transcriptional effect on downstream targets (O'Brate & Giannakakou, 2003). Cytoplasmic p21 may enhance p53 binding to a nuclear import protein or block p53 interaction with a cytoplasmic anchor, leading to increased nuclear localisation. A detailed analysis of cytoplasmic binding partners of p21 and p53 may yield new insight into the mechanisms of p21-dependent regulation of p53, and of intracellular trafficking of p53.

6.1.2 p53-dependent gene expression is associated with p21 gene dose

Microarray analysis of primary cells derived from transgenic mice nullizygous, heterozygous and wild-type for p21 provided new insight into p21-dependent regulation of p53-dependent gene expression. Loss of one allele of *p21* caused a 21 % decrease in p53-dependent gene expression, whilst loss of both *p21* alleles resulted in a 68 % decrease compared to wild-type cells (Figure 4.17). These striking and significant findings illustrate that p53-dependent gene expression is mediated by *p21* gene dose.

Culture cell models with inducible p21 expression would provide an important experimental tool to further characterise the dependence of p53 activity on

p21 levels. Long-term over-expression of exogenous p21 in cells may have cytotoxic side effects as p21 is a negative regulator of cell growth. Future work could therefore include development of constructs that enable the controlled induction of p21 activity. Expression of p21 from a promoter induced by isopropyl- β -thio-galactoside (IPTG) has previously been characterised (Broude *et al.*, 2007). This would allow temporal regulation of p21 activity, and enable examination of the kinetics of p21-dependent regulation of p53 localisation. Similarly, we used transient expression of siRNA to mediate gene knockdown of p21 (Figure 3.6, Figure 4.8). Stable expression of siRNAs to target p21 would mediate persistent suppression of p21 gene expression (Fritah *et al.*, 2005), and allow detailed analysis of the p21 loss-of-function phenotype over a longer period of time. To further investigate the relationship between the level of p53 activity and the amount of p21 protein, commercially available tetracycline-regulated expression systems (T-REx™ System, Invitrogen) allow expression levels of, for example, p21 to be gradually modulated in accordance tetracycline concentration. This system would provide a cell culture model to compare to our previous observations in mice (Figure 4.17) and enable detailed characterisation of p53 dependence on p21 levels.

Mouse models with p21 expression under inducible control, would also provide a versatile experimental tool as over-expression of p21 in a transgenic animal would probably have catastrophic effects. An elegant system has previously been used to investigate p53 tumour suppressor functions, consisting of a switchable knock-in mouse model in which endogenous p53 can be reversibly switched between functional and non-functional states, by substituting the endogenous *p53* gene with one encoding a p53 fusion protein whose function is dependent on ectopic provision

of 4-hydroxytamoxifen (Christophorou *et al.*, 2005). Application of this system to p21 expression would allow detailed characterisation of p21-dependent regulation of p53 activity, in terms of kinetics, dependence, persistence, and reversibility. Also studies could be extended from B-cells to include specific tissues and additional primary cell lines.

6.2 Further characterisation of the ATM-p21 interaction

Evidence has been presented suggesting that ATM and p21 cooperate to maintain p53 nuclear localisation (Figure 5.5A) and therefore p53 transcriptional activity. Future work should focus on further characterisation of the ATM-p21 interaction. Findings presented here suggest that ATM and p21 do not interact to form a complex as they did not co-immunoprecipitate (Figure 5.6). However, in undamaged cells it is likely that only small pools of ATM and p21 specifically interact, making detection difficult. Therefore further optimisation of co-immunoprecipitation conditions and utilising additional methods of protein detection other than immunoblotting, for example, silver staining of SDS-PAGE gels and mass spectrometry analysis may yield greater insight into the ATM and p21 interaction. Alternatively, ATM and p21 may interact within the context of a multi-protein complex, and essential co-factors required to maintain binding may be lost during the co-immunoprecipitation procedure. However, no evidence of a multi-function complex involving ATM and p21 has been ascertained so far.

ATM has previously been shown to be involved in histone acetylation-mediated *p21* gene expression (Ju & Muller, 2003). Our findings suggest that ATM

functions upstream of p21 in the regulation of p53 localisation. This is based on the observation that specific inhibition of ATM produced the same phenotype as loss of p21, in regard to aberrant p53 localisation, in HCT116 WT cells. In HCT116 p21^{-/-} cells, inhibition of ATM was ineffective in altering p53 localisation (Figure 5.5A).

A model (Figure 6.2) can be presented to account for these observations, in which ATM maintains basal expression of p21 independent of p53, via histone acetylation-dependent gene expression. In unstressed cells, ATM may maintain low level expression of p21. Basal levels of p21 protein may regulate p53 subcellular localisation and transcriptional activity. In response to damage, p53-dependent p21 expression mechanisms may supersede ATM-dependent expression of p21, leading to enhanced p21 expression. Enhanced p21 protein levels would lead to further activation of p53 (Figure 6.2). Therefore specific inhibition or loss of ATM before damage would lead to decreased expression of p21 and loss of functional p53, which could no longer up-regulate p21 in response to damage. To test this model, inhibition of HDAC in HCT116 WT and NHF cells would be predicted to result in aberrant localisation of p53, as observed with ATM inhibition and loss of p21. This model would not require direct interaction between ATM and p21, nor would ATM kinase activity expected to be altered, which is consistent with previous *in vitro* data (Figure 5.4B, C; Figure 5.6). However in disagreement with this model, inhibition of ATM caused an increase in p21 protein levels, not the predicted decrease (Figure 5.5A). The observed accumulation of p21 protein may be via increased stabilisation of p21 rather than increased expression levels, and may be a consequence of treatment with small molecule inhibitors, as a similar elevation of p21 levels was observed with DNA-PK inhibition (Figure 5.5B). Validating the effects of the ATM inhibitor with

ATM siRNA mediated gene knockdown will further clarify non-specific effects of ATM inhibition by KU-55933.

ATM and p21 are both multi-functional proteins with important roles within the cell. Additional studies are required to begin understanding the ATM-p21 interaction, elucidate the mechanism by which these two important proteins impinge upon each other, and to determine the cellular consequences of this interaction.

6.3 Investigation of p21-dependent regulation of p53 within the cell cycle

During an unperturbed cell cycle, p53 shuttles between the nucleus and the cytoplasm. Nuclear p53 is only detected in cells at the G1/S transition, and cytoplasmic p53 is associated with S-phase cells (Shaulsky *et al.*, 1990b). Strikingly, expression levels of p21 are highest at the G1/S transition when p53 is localised to the nucleus and lowest at the S-phase of cell cycle when p53 is localised to the cytoplasm (Li *et al.*, 1994). The work presented here was carried out in asynchronous populations of cells. However, future studies involving synchronised cell populations and cell cycle analysis may show that in normal cells p21 plays an important role in coordinating the cell cycle and p53 transcriptional activity via its subcellular localisation.

p21 also accumulates in the cell during the G2/M transition (Li *et al.*, 1994), and is subsequently degraded in early mitosis to allow cell cycle progression (Li *et al.*, 1994). CDC20 associates with and activates the ubiquitin ligase APC/C (anaphase-promoting complex/cyclosome) (Fung & Poon, 2005) and controls ubiquitin-mediated degradation of p21 in mitosis (Amador *et al.*, 2007). Substrates of

APC/C^{CDC20} are often characterised by the presence of a “destruction box” or D box, which consists of a minimal RxxL motif. In the N-terminus of p21 (at positions 86-89 in human) one conserved RxxL motif was identified and shown to be necessary for p21 degradation (Amador *et al.*, 2007). Interestingly, the C-terminus of p21 is not required for restoration of p53 nuclear localisation (Figure 4.2B). In speculation the minimal domain of p21 required for regulation of p53 may include the D box motif, to block APC/C^{CDC20} ubiquitin-mediated degradation of p21 in response to cellular stress, therefore causing a G2 arrest and allowing p21 accumulation and subsequent activation of p53. Further identification and characterisation of the minimal domain of p21 essential to restore p53 activity is required.

CDC20 expression is repressed by genotoxic stresses in a p53-dependent manner (Kidokoro *et al.*, 2007). In context of our results, a model can be proposed where p21 is an essential co-factor of p53 transcriptional activity by maintaining p53 nuclear localisation (Figure 6.3). In unstressed cells, CDC20 may maintain cytoplasmic localisation and inactivation of p53 by degrading p21. In response to cellular insult, stabilisation of p53 may lead to inhibition of *CDC20* expression and decrease CDC20 protein levels accordingly. Subsequently, inhibition of CDC20 may enable accumulation of p21, leading to increased nuclear localisation and activation of p53. Future studies should focus on validating the role of CDC20 in this model. Consistent with this model, CDC20 is frequently up-regulated in a range of malignancies, including oral squamous cell carcinoma (Mondal *et al.*, 2007) and gastric cancer (Kim *et al.*, 2005). Increased expression of CDC20 may cause loss of p21 and inactivation of p53, which would be of selective advantage to cancer cells, enhancing tumour progression.

6.4 Potential therapeutics

6.4.1 Specific inhibition of ATM

Cells derived from Ataxia Telangiectasia patients are hypersensitive to IR and fail to arrest the cell cycle after the induction of DNA double strand breaks (Khanna *et al.*, 2001). Many current non-surgical cancer treatments target the integrity of cellular DNA, which is crucial to cell survival. These agents directly and/or indirectly damage DNA by inducing DNA breaks e.g. IR; forming crosslinks e.g. trizenes and platinum compounds; and targeting DNA-related proteins e.g. topoisomerase inhibitors (Ding *et al.*, 2006). However, the anticancer effectiveness of these agents is limited by the activation of DNA repair pathways (Hoeijmakers, 2001). Inhibition of these pathways may increase the effectiveness of DNA damaging agents and improve cancer therapy.

Specific inhibition of ATM by KU-55933 in a range of ATM-proficient cells significantly sensitised them to IR and DSB-inducing chemotherapeutics including etoposide, doxorubicin and camptothecin (Hickson *et al.*, 2004). Therefore combinational therapy against cancer may include KU-55933 as a novel radio- and chemosensitizer to enhance efficacy of conventional radio- and chemotherapy.

In this study ATM inhibition has also been shown to induce mislocalisation of p53 and possibly functional inactivation (Figure 5.5A). However this does not impinge on the radiosensitivity caused by ATM inhibition, and may indicate that cells are undergoing apoptosis independent of p53. Further understanding and

characterisation of ATM functions will allow judgement of the therapeutic benefits of specific ATM inhibition.

6.4.2 Specific p21 peptides for reactivation of p53

Loss of p53 function is a common feature of human cancers (Sherr, 2004). Several pharmacological strategies aimed at restoring p53 have been proposed including: small molecules that restore mutant p53 protein to conformationally active p53 (Bykov *et al.*, 2002); compounds that interfere with the MDM2-p53 interaction (Vasilev *et al.*, 2004); and gene-therapy based approaches aimed at introducing a wild-type copy of the p53 gene into tumour cells (Roth, 2006). Here, a novel mechanism of p53 inactivation has been identified, mediated by loss of p21. The C-terminus of p21 is not required to restore nuclear localisation of p53 in HCT116 cells (Figure 4.2B). Hence, further mapping of the domain of p21 required to restore p53 activity by mutational analysis, may provide novel drug targets. If this domain of p21 directly binds p53, or blocks interaction of p53 with a cytoplasmic anchor, direct targeting of these interactions could counteract aberrant p53 localisation and restore p53 transcriptional activity. These interactions are relatively uncharacterised therefore the development, screening and effective targeting with small-molecule drugs may be difficult (Baines & Colas, 2006). However with the advances in cell-permeable peptide technology, the development of specific peptides of the minimum domain of p21 required to restore p53 nuclear localisation may be more therapeutically viable. Specific peptides can be fused to specific protein transduction domains, consisting of short amino acid peptide motifs, which penetrate virtually all

cells, independent of surface transporters and of cell cycle phase (Privé & Melnick, 2006). Commonly used protein transduction domains include the penetratin motif, derived from the *Drosophila* antennapedia protein, and the pTAT motif, derived from the HIV transactivator protein (Joliot & Prochiantz, 2004). As these domains are naturally occurring, and have physiological roles in protein transduction, they are generally non-toxic to cells. The validity of this technique has been illustrated by a specific peptide inhibitor of HSP90 (Plescia *et al.*, 2005). HSP90 is strongly activated in cancer and stabilises proteins required for survival and proliferation (Calderwood *et al.*, 2006). Specific peptide inhibition of HSP90 caused massive cell death *in vitro* and *in vivo*, with greater potency and less toxicity than equivalent small molecule inhibitors (Plescia *et al.*, 2005).

In human cancer loss of p21 correlates with tumour progression and has been characterised in a range of different malignancies, including lung (Komiya *et al.*, 1997), breast (Wakasugi *et al.*, 1997), bladder (Stein *et al.*, 1998), ovarian (Anttila *et al.*, 1999), cervical (Lu *et al.*, 1998), head and neck (Kapranos *et al.*, 2001), and anal carcinomas (Holm *et al.*, 2001). In light of our data, malignancies under-expressing p21 may have defects in p53 transcriptional activity. Specific peptides corresponding to the minimal domain of p21 required for maintaining p53 nuclear localisation, fused to a protein transduction domain, may stimulate reactivation of p53 and be of important therapeutic value in cancers lacking p21.

6.5 Conclusion

The p53 tumour suppressor protein is an essential component of an intricate network of proteins which communicate with each other throughout the cell cycle to preserve DNA integrity by eliciting appropriate cellular responses, such as DNA repair, cell cycle arrest or apoptosis. An established downstream effector of the p53 pathway is the cyclin-dependent kinase inhibitor, p21. This study has identified and characterised a novel p21 feedback loop in the regulation of p53, where levels of p21 protein maintain p53 nuclear localisation and transcriptional activity. Additional work is required to unravel the molecular mechanisms that underlie p21-dependent regulation of p53. However, these exciting observations have provided insight into a novel mechanism of p53 regulation, the intricacies of the ATM-p21 interaction, and have further defined the role of p21 in tumour progression.

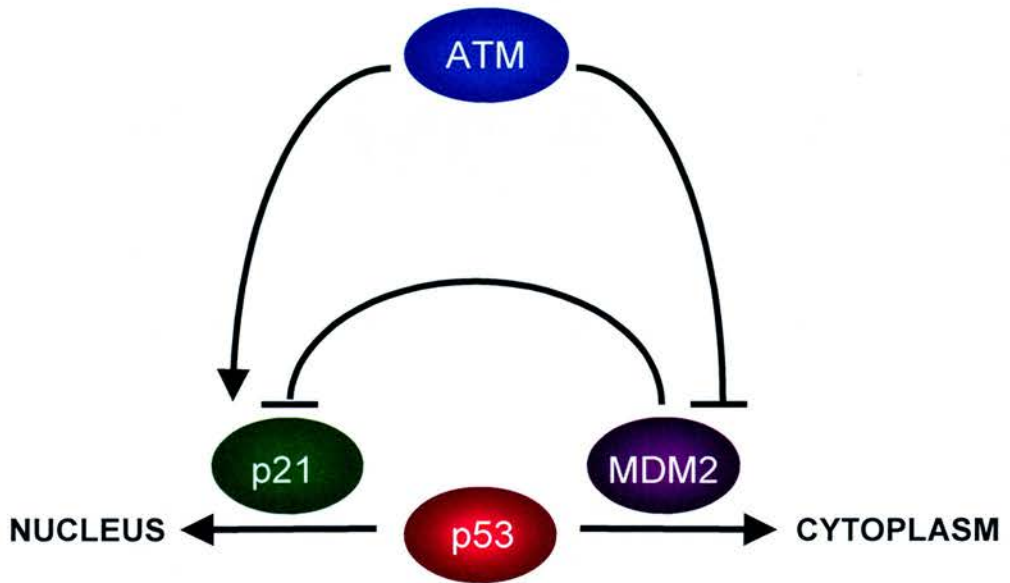


Figure 6.1 A model of the regulation of p53 subcellular localisation. Transcriptional activity of p53 is regulated by its subcellular localisation. MDM2 mediates p53 nuclear export, driving cytoplasmic localisation of p53 and transcriptional inactivation. p21 mediates p53 nuclear import, driving p53 nuclear localisation and transcriptional activation. ATM cooperates with p21 to ensure activation of p53, and by inhibiting MDM2 activity. Inhibition represented by T-shaped lines. Activation represented by arrows.

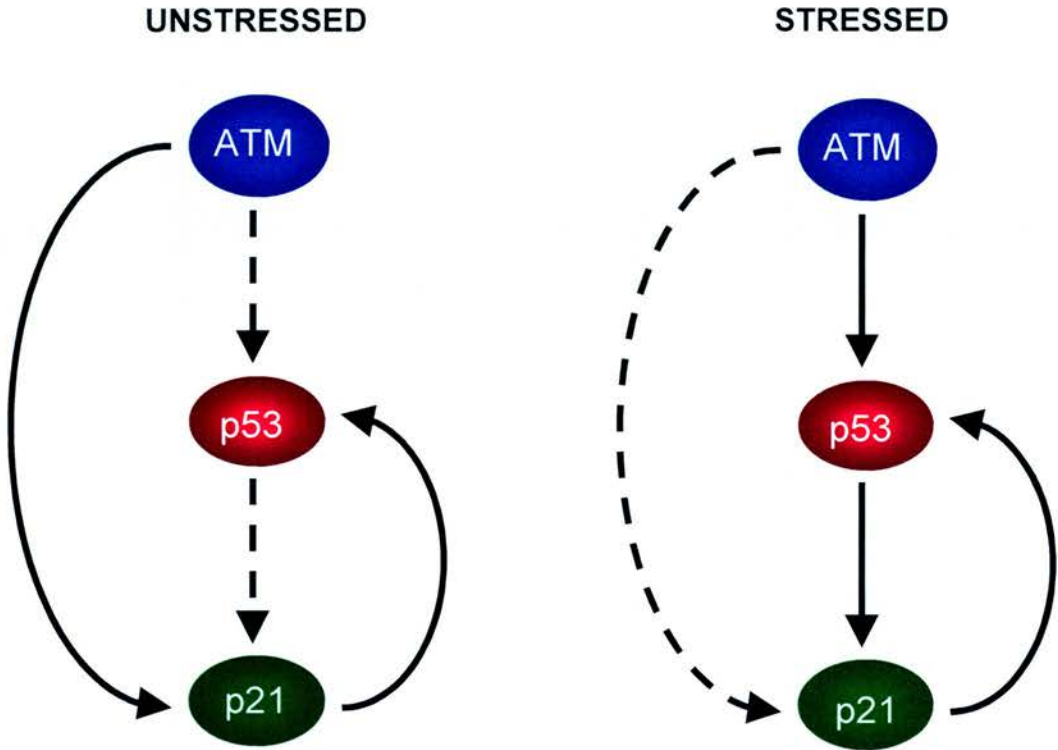


Figure 6.2 A model of ATM-dependent regulation of p21 expression and activation of p53. In unstressed cells ATM mediates histone acetylation-dependent gene expression of p21 and maintains low basal expression of p21 independent of p53. Low levels of p21 maintains nuclear localisation of basal levels of p53. In stressed cells ATM stabilises and activates p53. p53 specifically up-regulates p21 expression. Increased levels of p21 feedback to maintain p53 nuclear localisation and activation. Solid lines represent the dominant pathway regulating *p21* gene expression. Dashed lines represent the minor pathway regulating *p21* gene expression.

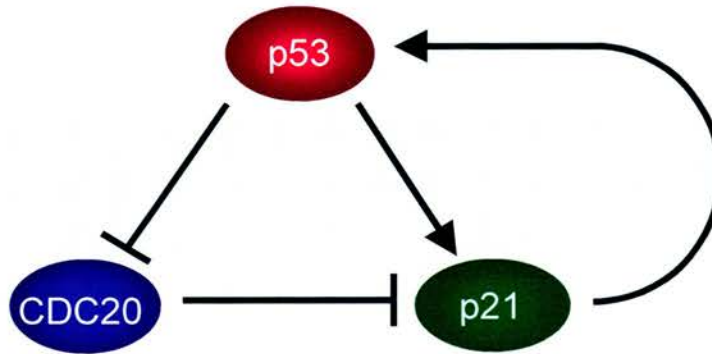


Figure 6.3 A model of a novel p21 feedback loop in the regulation of p53. CDC20 mediates p21 degradation preventing p21 activation of p53. Stabilisation of p53 in response to cellular stress inhibits CDC20 expression and up-regulates p21 expression. Inhibition of CDC20 prevents p21 degradation, enabling p21 accumulation and activation of p53 transcriptional activity. Inhibition represented by T-shaped lines. Activation represented by arrows.

APPENDIX A

IDENTIFICATION OF NOVEL SMALL MOLECULE COMPOUND INHIBITORS OF hSMG-1

A. 1 Introduction

Human suppressor of morphogenesis in genitalia-1 (hSMG-1) is the newest member of the phosphoinositide 3-kinase related kinase (PIKK) family of serine/threonine protein kinases. hSMG-1 has been shown to play a crucial role in non-sense mediated mRNA decay (Yamashita *et al.* 2001; Denning *et al.* 2001), and has been implicated as a genotoxic stress activated kinase (Brumbaugh *et al.*, 2004).

KuDOS Pharmaceuticals Ltd. (Cambridge) aims to discover and develop novel small molecule inhibitors that will significantly improve the treatment of cancer by inhibiting DNA repair and overcoming cancer cell resistance to radio- and chemotherapy. hSMG-1 is a very attractive target, as hSMG-1 deficient cells accumulate DNA damage indicating that hSMG-1 functions as a tumour suppressor gene product (Brumbaugh *et al.*, 2004) and therefore specific small molecule inhibitors of hSMG-1 could sensitise cells to conventional cancer therapies. During a six week placement at KuDOS Pharmaceuticals, small molecule compound libraries designed for the PIKK family were screened to identify specific small molecule inhibitors of hSMG-1.

A.1.1 Biochemistry of the PIKK family

The PIKK family consists of high molecular mass signaling proteins that initiate cellular stress responses when genome integrity, mRNA translation, or nutrient availability is compromised (Abraham, 2004a; Bakkenist & Kastan, 2004). Mammalian cells express six PIKK family members, ATM, ATR, DNA-PK, mammalian target of rapamycin (mTOR), transformation/transcription domain associated protein (TRRAP) and the newest member of the family, hSMG-1.

The five mammalian PIKKs which have been identified as active protein kinases, share a strong preference for protein substrates containing serine/threonine followed by a glutamine (S/T-Q) motif, which are frequently found in multiple copies localized in “S/T-Q rich domains” (Kruz & Lees-Miller, 2004). In addition, the PIKK family members exhibit similar overall structural organisation (Figure A.1). The most characteristic feature of these proteins is the catalytic domain (~300 amino acids), located near their C-terminus, which shows homology to the catalytic domain of phosphatidylinositol 3-kinase (PI3-K). The catalytic domain is flanked by two conserved domains termed FAT (*FRAP/ATR/TRRAP*) and FAT-C (C indicates C-terminus). The functions of the FAT (~600 residues) and FAT-C (~30 residues) regions are as yet unknown, however it is speculated that they may interact to stabilise the conformation of the interposed kinase domain (Abraham, 2001; Abraham, 2004a; Bakkenist & Kastan, 2004).

Typically the catalytic domain and the FAT-C domain are separated by no more than a few hundred residues, except in hSMG-1 which contains a large insert (~1000 amino acids) between these two conserved domains (Brumbaugh *et al*, 2004;

Abraham, 2004b; Bakkenist & Kastan, 2004). Therefore the kinase domain of hSMG-1 is located in the central region of the molecule rather than the near C-terminus (Figure A.1). Interestingly the hSMG-1 ortholog in *Caenorhabditis elegans* does not contain this large insert region, and Abraham (2004b) has speculated that its late appearance in metazoan evolution may enable hSMG-1 to interact with a broader range of upstream regulatory proteins and downstream targets.

The structure and function of the N-terminus of PIKK family members is relatively unknown. However the N-termini of ATM, ATR and mTOR have been predicted by bioinformatics, to contain 40-54 HEAT (*Huntington disease protein, Elongation factor 3, a subunit of phosphatase 2A and TOR1*) repeats (Perry & Kleckner, 2003). This is also likely to apply to hSMG-1 and DNA-PK. Each HEAT repeat is ~40 residues long, consisting of two anti-parallel alpha helices linked by a flexible loop, and the multiple repeats stack to form a large superhelical structure, which may act as a surface for protein-protein interactions (Khanna *et al.*, 2001; Kruz & Lees-Miller, 2004).

A.1.2 Suppressor of morphogenesis in genitalia-1 (hSMG-1)

The newest addition to the PIKK family was cloned independently by Yamashita *et al.* (2001), Denning *et al.* (2001) and Brumbaugh *et al.* (2004) and was termed human SMG-1, based on its sequence and functional homology to the *Caenorhabditis elegans* protein CeSMG-1. The *hSMG-1* gene has been mapped to 16p12 in human chromosomes (Yamashita *et al.*, 2001). However each group found mRNAs encoding hSMG-1 proteins of varying lengths. Yamashita *et al.* (2001)

isolated overlapping cDNA clones encoding an open reading frame (ORF) of 3657 amino acids residues with a deduced molecular mass of 409 kDa; Denning *et al.* (2001) isolated a cDNA encoding a 3031 amino acid polypeptide with a molecular mass of 340 kDa; and Brumbaugh *et al.* (2004) cDNA encodes a 3521 amino acid polypeptide with a deduced molecular mass of 395 kDa. The principle disparity between the three variants occurs at the N-terminus, indicating different splice variants of hSMG-1. However, whether these different splice variants are actually expressed in mammalian cells and their biological significance remains to be determined.

A.1.3 The role of hSMG-1 in nonsense mediated mRNA decay

Yamashita *et al.* (2001) and Denning *et al.* (2001) have shown that hSMG-1 plays a central role in nonsense-mediated mRNA decay (NMD). NMD is a conserved surveillance mechanism that eliminates imperfect mRNAs that contain premature translation termination codons (PTCs) and therefore protects against potential deleterious gain of function and consequent dominant negative effects of aberrant truncated proteins.

In mammals, human Upf (hUpf) proteins cooperate with an exon-junction complex (EJC) to identify PTCs in mRNA (Figure A.2). The EJC consists of multiple proteins deposited 20-24 nucleotides upstream of exon-exon junctions after splicing. A central regulator of NMD is hUpf-1, an ATPase/helicase which interacts with hUpf-3/hUpf-2 bound to EJCs located >50-55 nucleotides downstream of the

termination codon. This leads to hUpf-1 dependent exonucleolytic degradation of substrate mRNAs (Singh & Lykke-Andersen, 2003).

hUpf-1 is a phosphoprotein, containing multiple potential S/T-Q phosphorylation site motifs, and under normal conditions is subject to continuous cycles of phosphorylation and dephosphorylation (Denning *et al.*, 2001). Recent studies by Grimson *et al.* (2004) in *C.elegans* and in human cells, has clearly implicated hSMG-1 as the major upstream kinase for hUpf-1. Genetic evidence in *C.elegans* shows that *ceSMG-1* mutants block phosphorylation of *ceSMG-2*, the orthologue of hUpf-1, and that *ceSMG-1* kinase activity is required *in vivo* for NMD (Grimson *et al.*, 2004). Yamashita *et al.* (2001) provided evidence that in mammalian cells inhibition of hSMG-1, using wortmannin and caffeine, leads to suppression of NMD. However these drugs also inhibit other PIKKs and will therefore have pleiotropic effects. Furthermore, silencing of *hSMG-1* or *hUPF-1* gene expression in mammalian cells with small interfering RNA (siRNA) leads to dramatic decline in cell viability and proliferation, highlighting the importance of NMD (Brumbaugh *et al.*, 2004).

A.1.4 The Role of hSMG-1 in the stress response

Abraham (2004b) has reasoned that the incorporation of a protein kinase, hSMG-1 into the NMD pathway indicates that this pathway is capable of responding to environmental factors, such as growth factors and stress inducing stimuli, such as IR. In support of this, hSMG-1 has been found in both the cytoplasmic and nuclear

compartments of human cells and hUpf-1 undergoes nuclear-cytoplasmic shuffling (Brumbaugh *et al.*, 2004).

A compelling study by Brumbaugh *et al.* (2004) provides evidence that hSMG-1 is a genotoxic stress activated protein kinase, displaying functional overlap with ATM. They initially established hSMG-1 as p53 serine-15 kinase and showed that the specific kinase activity of hSMG-1 towards p53 is 3.5-fold higher than that of ATM in *in vitro* kinase assays. Interestingly, exposure of cells transfected with recombinant hSMG-1 to IR or UV stimulated hSMG-1 p53 serine-15 kinase activity, with IR proving to be the more effective stimulus. In line with this, transfection with kinase dead hSMG-1 or knockdown of endogenous hSMG-1 using siRNA, led to impaired accumulation and phosphorylation of p53 in IR treated cells (Brumbaugh *et al.*, 2004). However in the absence of extrinsic genotoxic stress, hSMG-1 depleted cells displayed elevated basal levels of p53 and phosphorylation, as well as histone H2AX serine-139 phosphorylation, indicating that loss of hSMG-1 is sufficient to trigger a spontaneous DNA damage response. hSMG-1 depleted cells also exhibit a loss of cell viability and accumulate at the G2 DNA damage checkpoint (Brumbaugh *et al.*, 2004). Interestingly, these phenotypic abnormalities are similar to those of ATR-depleted cells.

The role of hSMG-1 in mammalian cells requires further clarification, but present published evidence indicates that hSMG-1 may mediate mRNA and DNA surveillance mechanisms in human cells to ensure the quality of the proteome pool. Development of small molecule compound inhibitors of hSMG-1 will be a valuable tool in elucidating its biological function, and may yield therapeutic value beyond cancer treatment, because although NMD protects the cell from the dominant effects

of aberrant truncated proteins, there are some cases where truncated proteins contain residual activity and can compensate for normal gene function. Therefore specific inhibitors of hSMG-1 would be of potential therapeutic importance for all genetic diseases associated with PTC mutations, such as β -thalassemia.

A.2 Materials and Methods

A.2.1 Screening for Small Molecule Compound Inhibitors of hSMG-1

This work was carried out during a six week placement at KuDOS Pharmaceuticals (Cambridge).

A.2.2 General Equipment and Reagents

Equipment used included 8-channel multi-pipette (10, 50, 300 μ l Finn pipette); 96 well V-bottomed polypropylene plate (Greiner); 96 well white opaque non-treated plate (Corning); Adhesive plate covers (Greiner); Stepper (multipette[®] Eppendorf); Incubated plate shaker (Titramax 1000, Heidolph); Chemiluminescence counter (Topcount Packard); Refrigerated centrifuge (ALC 4237R, Jencons PLS); Buckets for 96 well plates for the above centrifuge (Jencons PLS); Refrigerated centrifuge (RC5C, Sorvall); Rotor SS-34 for RC5C (Sorvall); and Rotor Mixer (Agar Scientific). hSMG-1 mouse monoclonal (In house, KuDOS). Test Compounds were made up at 100 μ M in 50 % (v/v) DMSO and used at a final concentration of 10 μ M.

A.2.3 Immunoprecipitation of hSMG-1

25 ml HeLa Nuclear Extract (Computer Cell Culture Centre, Belgium) was thawed on ice and clarified by centrifugation at 2000 g for 15 min at 4 °C. The clarified supernatant was transferred to a 50 ml falcon tube, and 250 µl 100x protease inhibitor mix (Roche), and 125 µl anti-SMG-1 antibody (mouse monoclonal, in house) was added. The mixture (NE mix) was incubated for 3 hr at 4 °C on a rotary mixer. 6.25 ml Protein A sepharose (Sigma) slurry, (pre-washed in PBS three times) was added to the NE mix and incubated for a further 1 hr on the rotary mixer at 4 °C. The immune complexes were sedimented by centrifugation at 200 g for 2 min at 4 °C. The hSMG-1 depleted nuclear extract was decanted. The beads were washed twice in 50 ml ice cold IP buffer (250 mM KCl, 25 mM Hepes, 10 % Glycerol, 2 mM MgCl₂, 0.5 mM EDTA, 0.1 mM Na₃VO₄, 1 % NP-40) then once in 50 ml ice cold high salt buffer (100 mM Tris-HCl pH 7.4, 500 mM LiCl), and twice in ice cold incomplete kinase buffer (10 mM Hepes, 50 mM β-glycerol Phosphate, 50 mM NaCl). The final bead pellet was resuspended in 18.75 ml complete kinase buffer (10 mM Hepes, 50 mM β-glycerol phosphate, 50 mM NaCl, 10 % Glycerol, 1 mM DTT, 10 mM MnCl₂, 0.1 mM Na₃VO₄), aliquoted into cryogenic vials and stored at -80°C.

A.2.4 hSMG-1 *in vitro* Kinase Assay

The hSMG-1 beads from the IP were resuspended and 35 µl was added per well to a V-bottomed 96 well polypropylene plate. Test compounds (100 µM in 50 % DMSO)

from the KuDOS library were replicated in microtitre plates (Greiner). In the primary screen 5 μ l of each compound was added to the beads to give a final working concentration of 10 μ M. This was incubated for 15 mins at room temperature with shaking. 10 μ l of the substrate mix (p53N₁₋₆₆ GST fragment (1 μ l, 1 μ g/ μ l), ATP (1 μ l, 2.5 mM), 8 μ l Kinase Buffer (10 mM Hepes pH 7.6, 50 mM NaCl, 50 mM β -glycerol phosphate, 1 mM DTT, 10 mM MnCl₂, 0.1 mM Na₃VO₄) was added per well. For the negative control the p53N₁₋₆₆ fragment was substituted with a p53N₁₋₆₆ double mutant (ser15 \rightarrow ala, ser37 \rightarrow ala). The plate was incubated on the plate shaker for 40 min at 30°C. The reaction was terminated by adding 25 μ l PBS per well. To pellet the beads the plate was centrifuged at 250 g for 10 min at 4 °C.

50 μ l of the assay mix was transferred to the corresponding wells of an opaque white ELISA (enzyme linked immunosorbent assay) plate (Corning), incubated for 1.5 hr on a shaker at room temperature. The plate content was discarded and washed twice in 300 μ l PBS. The plate was blocked in 3 % BSA (w/v) in PBS (300 μ l per well) for 16 hr at room temperature. The plate was washed as before, and 50 μ l of a 1:10,000 dilution of anti-Phospho-p53ser15 mouse monoclonal antibody (Cell Signalling Technology) in 3 % BSA was added to each well and incubated for 1 hr on a shaker at room temperature. The contents were then discarded and washed four times in 300 μ l PBS. 50 μ l of a 1:25,000 dilution of goat-anti-mouse-HRP antibody (Pierce) in 3% BSA was added per well and incubated for 1 hr on a shaker at room temperature. The plate was then washed 4 times in PBS as before. 50 μ l of ECL (1:1 ratio ECL I: ECL II (Amersham Pharmacia Biotech) was added to each well and the luminescence detected by a Packard Scintillation counter,

Top Count™. The raw data was tabulated in Microsoft Excel and the KuDOS Pharmaceuticals database program, Activity Base.

The percentage inhibition for each compound was then calculated using the following equation:

$$\% \text{ Inhibition} = 100 - \left[\frac{(\text{cps of well-mean negative cps})}{(\text{mean positive cps-mean negative cps})} \right] \times 100$$

A.3 Results

A.3.1 Screening small molecule compound libraries

The hSMG-1 *in vitro* ELISA assay was used to screen small molecule compound libraries. The assay is based on the ability of hSMG-1 to phosphorylate p53 at serine-15 (Braumbaugh *et al*, 2004). Immuno-purified hSMG-1 was used to phosphorylate a recombinant GST-fused N-terminal fragment of p53 (p53N₁₋₆₆ GST fragment). The specific phosphorylation event at serine-15 was detected by a phospho-specific p53 serine-15 monoclonal antibody (Cell Signaling Technology). In turn, this was detected by the secondary HRP-conjugated anti-mouse antibody through the oxidation of luminol resulting in the emission of light, which is detected and measured by a plate reader (Packard Scintillation counter, Top Count™). In the presence of an inhibitor of hSMG-1 the extent of p53 serine-15 phosphorylation would decrease resulting in a corresponding decrease in chemiluminescence. The positive control represents hSMG-1 activity in the absence of any drug. In the

negative control a p53 double mutant lacking the hSMG-1 phosphorylation site, was used as the substrate and is representative of the background reading.

Small molecule compound libraries (2480 compounds in total) were primarily screened at a final concentration of 10 μM to identify any potential inhibitors. From this initial screen 240 compounds were identified to have a percentage inhibition of 45 % and above. All 240 hits were then re-screened in duplicate at both 10 μM and 1 μM . The secondary screen highlighted 18 compounds which showed 45 % inhibition and above at 1 μM (Table A.1).

A.3.2 IC₅₀ Determination

IC₅₀ is a common method for assaying drug efficiency in pharmaceutical screening regimens. In this case, IC₅₀ would be defined as the concentration of the drug needed to inhibit hSMG-1 activity by 50%. Therefore to determine the potency of the 18 hits, each compound was tested in duplicate at semi-log concentrations (Figure A.3) on two separate occasions, termed A and B. The raw data generated was used to calculate the percentage hSMG-1 activity in the presence of each compound at each concentration, this was then transferred to a graphical form and the IC₅₀ deduced. The IC₅₀ values of the hits identified in the secondary screen range from 254 nM to inactive (Table A.2). The most potent inhibitor identified on the first testing was KU-0055958 with an IC₅₀ of 289 nM. The IC curve for KU-0055958 is shown in Figure A.4 and this is contrasted with less potent compounds tested.

The IC₅₀ screen highlighted the effectiveness of the drugs identified in the secondary screen. To determine if the drugs were specific to hSMG-1, IC₅₀ databases

held within KuDOS Pharmaceuticals were analysed to determine the effect of each compound towards other members of the PIKK family including ATM, ATR, DNA-PK, mTOR and PI3 Kinase (table A.3). Analysis of the IC₅₀ records show that KU-0055958 is the only specific h-SMG-1 inhibitor identified with an IC₅₀ of 289 nM, this is a ten-fold order of magnitude less than the IC₅₀ for ATM (3 µM) and the compound is not active towards DNA-PK, ATR, mTOR or PI3 Kinase. The majority of the other inhibitors of hSMG-1 identified in this screen were shown to be approximately ten times more potent for ATM than hSMG-1, indicating that the structure of the hSMG-1 active site is most closely related to that of ATM as opposed to other members of the PIKK family.

KU-0055958 has therefore been identified as a specific and potent inhibitor of hSMG-1 and is the lead compound identified in this screen.

A.4 Discussion

Genome instability is one of the main forces driving the onset and progression of carcinogenesis. Genetic degradation is intimately linked with DNA maintenance mechanisms. Therefore further study into these mechanisms will not only reveal the biological impact of damage on the genome, but also uncover new paradigms for prevention, genetic susceptibility, diagnosis and therapeutic intervention (Hoeijmakers, 2001). On this basis, KuDOS pharmaceuticals have developed small molecule inhibitors of DNA repair proteins, including ATM and DNA-PK, and aim to extend this to other members of the PIKK family. These inhibitors may not only

lead to the development of therapeutics but will also provide useful probes for elucidating the role of each PIKK and defining the signalling pathways they regulate.

The newest member of the PIKK family, hSMG-1 has been characterised by Brumbaugh *et al.* (2004) as a genotoxic stress activated protein kinase that displays some functional overlap with ATM, in human cells. Therefore identification of a novel and specific small molecule inhibitor of hSMG-1 could be used to dissect out the role of hSMG-1 in the cells and to determine the extent of functional overlap with ATM.

A high throughput *in vitro* kinase assay for hSMG-1 was developed at KuDOS Pharmaceuticals. This was utilised to screen small molecule compound libraries developed for the PIKK family. We identified an ATP-competitive inhibitor, KU-0055958 that inhibits hSMG-1 with an IC_{50} of 0.289 μ M. KU-0055958 shows specificity with respect to inhibition of other PIKK family members (Table A.3). Figure A.5 shows the chemical structure of KU-0055958. The critical oxygen (highlighted in red) is believed to form a hydrogen bond within the hinge region of the ATP binding site of hSMG-1. The aryl group (highlighted in green) is hydrophobic and has been proposed to fill the ATP-binding site. The unmarked region may act as a scaffold to correctly orientate the critical oxygen molecule for hydrogen bond formation. Potentially, these areas could be modified to increase the compounds selectivity, efficiency for hSMG-1 or cellular penetrance. However it is important to note that the structural relationship of these regions with the ATP-binding site of hSMG-1 can only be fully established from a crystal structure determination of hSMG-1 bound to KU-0055958.

This screen, as well as identifying a novel and specific inhibitor of hSMG-1, also gave insight into the structure of the active site of hSMG-1. Most of the other inhibitors of hSMG-1 identified in the second screen were approximately ten times more potent for ATM indicating that the structure of the hSMG-1 active site is most closely related to that of ATM, compared to other members of the PIKK family.

KU-0055958 has therefore been identified as a specific and potent inhibitor of hSMG-1 with an IC_{50} of 289 nM and is the lead compound identified in this screen. However systematic modification and evaluation of this lead inhibitor will be continued until an IC_{50} value in the low nanomolar range is obtained.

In addition, kinetic analysis of KU-0055958 will be carried out to confirm that inhibition of hSMG-1 by KU-0055958 is ATP competitive. Lineweaver-Burke plots will be produced to determine the mode of inhibition and the K_i value of the compound. KU-0055958 will also be subject to cell based assays to evaluate its ability to inhibit hSMG-1 at a cellular level. Compounds which are promising in the *in vitro* assay can behave unexpectedly in cells, showing little or no activity. This may be because compounds are insoluble and therefore not taken up by the cell, or if compounds are taken up, they could be rapidly broken down to give inactive products. KU-0055958 may also be toxic to cells as hSMG-1 has been shown to play a crucial role in NMD. To initially assess the effect of KU-0055958 at the cellular level, an *in vitro* clonogenic survival assay will be used to study the effect of KU-0055958 on ionising radiation induced cytotoxicity on different cell lines. The data obtained can be used to determine the percentage cell survival in the presence of different concentrations of the drug in combination with irradiation. Cellular IC_{50} value has also to be determined as a measure of effectiveness *in vivo*. Yamashita *et al.*

(2001) have shown that hSMG-1 directly phosphorylates hUPF-1 at serine-1078 and serine-1096 *in vivo* and *in vitro*. Therefore the phosphorylation status of these sites of hUPF-1 could be used as a marker of hSMG-1 activity and used to assess the function of hSMG-1 at the cellular level.

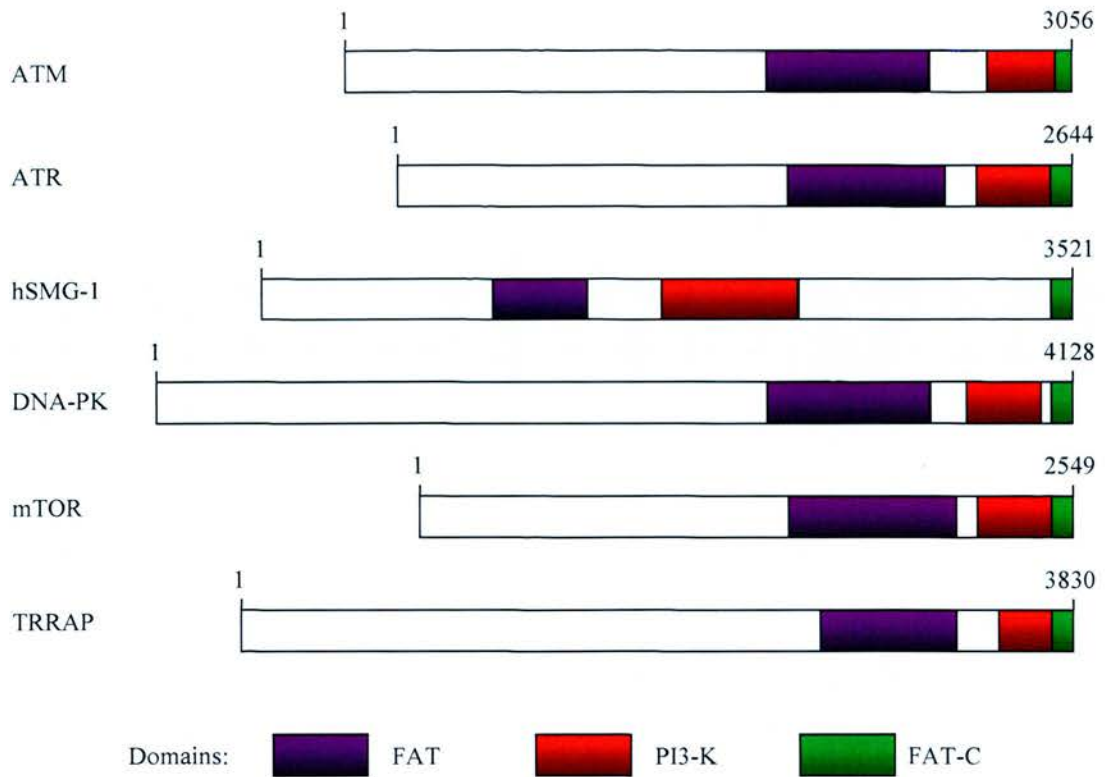


Figure A.1 Schematic representation of the human PIKK proteins. The number of residues is indicated for each protein. Three domains are common to all members of the PIKK family, FAT, PI3-K catalytic domain and the FAT-C domain (Adapted from Shiloh *et al.*, 2004; Khanna *et al.*, 2001)

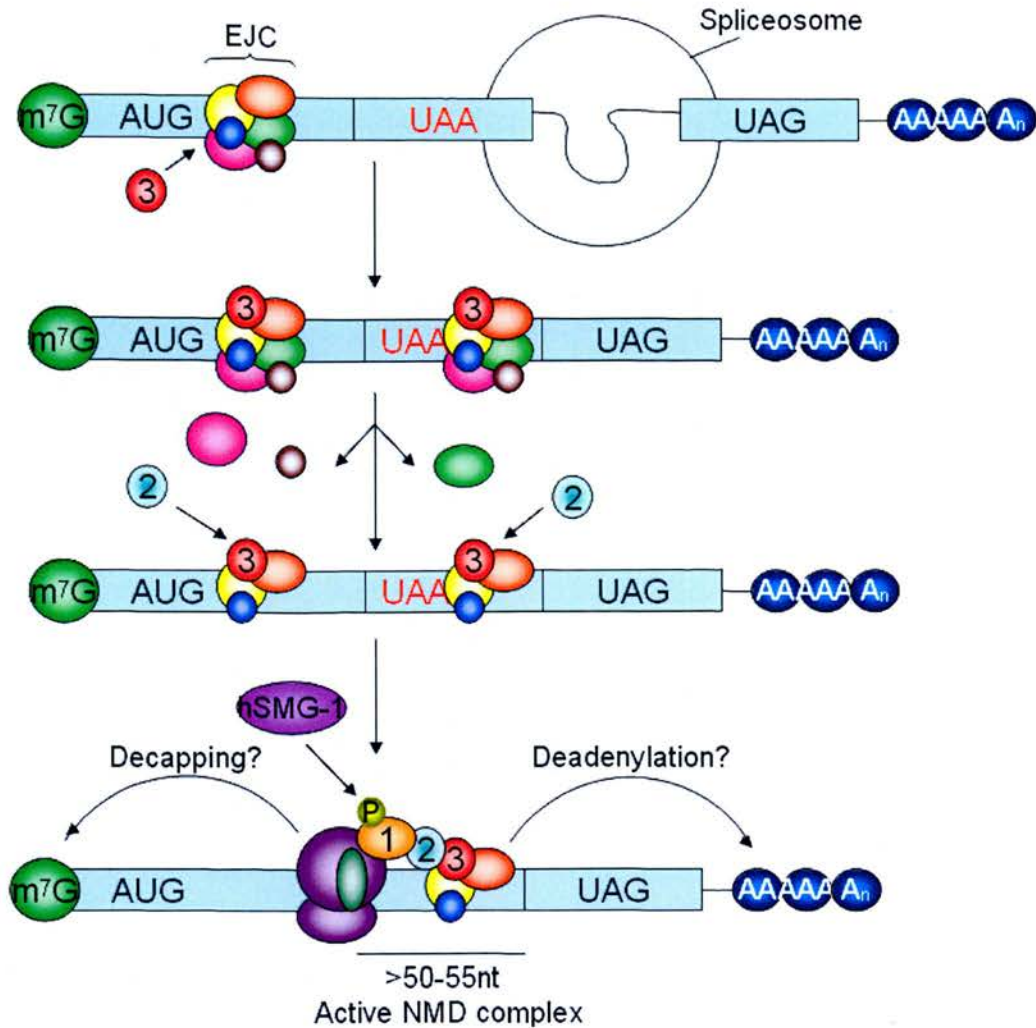


Figure A.2 A model of nonsense mediated mRNA decay pathway. A multi-protein exon junction complex (EJC) is deposited 20-24 nucleotides upstream of each exon-exon junction after splicing. hUpf-3 is recruited to the EJC followed by hUpf-2. The first translation event removes the EJCs from the mRNA. If translation terminates >50-55 nucleotides upstream of the last exon-exon junction, one or more EJC remain associated with the mRNA downstream of the termination complex. hUpf-1 is then recruited to bridge the terminated ribosome and the downstream EJC, this interaction may trigger hSMG-1 dependent phosphorylation of hUpf-1, forming an active NMD complex that triggers rapid decay of mRNA. The proteins hUpf-1, hUpf-2, and hUpf-3 are labelled 1, 2 and 3 respectively. The translation apparatus consists of the cap-binding complex (green), the ribosome (purple) and the poly(A)-binding protein (dark blue), and release factors (dark green) (Adapted from Abraham, 2004; Singh & Lykke-Andersen, 2003).

Compound ID	% Inhibition 10 μ M	% Inhibition 1 μ M	Compound ID	% Inhibition 10 μ M	% Inhibition 1 μ M
KU-0051664	74.5	50	KU-0059083	86.5	79.5
KU-0055958	98.3	94.4	KU-0059089	90.7	45
KU-0059473	84.5	60.5	KU-0059090	86	46
KU-0056296	53.5	56	KU-0059097	96.8	79.4
KU-0056788	86.4	55	KU-0059098	97	44
KU-0058315	78	56.3	KU-0059103	94.2	61
KU-0058321	86.7	52.8	KU-0059919	64.5	50.5
KU-0058541	65.4	44	KU-0060027	80	46.4
KU-0058545	83.3	55.3	KU-0051840	74	60

Table A.1 Hits identified in the secondary screen. Values for percentage inhibition are averages of duplicates.

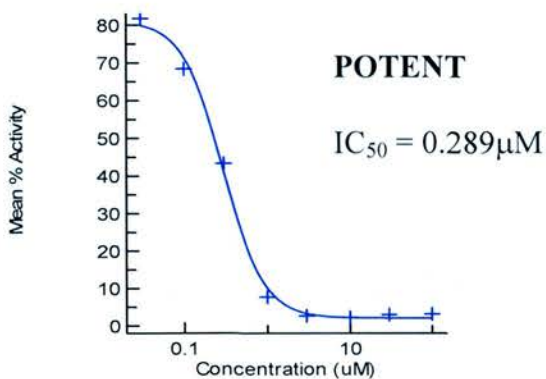
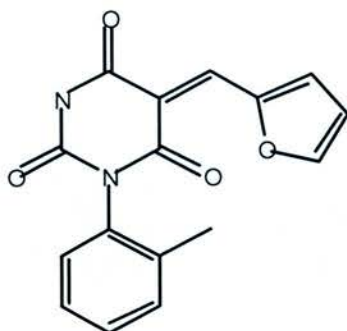
Cmpd1 100	Cmpd1 100	Cmpd2 100	Cmpd2 100	Cmpd3 100	Cmpd4 100	Cmpd4 100	Cmpd4 100	Std 100	Std 100	DMSO	DMSO
Cmpd1 30	Cmpd1 30	Cmpd2 30	Cmpd2 30	Cmpd3 30	Cmpd4 30	Cmpd4 30	Cmpd4 30	Std 30	Std 30	DMSO	DMSO
Cmpd1 10	Cmpd1 10	Cmpd2 10	Cmpd2 10	Cmpd3 10	Cmpd4 10	Cmpd4 10	Cmpd4 10	Std 10	Std 10	DMSO	DMSO
Cmpd1 3	Cmpd1 3	Cmpd2 3	Cmpd2 3	Cmpd3 3	Cmpd4 3	Cmpd4 3	Cmpd4 3	Std 3	Std 3	DMSO	DMSO
Cmpd1 1	Cmpd1 1	Cmpd2 1	Cmpd2 1	Cmpd3 1	Cmpd4 1	Cmpd4 1	Cmpd4 1	Std 1	Std 1	DMSO	DMSO
Cmpd1 0.3	Cmpd1 0.3	Cmpd2 0.3	Cmpd2 0.3	Cmpd3 0.3	Cmpd4 0.3	Cmpd4 0.3	Cmpd4 0.3	Std 0.3	Std 0.3	DMSO	DMSO
Cmpd1 0.01	Cmpd1 0.01	Cmpd2 0.01	Cmpd2 0.01	Cmpd3 0.01	Cmpd4 0.01	Cmpd4 0.01	Cmpd4 0.01	Std 0.01	Std 0.01	DMSO	DMSO
Cmpd1 0.03	Cmpd1 0.03	Cmpd2 0.03	Cmpd2 0.03	Cmpd3 0.03	Cmpd4 0.03	Cmpd4 0.03	Cmpd4 0.03	Std 0.03	Std 0.03	DMSO	DMSO

Figure A.3 Plate layout for IC₅₀ determination. All compounds were tested in duplicate. DMSO (5% v/v) was used as a control. Positive control is shown in green. Negative control is shown in red. p53 double mutant (S15A/ S37A) substrate was used as the negative control.

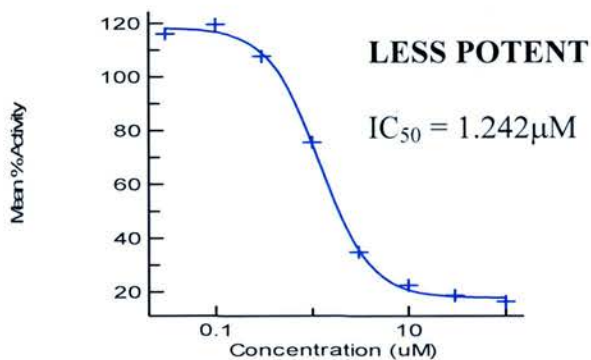
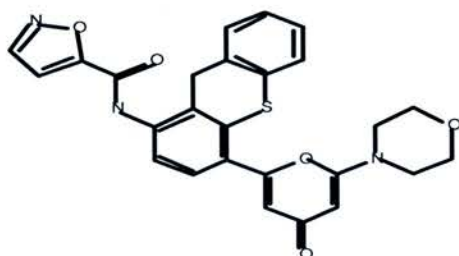
Compound ID	IC₅₀ A (μM)	IC₅₀ B (μM)	Average IC₅₀ (μM)
KU-0051664	2.226	1.485	1.856
KU-0055958	0.289	0.412	0.350
KU-0059473	1.983	1.620	1.802
KU-0056296	Inactive	Inactive	Inactive
KU-0056788	unavailable	unavailable	unavailable
KU-0058315	0.707	0.556	0.632
KU-0058321	0.527	0.204	0.366
KU-0058541	0.841	0.982	0.912
KU-0058545	1.242	0.752	0.997
KU-0059083	0.338	0.170	0.254
KU-0059089	0.318	0.963	0.641
KU-0059090	0.898	0.792	0.845
KU-0059097	0.541	0.187	0.364
KU-0059098	0.620	1.308	0.955
KU-0059103	0.598	0.832	0.715
KU-0059919	37.757	Inactive	37.757
KU-0060027	4.100	4.631	4.366
KU-0051840	Inactive	Inactive	Inactive

Table A.2 Compounds identified in the secondary screen and their IC₅₀ values.

KU-0055958



KU-0058545



KU-0060027

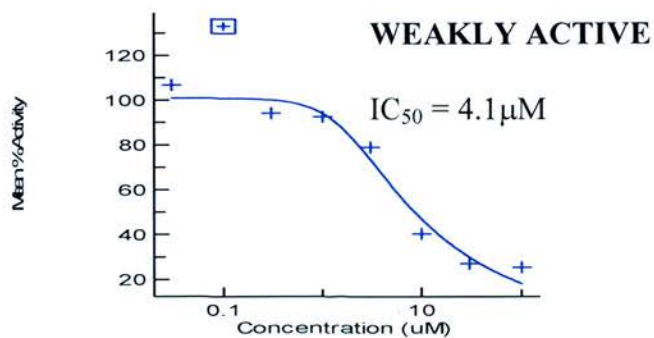
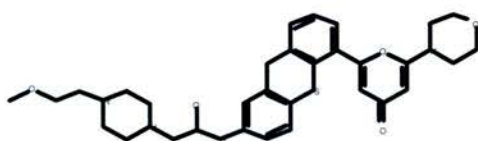
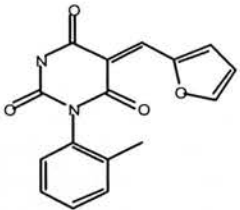
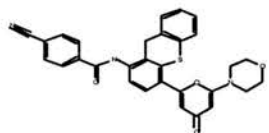
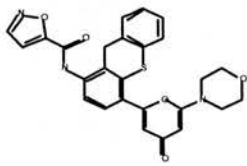
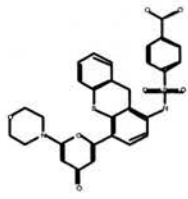
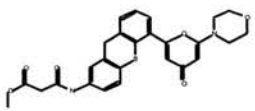


Figure A.4 Inhibitors of hSMG-1. Three examples of hSMG-1 inhibitors tested. KU-0055958 was shown to be the most potent inhibitor tested, KU-0058545 was less potent where KU-0060027 was shown to be a weakly active compound. The structures and IC_{50} values (μM) are shown

Compound ID	Structure	IC ₅₀ /μM					
		hSMG-1	ATM	ATR	DNA-PK	mTOR	PI3 Kinase
KU-0055958		0.289	3.0	>100	>10	>10	10
KU-0058321		0.527	0.041	NA	>1	>10	>10
KU-0058545		1.242	0.034	NA	10	>10	>10
KU-0059083		0.338	0.057	NA	>1	>10	>10
KU-0059089		0.318	0.008	NA	>1	>10	>10

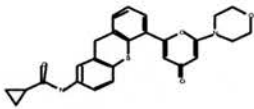
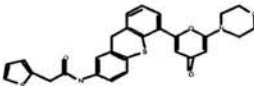
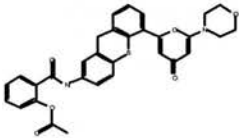
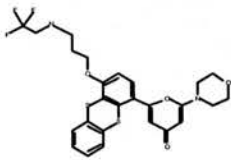
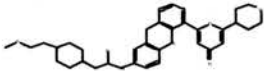
Compound ID	Structure	IC ₅₀ /μM					
		hSMG-1	ATM	ATR	DNA-PK	mTOR	PI3 Kinase
KU-0059090		0.898	0.006	NA	>1	<10	10.539
KU-0059097		0.541	0.008	NA	>1	>10	10
KU-0059103		0.598	0.007	NA	>1	>10	10
KU-0059919		37.78	0.1	NA	NA	>10	>10
KU-0060027		4.1	0.022	NA	NA	>10	>10

Table A.3 Comparison of IC₅₀ Values. IC₅₀ values are in μM. NA = data not available

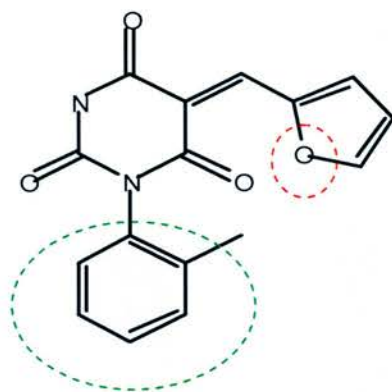


Figure A.5 Chemical structure of KU-0055958. The oxygen highlighted in red is likely to form a critical hydrogen bond within the ATP binding site. The hydrophobic aryl group highlighted in green may fill the ATP binding site. The unmarked region may act as a scaffold.

APPENDIX B

BUFFERS AND SOLUTIONS

Ampicillin – a stock solution of 100 mg/ml was prepared and used at a final concentration of 100 µg/ml. The solution was stored at -20 °C.

ATP (Boehringer) – a stock solution of 2.5 mM was made and used at a final concentration of 0.5 µM. The solution was stored at -20 °C.

ATM Kinase Buffer - Hepes (50 mM, pH 7.5), Sodium Chloride (150 mM), Managanese (II) Chloride (4 mM), Magnesium Chloride (6mM), Glycerol (10 %), DTT (1 mM), Sodium Orthovanadate (0.1 mM).

Bovine Serum Albumin (Sigma) – 3 % Bovine Serum Albumin (BSA) was prepared in Phosphate Buffered Saline (PBS) and used as a blocking agent. The solution was stored at 4 °C.

Coomassie Blue stain –Methanol (45 %), Acetic acid (10 %), Coomassie Blue R250 (0.1 % (w/v)).

Destain 1 –Methanol (5 % (v/v)), Acetic Acid (7 % (v/v)).

Destain 2 –Methanol (50 % (v/v)), Acetic Acid (10 % (v/v)).

Dithiothreitol – a stock solution of 1 M Dithiothreitol (DTT) was stored at -20°C.

DNA Loading Buffer – Glycerol (40 % (v/v)), EDTA (50 mM), Bromophenol Blue (0.1 % (w/v))

ECL[®] Solution I – Luminol (2.5 mM), Coumaric Acid (396 µM), Tris (100 mM, pH 8.5). The solution was stored at 4 °C protected from light.

ECL[®] Solution II - Hydrogen peroxide (0.02 % (v/v)), Tris (100 mM, pH 8.5). The solution was stored at 4 °C protected from light.

Ethidium bromide – a stock solution of 10 mg/ml was made and used at a final concentration of 5 µg/ml. The solution was stored at room temperature protected from light.

Freezing Media - Tissue culture media (50% (v/v)), FBS (40 % (v/v)), DMSO (10% (v/v))

High Salt Buffer - Tris-HCl (50 mM, pH 8), Glycerol (5 %), EDTA (1 mM), Magnesium Chloride (10 mM), Potassium Chloride (400 mM)

IP Buffer – Potassium Chloride (250 mM), Hepes (25 mM), Glycerol (10 %), Magnesium Chloride (2 mM), EDTA (0.5 mM), Sodium Orthovanadate (0.1 mM), NP-40 (1 %).

Low Salt Buffer - Hepes pH 7.4 (10 mM), Potassium Chloride (25 mM), Sodium Chloride (10 mM), Magnesium Chloride (1 mM), EDTA (0.1 mM)

Luria Bertani (LB) –bacto-tryptone (1 % (w/v)), bacto–yeast extract (0.5% (w/v)), Sodium Chloride (1 % (w/v)). Adjust to pH 7.5.

Marvel – Marvel powdered milk (5 % (w/v)) dissolved in PBS-Tween.

NBA - Potassium Chloride (85 mM), Sucrose (5.5 % (w/v)), Tris-HCl (10 mM pH 7.5), EDTA (0.2 mM), Spermidine (0.5 mM), PMSF (250 μ M)

NBB - Potassium Chloride (85 mM), Sucrose (5.5 % (w/v)), Tris-HCl (10 mM pH 7.5), EDTA (0.2 mM), Spermidine (0.5 mM), PMSF (250 μ M), NP40 (1 %).

NBR - Potassium Chloride (85 mM), Sucrose (5.5 % (w/v)), Tris-HCl (10 mM pH 7.5), Calcium Chloride (1.5 mM), Magnesium Chloride (3 mM), PMSF (250 μ M).

NP40 Lysis Buffer - NP40 (1 %), Hepes (25 mM pH 7.6), Potassium Chloride (400 mM), Sodium Orthovanadate (200 μ M)

NP40 Lysis Buffer 2 - NP40 (1 %), Tris-HCl (50 mM, pH 7.4), EDTA (1 mM pH 7.4), Sodium Chloride (150 mM), glycerol (10 %).

Phosphate Buffered Saline (10x) – 100 tablets (Oxoid) are dissolved in 1 litre distilled water. (Typical formula (g/l) Sodium Chloride (8 g), Potassium Chloride (0.2 g), Di-Sodium hydrogen Orthophosphate (1.44 g), Potassium dihydrogen orthophosphate (0.24 g))

PBS-Tween – Tween (0.1 % (v/v)) in PBS.

Proteasome Lysis Buffer - Tris-HCl (20 mM, pH 7.2), EDTA (0.1 mM), 2-mercaptoethanol (1 mM), ATP (5 mM), glycerol (20 %), NP40 (0.04 %).

Resolving Gel - Acrylamide (6 - 15 %), Tris-HCl (390 mM, pH 8.8), SDS (0.1 %), Ammonium peroxodisulphate (0.1 %), TEMED (0.08 %)

SDS-PAGE Running Buffer - Glycine (192 mM), Tris (25 mM), SDS (0.1 % (w/v))

SDS sample buffer (4x) – SDS (4 % (w/v)), Tris-HCl (250 mM, pH 6.8), EDTA (10 mM), DTT (0.2 M), Bromophenol blue (1% (w/v)).

Separation Buffer – EDTA (2 mM), BSA (0.5 % (w/v)) in PBS pH 7.2

Stacking Gel - Acrylamide (5 %), Tris-HCl (123 mM, pH 6.8), SDS (0.1 %), Ammonium peroxodisulphate (0.1 %), TEMED (0.1 %)

TAE Electrophoresis Buffer (10x) – Tris-HCl (0.4 M, pH 8.0), Sodium Acetate (0.2 M), EDTA (0.02 M, pH 8.0)

TEEP₂₀ - Tris-HCl (10 mM pH 8.0), EDTA (1 mM), EGTA (1 mM), PMSF (250 μ M), Sodium Chloride (20 mM)

Transformation Buffer 1 – Rubidium Chloride (100 mM), Manganese (II) Chloride (79 mM), Potassium Acetate (30 mM pH 7.5), Calcium Chloride (13.5 mM), Glycerol (15 %). Adjust to pH 5.8 with Acetic acid (0.2 M).

Transformation Buffer 2 - MOPS (10 mM pH 6.8), Rubidium Chloride (10 mM), Calcium Chloride (13.5 mM), Glycerol (15 %). Adjust to pH 6.8 with Sodium Hydroxide.

Transfer Buffer –Glycine (192 mM), Tris (25 mM), Methanol (20 % (v/v)).

Urea Lysis Buffer – Urea (7 M), DTT (0.1 M), Triton x-100 (0.05 % (v/v)), Sodium Chloride (25 mM), Hepes (20 mM, pH 7.6).

Wash Buffer -, Hepes (25 mM pH 7.4), Potassium Chloride (150 mM), EDTA (1 mM), Sodium Orthovanadate (200 μ M)

REFERENCES

- Abraham, R.T. (2001). Cell cycle checkpoint signalling through the ATM and ATR kinases. *Genes Dev.* **15**, 2177-2196.
- Abraham, R.T. (2004a). PI 3-kinase related kinases: “big” players in stress-induced signalling pathways. *DNA Repair* **3**, 883-887.
- Abraham, R.T. (2004b). The ATM-related kinase, hSMG-1, bridges genome and RNA surveillance pathways. *DNA Repair* **3**, 919-925.
- Achanta, G & Haung, P. (2004). Role of p53 in sensing oxidative DNA damage in response to reactive oxygen species-generating agents. *Cancer Res.* **64**, 6233-6239.
- Adams, P.D., Sellers, W.R., Sharma, S.K., Wu, A.D., Nalin, C.M., Kaelin, W.G., Jr. (1996). Identification of a cyclin-cdk2 recognition motif present in substrates and p21-like cyclin-dependent kinase inhibitors. *Mol. Cell Biol.* **16**, 6623-6633.
- Adnane, J., Jackson, R.J., Nicosia, S.V., Cantor, A.B., Pledger, W.J., Sefti, S.M. (2000). Loss of p21WAF1/CIP1 accelerates Ras oncogenesis in a transgenic/knockout mammary cancer model. *Oncogene* **19**, 5338-47.
- Akey, C.W. & Luger, K. (2003). Histone chaperones and nucleosome assembly. *Curr. Opin. Struct. Biol.* **13**, 6-14.
- Albertella, M.R., Lau, A., O'Connor, M.J. (2005). The overexpression of specialised DNA polymerases in cancer. *DNA Repair* **4**, 583-593.
- Ali, A., Zhang, J., Bao, S., Liu, I., Otterness, D., Dean, N.M., Abraham, R.T., Wang, X.F. (2004). Requirement of protein phosphatase 5 in DNA-damage-induced ATM activation. *Genes Dev.* **18**, 249-254.
- Alt, J.R., Gladden, A.B., Diehl, J.A. (2002). p21 (Cip1) promotes cyclin D1 nuclear accumulation via direct inhibition of nuclear export. *J. Biol. Chem* **277**, 8517-8523.

- Amador, V., Ge, S., Santamaría, P.G., Guardavaccaro, D., Pagano, M. (2007). APC/CCdc20 controls the ubiquitin-mediated degradation of p21 in prometaphase. *Mol. Cell* **27**, 462-473.
- An, W., Kim, J., Roeder, R.G. (2004). Ordered cooperative functions of PRMT1, p300, and CARM1 in transcriptional activation by p53. *Cell* **117**, 735-748.
- Andegeko, Y., Moyal, L., Mittelman, L., Tsarfaty, I., Shiloh, Y., Rotman, G. (2001). Nuclear retention of ATM at sites of DNA double strand breaks. *J. Biol. Chem.* **276**, 38224-38230.
- Andrews, P., He, Y.J., Xiong, Y. (2006). Cytoplasmic localised ubiquitin ligase cullin 7 binds to p53 and promotes cell growth by antagonising p53 function. *Oncogene* **25**, 4534-4548.
- Antignani, A. & Youle, R.J. (2006) How do Bax and Bak lead to permeabilization of the outer mitochondrial membrane? *Curr. Opin. Cell Biol.* **18**, 685-689.
- Anttila, M. A., Kosma, V. M., Hongxiu, J., Puolakka, J., Juhola, M., Saarikoski, S., Syrjanen K. (1999). p21/WAF1 expression as related to p53, cell proliferation and prognosis in epithelial ovarian cancer. *Br. J. Cancer.* **79**, 11-12.
- Appella, E. & Anderson, C.W. (2001). Post-translational modifications and activation of p53 by genotoxic stresses. *Eur. J. Biochem.* **268**, 2764-2772.
- Araya, J., Maruyama, M., Inoue, A, Fujita, T., Kawahara, J., Sassa, K., Hayashi, R., Kawagishi, Y., Yamashita, N., Sugiyama, E., Kobayashi, M. (2002). Inhibition of proteasome activity is involved in cobalt-induced apoptosis of human alveolar macrophages. *Am. J. Physiol. Lung Cell Mol. Physiol.* **283**, L849 – L858.
- Ard, P.G., Chatterjee, C., Kunjibettu, S., Adside, L.R., Gralinski, L.E., McMahon, S.B. (2002). Transcriptional regulation of the mdm2 oncogene by p53 requires TRRAP acetyltransferase complexes. *Mol. Cell Biol.* **22**, 5650-5661.
- Armstrong, J., Kaufman, M.H., Darrison, D.J., Clarke, A.R. (1995). High-frequency developmental abnormalities in p53-deficient mice. *Curr. Biol.* **5**, 931-936.

Ashcroft, M. & Vousden, K.H. (1999). Regulation of p53 stability. *Oncogene* **18**, 7637-7643.

Ashcroft, M., Kubbutat, M.H., Vousden, K.H. (1999). Regulation of p53 function and stability by phosphorylation. *Mol. Cell Biol.* **19**, 1751-1758.

Ashcroft, M., Yoichi, T., & Vousden, K.H. (2000). Stress signals utilize multiple pathways to stabilize p53. *Mol. Cell Biol.* **20**, 3224-3233.

Attardi, L.D. & Jacks, T. (1999). The role of p53 in tumour suppression: lessons from mouse models. *Cell. Mol. Life. Sci.* **55**, 48-63.

Badie, C., Itzhaki, J.E., Sullivan, M.J., Carpenter, A.J., Porter, A.C. (2000). Repression of CDK1 and other genes with CDE and CHR promoter elements during DNA damage-induced G(2)/M arrest in human cells. *Mol. Cell Biol.* **20**, 2358-2366.

Baines, I.C. & Colas, P. (2006). Peptide aptamers as guides for small-molecule drug discovery. *Drug Discov. Today* **11**, 334-341.

Bakkenist, C.J. & Kastan, M.B. (2003). DNA damage activates ATM through intermolecular autophosphorylation and dimer dissociation. *Nature* **421**, 499-506.

Bakkenist, C.J. & Kastan, M.B. (2004). Initiating cellular stress responses. *Cell* **118**, 9-17.

Banin, S., Moyal, L., Shieh, S., Taya, Y., Anderson, C.W., Chessa, L., Smorodinsky, N.I., Prives, C., Reiss, Y., Shiloh, Y., Ziv, Y. (1998). Enhanced phosphorylation of p53 by ATM in response to DNA damage. *Science* **281**, 1674-1677.

Barlow C., Ribaut-Barassin, C., Zwingman, T.A., Pope, A.J., Brown, K.D., Owens, J.W., Larson, D., Harrington, E.A., Haerberle, A.M., Mariani, J., Eckhaus, M., Herrup, K., Bailly, Y., Wynshaw-Boris, A. (2000). ATM is a cytoplasmic protein in mouse brain required to prevent lysosomal accumulation. *Proc. Natl. Acad. Sci. USA* **97**, 871-876.

Bartek, J., Falck, J., Lukas, J. (2001). CHK2 kinas- a busy messenger. *Nat. Rev. Mol. Cell Biol.* **2**, 877-886.

Bartek, J. & Lukas, J. (2001). Mammalian G1- and S-phase checkpoints in response to DNA damage. *Curr. Opin. Cell Biol.* **13**, 738-747.

Bartkova, J., Rezaei, N., Liontos, M., Karakaidos, P., Kletsas, D., Issaeva, N., Vassiliou, L-V.F., Kolettas, E., Niforou, K., Zoumpourlis, V.S. *et al.* (2006). Oncogene-induced senescence is part of the tumourigenesis barrier imposed by DNA damage checkpoints. *Nature* **444**, 633-636.

Bates, S., Ryan, K.M., Phillips, A.C., Vousden, K.H. (1998). Cell cycle arrest and DNA endoreduplication following p21Waf1/Cip1 expression. *Oncogene* **17**, 1691-1703.

Beamish, H., Williams, R., Chen, P., Lavin, M.F. (1996). Defect in multiple cell cycle checkpoints in ataxia-telangiectasia post irradiation. *J. Biol. Chem.* **271**, 20486-20493.

Bell, S., Klein, C., Muller, L., Hansen, S., Buchner, J. (2002). p53 contains large unstructured regions in its native state. *J Mol. Biol.* **322**, 917-927.

Bellido, T., O'Brien, C.A., Roberson, P.K., Manolagas, S.C. (1998). Transcriptional activation of the p21(WAF1,CIP1,SDI1) gene by interleukin-6 type cytokines. A prerequisite for their pro- differentiating and anti-apoptotic effects on human osteoblastic cells. *J. Biol. Chem.* **273**, 21137-21144.

Benchimol, S. (2001). p53-dependent pathways of apoptosis. *Cell Death Differ.* **8**, 1049-1051.

Bendjennat, M., Boulaire, J., Jascur, T., Brickner, H., Barbier, V., Sarasin, A., Fotedar, A., Fotedar, R. (2003). UV irradiation triggers ubiquitin-dependent degradation of p21(WAF1) to promote DNA repair. *Cell* **114**, 599-610.

Bensaad, K., Tsuruta, A., Selak, M.A., Vidal, M.N., Nakano, K., Bartrons, R., Gottlieb, E., Vousden, K.H. (2006). TIGAR, a p53-inducible regulator of glycolysis and apoptosis. *Cell* **126**, 107-120.

Bialik, S. & Kimchi, A. (2006). The Death-Associated Protein Kinases: Structure, Function, and Beyond. *Annu. Rev. Biochem.* **75**, 189-210.

Bischoff, J.R., Casso, D., Beach, D. (1992). Human-p53 inhibits growth in schizosaccharomyces-pombe. *Mol. Cell Biol.* **12**, 1405-1411.

Blanco-Aparicio, C., Renner, O., Leal, J.F.M., Carnero, A. (2007). PTEN, more than AKT pathway. *Carcinogenesis* **28**, 1379-1386.

Blattner, C., Tobiasch, E., Litfen, M., Rahmsdorf, H.J., Herrlich, P. (1999). DNA damage induced p53 stabilization: no indication for an involvement of p53 phosphorylation. *Oncogene* **18**, 1723-1732.

Bode, A.M. & Dong, Z. (2004). Post-translational modification of p53 in tumourigenesis. *Nat. Rev. Can.* **4**, 793-805.

Boisvert, F.M., Kruhlak, M.J., Box, A.K., Hendzel, M.J., Bazett-Jones, D.P. (2001). The transcriptional co-activator CBP is a dynamic component of the promyelocytic leukaemia nuclear body. *J. Cell Biol.* **152**, 1099-1106.

Bornstein, G., Bloom, J., Sitry-Shevah, D., Nakayama, K., Pagano, M., Hershko, A. (2003). Role of the SCFSkp2 ubiquitin ligase in the degradation of p21Cip1 in S phase. *J. Biol. Chem.* **278**, 25752-25757.

Bosari, S., Viale, G., Roncalli, M., Graziani, D., Borsani, G., Lee, A.K.C., Coggi, G. (1995) p53 gene mutations, p53 protein accumulation and compartmentalisation in colorectal adenocarcinoma. *Am. J. Pathol.* **147**, 790-798.

Braumbaugh, K.M., Otternes, D.M., Geisen, C., Oliveira, V., Brognard, J., Li, X., Lejeune, F., Tibbetts, R.S., Maquat, L.E., Abraham, R.T. (2004). The mRNA surveillance protein hSMG-1 functions in genotoxic stress response pathways in mammalian cells. *Mol. Cell* **14**, 585-598.

Brenner, C., Deplus, R., Didelot, C., Loriot, A., Viré, E., De Smet, C., Gutierrez, A., Danovi, D., Bernard, D., Boon, T., Pelicci, P.G., Amati, B., Kouzarides, T., de Launoit, Y., Di Croce, L., Fuks, F. (2005). Myc represses transcription through recruitment of DNA methyltransferase co-repressor. *EMBO J.* **24**, 336-346.

Brooks, C.L. & Gu, W. (2004). Dynamics in the p53-MDM2 Ubiquitination Pathway. *Cell Cycle* **3**, 895-899.

Broude, E.V., Swift, M.E., Vivo, C., Chang, B-D., Davis, B.M., Kalurupalle, S., Blagosklonny, M.V., Roninson, I.B. (2007). p21Waf1/Cip1/Sdi1 mediates retinoblastoma protein degradation. *Oncogene* **26**, 6954-6958.

Brown, P.O. & Botstein, D. (1999). Exploring the new world of the genome with DNA microarrays. *Nat. Genet.* **21**, S33-S37.

Brown, K.D., Lataxes, T.A., Shangary, S., Mannino, J.L., Giardina, J.F., Chen, J., Baskaran, R. (2000). Ionizing radiation exposure results in up-regulation of Ku70 via a p53/Ataxia telangiectasia-mutated protein-dependent mechanism. *J. Biol. Chem.* **275**, 6651-6656.

Brownell, J.E. & Allis, C.D. (1996). Special HATs for special occasions: linking histone acetylation to chromatin assembly and gene activation. *Curr. Opin. Genet. Dev.* **6**, 176-184.

Brugarolas, J., Bronson, R.T. & Jacks, T. (1998). p21 is a critical CDK2 regulator essential for proliferation control in Rb-deficient cells *J. Cell Biol.* **141**, 503-14.

Bunz, F., Dutriaux, A., Lengauer, C., Waldman, T., Zhou, S., Brown, J.P., Sedivy, J.M., Kinzler, K.W., Vogelstein, B. (1998). Requirement for p53 and p21 to sustain G2 arrest after DNA damage. *Science* **282**, 1497-1500.

Buschmann, T., Adler, V., Matusevich, E., Fuchs, S.Y., Ronai, Z. (2000). p53 phosphorylation and association with murine double minute 2, c-Jun NH2-terminal kinase, p14ARF, and p300/CBP during the cell cycle and after exposure to ultraviolet irradiation. *Cancer Res.* **60**, 896-900.

Butler, J.S. & Loh, S.N. (2003). Structure, function, and aggregation of the zinc-free form of the p53 DNA binding domain. *Biochemistry* **42**, 2396-2403.

Caelles, C., Helmborg, A., Karin, M. (1994). p53-dependent apoptosis in the absence of transcriptional activation of p53-target genes. *Nature* **370**, 220-223.

Calderwood, S.K., Khaleque, M.A., Sawyer, D.B., Ciocca, D.R. (2006). Heat shock proteins in cancer: chaperones of tumorigenesis. *Trends. Biochem. Sci.* **31**, 164-172.

Campbell, W.A., et al. (2006). Zebrafish lacking Alzheimer presenilin enhancer 2 (Pen-2) demonstrate excessive p53-dependent apoptosis and neuronal loss. *J. Neurochem.* **96**, 1423-1440.

Campisi, J. (2001). Cellular senescence as a tumour suppressor mechanism. *Trends Cell Biol.* **11**, S27-S31.

Canman, C.E. & Lim, D. (1998). The role of ATM in DNA damage responses and cancer. *Oncogene* **17**, 3301-3308.

Canman, C.E., Lim, D.S., Cimprich, K.A., Taya, Y., Tamai, K., Sakaguchi, K., Appella, E., Kastan, M.B., Siliciano, J.D. (1998). Activation of the ATM kinase by ionising radiation and phosphorylation of p53. *Science*, **281**, 1677-1679.

Casini, T. & Pelicci, P.G. (1999). A function of p21 during promyelocytic leukaemia cell differentiation independent of CDK inhibition and cell cycle arrest. *Oncogene* **18**, 3235-3243.

Chan, D.W., Gately, D.P., Urban, S., Galloway, A.M., Lees-Miller, S.P., Yen, T., Allalunis-Turner, J. (1998). Lack of correlation between ATM protein expression and tumour cell radiosensitivity. *Int. J. Radiat. Biol.* **74**, 217-224.

Chan, T.A., Hermeking, H., Lengauer, C., Kinzler, K.W., Vogelstein, B. (1999). 14-3-3Sigma is required to prevent mitotic catastrophe after DNA damage. *Nature* **401**, 616-620.

Chang, B-D., Broude, E.V., Fang, J., Kalinichenko, T.V., Abdryashitov, R., Poole, J.C., Roninson, I.B. (2000). p21^{Waf1/Cip1/Sid1} - induced growth arrest is associated with depletion of mitosis control proteins and leads to abnormal mitosis and endoreduplication in recovering cells. *Oncogene* **19**, 2165-2170.

Chen, C.Y., Oliner, J.D., Zhan, Q., Fornace, A.J., Jr., Vogelstein, B., Kastan, M.B. (1994). Interactions between p53 and MDM2 in a mammalian cell cycle checkpoint pathway. *Proc. Natl. Acad. Sci. USA* **91**, 2684-8.

Chen, J., Jackson, P.K., Kirschner, M.W., Dutta, A. (1995). Separate domains of p21 involved in the inhibition of Cdk kinase and PCNA. *Nature* **374**, 386-388.

Chen, J., Saha, P., Kornbluth, S., Dynlacht, B.D., Dutta, A. (1996). Cyclin-binding motifs are essential for the function of p21CIP1. *Mol. Cell Biol.* **16**, 4673-4682.

Chen, G. & Lee, E.Y.-H.P. (1996). The product of the ATM gene is a 370 kDa nuclear phosphoprotein. *J. Biol. Chem.* **271**, 33693-33697.

Chen, X., Chi, Y., Bloecher, A., Aebersold, R., Clurman, B.E., Roberts, J.M. (2004). N-acetylation and ubiquitin-independent proteasome degradation of p21 (Cip1). *Mol. Cell* **16**, 839-847.

Chen, D., Kon, N., Li, M., Zhang, W., Qin, J., Gu, W. (2005). ARF-BP1/Mule is a critical mediator of the ARF tumour suppressor. *Cell* **121**, 1071-1083.

Chen, J., Ruan, H., Ng, S.M., Gao, C., Soo, H.M., Wu, W., Zhang, Z., Wen, Z., Lane, D.P., Peng, J. (2006). Loss of function of *def* selectively up-regulates $\Delta 113p53$ expression to arrest expansion growth of digestive organs in zebrafish. *Genes Dev.* **19**, 2900-2911.

Cheng, M., Olivier, P., Diehl, J.A., Fero, M., Roussel, M.F., Roberts, J.M., Sherr, C.J. (1999). The p21(Cip1) and p27(Kip1) CDK 'inhibitors' are essential activators of cyclin D-dependent kinases in murine fibroblasts. *EMBO J.* **18**, 1571-1583.

Chène, P. (2001). The role of tetramerization of p53 function. *Oncogene* **20**, 2611-2617.

Chin, Y.E., Kitagawa, M., Su, W-C.S., You, Z-H., Iwamoto, Y., Fu, X-Y. (1996). Cell growth arrest and induction of cyclin-dependent kinase inhibitor p21 WAF1/CIP1 mediated by STAT1. *Science* **272**, 719-722.

Cho, Y., Gorina, S., Jeffrey, P.D., Pavletich, N.P. (1994). Crystal structure of a p53 tumor suppressor-DNA complex: understanding tumorigenic mutations. *Science* **265**, 246-355.

Christophorou, M.A., Martin-Zanca, D., Soucek, L., Lawlor, E.R., Brown-Swigart, L., Verschuren, E.W., Evan, G.I. (2005). Temporal dissection of p53 function in vitro and in vivo. *Nat. Genet.* **37**, 718-726.

Coates, P.J., Lorimore, S.A., Lindsay, S.A., Wright, E.G. (2003). Tissue specific p53 responses to ionising radiation and their genetic modification: the key to tissue-specific tumour susceptibility? *J. Pathol.* **201**, 377-388.

Copper, M.P., Balajee, A.S., Bohr, V.A. (1999). The C-terminal domain of p21 inhibits nucleotide excision repair in vitro and in vivo. *Mol. Biol. Cell* **10**, 2119-2129.

Coqueret, O. & Gascan, H. (2000). Functional interaction of STAT3 transcription factor with the cell cycle inhibitor p21^{WAF1/CIP1/SDI1}. *J. Biol. Chem.* **275**, 18794-18800.

Cordenonsi, M., Dupont, S., Maretto, S., Insinga, A., Imbriano, C., Piccolo, S. (2003). Links between tumour suppressors: p53 is required for TGF-beta gene responses by cooperating with Smads. *Cell* **113**, 301-314.

Corryer, S., Nabeyrat, E., Clemant, A. (1997). Involvement of the cell cycle inhibitor CIP1/WAF1 in lung alveolar epithelial cell growth arrest induced by glucocorticoids. *Endocrinology* **138**, 3677-3685.

Cory, S. & Adams, J.M. (2002). The Bcl2 family: regulators of the cellular life-or-death switch. *Nat. Rev. Cancer* **2**, 647-656.

Craig, A.L., Burch, L., Vojtesek, B., Mikutowska, J., Thompson, A., Hupp, T.R. (1999). Novel phosphorylation sites of human tumour suppressor protein p53 at Ser20 and Thr18 that disrupt the binding of mdm2 (mouse double minute 2) protein are modified in human cancers. *Biochem. J.* **342**, 133-141.

Crook, T., Parker, G.A., Rozycka, M., Crossland, S., Allday, M.J. (1998). A transforming p53 mutant, which binds DNA, transactivates and induces apoptosis reveals a nuclear: cytoplasmic shuttling defect. *Oncogene* **16**, 1429-1441.

Damalas, A., Kahan, S., Shtutman, M., Ben-Ze'ev, A., Oren, M. (2001). Deregulated beta-catenin induces a p53- and ARF-dependent growth arrest and cooperates with Ras in transformation. *EMBO J.* **20**, 4912-4922.

Dang, C.V. & Lee, W.M. (1989). Nuclear and nucleolar targeting sequences of c-erb-A, c-myb, N-myc, p53, HSP70, and HIV tat proteins. *J. Biol. Chem.* **264**, 18019-18023.

Das, S., Raj, L., Zhao, B., Kimura, Y., Bernstein, A., Aaronson, S.A., Lee, S.W. (2007). Hzf Determines cell survival upon genotoxic stress by modulating p53 transactivation. *Cell* **130**, 624-637.

Delavaine, L. & La Thangé, N.B. (1999). Control of E2F activity by p21^{Waf1/Cip1}. *Oncogene* **18**, 5381-5392.

Deng, C., Zhang, P., Harper, J.W., Elledge, S.J., Leder, P. (1995). Mice lacking p21^{CIP1/WAF1} undergo normal development, but are defective in G1 checkpoint control. *Cell* **82**, 675-84.

Denning, G., Jamieson, L., Maquat, L.E., Thompson, E.A., Fields, A.P. (2001). Cloning of a novel phosphatidylinositol kinase-related kinase. *J. Biol. Chem.* **276**, 22709-22714.

Derry, W.B., Putzke, A.P., Rothman, J.H. (2001). *Caenorhabditis elegans* p53: role in apoptosis, meiosis, and stress resistance. *Science* **294**, 591-595.

Di Cunto, F., Topley, G., Calautti, E., Hsiao, J., Ong, L., Seth, P.K., Dotto, G.P. (1998). Inhibitory function of p21^{Cip1/WAF1} in differentiation of primary mouse keratinocytes independent of cell cycle control. *Science* **280**, 1069-1072.

Ding, J., Miao, Z-H, Meng, L-H, Geng, M-Y. (2006). Emerging cancer therapeutic opportunities target DNA-repair systems. *Trends Pharm. Sci.* **27**, 338-344.

Donehower, L.A., Harvey, M, Slagle, B.L., McArthur, M.J., Montgomery, C.A., Jr., Butel, J.S., Bradley, A. (1992). Mice deficient for p53 are developmentally normal but susceptible to spontaneous tumours. *Nature* **356**, 215-21.

Dornan, D. & Hupp, T.R. (2001). Inhibition of p53-dependent transcription by BOX-I phospho-peptide mimetics that bind to p300. *EMBO Rep.* **2**, 139-144.

Dornan, D., Shimizu, H., Burch, L., Smith, A.J., Hupp, T.R. (2003). The proline repeat domain of p53 binds directly to the transcriptional coactivator p300 and allosterically controls DNA-dependent acetylation of p53. *Mol. Cell Biol.* **23**, 8846-8861.

Dornan, D., Wertz, I., Shimizu, H., Arnott, D., Frantz, G.D., Dowd, P., O'Rourke, K., Koeppen, H., Dixit, V.M. (2004). The ubiquitin ligase COP1 is a critical negative regulator of p53. *Nature* **429**, 86-92.

Dotto, G.P. (2000). p21WAF1/Cip1: more than a break to the cell cycle? *Biochimica et Biophysica. Acta.* **1471**, M43-M56.

Draghici, S., Khatri, P., Eklund, A.C., Szallasi, Z. (2006). Reliability and reproducibility issues in DNA microarray measurements. *Trends Genetics* **22**, 101-109.

Dulic, V., Kaufmann, W.K., Wilson, S.J., Tlsty, T.D., Lees, E., Harper, J.W., Elledge, S.J., Reed, S.I. (1994). p53-dependent inhibition of cyclin-dependent kinase activities in human fibroblasts during radiation-induced G1 arrest. *Cell* **76**, 1013-1023.

Dumaz, N. & Meek, D.W. (1999). Serine 15 phosphorylation stimulates p53 transactivation but does not directly influence interaction with HDM2. *EMBO J.* **18**, 7002-7010.

Dunker, A.K., Cortese, M.S., Romero, P., Iakoucheva, L.M., Uversky, V.N. (2005). Flexible nets. The roles of intrinsic disorder in protein interaction networks. *FEBS J.* **272**, 5129-5148.

Dutto, A. & Bell, S.P. (1997). Initiation of DNA replication in eukaryotic cells. *Annu. Rev. Cell Dev.* **13**, 293-332.

el-Deiry, W.S., Kern, S.E., Pietenpol, J.A., Kinzler, K.W., Vogelstein, B. (1992). Definition of a consensus binding site for p53. *Nat. Genet.* **1**, 45-49.

el-Deiry, W.S., Tokino, T., Velculescu, V.E., Levy, D.B., Parsons, R., Trent, J.M., Lin, D., Mercer, W.E., Kinzler, K.W., Vogelstein, B. (1993). WAF1, a potent mediator of p53 tumour suppression. *Cell* **75**, 817-825.

el-Deiry, W.S, Harper, J.W., O'Connor, P.M., Velculescu, V.E., Canman, C.E., Jackman, J., Pietenpol, J.A., Burrell, M., Hill, D.E., Wang, Y., *et al.* (1994). WAF1/CIP1 is induced in p53-mediated G1 arrest and apoptosis. *Cancer Res.* **54**, 1169-1174.

el-Deiry, W.S., Tokino, T., Waldman, T., Oliner, J.D., Velculescu, V.E., Burrell, M., Hill, D.E., Healy, E., Rees, J.L., Hamilton, S.R., *et al.* (1995). Topological control of p21 WAF1/CIP1 expression in normal and neoplastic tissues. *Cancer Res.* **55**, 2910-2919.

Elledge, R.M. & Allred, D.C. (1998). Prognostic and predictive value of p53 and p21 in breast cancer. *Breast Cancer Res Treat* **52**, 79-98.

Esser, C., Scheffner, M., Hohfeld, J. (2005). The chaperone associated ubiquitin ligase CHIP is able to target p53 for proteasomal degradation. *J. Chem. Biol.* **280**, 27443-27448.

Evan, G.I. & Vousden, K.H. (2001). Proliferation, cell cycle and apoptosis in cancer. *Nature* **411**, 342-348.

Falck, J., Coates, J., Jackson, S.P. (2005). Conserved modes of recruitment of ATM, ATR, and DNA-PK to sites of DNA damage. *Nature*, **434**, 605-611.

Fang, S., Jensen, J.P., Ludwig, R.L., Vousden, K.H., Weissman, A.M. (2000). Mdm2 is a RING finger-dependent ubiquitin protein ligase for itself and p53. *J. Biol. Chem.* **275**, 8945-8951.

Fei, P. & El-Deiry, W.S. (2003). P53 and radiation responses. *Oncogene* **22**, 5774-5783.

Feldman, D.E., Chauhan, V., Koong, A.C. (2005). The unfolded response: A novel component of the hypoxic stress response in tumours. *Mol. Cancer Res.* **3**, 597-605.

Fields, S. & Jang, S.K. (1990). Presence of a potent transcription activating sequence in the p53 protein. *Science* **249**, 1046-1049.

Fiucci, G., Beaucourt, S., Duflaut, D., Lespagnol, A., Stumptner-Cuvelette, P., Géant, A., Buchwalter, G., Tuynder, M., Susini, L., Lassalle, J.M., Wasyluk, C., Wasyluk, B., Oren, M., Amson, R., Telerman, A. (2004). Siah-1b is a direct transcriptional target of p53: identification of the functional p53 responsive element in the siah-1b promoter. *Proc. Natl. Acad. Sci. USA* **101**, 3510-3515.

Fortier, M., Kent, S., Ashdown, H., Poole, S., Boksa, P., Luheshi, G.N. (2004). The viral mimic, polyinosinic: polycytidylic acid, induces fever in rats via an interleukin-1-dependent mechanism. *AJP-Regul Intergr Comp Physiol.* **287**, R759-R766.

Franklin, D.S., Godfrey, V.L., O'Brien, D.A., Deng, C., Xiong, Y. (2000). Functional collaboration between different cyclin-dependent kinase inhibitors suppresses tumor growth with distinct tissue specificity. *Mol. Cell Biol.* **20**, 6147-58.

Fraser, J.A. & Hupp, T.R. (2007). Chemical genetics approach to identify peptide ligands that selectively stimulate DAPK-1 kinase activity. *Biochemistry* **46**, 2655-2673.

Friedler, A., Veprintsev, D.B., Freund, S.M., von Glos, K.I., Fersht, A.R. (2005). Modulation of binding of DNA to the C-terminal domain of p53 by acetylation. *Structure* **13**, 629-636.

Friedman, P.N., Chen, X., Bargonetti, J., Prives, C. (1993). The p53 protein is an unusually shaped tetramer that binds directly to DNA. *Proc. Natl. Acad. Sci. USA* **90**, 3319-3323.

Fritah, A. Saucier, C., Mester, J., Redeuilh, G., Sabbah, M. (2005). p21WAF1/CIP1 selectively controls the transcriptional activity of estrogen receptor alpha. *Mol. Cell Biol.* **25**, 2419 -2430.

Fung, T.K. & Poon, R.Y. (2005). A roller coaster ride with the mitotic cyclins. *Semin. Cell Dev. Biol.* **16**, 335-342.

Gaiddon, C., Moorthy, N.C., Prives, C. (1999). Ref-1 regulates the transactivation and pro-apoptotic functions of p53 in vivo. *EMBO J.* **18**, 5609-5621.

Gartel, A.L., Serfas, M.S., Gartel, M., Goufman, E., Wu, G.S., el-Deiry, W.S., Tyner, A.L. (1996). p21 (WAF1/CIP1) expression is induced in newly nondividing cells in diverse epithelia and during differentiation of the Caco-2 intestinal cell line. *Exp. Cell Res.* **227**, 171-181.

Gartel, A.L., Goufman, E., Tevosian, S.G., Shih, H., Yee, A.S., Tyner, A.L. (1998). Activation and repression of p21(WAF1/CIP1) transcription by RB binding proteins. *Oncogene* **17**, 3463-3469.

Gartel, A.L. & Tyner, A.L. (1999). Transcriptional regulation of the p21 WAF1/CIP1 gene. *Exp. Cell Res.* **246**, 280-289.

Gartel, A.L., Ye, X., Goufman, E., Shianov, P., Hay, N., Najmabadi, F., Tyner, A.L. (2001). Myc represses the p21 (WAF1/CIP1) promoter and interacts with Sp1/Sp3. *Proc. Natl. Acad. Sci. USA* **98**, 4510-4515.

Gartel, A.L. & Tyner, A.L. (2002). The role of the cyclin-dependent kinase inhibitor p21 in apoptosis. *Mol. Cancer Ther.* **1**, 639-649.

Gately, D.P., Hittle, J.C., Chan, G.K.T., Yen, T.J. (1998) Characterisation of ATM expression, localisation, and associated DNA-dependent protein kinase activity. *Mol. Biol. Cell* **9**, 2361-2374.

Giannakaou, P., Sackett, D.L., Ward, Y., Webster, K.R., Blagosklonny, M.V., Fojo, T. (2000). p53 is associated with cellular microtubules and is transported to the nucleus by dynein. *Nat. Cell Biol.* **2**, 709-717.

Gilbert, N. & Allan, J. (2001). Distinctive higher-order chromatin structure at mammalian centrosomes. *Proc. Natl. Acad. Sci. USA* **98**, 11949 - 11954.

Ginsberg, D., Michael-Michalovitz, D., Oren, M. (1991). Induction of growth arrest by a temperature-sensitive p53 mutant is correlated with increased nuclear localization and decreased stability of the protein. *Mol. Cell Biol.* **11**, 582-585.

Goodarzi, A.A. & Lees-Miller, S.P. (2004). Biochemical characterisation of the ataxia-telangiectasia mutated (ATM) protein from human cells. *DNA Repair* **3**, 753-767.

Goodarzi, A.A., Jonnalagadda, J.C., Douglas, P., Young, D., Ye, R., Moorhead, G.B., Lees-Miller, S.P., Khanna, K.K. (2004). Autophosphorylation of ataxia-telangiectasia mutated is regulated by protein phosphatase 2A. *EMBO J.* **23**, 4451-4461.

Gorospe, M., Wang, X., Guyton, K., Holbrook, N. (1996a). Protective role of p21 (WAF1/CIP1) against prostaglandin A2-mediated apoptosis of human colorectal carcinoma cells. *Mol. Cell Biol.* **16**, 6654-6660.

Gorospe, M., Shack, S., Guyton, K., Samid, D., Holbrook, N. (1996b). Up-regulation and functional role of p21 (WAF1/CIP1) during growth arrest of human breast carcinoma MCF-7 cells by phenylacetate. *Cell Growth Differ.* **7**, 1609-1615.

Gostissa, M., Hengstermann, A., Fogal, V., Sandy, P., Schwarz, S.E., Scheffner, M., Del Sal, G. (1999). Activation of p53 by conjugation to the ubiquitin-like protein SUMO-1. *EMBO J.* **18**, 6462-6471.

Grimson, A. O'Conner, S., Newman, C.L., Anderson, P. (2004). SMG-1 is a phosphatidylinositol kinase related protein kinase required for non-sense mediated mRNA decay in *Caenorhabditis elegans*. *Mol. Cell Biol.* **24**, 7483-7490.

Grob, T.J., Novak, U., Maisse, C., Barcaroli, D., Lüthi, A.U., Pirnia, F., Hügli, B., Graber, H.U., De Laurenzi, V., Fey, M.F., Melino, G., Tobler, A. (2001). Human delta Np73 regulates a dominant negative feedback loop for TAp73 and p53. *Cell Death Differ.* **8**, 1213-1223.

Gronroos, E., Terentiev, A.A., Punga, T., Ericsson, J. (2004). YY1 inhibits the activation of the p53 tumour suppressor in response to genotoxic stress. *Proc. Natl. Acad. Sci. USA* **101**, 12165 - 12170.

Grossman, S.R., Deato, M.E., Brignone, C., Chan, H.M., Kung, A.L., Tagami, H., Nakatani, Y., Livingstone, D.M. (2003). Polyubiquitination of p53 by an ubiquitin ligase activity of p300. *Science* **300**, 342-344.

Grunstein, M. (1997). Histone acetylation and chromatin structure and transcription. *Nature* **389**, 349-352.

Gu, Y., Turck, C.W., Morgan, D.O. (1993). Inhibition of the CDK2 activity in vivo by associated 20K regulatory subunit. *Nature* **366**, 707-710.

Gu, W., Shi, X.L., Roeder, R.G. (1997). Synergistic activation of transcription by CBP and p53. *Nature* **387**, 819-823.

Gu J., Nie, N., Wiederschain, D., Yuan, Z.M. (2001). Identification of p53 sequence elements that are required for MDM2-mediated nuclear export. *Mol. Cell Biol.* **21**, 8533-8546.

Hahn, W.C. & Weinberg, R.A. (2002). Modelling the molecular circuitry of cancer. *Nat. Rev. Can.* **2**, 331-341.

Hainut, P. & Hollstein, M. (2000). p53 and human cancer: the first ten thousand mutations. *Adv. Cancer Res.* **77**, 81-137.

Han, Z., Wei, W., Dunaway, S., Darnowski, J.W., Calabresi, P., Sedivy, J., Hendrickson, E.A., Balan, K.V., Pantazis, P., Wyche, J.H. (2002) Role of p21 in apoptosis and senescence of human colon cancer cells treated with camptothecin. *J. Biol. Chem.* **277**, 17154-17160.

Hardy, R.R, Kincade, P.W., Dorshkind, K. (2007). The protean nature of cells in the B lymphocyte lineage. *Immunity* **26**, 703-714

Harper, J.W., Adami, G.R., Wei, N., Keyomarsi, K., Elledge, S.J. (1993). The p21 Cdk-interacting protein Cip1 is a potent inhibitor of G1 cyclin- dependent kinases. *Cell* **75**, 805-816.

Harper, J.W., Elledge, S.J., Keyomasi, K., Dynlacht, B., Tsai, L.-H., Zhang, P. (1995). Inhibition of cyclin-dependent kinases by p21. *Mol. Biol. Cell* **6**, 387-400.

Harris, S.L. & Levine, A.J. (2005). The p53 pathway: positive and negative feedback loops. *Oncogene* **24**, 2899-2908.

Harvey, M., McArthur, M.J., Montgomery, C.A., Jr., Butel, J.S., Bradley, A, Donehower, L.A. (1993). Spontaneous and carcinogen-induced tumorigenesis in p53-deficient mice. *Nat. Genet.* **5**, 225-9.

Haupt, Y., Maya, R., Kazaz, A., Oren, M. (1997). Mdm2 promotes the rapid degradation of p53. *Nature* **387**, 296-299.

Hayon, I.L. & Haupt, Y. (2002). p53: An internal investigation. *Cell Cycle* **1**, 111-116.

Hayward, R.L., Schornagel, Q.C., Tente, R., Macpherson, J.S., Aird, R.E., Guichard, S., Habtemariam, A., Sadler, P., Jodrell, D.I. (2005). Investigation of the role of Bax, p21/Waf1 and p53 as determinants of cellular responses in HCT116 colorectal cancer cells exposed to novel cytotoxic ruthenium(II) organometallic agent, RM175. *Cancer Chemother. Pharmacol.* **55**, 577-583.

Hengartner, M.O. (2000). The biochemistry of apoptosis. *Nature* **407**, 770-776.

Hermeking, H., Lengauer, C., Polyak, K., He, T.C., Zhang, L., Thiagalingam, S., Kinzler, K.W., Vogelstein, B. (1997). 14-3-3 sigma is a p53 regulated inhibitor of G2/M progression. *Mol. Cell* **1**, 3-11.

Hickson, I., Zhao, Y., Richardson, C.J., Green, S.J., Martin, N.M.B., Orr, A.I., Reaper, P.M., Jackson, S.P., Curtin, N.J., Smith, G.C.M. (2004). Identification and characterisation of a novel and specific inhibitor of the ataxia-telangiectasia mutated kinase ATM. *Cancer Res.* **64**, 9152-9159.

Higashitsuji, H., Itoh, K., Sakurai, T., Nagao, T., Sumitomo, Y. et al. (2005). The oncoprotein gankyrin binds to MDM2/HDM2, enhancing ubiquitination and degradation of p53. *Cancer Cell* **8**, 75-87.

Hirano, T. (1998). Interleukin 6 and its receptor: ten years later. *Int. Rev. Immunol.* **16**, 249-284.

Ho, J.S., Ma, W., Mao, D.Y., Benchimol, S. (2005). p53-dependent transcriptional repression of c-myc is required for G1 cell cycle arrest. *Mol. Cell Biol.* **25**, 7423-7431.

Hoeijmakers, J.H.J. (2001). Genome maintenance mechanisms for preventing cancer. *Nature* **411**, 366-374.

Hoffman, W.H., Biade, S., Zilfou, J.T., Chen, J., Murphy, M. (2002). Transcriptional repression of the anti-apoptotic survivin gene by wild type p53. *J. Biol. Chem.* **277**, 3247-3257.

Hofmann, T.G., Möller, A., Sirma, H., Zentgraf, H., Taya, Y., Dröge, W., Will, H., Schmitz, M.L. (2002). Regulation of p53 activity by its interaction with homeodomain-interacting protein kinase-2. *Nat. Cell Biol.* **4**, 1-10.

Hoheisel, J.D. (2006) Microarray technology: beyond transcript profiling and genotype analysis. *Nat. Rev. Genet.* **7**, 200-210.

Holm, R., Skovlund, E., Skomedal, H., Florenes, V.A., Tanum, G. (2001). Reduced expression of p21WAF1 is an indicator of malignant behaviour in anal carcinomas. *Histopathology* **39**, 43-9.

Honda, R. & Yasuda, H. (1999). Association of p19(ARF) with Mdm2 inhibits ubiquitin ligase activity of Mdm2 for tumor suppressor p53. *EMBO J.* **18**, 22-27.

Huang, L., Sowa, Y., Sakai, T., Pardee, A.B. (2000). Activation of the p21WAF1/CIP1 promoter independent of p53 by the histone deacetylase inhibitor suberoylanilide hydroxamic acid (SAHA) through Sp1 sites. *Oncogene* **19**, 5712-5719.

Hupp, T.R., Meek, D.W., Midgley, C.A., Lane, D.P. (1992). Regulation of the specific DNA binding function of p53. *Cell* **71**, 875-886.

Hupp, T.R. & Lane, D.P. (1994). Allosteric activation of latent p53 tetramers. *Curr. Biol.* **4**, 865-875.

Hupp, T.R., Lane, D.P., Ball, K.L. (2000). Strategies for manipulating the p53 pathway in the treatment of human cancer. *Biochem. J.* **352**, 1-17.

Hwang, B.J., Ford, J.M., Hanawalt, P.C., Chu, G. (1999). Expression of the p48 xeroderma pigmentosum gene is p53-dependent and is involved in global genomic repair. *Proc. Natl. Acad. Sci. USA* **96**, 424 - 428.

Ihle, J.N. (1996). STATs and MAPKs: obligate or opportunistic partners in signaling. *BioEssays* **18**, 95-98.

Ito, Y., Kobayashi, T., Takeda, T., Komoike, Y., Wakasugi, E., Tamaki, Y., Tsujimoto, M., Matsuura, N., Monden, M. (1996). Expression of p21 (WAF1/CIP1) protein in clinical thyroid tissues. *Br. J. Cancer* **74**, 1269-1274.

Iwai, A., Marusawa, H., Matsuzawa, S., Fukushima, T., Hijikata, M., Reed, J.C., Shimotohno, K., Chiba, T. (2004). Siah-1L, a novel transcript variant belonging to the human Siah family of proteins, regulates beta-catenin activity in a p53-dependent manner. *Oncogene* **23**, 7593-7600.

Izzard, R.A., Jackson, S.P., Smith, G.C.M. (1999). Competitive and noncompetitive inhibition of DNA-dependent protein kinase. *Cancer Res.* **59**, 2581-2586.

Janus, F., Albrechtsen, N., Dornreiter, I., Wiesmuller, L., Grosse, F., Deppert, W. (1999). The duel role model for p53 in maintaining genome integrity. *Cell Mol. Life Sci.* **55**, 12-27.

Janz, C., Susse, S., Wiesmuller, L. (2002). p53 and recombination intermediates: role of tetramerisation at DNA junctions in complex formation and exonucleolytic degradation. *Oncogene* **21**, 2130-2140.

Javelaud, D. & Besançon, F. (2002). Inactivation of p21^{WAF1} sensitizes cells to apoptosis via an increase of both p14^{ARF} and p53 levels and an alteration of the Bax/Bcl-2 ratio. *J. Biol. Chem.* **277**, 37949-37954.

Jazayeri, A., Falck, J., Lukas, C., Bartek, J., Smith, G.C.M., Lukas, J., Jackson, S. P. (2006). ATM- and cell cycle-dependent regulation of ATR in response to DNA double-strand breaks. *Nat. Cell Biol.* **8**, 37-45.

Jeffrey, P.D., Gorina, S., Pavletich, N.P. (1995). Crystal structure of the tetramerization domain of the p53 tumor suppressor at 1.7 angstroms. *Science* **267**, 1498-1502.

Jenkins, J.R., Chumakov, P., Addison, C., Struzbecher, H.W. (1985). The cellular oncogene p53 can be activated by mutagenesis. *Nature* **317**, 816-818.

Jiang, H., Lin, J., Su, Z.Z., Herlyn, M., Kerbel, R.S., Weissman, B.E., Welch, D.R., Fisher, P.B. (1995). The melanoma differentiation-associated gene mda-6, which encodes the cyclin-dependent kinase inhibitor p21, is differentially expressed during growth, differentiation and progression in human melanoma cells. *Oncogene* **10**, 1855-1864.

Jiang, M., Shao, Z.M., Wu, J., Lu, J.S., Yu, L.M., Yuan, J.D., Han, Q.X., Shen, Z.Z., Fontana, J.A. (1997). p21/waf1/cip1 and mdm-2 expression in breast carcinoma patients as related to prognosis. *Int. J. Cancer* **74**, 529-34.

Jimenez, G.S., Khan, S.H., Stommel, J.M., Wahl, G.M. (1999) p53 regulation by post-translational modification and nuclear retention in response to diverse stresses. *Oncogene* **18**, 7656-7665.

Joliot, A. & Prochiantz, A. (2004). Transduction peptides: from technology to physiology. *Nat. Cell Biol.* **6**, 189-196.

Jones, S.N., Roe, A.E., Donehower, L.A., Bradley, A. (1995). Rescue of embryonic lethality in Mdm2-deficient mice by absence of p53. *Nature* **378**, 206-208.

Jones, R.G., Plas, D.R., Kubek, S., Buzzai, M., Mu, J., Xu, Y., Birnbaum, M.J., Thompson, C.B. (2005). AMP-activated protein kinase induces a p53-dependent metabolic pathway. *Mol. Cell* **18**, 283-293.

Ju, R. & Muller, M.T. (2003). Histone deacetylase inhibitors activate p21^{WAF1} expression via ATM. *Cancer Res.* **63**, 2891-2897.

Kannan, K., Amariglio, N., Rechavi, G., Jakob-Hirsch, J., Kela, I., Kaminski, N., Getz, G., Domany, E., Givol, D. (2001) DNA microarrays identification of primary and secondary target genes regulated by p53. *Oncogene* **20**, 2225-2234.

Kapranos, N., Stathopoulos, G.P., Manolopoulos, L., Kokka, E., Papadimitriou, C., Bibas, A., Yiotakis, J., Adamopoulos, G. (2001). p53, p21 and p27 protein expression in head and neck cancer and their prognostic value. *Anticancer Res.* **21**, 521-8.

Kartasheva, N.N., Contente, A., Lenz-Stöppler, C., Roth, J., Dobbelstein, M. (2002). p53 induces the expression of its antagonist p73 Delta N, establishing an autoregulatory feedback loop. *Oncogene* **21**, 4715-4727.

Kastan, M.B., Onyekwere, O., Sidransky, D., Vogelstein, B., Craig, R. W. (1991). Participation of p53 protein in the cellular response to DNA damage. *Cancer Res.* **51**, 6304-6311.

Kastan, M.B. & Bartek, J. (2004). Cell-cycle checkpoints and cancer. *Nature* **432**, 316-323.

Khanna, K.K., Lavin, M.F., Jackson, S.P. Mulhern, T.D. (2001). ATM, a central controller of cellular responses to DNA damage. *Cell Death Diff.* **8**, 1052-1065.

Khosravi, R, Maya, R, Gottlieb, T, Oren, M, Shiloh, Y and Shkedy, D. (1999). Rapid ATM-dependent phosphorylation of MDM2 precedes p53 accumulation in response to DNA damage. *Proc. Natl. Acad. Sci. USA* **96**, 14973-14977.

Kidokoro, T., Tanikawa, C., Furukawa, Y., Katagiri, T., Nakamura, Y., Matsuda, K. (2007). CDC20, a potential cancer therapeutic target, is negatively regulated by p53. *Oncogene* [Epub ahead of print]

Kim, J.M, Sohn, H.Y., Yoon, S.Y., Oh, J.H., Yang, J.O., Kim, J.H. *et al.* (2005). Identification of gastric cancer-related genes using a cDNA microarray containing novel expressed sequence tags expressed in gastric cancer cells. *Clin. Cancer Res.* **11**, 473-482.

Kitaura, H., Shinshi, M., Uchikoshi, Y., Ono, T. Tsurimoto, T., Yoshikawa, H., Iguchi-Arigo, S.M.M., Ariga, H. (2000). Reciprocal regulation via protein-protein interaction between c-Myc and p21(cip1/waf1/sdi1) in DNA replication and transcription. *J. Biol. Chem.* **275**, 10477-10483.

Kitayner, M., Rozenberg, H., Kessler, N., Rabinovich, D., Shaulov, L., Haran, T.E., Shakked, Z. (2006). Structural basis of DNA recognition by p53 tetramers. *Mol. Cell* **22**, 741-753.

Ko, L.J. & Prives, C. (1996). p53: puzzle and paradigm. *Genes Dev.* **10**, 1054-1072.

Komiya, T., Hosono, Y., Hirashima, T., Masuda, N., Yasumitsu, T., Nakagawa, K., Kikui, M., Ohno, A., Fukuoka, M., Kawase, I. (1997). p21 expression as a predictor for favourable prognosis in squamous cell carcinoma of the lung. *Clin. Cancer Res.* **3**, 1831-1835.

Kortlever, R.M., Higgins, P.J., Bernards, R. (2006). Plasminogen activator inhibitor-1 is a critical downstream target of p53 in the induction of replicative senescence. *Nat. Cell Biol.* **8**, 878-884.

Koumenis, C., Alarcon, R., Hammond, E., Sutphin, P., Hoffman, W., Murphy, M., Derr, J., Taya, Y., Lowe, S.E., Kastan, M., Giaccia, A. (2001). Regulation of p53 by hypoxia: Dissociation of transcriptional repression and apoptosis from p53-dependent transcription. *Mol. Cell Biol.* **21**, 1297-1310.

Kovlov, S.V., Graham, M.E., Peng, C., Chen, P., Robinson, P.J., Lavin, M.F. (2006). Involvement of novel autophosphorylation sites in ATM activation. *EMBO J.* **25**, 3504-3514.

Kriwacki, R.W., Hengst, L., Tennant, L., Reed, S.I., Wright, P.E. (1996). Structural studies of p21Waf1/Cip1/Sdi1 in the free and Cdk2-bound state: conformational disorder mediates binding diversity. *Proc. Natl. Acad. Sci. USA* **93**, 11504-11509.

Krummel, K.A., Lee, C.J., Toledo, F., Wahl, G.M. (2005). The C-terminal lysines fine-tune p53 stress responses in a mouse model but are not required for stability control or transactivation. *Proc. Natl. Acad. Sci. USA* **102**, 10188-10193.

Kruz, E.U & Lees-Miller, S.P. (2004). DNA damage-induced activation of ATM and ATM-dependent signaling pathways. *DNA Repair* **3**, 889-900.

Kubbutat, M.H., Jones, S.N., Vousden, K.H. (1997). Regulation of p53 stability by Mdm2. *Nature* **387**, 299-303.

Kuo, M.H. & Allis, C.D. (1998). Roles of histone acetyltransferases and deacetylases in gene regulation. *Bioessays* **20**, 615-626.

Kussie, P.H., Gorina, S., Marechal, V., Elenbaas, B., Moreau, J., Levine, A.J. *et al.* (1996). Structure of the MDM2 oncoprotein bound to the p53 tumour suppressor transactivation domain. *Science* **274**, 948-953.

Laherty, C., Yang, W-M., Sun, J-M., Davie, J.R., Seto, E., Eisenman, R.N. (1997). Histone deacetylases associated with mSin3 co-repressor mediate mad transcriptional repression. *Cell* **89**, 349-456.

Laine, A. & Ronai, Z. (2007). Regulation of p53 localisation and transcription by HECT domain E3 ligase WWP1. *Oncogene* **26**, 1477-1483.

Lakin, N.D., Weber, P., Stankovic, T., Rottinghaus S.T., Taylor, A.M., Jackson, S.P. (1996). Analysis of the ATM protein in wild-type and ataxia telangiectasia cells. *Oncogene* **13**, 2707-2716.

Lakin, N.D. & Jackson, S.P. (1999). Regulation of p53 in response to DNA damage. *Oncogene* **18**, 7644-7655.

Lane, D.P. & Crawford, L.V. (1979). T antigen is bound to a host protein in SV40-transformed cells. *Nature* **278**, 261-263.

Lane, D.P. & Hupp, T.R. (2003). Drug Discovery and p53. *Drug Discovery Today* **8**, 347-355

Lane, D.P. (1992). Cancer. p53, guardian of the genome. *Nature* **358**, 15-16.

Laptenko, O. & Prives, C. (2006). Transcriptional regulation by p53:one protein, many possibilities. *Cell Death Differ.* **13**, 951-961.

Lau, A., Swinbank, K.M., Ahmed, P.S., Taylor, D.L., Jackson, S.P., Smith, G.C.M., O'Connor, M. (2005). Suppression of HIV-1 infection by a small molecule inhibitor of the ATM kinase. *Nat. Cell Biol.* **7**, 493-500.

Lavin, M.F. & Shiloh, Y. (1997). The genetic defect in ataxia-telangiectasia. *Annu. Rev. Immunol.* **15**, 177-202.

Le, H-V., Minn, A.J., Massagué, J. (2005). Cyclin-dependent kinase inhibitors uncouple cell cycle progression from mitochondrial apoptotic functions in DNA-damaged cancer cells. *J. Biol. Chem.* **280**, 32018-32025.

Leahy, J.J.J., Golding, B.T., Griffin, R.J., Hardcastle, I.R., Richardson, C., Rigoreau, L., Smith, G.C.M. (2004). Identification of a highly potent and selective DNA-dependent protein kinase (DNA-PK) inhibitor (NU7441) by screening of chromenone libraries. *Bioorg. Med. Chem. Lett.* **14**, 6083-6087.

Legube, G., Linares, L.K., Tyteca, S., Caron, C., Scheffner, M., Chevillard-Briet, M., Trouche, D. (2004). Role of the histone acetyltransferase Tip60 in the p53 pathway. *J. Biol. Chem.* **279**, 44825-44833.

Leng, R.P., Lin, Y., Ma, W., Wu, H., Lemmers, B., Chung, S., Parant, J. M., Lozano, G., Hakem, R., Benchimol, S. (2003). Pirh2, a p53-induced ubiquitin-protein ligase, promotes p53 degradation. *Cell* **112**, 779-791.

Leu, J.I., Dumont, P., Hafey, M., Murphy, M.E., George, D.L. (2004). Mitochondrial p53 activates Bak and causes disruption of a Bak-Mcl1 complex. *Nat. Cell Biol.* **6**, 443-450.

Lev Bar-Or, R., Maya, R., Segel, L.A., Alon, U., Levine, A.J., Oren, M. (2000). Generation of oscillations by the p53-Mdm2 feedback loop: a theoretical and experimental study. *Proc. Natl. Acad. Sci. USA* **97**, 11250-11255.

Levine, A.J., Momand, J., Finlay, C.A. (1991). The p53 tumour suppressor gene. *Nature* **351**, 453-456.

Levine, A.J. (1997). p53, the cellular gatekeeper for growth and division. *Cell* **88**, 323-331.

Li, Y., Jenkins, C.W., Nichols, M.A., Xiong, Y. (1994a). Cell cycle expression and p53 regulation of the cyclin-dependent kinase inhibitor p21. *Oncogene* **9**, 2261-2268.

Li, R., Waga, S., Hannon, G.J., Beach, D., Stillman, B. (1994b). Differential effects by the p21 CDK inhibitor on PCNA-dependent DNA replication and repair. *Nature* **371**, 534-537.

Li, C.Y., Suardet, L., Little, J.B. (1995). Potential role of WAR1/Cip1/p21 as a mediator of TGF-beta cytoinhibitory effect. *J. Biol. Chem.* **270**, 4971-4974.

Li, Y., Dowbenko, D., Lasky, L.A. (2002a). AKT/PKB phosphorylation of p21 Cip/WAF1 enhances protein stability of p21 Cip/WAF1 and promotes cell survival. *J. Biol. Chem.* **277**, 11352-11361.

Li, M. Chen, D., Shiloh, A., Luo, J., Nikolaev, A.Y., Qin, J., Gu, W. (2002b). Deubiquitination of p53 by HAUSP is an important pathway for p53 stabilisation. *Nature* **416**, 648-653.

- Li, M., Brooks, C.L., Wu-Baer, F., Chen, D., Baer, R., Gu, W. (2003). Mono- versus polyubiquitination: differential control of p53 fate by Mdm2. *Science* **302**, 1972-1975.
- Lill, N.L., Grossman, S.R., Ginsberg, D., DeCaprio, J., Livingston, D.M. (1997). Binding and modulation of p53 by p300/CBP coactivators. *Nature* **387**, 823-827.
- Lim D., Kirsch, D.G., Canman, C.E., Ahn, J.H., Ziv, Y., Newman, L.S., Darnell, R.B., Shiloh, Y., Kastan, M.B. (1998). ATM binds to β -adapin in cytoplasmic vesicles. *Proc. Natl. Acad. Sci. USA* **95**, 10146-10151.
- Lin, X., Ramamurthi, K., Mishima, M., Kondo, A., Christen, R.D., Howell, S.B. (2001). p53 modulates the effect of loss of DNA mismatch repair on the sensitivity of human colon cancer cells to the cytotoxic and mutagenic effects of cisplatin. *Cancer Res.* **61**, 1508-1516.
- Lin, Y., Waldman, B.C., Waldman, A.S. (2003). Suppression of high-fidelity double-strand break repair in mammalian chromosomes by pifithrin- α , a chemical inhibitor of p53. *DNA Repair* **2**, 1-11.
- Lipponen, P., Aaltomaa, S., Eskelinen, M., Ala-Opas, M., Kosma, V.M. (1998). Expression of p21(waf1/cip1) protein in transitional cell bladder tumours and its prognostic value. *Eur. Urol.* **34**, 237-243.
- Liu, Y., Martindale, J.L., Gorospe, M., Holbrook, N.J. (1996a). Regulation of p21 WAF/CIP1 expression through mitogen activated protein kinase signalling pathway. *Cancer Res.* **56**, 31-35.
- Liu, M., Iavarone, A., Feedman, L.P. (1996b). Transcriptional activation of the human p21 (WAF1/CIP1) gene by retinoic acid receptor. Correlation with retinoid induction of U937 cell differentiation. *J. Biol. Chem.* **271**, 31723-31728.
- Liu, S., Robert Bishop, W., Liu, M. (2003). Differential effects of cell cycle regulatory protein p21^{WAF1/CIP1} on apoptosis and sensitivity to cancer chemotherapy. *Drug Resist. Updat.* **6**, 183-195.
- Loeb, L.A., Springgate, C.F., Battula, N. (1974). Errors in DNA replication as a basis in malignant changes. *Cancer Res.* **34**, 761-763.

Löhr, K., Möritz, C., Contente, A., Dobbelstein, M. (2003). p21/CDKN1A mediates negative regulation of transcription by p53. *J. Biol. Chem.* **278**, 32507-32516.

Lohrum, M.A., Woods, D.B., Ludwig, R.L., Balint, E., Vousden, K.H. (2001). C-terminal ubiquitination of p53 contributes to nuclear export. *Mol. Cell Biol.* **21**, 8521-8532.

Lomax, M.E., Barnes, D.M., Hupp, T.R., Picksley, S.M., Campjohn, R.S. (1998). Characterization of p53 oligomerization domain mutations isolated from Li-Fraumeni and Li-Fraumeni like family members. *Oncogene* **17**, 643-649.

Louria-Hayon, I., Grossman, T., Sionov, R.V., Alsheich, O., Panodolfi, P.P., Haupt, Y. (2003). The promyelocytic leukaemic protein protects p53 from MDM2 mediated inhibition and degradation. *Biol. Chem.* **278**, 33134-33141.

Lowe, S.W., Cepero, E., Evan, G. (2004). Intrinsic tumour suppression. *Nature* **432**, 307-315.

Lu, H. & Levine, A.J. (1995). Human TAFII31 protein is a transcriptional coactivator of the p53 protein. *Proc. Natl. Acad. Sci. USA* **92**, 5154-5158.

Lu, X., Toki, T., Konishi, I., Nikaido, T., Fujii, S. (1998). Expression of p21WAF1/CIP1 in adenocarcinoma of the uterine cervix: a possible immunohistochemical marker of a favourable prognosis. *Cancer* **82**, 2409-17.

Luger, K., Mader, A.W., Richmond, R.K., Sargent, D.F., Richmond, T.J. (1997). Crystal structure of the nucleosome core particle at 2.8 Å resolution. *Nature* **389**, 251-260.

Luo, Y., Lin, F.T., Lin, W.C. (2004). ATM-mediated stabilisation of hMutL DNA mismatch repair proteins augments p53 activation during DNA damage. *Mol. Cell Biol.* **24**, 6430-6444.

MacLachlan, T.K., Dash, B.C., Dicker, D.T., El-Diery, W.S. (2000). Repression of BRCA1 through a feedback loop involving p53. *J. Biol. Chem.* **275**, 31869-31875.

Macleod, K.F., Sherry, N., Hannon, G., Beach, D., Tokino, T., Kinzler, K., Vogelstein, B., Jacks, T. (1995). p53-dependent and independent expression of p21 during cell growth, differentiation, and DNA damage. *Genes Dev.* **9**, 935-944.

MacPherson, D., Kim, J., Kim, T., Rhee, B.K., Van Oostrom, C.T., DiTullio, R.A., Venere, M., Halazonetis, T.D., Bronson, R., De Vries, A., Fleming, M., Jacks, T. (2004). Defective apoptosis and B-cell lymphomas in mice with p53 point mutation at Ser 23. *EMBO J.* **23**, 3689-3699.

Maki, C.G. & Howley, P.M. (1997). Ubiquitination of p53 and p21 is differentially affected by ionising radiation and UV radiation. *Mol. Cell Biol.* **17**, 355-363.

Malkin, D., Li, F.P., Strong, L.C., Fraumini, Jr. J.F., Nelson, C.E., Kim, D.H., *et al.* (1990). Germ line p53 mutations in familial syndrome of breast cancer, sarcomas, and other neoplasms. *Science* **250**, 1233-1238.

Maltzman, W. & Czyzyk, L. (1984). UV irradiation stimulates levels of p53 cellular tumour antigen in nontransformed mouse cells. *Mol. Cell Biol.* **4**, 1689-1694.

Manning, A.T., Garvin, J.T., Shahbazi, N., Miller, R.E., McNeill, R.E., Kerin, M.J. (2007). Molecular profiling techniques and bioinformatics in cancer research. *EJSO.* **33**, 255-265.

Marches, R., Hsueh, R., Uhr, J.W. (1999). Cancer dormancy and cell signaling: induction of p21 (waf1) initiated by membrane IgM engagement increases the survival of B-lymphoma cells. *Proc. Natl. Acad. Sci. USA* **96**, 8711-8715.

Martin-Caballero, J., Flores, J. M., Garcia-Palencia, P., Serrano, M. (2001). Tumor susceptibility of p21 (Waf1/Cip1)- deficient mice. *Cancer Res.* **61**, 6234-6238.

Martinez, L.A., Yang, J., Vazquez, E.S., Rodriguez-Vargas, M.D.C., Olive, M., Hsieh, J-T., Logothetis, C.J., Navone, N.M. (2002). p21 modulates the threshold of apoptosis induced by DNA damage and growth factor withdrawal in prostate cancer cells. *Carcinogenesis* **23**, 1289-1296.

Marchenko, N.D., Zaika, A., Moll, U.M. (2000). Death signal-induced localisation of p53 protein to the mitochondria: a potential role in apoptotic signalling. *J. Biol. Chem.* **275**, 16202-16212.

Matoba, S., Kang, J.G., Patino, W.D., Wragg, A., Boehm, M., Gavrillova, O., Hurley, P.J., Bunz, F., Hwang, P.M. (2006). p53 regulates mitochondrial metabolism. *Science* **312**, 1650-1653.

Matsumura, I., Ishikawa, J., Nakajima, K., Oritani, K., Tomiyama, Y., Miyagawa, J., Kato, T., Miyazaki, H., Matsuzawa, Y., Kanakura, Y. (1997). Thrombopoietin-induced differentiation of a human megakaryoblastic leukemia cell line, CMK, involves transcriptional activation of p21(WAF1/Cip1) by STAT5. *Mol. Cell Biol.* **17**, 2933-2943.

Matsuoka, S., Rotman, G., Ogawa, A., Shiloh, Y., Tamai, K., Elledge, S. J. (2000). Ataxia telangiectasia mutated phosphorylates Chk2 *in vivo* and *in vitro*. *Proc. Natl. Acad. Sci. USA* **97**, 10389-10394.

Matsuoka, S., Ballif, B.A., Smogorzewska, A., McDonald, E.R. III, Hurov, K.E., Luo, J., Bakalarski, C.E., Zhao, Z., Solimini, N., Lerenthal, Y., Shiloh, Y., Gygi, S.P., Elledge, S.J. (2007). ATM and ATR substrate analysis reveals extensive protein networks responsive to DNA damage. *Science* **316**, 1160-1166.

May, P. & May, E. (1999). Twenty years of p53 research: Structural and functional aspects of the p53 protein. *Oncogene* **18**, 7621-7636.

Maya, R., Balass, M., Kim, S.T., Shkedy, D., Leal, J.F., Shifman, O., Moas, M., Buschmann, T., Ronai, Z., Shiloh, Y., Kastan, M.B., Katzir, E., Oren, M. (2001). ATM-dependent phosphorylation of Mdm2 on serine 395: role in p53 activation by DNA damage. *Genes Dev.* **15**, 1067-1077.

Mayher-Roemer, M., Roemer, K. (2001). p21 Waf1/Cip1 can protect human colon carcinoma cells against p53-dependent and p53-independent apoptosis induced by natural chemopreventive and therapeutic agents. *Oncogene* **20**, 3387-3398.

McBride, O.W., Merry, D., Givol, D. (1986). The gene for human p53 cellular tumour antigen is located on chromosome 17 short arm (17p13). *Proc. Natl. Acad. Sci. USA* **83**, 130-134.

Meek, D.W. (2004). The p53 response to DNA damage. *DNA Repair* **3**, 1049-1056.

Michor, F., Iwasa, Y., Nowark, M.A. (2004). Dynamics of cancer progression. *Nat. Rev. Can.* **4**, 197-205.

Miller, S.D., Moses, K., Jayaraman, L., Prives, C. (1997). Complex formation between p53 and replication protein A inhibits the sequence-specific DNA binding of p53 and is regulated by single- stranded DNA. *Mol. Cell Biol.* **17**, 2194-2201.

Miller, F.D., Pozniak, C.D., Walsh, G.S. (2000). Neuronal life and death: an essential role of for the p53 family. *Cell Death Differ.* **7**, 880-888.

Miyashita, T. & Reed, J.C. (1995). Tumor suppressor p53 is a direct transcriptional activator of the human bax gene. *Cell* **80**, 293-299.

Moll, U.M., Riou, G., Levine, A.J. (1992). Two distinct mechanisms alter p53 in breast cancer: mutation and nuclear exclusion. *Proc. Natl. Acad. Sci. USA* **15**, 7262-7266.

Moll, U.M., LaQuaglia, M., Bénard, J., Riou, G. (1995). Wild-type p53 protein undergoes cytoplasmic sequestration in undifferentiated neuroblastomas but not in differentiated tumours. *Proc. Natl. Acad. Sci. USA* **92**, 4407-4411.

Moll, U.M., Ostermeyer, A.G., Haladay, R., Winkfield, B., Frazier, M., Zambetti, G. (1996). Cytoplasmic sequestration of wild-type p53 protein impairs the G1 checkpoint after DNA damage. *Mol. Cell Biol.* **16**, 1126-1137.

Moll, U.M. & Petrenko, O. (2003). The MDM2-p53 interaction. *Mol. Cancer Res.* **1**, 1001-1008.

Moll, U.M., Wolff, S., Speidel, D., Deppart, W. (2005). Transcription-independent pro-apoptotic functions of p53. *Curr. Opin. Cell Biol.* **17**, 631-636.

Moll, U.M., Marchenko, N., Zhang, X-k., (2006). p53 and Nur77/TR3 - transcription factors that directly target the mitochondria for cell death induction. *Oncogene* **25**, 4725-4743.

Mondal, G., Sengupta, S., Panda, C.K., Gollin, S.M., Saunders, W.S., Roychoudhury, S. (2007). Overexpression of Cdc20 leads to impairment of the spindle assembly checkpoint and aneuploidization in oral cancer. *Carcinogenesis* **28**, 81-92.

Müller, H., Bracken, A.P., Vernell, R., Moroni, M.C., Christians, F., Grassilli, E., Prosperini, E., Vigo, E., Oliner, J.D., Helin, K. (2001). E2Fs regulate the expression of genes involved in differentiation, development, proliferation, and apoptosis. *Genes Dev.* **15**, 267-285.

Murphy, M., Ahn, J., Walker, K.K., Hoffman, W.H., Evans, R.M., Levine, A.J., George, D.L. (1999). Transcriptional repression by wild-type p53 utilizes histone deacetylases, mediated by interaction with mSin3a. *Genes Dev.* **13**, 2490-2501.

Nigro, J.M., Sikorski, R., Reed, R.I., Vogelstein, B. (1992). Human p53 and CDC2Hs genes combine to inhibit the proliferation of *saccharomyces-cerevisiae*. *Mol. Cell Biol.* **12**, 1357-1365.

Noda, A., Ning, Y., Venable, S.F., Pereira-Smith, O.M., Smith, J.R. (1994). Cloning of senescent cell-derived inhibitors of DNA synthesis using an expression screen. *Exp. Cell Res.* **211**, 90-98.

Nurse, P. (1990). Universal control mechanism regulating the onset of M-phase. *Nature* **344**, 503-508.

O' Brate, A. & Giannakakou, P. (2003). The importance of p53 nuclear localisation: nuclear or cytoplasmic zip code? *Drug Resist. Updat.* **6**, 313-322.

Ocker, M. & Schneider-Stock, R. (2007). Histone deacetylase inhibitors: Signalling towards p21cip1/waf1. *Int. J. Biochem. Cell Biol.* **39**, 1367-1374.

Ogawa, M., Maeda, K., Onoda, N., Chung, Y.S., Sowa, M. (1997). Loss of p21WAF1/CIP1 expression correlates with disease progression in gastric carcinoma. *Br. J. Cancer* **75**, 1617-20.

Olivier, M., Goldgar, D.E., Sodha, N., Ohgaki, H., Kleiheus, P., Hainaut, P., Eeles, R.A. (2003). Li-Fraumeni and related syndromes: correlations between tumour type, family structure, and TP53 genotype. *Cancer Res.* **63**, 6643-6650.

Oren, M. & Levine, A.J. (1983). Molecular cloning of a cDNA specific for the murine p53 cellular tumour antigen. *Proc. Natl. Acad. Sci. USA* **80**, 56-59.

Ostermeyer, A.G., Runko, E., Winkfield, B., Ahn, B., Moll, U.M. (1996) Cytoplasmically sequestered wild-type p53 protein in neuroblastoma is relocated to the nucleus by a C-terminal peptide. *Proc. Natl. Acad. Sci. USA* **93**, 15190-15194.

Pantoja, C. & Serrano, M. (1999). Murine fibroblasts lacking p21 undergo senescence and are resistant to transformation by oncogenic Ras. *Oncogene* **18**, 4974-4982.

Papp, T., Jafari, M., Schiffmann, D. (1996). Lack of p53 mutations and loss of heterozygosity in non-cultured human melanocytic lesions. *J. Cancer Res. Clin. Oncol.* **122**, 541-8.

Passalaris, T.M., Benanti, J.A., Gewin, L., Kiyono, T., Galloway, D.A. (1999). The G(2) checkpoint is maintained by redundant pathways. *Mol. Cell Biol.* **19**, 5872-5881.

Pearson, M., Carbone, R., Sebastiani, C., Cioce, M., Fagioli, M., Saito, S., Higashimoto, Y., Appella, E., Minucci, S., Pandolfi, P.P., Pelicci, P.G. (2000). PML regulates p53 acetylation and premature senescence induced by oncogenic Ras. *Nature* **406**, 207-210.

Perkins, N.D. Felzien, L., Betts, J.C., Leung, K., Beach, D.H., Nabel, G.J. (1997). Regulation of NF-KappaB by cyclin dependent kinases associated with the p300 co-activator. *Science* **275**, 523-527.

Perkins, N.D. (2002). Not just a CDK inhibitor: Regulation of transcription by p21^{WAF1/CIP1/SDI1}. *Cell Cycle* **1**, 39-41.

Perry, J. & Kleckner, N. (2003). The ATRs, ATMs, and mTORs are giant HEAT repeat proteins. *Cell* **112**, 151-155.

Plaster, N., Sonntag, C., Busse, C.E., Hammerschmidt, M. (2006). p53 deficiency rescues apoptosis and differentiation of multiple cell types in zebrafish flathead mutants deficient for zygotic DNA polymerase $\delta 1$. *Cell Death Differ.* **13**, 223-235.

Plescia, J., Salz, W., Xia, F., Pennati, M., Zaffaroni, N., Daidone, M.G., Meli, M., Dohi, T., Fortugno, P., Nefedova, Y. *et al.* (2005). Rational design of shepherdin, a novel anticancer agent. *Cancer Cell* **7**, 457-468.

Plomin, R. & Schalkwyk, L.C. (2007). Microarrays. *Dev. Sci.* **10**, 19-23.

Podust, V.N., Podust, L.M., Goubin, F., Ducommun, B., Hubscher, U. (1995). Mechanism of inhibition of proliferating cell nuclear antigen-dependent DNA synthesis by the cyclin-dependent kinase inhibitor p21. *Biochemistry* **34**, 8869-8875.

Ponten, F., Berne, B., Ren, Z.P., Nister, M., Ponten, J. (1995). Ultraviolet light induces expression of p53 and p21 in human skin: effect of sunscreen and constitutive p21 expression in skin appendages. *J. Invest. Dermatol.* **105**, 402-406.

Price, B.D. & Youmell, M.B. (1996). The phosphatidylinositol 3-kinase inhibitor wortmannin sensitises murine fibroblasts and humour tumour cells to radiation and blocks induction of p53 following DNA damage. *Cancer Res.* **56**, 246-250.

Privé, G.G. Melnick, A. (2006). Specific peptides for the therapeutic targeting of oncogenes. *Curr. Opin. Genet. Dev.* **16**, 71-77.

Purdie, C.A., Harrison, D.J., Peter, A., Dobbie, L., White, S., Howie, S.E., Salter, D.M., Bird, C.C., Wyllie, A.H., Hooper, M.L. *et al.* (1994). Tumour incidence, spectrum and ploidy in mice with a large deletion in the p53 gene. *Oncogene* **9**, 603-9.

Qu, L., Huang S., Baltzis, D., Rivas-Estilla, A.M., Pluquet, O., Hatzoglou, M., Koumenis, C., Taya, Y., Yoshimura, A., Koromilas, E.S. Endoplasmic reticulum stress induces p53 cytoplasmic localization and prevents p53-dependent apoptosis by a pathway involving glycogen synthase kinase-3beta. (2004). *Genes Dev.* **18**, 261-277.

Radhakrishnan, S.K., Feliciano, C.S., Najmabadi, F., Haegrbarth, A., Kandel, E.S., Tyner, A.L., Gartel, A.L. (2004). Constitutive expression of E2F-1 leads to p21-dependent cell cycle arrest in S phase of the cell cycle. *Oncogene* **23**, 4173-4176.

Radhakrishnan, S.K., Gierut, J., Gartel, A.L. (2006). Multiple alternative p21 transcripts are regulated by p53 in human cell. *Oncogene* **25**, 1812-1815.

Rahman-Roblick, R., Roblick, U.J., Hellman, U., Conrotto, P., Liu, T., Becker, S., Hirschberg, D., Jörnvall, H., Auer, G., Wiman, K.G. (2007). p53 targets identified by protein expression profiling. *Proc. Natl. Acad. Sci. USA* **104**, 5401-5406.

Ramondetta, L., Mills, G.B., Burke, T.W., Wolf, J.K. (2000). Adenovirus-mediated expression of p21 and p53 in a papillary serous endometrial carcinoma cell line (SPEC-2) results in both growth inhibition and apoptotic cell death: potential application of gene therapy to endometrial cancer. *Clin. Cancer Res.* **6**, 278-284.

Raveh, T., Droguett, G., Horwitz, M.S., DePinho, R.A., Kimchi, A. (2001). DAP kinase activates a p19ARF/p53-mediated apoptotic checkpoint to suppress oncogenic transformation. *Nat. Cell Biol.* **3**, 1-7.

Rhodes, D.R. & Chinnaiyan, A.M. (2005). Integrative analysis of the cancer transcriptome. *Nat. Genet.* **37**, S31-S37.

Rocha, S., Martin, A.M., Meek, D.W., Perkins, N.D. (2003). p53 represses cyclin D1 transcription through down regulation of Bcl-3 and inducing increased association of the p52 NF-kappaB subunit with histone deacetylase 1. *Mol Cell Biol.* **23**, 4713-4727.

Rodriguez, M.S., Desterro, J.M., Lain, S., Lane, D.P., Hay, R.T. (2000). Multiple C-terminal lysine residues target p53 for ubiquitin-proteasome-mediated degradation. *Mol. Cell Biol.* **20**, 8458-8467.

Rodriguez-Vilarrupa, A., Diaz, C., Canela, N., Rahn, H.P., Bachs O., Agell, N. (2002). Identification of the nuclear localisation signal of p21(cip1) and consequences of its mutation on cell proliferation. *FEBS Lett.* **531**, 319-323.

Rogakou, E.P., Pilch, D.R., Orr, A.H., Ivanova, V.S., Bonner, W.M. (1998). DNA double strand breaks induce histone H2AX phosphorylation on serine 139. *J. Biol. Chem.* **273**, 5858-5868.

Roninson, I.B. (2002). Oncogenic functions of tumour suppressor p21 Waf1/Cip1/Sdi1: association with cell senescence and tumour-promoting activities of stromal fibroblasts. *Cancer Lett.* **179**, 1-14.

Roth, J.A. (2006). Adenovirus p53 gene therapy. *Expert Opin. Biol. Ther.* **6**, 55-61.

Roth, D.M., Moseley, G.W., Glover, D., Pouton, C.W., Jans, D.A. (2007). A microtubule-facilitated nuclear import pathway for cancer regulatory proteins. *Traffic* **8**, 673-686.

Rozan, L.M. & el-Deiry, W.S. (2007). p53 and downstream target genes and tumour suppression: a classical view in evolution. *Cell Death Differ.* **14**, 3-9.

Russo, A.A., Jeffrey, P.D., Patten, A.K., Massague, J., Pavletich, N.P. (1996). Crystal structure of the p27Kip1 cyclin-dependent-kinase inhibitor bound to the cyclin A-Cdk2 complex. *Nature* **382**, 325-331.

Saito, T., Oda Y, Kawaguchi, K., Takahira, T., Yamamoto, H., Sakamoto, A., Tamiya, S., Iwamoto, Y., Tsuneyoshi, M. (2003a). Possible association between tumour suppressor gene mutations and hMSH2/hMLH1 inactivation in alveolar soft part sarcoma. *Hum. Pathol.* **34**, 841-849.

Saito, S., Yamaguchi, H., Higashimoto, Y., Chao, C., Xu, Y., Fornace, A.J., Jr., Appella, E., Anderson, C. W. (2003b). Phosphorylation site interdependence of human p53 post-translational modifications in response to stress. *J. Biol. Chem.* **278**, 37536-37544.

Sakaguchi, K., Sakamoto, H., Xie, D., Erickson, J.W., Lewis, M.S., Anderson, C.W., Appella, E. (1997). Effect of phosphorylation on tetramerisation of the tumour suppressor protein p53. *J. Protein Chem.* **16**, 553-556.

Samuels-Lev, Y., O'Connor, D.J., Bergamaschi, D., Trigiante, G., Hsieh, J.K., Zhong, S., Campargue, I., Naumovski, L., Crook, T., Lu, X. (2001). ASPP proteins specifically stimulate the apoptotic function of p53. *Mol. Cell* **8**, 781-794.

Sarkaria, J.N., Tibbets, R.S., Busby, E.C., Kennedy, A.P., Hill, D.E., Abraham, R.T. (1998). Inhibition of the Phosphoinositide 3-kinase related kinases by the radiosensitising agent wortmannin. *Cancer Res.* **58**, 4375-4382.

Sarkaria, J.N., Busby, E.C., Tibbets, R.S., Roos, P., Taya, Y., Karnitz, L.M., Abraham, R.T. (1999). Inhibition of ATM and ATR kinase activities by the radiosensitising agent, caffeine. *Cancer Res.* **59**, 4375-4382.

Sarnow, P., Ho, Y.S., Williams, J., Levine, A.J. (1982). Adenovirus E1b 58kd tumor antigen and SV40 large tumour antigen are physically associated with the same 54kd cellular protein in transformed cells. *Cell* **28**, 387-394.

Scheffner, M., Werness, B.A., Huibregtse, J.M., Levine, A.J., Howley, P.M. (1990). The E6 oncoprotein encoded by human papillomavirus types 16 and 18 promotes the degradation of p53. *Cell* **63**, 1129-1136.

Scherer, S.J., Maier, S.M., Seifert, M., Hanselmann, R.G., Zang, K.D., Muller-Hermelink, H.K., Angel, P., Welter, C., Scharl, M. (2000). p53 and c-Jun functionally synergise in the regulation of the DNA repair gene hMSH2 in response to UV. *J. Biol. Chem.* **275**, 37469-37473.

Scolnick, D.M., Chehab, N.H., Stavridi, E.S., Lien, M.C., Caruso, L., Moran, E., Berger, S.L., Halazonetis, T.D. (1997). CREB-binding protein and p300/CBP-associated factor are transcriptional coactivators of the p53 tumor suppressor protein. *Cancer Res.* **57**, 3693-3696.

Scott, M.T., Morrice, N., Ball, K.L. (2000). Reversible phosphorylation at the C-terminal regulatory domain of p21(Waf1/Cip1) modulates proliferating cell nuclear antigen binding. *J. Biol. Chem.* **275**, 11529-11537.

Scott, M.T., Ingram, A., Ball, K.L. (2002). PDK1-dependent activation of atypical PKC leads to degradation of the p21 tumour modifier protein. *EMBO. J.* **21**, 6771-6780.

Seemann, S. & Hainaut, P. (2005). Roles of thioredoxin reductase 1 and APE/Ref-1 in the control of basal p53 stability and activity. *Oncogene* **24**, 3853-3863.

Shaulsky, G., Goldfinger, N., Ben-Ze'ev, A., Rotter, V. (1990a). Nuclear accumulation of p53 protein is mediated by several nuclear localization signals and plays a role in tumorigenesis. *Mol. Cell Biol.* **10**, 6565-6577.

Shaulsky, G., Ben-Ze'ev, A., Rotter, V. (1990b). Subcellular distribution of the p53 protein during the cell cycle of Balb/c 3T3 cells. *Oncogene* **5**, 1707-1711.

Shaulsky, G., Goldfinger, N., Tosky, M.S., Levine, A.J., Rotter, V. (1991). Nuclear localization is essential for the activity of p53 protein. *Oncogene* **6**, 2055-2065.

Shen, K.C., Heng, H., Wang, Y., Lu, S., Liu, G., Deng, C-X., Brooks, S.C., Wang, Y.A. (2005). ATM and p21 cooperate to suppress aneuploidy and subsequent tumour development. *Cancer Res.* **19**, 8747-8752.

Sherr, C.J. (2004). Principles of tumour suppression. *Cell* **116**, 235-246.

Sherr, C.J. (1994). G1 phase progression: Cycling on cue. *Cell* **79**, 551-555.

Shiloh, Y. (2003). ATM and related protein kinases: safeguarding genome integrity. *Nat. Rev. Can.* **3**, 155-168.

Shim, J., Lee, H., Park, J., Kim, H., Choi, E-J. (1996). A non-enzymatic p21 protein inhibitor of stress-activated protein kinases. *Nature* **381**, 804-807.

Shimizu, H., Saliba, D., Wallace, M., Finlan, L., Langridge-Smith, P. R., Hupp, T. R. (2006). Destabilizing missense mutations in the tumour suppressor protein p53 enhance its ubiquitination in vitro and in vivo. *Biochem. J.* **397**, 355-67.

Shiohara, M., el-Deiry, W.S., Wada, M., Nakamaki, T., Takeuchi, S., Yang, R., Chen, D.L., Vogelstein, B., Koefler, H. P. (1994). Absence of WAF1 mutations in a variety of human malignancies. *Blood* **84**, 3781-4.

Siliciano, J.D., Canman, C.E., Taya, Y., Sakaguchi, K., Appella, E., Kastan, M.B. (1997). DNA damage induces phosphorylation of the amino terminus of p53. *Genes Dev.* **11**, 3471-3481.

Singh, G. & Lykke-Andersen, J. (2003). New insights into the formation of active nonsense mediated decay complexes. *Trends Biochem. Sci.* **28**, 464-466.

Sluss, H.K., Armata, H., Gallant, J., Jones, J.N. (2004). Phosphorylation of serine-18 regulates distinct p53 functions in mice. *Mol. Cell Biol.* **24**, 976-984.

Smith, M.L., Kontny, H.U., Zhan, Q., Sreenath, A., O'Connor, P.M., Fornace, A.J. Jr. (1996). Antisense GADD45 expression results in decreased DNA repair and sensitises cells to UV irradiation or cisplatin. *Oncogene* **13**, 2255-2263.

Snowden, A.W. Anderson, L.A., Webster, G.A., Perkins, N.D. (2000). A novel transcriptional repression domain mediates p21 (WAF1/CIP1) induction of p300 transactivation. *Mol. Cell Biol.* **20**, 2676-2686.

Sohn, D., Essmann, F., Schulze-Osthoff, K., Jänicke, R.U. (2006). p21 blocks irradiation-induced apoptosis downstream of mitochondria by inhibition of cyclin-dependent kinase mediated caspase-9 activation. *Cancer Res.* **66**, 11254-11262.

Sogame, N., Kim, M., Abrams, J.M. (2003). Drosophila p53 preserves genomic stability by regulating cell death. *Proc. Natl. Acad. Sci. USA* **100**, 4696-4701.

Soussi, T., Caron de Fromentel, C., Mechali, M., May, P., Kress, M. (1987). Cloning and characterization of a cDNA from *Xenopus laevis* coding for a protein homologous to human and murine p53. *Oncogene* **1**, 71-78.

Soussi, T., Caron de Fromentel, C., May, P. (1990). Structural aspects of the p53 protein in relation to gene evolution. *Oncogene* **5**, 945-952.

Soussi, T & May, P. (1996). Structural aspects of the p53 protein in relation to gene evolution: A second look. *J. Mol. Biol.* **260**, 623-637.

Speir, E., Modali, R., Huang, E.S., Leon, M.B., Shawl, F., Finkel, T., Epstein, S.E. (1994). Potential role of human cytomegalovirus and p53 interaction in coronary restenosis. *Science* **265**, 391-394.

Stanley, J.S., Griffin, J.B., Zemleni, J., (2001). Biotinylation of histones in human cells. Effects of cell proliferation. *Eur. J. Biochem.* **268**, 5424-5429.

Steegenga, W.T., van Laar, T., Riteco, N., Mandarino, A., Shvarts, A., van der Eb, A.J., Jochemsen, A.G. (1996). Adenovirus E1A proteins inhibit activation of transcription by p53. *Mol. Cell Biol.* **16**, 2101-2109.

Stein, J. P., Ginsberg, D.A., Grossfeld, G.D., Chatterjee, S.J., Esrig, D., Dickinson, M.G., Groshen, S., Taylor, C.R., Jones, P.A., Skinner, D.G., Cote, R.J. (1998). Effect of p21WAF1/CIP1 expression on tumor progression in bladder cancer. *J. Natl. Cancer. Inst.* **90**, 1072-1079.

Stiff, T., Walker, S.A., Cersaletti, K., Goodarzi, A.A., Petermann, E., Concannon, P., O'Driscoll, M., Jeggo, P.A. (2006). ATR-dependent phosphorylation and activation of ATM in response to UV treatment or replication fork stalling. *EMBO J.* **25**, 5775-5782.

Stommel, J.M., Marchenko, N.D., Jimenez, G.S., Moll, U.M., Hope, T.J., Wahl, G.M. (1999). The leucine-rich nuclear export signal in the p53 tetramerisation domain: regulation of subcellular localization and p53 activity by NES masking. *EMBO J.* **18**, 1660-1672.

Stoughton, R.B. (2005). Applications of DNA microarrays in biology. *Annu. Rev. Biochem.* **74**, 53-82.

Sun, Y., Jiang, X., Chen, S., Fernandes, N., Price, B.D. (2005). A role for the Tip60 histone acetyltransferase in the acetylation and activation of ATM. *Proc. Natl. Acad. Sci. USA* **102**, 13182-13187.

Suzuki, A., Tsutomi, Y., Akahane, K., Araki, T., Miura, M. (1998). Resistance to Fas-mediated apoptosis: activation of caspase-3 is regulated by cell cycle regulator p21WAF1 and IAP gene family ILP. *Oncogene* **17**, 931-939.

Szekely, L., Selivanova, G., Magnusson, K.P., Klein, G., Wiman, K.G. (1993). EBNA-5, an Epstein-Barr virus encoded nuclear antigen, binds the retinoblastoma and p53 proteins. *Proc. Natl. Acad. Sci. USA* **90**, 5455-5459.

Takaoka, A., Hayakawa, S., Yanai, H., Stoiber, D., Negishi, H., Kikuchi, H., Sasaki, S., Imai, K., Shibue, T., Honda, K., Taniguchi, T. (2003). Integration of interferon- α/β signalling to p53 responses in tumour suppression and antiviral defence. *Nature* **424**, 516-523.

Takekawa, M., Adachi, M., Nakahata, A., Nakayama, I., Itoh, F., Tsukuda, H., Taya, Y., Imai, K. (2000). p53-inducible wip1 phosphatase mediates a negative feedback regulation of p38 MAPK-p53 signaling in response to UV radiation. *EMBO J.* **19**, 6517-6526.

Tanaka, H., Arakawa, H., Yamaguchi, T., Shiraishi, K., Fukuda, S., Matsui, K., Takei, Y., Nakamura, Y. (2000). A ribonucleotide reductase gene involved in a p53-dependent cell cycle checkpoint for DNA damage. *Nature* **404**, 42-49.

Tang, W., Willers, H., Powell, S.N. (1999). p53 directly enhances rejoining of DNA double strand breaks with cohesive ends in γ -irradiated mouse fibroblasts. *Cancer Res.* **59**, 2562-2565.

Tang, J.J., Shen, C., Lu, Y.J. (2006a). Requirement for pre-existing of p21 to prevent doxorubicin-induced apoptosis through inhibition of caspase-3 activation. *Mol. Cell. Biochem.* **291**, 139-144.

Tang, J., Qu, L.K., Zhang, J., Wang, W., Michealson, J.S., Degenhardt, Y.Y. (2006b). Critical role for Daxx in regulating MDM2. *Nat. Cell Biol.* **8**, 855-862.

Taso, Y-P., Huang, S-J., Chang, J-L., Hsieh, J-T, Pong, R-C., Chen, S-L. (1999). Adenovirus mediated p21 (Waf1/SdII/Cip1) gene transfer induces apoptosis of human cervical cancer cell lines. *J. Virol.* **73**, 4983-4990.

Thompson, T., Tovar, C., Yang, H., Carvajal, D., Vu, B.T., Xu, Q., Wahl, G.M., Heimbrook, D.C., Vassilev, L.T. (2004). Phosphorylation of p53 on key serines is dispensable for transcriptional activation and apoptosis. *J. Biol. Chem.* **279**, 53015-53022.

Tibbetts, R.S., Brumbaugh, K.M., Williams, J.M., Sarkaria, J.N., Cliby, W.A., Shieh, S.Y., Taya, Y., Prives, C., Abraham, R.T. (1999). A role for ATR in the DNA damage-induced phosphorylation of p53. *Genes Dev.* **13**, 152-157.

Toledo, F., Krummel, K.A., Lee, C.J., Liu, C.W., Rodewald, L.W., Tang, M., Wahl, G.M. (2006). A mouse p53 mutant lacking the proline-rich domain rescues Mdm4 deficiency and provides insight into the Mdm2-Mdm4-p53 regulatory network. *Cancer Cell* **9**, 273-285.

Trapman, J. (1979). A systematic study of interferon production by mouse L-929 cells induced with poly(I).poly(C) and DEAE-dextran. *FEBS Let.* **98**,107-110.

Trenz, K., Smith, E., Smith, S., Costanzo, V. (2006). ATM and ATR promote Mre11 dependent restart of collapsed replication forks and prevent accumulation of DNA breaks. *EMBO J.* **19**, 1764-1774.

Vale, R.D. & Milligan, R.A. (2000). The way things move: Looking under the hood of molecular motor proteins. *Science* **288**, 88-95.

Van Lint, C., Emiliani, S., Verdin, E. (1996). The expression of a small fraction of cellular genes is changed in response to histone hyperacetylation. *Gene Expr.* **5**, 245-253.

Vassilev, L.T., Vu, B.T., Graves, B., Carvajal, D., Podlaski, F., Filipovic, Z., Kong, N., Kammlott, U., Lukacs, C., Klein, C., Fotouhi, N., Liu, E. A. (2004). In vivo activation of the p53 pathway by small-molecule antagonists of MDM2. *Science* **303**, 844-848.

Vaziri, C., Saxena, S., Jeon, Y., Lee, C., Murata, K., Machida, Y., Wagle, N., Hwang, D.S., Dutta, A. (2003). A p53-dependent checkpoint pathway prevents rereplication. *Mol. Cell* **11**, 997-1008.

Vogelstein, B. & Kinzler, K. W. (2004). Cancer genes and the pathways they control. *Nat. Med.* **10**, 789-799.

Vousden, K.H. (2000). p53: Death Star. *Cell* **103**, 691-694.

Vousden, K.H. & Lane, D.P. (2007). p53 in health and disease. *Nat. Rev. Mol. Cell Biol.* **8**, 275-283.

Wadhwa, R., Takano, S., Mitsui, Y., Kaul, S.C. (1999). NIH 3T3 cells malignantly transformed by mot-2 show inactivation and cytoplasmic sequestration of the p53 protein. *Cell Res.* **9**, 261-269.

Wadhwa, R., Yaguchi, T., Hasan, M.K., Mitsui, Y., Reddel, R.R., Kaul, S.C. (2002). HSP70 family member, mot/mthsp70/GRP75, binds to the cytoplasmic sequestration domain of the p53 protein. *Exp. Cell Res.* **274**, 246-253.

Waga, S., Hannon, G.J., Beach, D., Stillman, B. (1994). The p21 inhibitor of cyclin-dependent kinases controls DNA replication by interaction with PCNA. *Nature* **369**, 574-578.

Wakasugi, E., Kobayashi, T., Tamaki, Y., Ito, Y., Miyashiro, I., Komoike, Y., Takeda, T., Shin, E., Takatsuka, Y., Kikkawa, N., Monden, T., Monden, M. (1997). p21(Waf1/Cip1) and p53 protein expression in breast cancer. *Am. J. Clin. Pathol.* **107**, 684-691.

Walczak, H. & Krammer, P.H. (2000). The CD95 (APO-1/FAS) and the TRAIL (APO-2L) apoptosis system. *Exp. Cell Res.* **256**, 58-66.

Waldman, T., Lengauer, C., Kinzler, K.W., Vogelstein, B. (1996). Uncoupling of S phase and mitosis induced by anticancer agents in cells lacking p21. *Nature* **381**, 713-716.

Walker, K.K. & Levine, A.J. (1996). Identification of a novel p53 functional domain that is necessary for efficient growth suppression. *Proc. Natl. Acad. Sci. USA* **93**, 15335-15340.

Wallace, M., Worall, E., Pettersson, S., Hupp, T.R., Ball, K.L. (2006). Dual-site regulation of MDM2 E3-ubiquitin ligase activity. *Mol. Cell* **23**, 251-263.

Wallingford, J.B., Seufert, D.W., Virta, V.C., Vize, P.D. (1997). p53 activity is essential for normal development in *Xenopus*. *Curr. Biol.* **7**, 747-757.

Wan, M., Cofer, K.F., Dubeau, L. (1996). WAF1/CIP1 structural abnormalities do not contribute to cell cycle deregulation in ovarian cancer. *Br. J. Cancer*, **73**, 1398-400.

Wang, X.W., Forrester, K., Yeh, H., Feitelson, M.A., Gu, J.R., Harris, C.C. (1994). Hepatitis B virus X protein inhibits p53 sequence-specific DNA binding, transcriptional activity and association with the transcription factor ERCC3. *Proc. Natl. Acad. Sci. USA* **91**, 2230-2234.

Wang, X.W., Yeh, H., Schaeffer, L., Roy, R., Moncollin, V., Egly, J.M., Wang, Z., Friedberg, E.C., Evans, M.K., Taffe, B.G., et al. (1995). p53 modulation of TFIIH-associated nucleotide excision repair activity. *Nat. Genet.* **10**, 188-195.

Wang, Y.A., Elson, A., Leder, P. (1997). Loss of p21 increases sensitivity to ionising radiation and delays the onset of lymphoma in atm-deficient mice. *Proc. Natl. Acad. Sci. USA* **94**, 14590-14595.

Wang, Y., Blandino, G., Givol, D. (1999). Induced p21^{waf} expression in H1299 cell lines promotes cell senescence and protects against cytotoxic effect of irradiation and doxorubicin. *Oncogene* **18**, 2643-2649.

Wang, T., Kobayashi, T., Takimoto, R., Denes, A.E., Snyder, E.L., el-Deiry, W.S., Brachmann, R.K. (2001). hADA3 is required for p53 activity. *EMBO J.* **20**, 6404-6413.

Warbrick, E., Lane, D.P., Glover, D.M., Cox, L.S. (1995). A small peptide inhibitor of DNA replication defines the site of interaction between the cyclin-dependent kinase inhibitor p21WAF1 and proliferating cell nuclear antigen. *Curr. Biol.* **5**, 275-282.

Warburg, O. (1956). On respiratory impairment in cancer cells. *Science* **124**, 269-270.

Wei, X., Hu, H., Kufe, D. (2005). Human MUC1 oncoprotein regulates p53-responsive gene transcription in the genotoxic stress response. *Cancer Cell* **7**, 167-178.

Weinberg, R.L., Veprintsev, D.B., Bycroft, M., Fersht, A.R. (2005). Comparative binding of p53 to its promoter and DNA recognition elements. *J. Mol. Biol.* **348**, 589-596.

Westphal, C.H., Rowan, S., Schmaltz, C., Elson, A., Fisher, D.E., Leder, P. (1997). Atm and p53 cooperate in apoptosis and suppression of tumorigenesis, but not in resistance to acute radiation toxicity. *Nat. Genet.* **16**, 397-401.

Wilkinson, D.S., Ogden, S.K., Stratton, S.A., Piechan, J.L., Nguyen, T.T., Smulian, G.A., Barton, M.C. (2005). A direct intersection between p53 and transforming growth factor beta pathway targets chromatin modification and transcription repression of the alpha fetoprotein gene. *Mol. Cell Biol.* **25**, 120-1212.

Wohlschlegel, J.A., Dwyer, B.T., Takeda, D.Y., Dutta, A. (2001). Mutational analysis of the Cy motif from p21 reveals sequence degeneracy and specificity for different cyclin-dependent kinases. *Mol. Cell Biol.* **21**, 4868-4874.

Wu, X., Bayle, J.H., Olson, D., Levine, A.J. (1993). The p53-mdm-2 autoregulatory feedback loop. *Genes Dev.* **7**, 1126-32.

Wu, Q., Kirschmeier, P., Hockenberry, T., Yang, T-Y., Brassard, D.L., Wang, L., McClanahan, T., Black, S., Rizzi, G., Musco-Hobkinson, M.L., Mirza, A., Liu, S. (2002). Transcriptional regulation during p21/WAF1/Cip1-induced apoptosis in human ovarian cancer cells. *J. Biol. Chem.* **277**, 36329-36337.

Wu, S., Cetinkaya, C., Munoz-Alonso, M.J., von der Lehr, N., Bahram, F., Beuger, V., Eilers, M., Leon, J., Larsson, L.G. (2003). Myc represses differentiation induced p21CIP1 expression via Miz-1-dependent interaction with the p21 core promoter. *Oncogene* **22**, 351-360.

Wu Z-H., Shi, Y., Tibbetts, R.S., Miyamoto, S. (2006). Molecular linkage between the kinase ATM and NF- κ B signalling in response to genotoxic stimuli. *Science* **311**, 1141-1146.

Wulf, G.M., Liou, Y.C., Ryo, A., Lee, S.W., Lu, K.P. (2002). Role of Pin1 in the regulation of p53 stability and p21 transactivation, and cell cycle checkpoints in response to DNA damage. *J. Biol. Chem.* **277**, 47976-47979.

Wymann, M.P., Bulgarelli-Leva, G., Zvelebil, M.J., Pirola, L., Vanhaesebroeck, B., Waterfield, M.J., Panayotou, G. (1996). Wortmannin inactivates phosphoinositide 3-kinase by covalent modification of Lys-802, a residue involved in the phosphate transfer reaction. *Mol. Cell. Biol.* **16**, 1722-1733.

Xiong, Y., Hannon, G.J., Zhang, H., Casso, D., Kobayashi, R., Beach, D. (1993). p21 is a universal inhibitor of cyclin kinases. *Genes Dev.* **7**, 1572-1583.

Xirodimas, D.P., Saville, M.K., Bourdon, J.C., Hay, R.T., Lane, D.P. (2004). Mdm2-mediated NEDD8 conjugation of p53 inhibits its transcriptional activity. *Cell* **118**, 83-97.

Xu, Y. & Baltimore, D. (1996). Dual roles of ATM in the cellular response to radiation and in cell growth. *Genes Dev.* **10**, 2401-2410.

Xu, Y., Yang, E.M., Brugarolas, J., Jacks, T., Baltimore, D. (1998). Involvement of p53 and p21 in cellular defects and tumorigenesis in atm^{-/-} mice. *Mol. Cell. Biol.* **18**, 4385-4390.

Yamashita, A., Ohnishi, T., Kashima, I., Taya, Y., Ohno, S. (2001). Human SMG-1, a novel phosphatidylinositol 3-kinase related protein kinase, associated with components of the mRNA surveillance complex and is involved in the regulation of nonsense-mediated mRNA decay. *Genes Dev.* **15**, 2215-2228.

Yang, W.C., Mathew, J., Velcich, A., Edelman, W., Kucherlapati, R., Lipkin, M., Yang, K., Augenlicht, L.H. (2001). Targeted inactivation of the p21(WAF1/cip1) gene enhances Apc-initiated tumor formation and the tumor-promoting activity of a Western-style high-risk diet by altering cell maturation in the intestinal mucosal. *Cancer Res.* **61**, 565-9.

Zacci, P., Gostissa, M., Uchida, T., Salvagno, C., Avolio, F., Volinia, S., Ronai, Z., Blandino, G., Schneider, C, Del Sal, G. (2002). The propyl isomerase Pin1 reveals a mechanism to control p53 functions after genotoxic stress. *Nature* **419.**, 853-857.

Zaika, A., Marchenko, N., Moll, U.M. (1999). Cytoplasmically "sequestered" wild type p53 is resistant to Mdm2-mediated degradation. *J. Biol. Chem.* **274**, 27474-27480.

Zhan, Q., Antinore, M.J., Wang, X.W., Carrier, F., Smith, M.L., Harris, C.C., Fornace, A.J., Jr. (1999). Association with cdc2 and inhibition of the cdc2/cyclin B1 kinase activity by the p53-regulated protein GADD45. *Oncogene* **18**, 2892-2900.

Zhang, H. & Burrows, F. (2004). Targeting multiple signal transduction pathways through inhibition of Hsp90. *J. Mol. Med.* **82**, 488-499.

Zhang, Z., Wang, H., Li, M., Agrawal, S., Chen, X., Zhang, R. (2004). MDM2 is a negative regulator of p21^{WAF1/CIP1}, independent of p53. *J. Biol. Chem.* **279**, 16000-16006.

Zhang, H., Xiong, Y., Beach, D. (1993). Proliferating cell nuclear antigen and p21 are components of multiple cell cycle kinase complexes. *Mol. Biol. Cell* **4**, 897-906.

Zhao, R., Gish, K., Murphy, M., Yin, Y., Notterman, D., Hoffman, W.H., Tom, E., Mack, D.H., Levine, A.J. (2000) Analysis of p53-regulated gene expression patterns using oligonucleotide arrays. *Genes Dev.* **14**, 981-993.

Zheng, H., You, H., Zhou, X.Z., Murray, S.A., Uchida, T., Wulf, G., Gu, L., Tang, X., Lu, K.P., Xiao, Z.X. (2002). The prolyl isomerase Pin1 is a regulator of p53 in genotoxic response. *Nature* **419**, 849-853.

Zhou, B.B. & Elledge, S.J (2000). The DNA damage response: putting checkpoints in perspective. *Nature* **408**, 433-439.

Ziyaie, D., Hupp, T. R., Thompson, A.M. (2000). p53 and breast cancer. *The Breast* **9**, 239-246.